ACOUSTICAL SCATTERING FROM THE IMPEDANCE COVERED STRAIGHT EDGE AND WEDGE; THE EXACT THEORY

E. J. Skudrzyk

Technical Memorandum
File No. TM 75-01
January 3, 1975
Contract No. N00017-73-C-1418

Copy No. 41

The Pennsylvania State University
Institute for Science and Engineering
APPLIED RESEARCH LABORATORY
Post Office Box 30
State College, PA 16801

NAVY DEPARTMENT

NAVAL SEA SYSTEMS COMMAND

(14) ARL/PSU/TM-75-01

UNCLASSIFIED
SECURITY CLASSIFICATION OF THIS PAGE (When Data Entered)

REPORT DOCUMENTATION PAGE

READ INSTRUCTIONS BEFORE COMPLETING FORM

1. REPORT NUMBER: TM 75-01	2. GOVT ACCESSION NO.: AD-A086003
3. RECIPIENT'S CATALOG NUMBER	
4. TITLE (and Subtitle): (6) Acoustical Scattering from the Impedance Covered Straight Edge and Wedge; The Exact Theory.	5. TYPE OF REPORT & PERIOD COVERED: (9) Technical Report
	6. PERFORMING ORG. REPORT NUMBER
7. AUTHOR(s): (10) E. J. Skudrzyk	8. CONTRACT OR GRANT NUMBER(s): (11) Jun 75
9. PERFORMING ORGANIZATION NAME AND ADDRESS: Applied Research Laboratory, P. O. Box 30, State College, PA 16801	10. PROGRAM ELEMENT, PROJECT, TASK AREA & WORK UNIT NUMBERS: (12) 177
11. CONTROLLING OFFICE NAME AND ADDRESS	12. REPORT DATE
	13. NUMBER OF PAGES
14. MONITORING AGENCY NAME & ADDRESS (if different from Controlling Office): (15) N00017-73-C-2448	15. SECURITY CLASS. (of this report)
	15a. DECLASSIFICATION/DOWNGRADING SCHEDULE

16. DISTRIBUTION STATEMENT (of this Report)

Approved for public release, distribution unlimited. Per Naval Sea Systems Command 4/1/80.

17. DISTRIBUTION STATEMENT (of the abstract entered in Block 20, if different from Report)

18. SUPPLEMENTARY NOTES

19. KEY WORDS (Continue on reverse side if necessary and identify by block number)

impedance, straight, edge, wedge, fourier, integral, sommerfeld, Malyuzhinets, theorems, diffraction

20. ABSTRACT (Continue on reverse side if necessary and identify by block number)

The analytic extension of the Fourier integral from the half space to wedge-like spaces leads to Sommerfeld type integrals. Theorems derived by Malyuzhinets in conjunction with new methods of handling Fourier Laplace integrals make it possible to apply the boundary conditions to the integrand to determine the integrand function and thus to determine the solution from the boundary conditions. The resulting Malyuzhinets functions can then be closely approximated by simple expressions for real and complex arguments.

DD FORM 1 JAN 73 1473 EDITION OF 1 NOV 65 IS OBSOLETE
S/N 0102-LF-014-6601

UNCLASSIFIED
SECURITY CLASSIFICATION OF THIS PAGE (When Data Entered)

JCL

24107

20. ABSTRACT (continued)

The diffracted field then depends on the shadow boundary and, in contrast to the classical theory, also on the orientation of the diffracting surface. The diffraction field is described by the sum of two terms. One term can be interpreted as a scattering effect because of the discontinuity in the medium caused by the impedance surfaces; the second could be interpreted as a field generated by reemission of some of the energy that is bent into the the diffractor near the edge. This term is equal to half the refelected amplitude at the shadow boundary of the reflected wave and to half the amplitude of the transmitted wave at the shadow-boundary of the transmitted wave. It describes the trivial condition of continuity in the transition from the insonnified region to the shadowed region. On the side of the incident wave, the amplitude is very nearly equal to the excitation as though due to the reflection factor that would obtain if the angle of exit (of diffraction) were produced by reflecting a ray on the wedge surface under the appropriate angle of incidence. As a consequence, this second term vanishes at two angles (the Brewster angles) that are equidistant from the normal of the surface. In this report, the diffraction is investigated of a great number of straight edges and wedges whose surfaces are covered with various impedances. The exact solutions are compared with approximations. However, even the exact solution can be easily derived because of a simple and very good approximation to the Malyuzhinets functions.

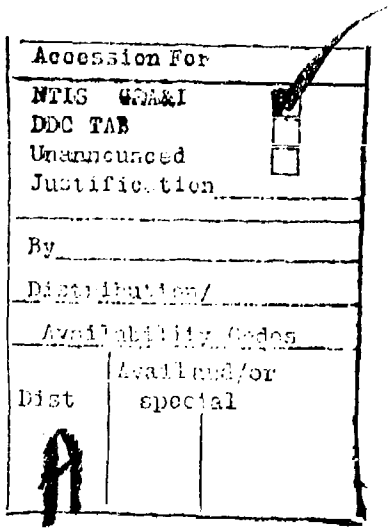

Subject: Acoustical Scattering from the Impedance Covered Straight Edge and Wedge; the Exact Theory

References: See pages 163-167

Abstract: See pages i and ii

ACOUSTICAL SCATTERING FROM THE IMPEDANCE COVERED STRAIGHT EDGE AND WEDGE; THE EXACT THEORY

ABSTRACT

The analytic extension of the Fourier integral from the half space to wedge-like spaces leads to Sommerfeld type integrals. Theorems derived by Malyuzhinets in conjunction with new methods of handling Fourier Laplace integrals make it possible to apply the boundary conditions to the integrand to determine the integrand function and thus to determine the solution from the boundary conditions. The resulting Malyuzhinets functions can then be closely approximated by simple expressions for real and complex arguments. The diffracted field then depends on the shadow boundary and, in contrast to the classical theory, also on the orientation of the diffracting surface. The diffraction field is described by the sum of two terms. One term can be interpreted as a scattering effect because of the discontinuity in the medium caused by the impedance surfaces; the second could be interpreted as a field generated by reemission of some of the energy that is bent into the diffractor near the edge. This term is equal to half the reflected amplitude at the shadow boundary of the reflected wave and to half the amplitude of the transmitted wave at the shadow-boundary of the transmitted wave. It describes the trivial condition of continuity in the transition from the insonnified region to the shadowed region. On the side of the incident wave, the amplitude is very nearly equal to the excitation as though due to the reflection factor that would obtain if the angle of exit (of diffraction) were produced by reflecting a ray on the wedge surface under the appropriate angle of incidence. As a consequence, this second term vanishes at two angles (the Brewster angles) that are equidistant from the normal of the surface. In this

report, the diffraction is investigated of a great number of straight edges and wedges whose surfaces are covered with various impedances. The exact solutions are compared with approximations. However, even the exact solution can be easily derived because of a simple and very good approximation to the Malyuzhinets functions.

I. INTRODUCTION

The Fourier Integral for the Half Space and Its Analytic Extension to Wedge Spaces

In dealing with propagation problems, we solved the wave equation in a suitable coordinate system. Because the wave equation is of second order, we obtain two independent solutions. Boundary conditions are usually prescribed at the coordinate surfaces and at infinity. One solution frequently has to be discarded because it represents energy sources at infinity. In the case of a straight edge (semi infinite plane), boundary conditions need to be prescribed at both surfaces, i.e. the solution must be discontinuous at the half plane. The coordinate surface is no longer a plane but is a degenerate cylindrical paraboloid.

The standard Fourier method is not applicable to wedge spaces nor to the straight edge. Fourier integrals converge only in the semi space.

The Fourier integral can be built up from plane two-dimensional waves:

$$p = S_o \, e^{j(wx + k_y y) - j\omega t} \tag{1.1}$$

where S_o is an amplitude constant, k is the wave number, and

$$k_y = \sqrt{k^2 - w^2} \tag{1.2}$$

The quantity w can be interpreted as the forced wave number in the x direction at the surface $y = 0$; the quantity k is the wave number of the wave that propagates in the medium as a consequence of the vibration forced with the wave number w along the plane $y = 0$. We may now prescribe the vibration amplitude at $y = 0$ by a Fourier integral and extend the integral to the y-space by including the k_y part in the exponent. Thus we have

$$p = \int_{-\infty}^{\infty} e^{j(wx + y\sqrt{k^2 - w^2})} S_o(w)dw \quad , \tag{1.3}$$

where $S_o(w)$ is the spectral amplitude function. The integral then represents a solution of the wave equation provided that it is absolutely convergent. This is the case in the upper half plane if the exponent has a negative real part for $y > 0$, and if $S_o(w)$ is bounded in the interval of integration.

The convergence properties of the integrand are not affected by a coordinate transformation. However, it will be of advantage to introduce cylindrical coordinates (see Fig. 1.1):

$$x = r \sin \varphi \ , \quad y = r \cos \varphi \ , \quad w = k \sin \alpha \quad . \tag{1.4}$$

Regardless of the sign of the square root in the integrand of Eq. (3), the transformation introduces once more an ambiginity of the sign. ($\sqrt{1 - \sin^2\alpha} = \pm \cos \alpha$). The exponent in the integrand thus becomes

$$jkr \ (\sin \alpha \sin \varphi \pm \cos \varphi \cos \alpha) = \pm jkr \cos \ (\varphi \mp \alpha) \tag{1.5}$$

The limits are given by

$$w/k = \sin \alpha = \sin \ (\alpha_r + j\alpha_i) = \sin \alpha_r \cosh \alpha_i + j \cos \alpha_r \sinh \alpha_i = \pm \infty \ , \tag{1.6}$$

We find that $\cos \alpha_r = 0$, $\alpha_i = \pm \infty$, $\alpha_r = \frac{\pi}{2}$ for $w = \infty$, and that

$\alpha_r = -\frac{\pi}{2}$, $\alpha_i = \pm \infty$ for $w = -\infty$.

We have a choice of two basically different values for each limit. It does not make much difference which sign we select for the square root; convergence can be obtained for each sign by selecting properly the new limits of integration. If we select the positive sign for the square root, the integral will converge if

$$kr \sin(\varphi - \alpha_r) \sinh \alpha_i \tag{1.7}$$

is positive. This means that we must have

$$0 < \varphi - \alpha_r < \pi , \quad \alpha_i \to \infty \tag{1.8}$$

$$-\pi < \varphi - \alpha_r < 0 , \quad \alpha_i \to -\infty \tag{1.9}$$

For $\alpha_i \to \infty$ we obtain for the limit $\pi/2$ of φ:

$$0 < -\pi/2 - \alpha_r < \pi \quad \text{or} \quad -\frac{3\pi}{2} < \alpha_r < -\pi/2 , \tag{1.10}$$

and for the limit $\pi/2$ of φ:

$$0 < \pi/2 - \alpha_r < \pi \quad \text{or} \quad -\frac{\pi}{2} < \alpha_r < \pi/2 \tag{1.11}$$

Thus $\alpha_r = -\frac{\pi}{2} - \epsilon$ when φ is negative ($\epsilon \to 0$) and $\alpha_r = -\frac{\pi}{2} + \epsilon$ when φ is positive, or we may assume that $\alpha_r = -\frac{\pi}{2}$, and that φ is restricted to the interval $-(\frac{\pi}{2} - \epsilon) \leq \varphi \leq (\frac{\pi}{2} - \epsilon)$. Similarly we find that $\alpha_r = +\pi/2$ for $\alpha_i \to -\infty$. The transformed integral is thus given by

$$P(r,\varphi) = \int_{-\frac{\pi}{2} - j\infty}^{-\frac{\pi}{2} + j\infty} e^{jkr \cos(\varphi - \alpha)} S_o(k \sin \alpha)\, k \cos \alpha \, d\alpha \tag{1.12}$$

If we assume that the path of integration passes from $+ j\infty - \frac{\pi}{2}$ to $- \frac{\pi}{2}$ and from there along to $- \pi/2$ and then straight up to $- \frac{\pi}{2} + j\infty$, then the contribution of the path along the real axis represents the field of waves in the direction φ that propagates at an angle $- \frac{\pi}{2} < \alpha < \frac{\pi}{2}$ with respect to the real axis. The contribution of the vertical parts of the path represents the field of waves in the direction φ that propagates along the axis $\alpha = 0$ and decays strongly with distance. We have no freedom in the path of integration if the integral is to converge for all values of φ that correspond to points in the upper half plane. Thus changing the variable did not change anything basically.

Equations (1.1) and (1.3) derive the field from the boundary condition at $y = 0$. This boundary condition is equivalent to a field that is generated by a source distribution somewhere between $y = 0$ and $y = - \infty$. In a wedge space or in case of a straight edge, we need solutions that converge also for $y < 0$ and that are discontinuous at the surfaces of the straight edge or wedge. This requirement excludes solutions in Cartesian coordinates. Such solutions have the period 2π and would lead to the same values at the two surfaces of the straight edge. If we want to perform an analysis in terms of simple harmonic functions, they must have a period that differs from 2π. We are therefore certain that $S_o(\alpha) \neq S_o(\alpha + 2\pi)$.

To introduce the preceding condition explicitly into the solution, we write the integrand in the following form:

$$S(\alpha + \pi) - S(\alpha - \pi) = 2\pi j \, S_o(k \sin \alpha) \, k \cos \alpha \quad . \tag{1.13}$$

$S(\alpha - \pi)$ can then be interpreted as the radiation from the front, $S(\alpha + \pi)$ from the back (see Fig. 1.2). Front and back are separated by the semi infinite plane, each point therefore contributes because it radiates into

the front space and because it also radiates into the shadow space. This particular geometry seems to be impressed on the whole space. The physical space is defined here as the space $-\pi < \varphi < \pi$ (Sommerfeld). All other angles ($|\varphi| > \pi$) represent a purely mathematical space (the Riemann space in the Sommerfeld theory). The reflected fields can then be interpreted as being generated by mirror image sources that are hidden in the Rieman space; this agrees with the assumption of having only one source in the physical space.

The solution then is represented by the expression

$$P(r,\varphi) = \frac{1}{2\pi j} \int_{-\frac{\pi}{2} + j\infty}^{+\frac{\pi}{2} - j\infty} e^{jkr\cos(\varphi - \alpha)}[S(\alpha + \pi) - S(\alpha - \pi)]\,d\alpha$$

$$= \frac{1}{2\pi j} \int_{\frac{\pi}{2} + j\infty}^{\frac{3\pi}{2} - j\infty} e^{-jkr\cos(\varphi - \alpha)} S(\alpha) + \frac{1}{2\pi j} \int_{-\frac{\pi}{2} - j\infty}^{-\frac{3\pi}{2} + j\infty} e^{-jkr\cos(\varphi - \alpha)} S(\alpha)\,d\alpha \qquad (1.14)$$

where we have introduced the new variable $\alpha' = \alpha + \pi$, $\alpha'' = \alpha - \pi$ in the two parts of the integral, written α again for α' and α'', and changed the limits of integration correspondingly. The new paths of integration are shown in Fig. 1.3a. We now assume that $S(\alpha)$ is regular in the range of integration except for a number of discrete poles at finite distance from the real axis. We combine the two halves of the path in each half plane into a loop, getting the path $\gamma(\varphi)$ as shown in Fig. 1.3b. Poles at infinite distances from the real axis can be accounted for by considering their residues. We thus obtain:

$$P(r,\varphi) = \frac{1}{2\pi j} \int_{\gamma(\varphi)} e^{-jkr\cos(\alpha - \varphi)} S(\alpha)\,d\alpha \qquad (1.15)$$

It is inconvenient to introduce limits that depend on φ. By changing variables

$$(\varphi - \alpha) = - u \ , \qquad u = \alpha - \varphi$$

$$\alpha = u + \varphi \ , \qquad d\alpha = du \tag{1.16}$$

and writing α again for u the integral transforms into

$$\int_{\Gamma} e^{-jkr \cos \alpha} S(\alpha + \varphi) \, du \tag{1.17}$$

we are free to move the path of integration within the regions of convergence of the integrand. Since the convergence of the integrand does not depend on φ, the path Γ is the same for all values of $- \Phi < \varphi < \Phi$. We have assumed implicity that $S(\alpha + \varphi)$ vanishes sufficiently strong at infinity so that we are allowed to start the path at $\pm j\infty$ and to proceed in any direction as long as we stay in the convergence range of the integrand. For positive α_i, these limits are now given by

$$kr \sin \alpha_i \sinh \alpha_i > 0 \ , \quad 0 < \alpha_r < \pi \ , \tag{1.18}$$

if $\alpha_i > 0$ and by

$$- 2\pi < \alpha_r < - \pi \ , \quad \text{if } \alpha_i < 0 \ .$$

An analogous result is obtained for the negative half plane. The path Γ is as shown in figure 1.4. It extends along the real axis from at least $- \pi$ to $+ \pi$. It is apparent that the function $S(\alpha)$ must be analytic for at least the range $- \pi \leq (\alpha_r \pm \Phi) \leq \pi$ for $\alpha_i > c = \text{const.}$,

or

$$-(\pi + \Phi) \leq \alpha_r \leq \pi + \Phi \tag{1.19}$$

(i.e. except for the poles near the real axis. We thus have arrived at a generalized Fourier integral which will converge in wedge-like spaces. We shall refer to this integral as the loop integral in the following.

II. PROPERTIES OF THE LOOP INTEGRAL

(a) Derivative with Respect to φ

The derivation of the loop integral is best performed in its form (1.14). Since a small displacement of the path $\gamma(\varphi)$ into $\gamma(\varphi + d\varphi)$ within the convergence range of the integral does not change its value, differentiation can be confined to that of the integrand. Thus

$$\frac{\partial I}{\partial \varphi} = \int_{\gamma(\varphi)} \frac{\partial\, e^{-jkr \cos(\varphi - \alpha)}}{\partial \varphi}\, s(\alpha)\, d\alpha \tag{2.1}$$

$$jkr \int_{\Gamma} e^{-jkr \cos \alpha} \sin \alpha\, s(\alpha + \varphi)\, d\alpha \tag{2.2}$$

where we have replaced $\varphi - \alpha$ by $-\alpha'$ and written α for α' again.

(b) Condition for Zero Value of the Integral

The most important theorem that applies to the loop integrals is Malyuzhinet's theorem I. A loop integral is zero

$$\int_{\Gamma} e^{-jkr \cos z}\, s(z)\, dz = 0 \tag{2.3}$$

if the function $s(z)$ is even, i.e. if

$$s(z) = s(-z) \tag{2.4}$$

where

$$z = u + jv$$

To prove this theorem, the path of integration is deformed into the two lines infinitely close to $u = -\pi$ and $u = +\pi$ (see Fig. 1.4) and integration is performed either to the left or to the right of these lines so that the exponent has a negative real part. Since $\cos(z) = \cos(-z)$ and $s(z) = s(-z)$, the integrands along the line $0 > v > -\infty$, $u = -\pi$ and $u = \pi$, $0 \leq v \leq \infty$ are equal. But since the directions of the two parts of the path are opposite, their contributions cancel.

If the function $s(z)$ increases at a high rate towards infinity, condition (5) has to be replaced by a more complex condition.*

(c) Inversion Formula for the Wedge Integral for φ = const.

Malyuzhinets also derived an inversion formula for the wedge integral. If

$$\Delta s - m^2 s = 0 \quad \left(-\frac{\pi}{2} \leq \arg m \leq \frac{\pi}{2}\right) \tag{2.5}$$

$$S(r) = \frac{1}{2\pi j} \int_{\gamma} e^{mr \cos \alpha} S(\alpha) d\alpha \tag{2.6}$$

then

$$s(\alpha) = -\frac{m \sin \alpha}{2} \int_{0}^{\infty} S(r)\, e^{-mr \cos \alpha}\, dr \tag{2.7}$$

*The derivation is straightforward and given in the reference: G. D. Malyuzhinets, Inversion Formula for the Sommerfeld Integral, Mathematical Soviet Physics Doklady 3, 1958, 52-54.

III. BOUNDARY CONDITIONS

The function $S(\alpha)$ is determined from the boundary conditions for the sound pressure at the surfaces $\varphi = \pm \Phi$. For a wedge with pressure release surfaces

$$P(r,\Phi) = \int_{\Gamma} e^{jkr\cos\alpha} S(\alpha \pm \Phi)\, d\alpha = 0 \tag{3.1}$$

To satisfy this relation, $S(\alpha \pm \Phi)$ must be an even function of α. Thus

$$\begin{aligned} S(\alpha + \Phi) &= S(-\alpha + \Phi) \\ S(\alpha - \Phi) &= S(-\alpha - \Phi) \end{aligned} \tag{3.2}$$

If we replace α by $\alpha - \Phi$ in the first and by $\alpha + \Phi$ in the second equation, the left hand sides become equal and

$$S(\alpha) = S(-\alpha - 2\Phi) = S(-\alpha + 2\Phi) \tag{3.3}$$

This result shows that the solution has the period 4Φ. As pointed out in Section I, Equation 1.19, the solution must be analytic in the band $|\mathrm{Re}(\alpha)| \leq \Phi + \pi$ except for a pole for $\varphi = \varphi_o$, whose contribution represents the incident wave. The simplest function that has a period 4Φ, has a pole at $\alpha = \varphi_o$. Such a function is

$$S(\alpha) = \frac{1}{\sin \frac{\pi}{2\Phi} (\alpha - \varphi_o)} \tag{3.4}$$

But this function does not satisfy condition (3.3) because

$$S(-\alpha + 2\Phi) = \sin[\frac{\pi}{2\Phi}(-\alpha + 2\Phi - \varphi_o)] = \sin[\frac{\pi}{2\Phi}(-\alpha - \varphi_o) + \pi] = \sin\frac{\pi}{2\Phi}(\alpha + \varphi_o) \neq S(\alpha) \quad . \tag{3.5}$$

But the product of two functions of the type $S(\alpha)$, one with $+\varphi_o$, the other with $-\varphi_o$ in the argument will satisfy our requirement because of the symmetry which is thus generated. We are thus led to assume that

$$S(\alpha) = \frac{1}{\sin\frac{\pi}{2\Phi}(\alpha - \varphi_o)\sin\frac{\pi}{2\Phi}(\alpha + \varphi_o)} \tag{3.6}$$

$S(\alpha)$ still has a pole at $\alpha = -\varphi_o$; but $\varphi = -\varphi_o$ represents an incident wave in the physical space ($-\Phi \leq \varphi \leq \Phi$). But there is no second incident wave, and this pole must be cancelled by multiplying by a periodic non-trivial factor, Λ, that has such a pole. The factor

$$\Lambda = \sin\frac{\pi}{2\Phi}\alpha + \sin\frac{\pi}{2\Phi}\varphi_o \tag{3.7}$$

fulfills all requirements. It cancels the pole and satisfies the conditions. Hence we have

$$S(\alpha) = \frac{B(\sin\frac{\pi}{2\Phi}\alpha + \sin\frac{\pi}{2\Phi}\varphi_o)}{\sin\frac{\pi}{2\Phi}(\alpha + \varphi_o)\sin\frac{\pi}{2\Phi}(\alpha - \varphi_o)} \tag{3.8}$$

The residue of $S(\alpha)$ at $\alpha = \varphi_o$ is unity if

$$B = \frac{\pi}{2\Phi}\cos\frac{\pi}{2\Phi}\varphi_o \tag{3.9}$$

We thus arrive at the solution

$$S(\alpha) = \frac{\pi}{2\Phi} \frac{\cos \frac{\pi}{2\Phi} \varphi_o \left[\sin \frac{\pi}{2\Phi} \alpha + \sin \frac{\pi}{2\Phi} \varphi_o\right]}{\sin \frac{\pi}{2\Phi} (\alpha + \varphi_o) \sin \frac{\pi}{2\Phi} (\alpha - \varphi_o)}$$

$$= \frac{\pi}{2\Phi} \frac{\cos \left(\frac{\pi}{2\Phi} \varphi_o\right) 2 \sin \frac{\pi}{4\Phi} (\alpha + \varphi_o) \cos \frac{\pi}{4\Phi} (\alpha - \varphi_o)}{4 \sin \frac{\pi}{4\Phi} (\alpha + \varphi_o) \cos \frac{\pi}{4\Phi} (\alpha + \varphi_o) \sin \frac{\pi}{4\Phi} (\alpha - \varphi_o) \cos \frac{\pi}{4\Phi} (\alpha - \varphi_o)}$$

$$= \frac{\pi}{4\Phi} \frac{\cos \frac{\pi}{2\Phi} \varphi_o}{\sin \frac{\pi}{4\Phi} (\alpha - \varphi_o) \cos \frac{\pi}{4\Phi} (\alpha + \varphi_o)} =$$

$$= \frac{\pi}{4\Phi} \frac{\cos \frac{\pi}{4\Phi} (\alpha - \varphi_o) \cos \frac{\pi}{4\Phi} (\alpha + \varphi_o) + \sin \frac{\pi}{4\Phi} (\alpha - \varphi_o) \sin \frac{\pi}{4\Phi} (\alpha + \varphi_o)}{\sin \frac{\pi}{4\Phi} (\alpha - \varphi_o) \cos \frac{\pi}{4\Phi} (\alpha + \varphi_o)} \tag{3.10}$$

$$= \frac{\pi}{4\Phi} \left[\cot \frac{\pi}{4\Phi} (\alpha - \varphi_o) + \tan \frac{\pi}{4\Phi} (\alpha + \varphi_o)\right]$$

For the stationary phase integration, $S(\alpha)$ is best written in the form

$$S(\alpha) = \frac{\pi}{2\Phi} \frac{\cos \frac{\pi}{2\Phi} \varphi_o}{\sin \frac{\pi}{2\Phi} \alpha - \sin \frac{\pi}{2\Phi} \varphi_o} \tag{3.11}$$

which is easily deduced from the third form on the right. The cosine factor in the numerator is a consequence of the pressure release boundary. This factor is zero for $\varphi_o = \Phi$. We thus have obtained the well known Sommerfeld integrand for the pressure release wedge; in constrast to Sommerfeld's heuristic procedure the method above is based only on mathematical deduction. The solution for the rigid wedge can be derived in a very similar manner.

Malyuzhinets has derived a new kind of Fourier-Laplace analysis which can also be used to derive the function $S(\alpha)$. But in case of the Sommerfeld wedge, the Malyuzhinets Method is impractical because of the complexity of the integrals that result and the preceding method is preferable.

IV. THE FOURIER LAPLACE ANALYSIS OF MALYUZHINETS

Functions that increase exponentially towards $\pm\infty$ or approach finite values at $\pm\infty$ can be represented by Laplace integrals by separating them into two parts, one part representing the function in the interval 0 to ∞, the other zero part representing the function in the interval $-\infty$ to 0. This procedure leads to two different spectral functions. To compute inverse transform because of their different regions of convergence, each of these two functions has to be integrated over a different path. The analysis that has been introduced by Malyuzhinets is based on a single spectral function $F(w)$ for the whole range of integration. However, the representation of this function depends on whether the line integral is at the left or right of the imaginary axis. This simplification becomes possible because the fields we are interested in either approach finite values or vanish at $\pm\infty$. The integrals that occur in the various computations usually contain sines, cosines, tangents, and groups of functions of a variable z that are regular in strips, $a < \mathrm{Re}\,(z) < b$. For instance, $1/\cos z$ is regular for $-\pi/2 < \mathrm{Re}\,(z) < \frac{\pi}{2}$. We therefore limit our study to functions which exponentially approach constant values for $\mathrm{Im}(z) \to \pm\infty$ when $a < \mathrm{Re}\, z < b$. We thus have by definition

$$f(z) \to f(j\infty) + O\{e^{-\lambda \mathrm{Im}(z)}\} = f(j\infty) + O\{e^{j\lambda z}\}, \quad \mathrm{Im}(z) \to j\infty \tag{4.1}$$

$$f(z) \to f(-j\infty) + O\{e^{-\mu\, \mathrm{Im}(z)}\} = f(-j\infty) + O\{e^{-j\mu z}\}, \quad \mathrm{Im}(z) \to -j\infty \tag{4.2}$$

λ, μ positive constants

The analysis we are going to develop could be extended to exponentially increasing functions as $|\mathrm{Im}(z)| \longrightarrow \infty$. However, we would then loose the effect of the constants $f(j\infty)$ and $f(-j\infty)$. That wave fields differ at $\pm$ infinity is easily illustrated for a half plane as diffractor, half the incident energy will be reflected back at the semi infinite plane. But at great distances from the plane, the shadow space will be filled up with energy by diffraction and the amplitude will approach $1/\sqrt{2}$ times that of the incident wave. Thus the wave amplitude will be S_o at $+\infty$, and $S_o/\sqrt{2}$ at $-\infty$.

The function $f(z) - f(-j\infty)$ can be represented by a two-sided Laplace integral because it vanishes exponentially for $\mathrm{Im}(z) \rightarrow -\infty$, and approaches a constant for $z = +j\infty$. To derive this integral, let us use the notation of Malyuzhinets and prove that the integral

$$F^{*}(w) = \frac{j}{\sqrt{2\pi}} \int_{-j\infty}^{j\infty} [f(z) - f(-j\infty)]\, e^{jwz}\, dz \quad , \quad 0 < \mathrm{Re}\ w < \mu \tag{4.3}$$

converges for $0 < \mathrm{Re}(w) < \mu$, and that the integral

$$F^{**}(w) = \frac{j}{\sqrt{2\pi}} \int_{-j\infty}^{j\infty} [f(z) - f(j\infty)]\, e^{jwz} dz \quad , \quad -\lambda < \mathrm{Re}(w) < 0 \tag{4.4}$$

converges for $-\lambda < \mathrm{Re}(w) < 0$. To perform this proof, we divide the integral (4.3) into the two integrals

$$\frac{j}{\sqrt{2\pi}} \int_{-j\infty}^{0} [f(z) - f(-j\infty)] e^{jwz} dz + \frac{j}{\sqrt{2\pi}} \int_{0}^{j\infty} [f(z) - f(-j\infty)]\, e^{jwz} dz \tag{4.5}$$

The first integral exists because $f(z)$ is analytic and $f(z) - f(-j\infty)$ vanishes at its lower limit. If we replace $f(z)$ by Eq. (4.1) the first integral reduces to

$$\int_{-j\infty}^{0} [f(-j\infty) - f(-j\infty) + 0\ \{e^{-j\mu z}\}\ ]\ e^{jwz} dz = \int_{-j\infty}^{0} 0\ \{e^{j(w-\mu)z}\}\ dz \quad . \tag{4.6}$$

This integral converges, provided $\mathrm{Re}(w) = \mu < 0$. In the second integral we write correspondingly

$$\int_{0}^{j\infty} [f(j\infty) - f(-j\infty) + 0\ \{e^{j\lambda z}\}]\ e^{jwz} dz \tag{4.7}$$

This integral converges if $\mathrm{Re}\ w > 0$ and $\mathrm{Re}(w) + \lambda > 0$. The three conditions then lead to

$$0 < \mathrm{Re}\ w < \mu \tag{4.8}$$

The preceding formulae can be inverted as is proved by methods well known in Fourier analysis

$$f(z) - f(j\infty) = \frac{j}{\sqrt{2\pi}} \int_{-j\infty}^{j\infty} F^{**}(w)\ e^{-jwz}\ dw \quad , \tag{4.9}$$

provided $-\lambda < \mathrm{Re}(w) < 0$ and

$$f(z) - f(-j\infty) = \frac{j}{\sqrt{2\pi}} \int_{-j\infty}^{j\infty} F^{*}(w)\ e^{-jwz}\ dw \quad , \tag{4.10}$$

provided $0 < \mathrm{Re}(w) < \mu$. If we substract the two equations from each other

$$[f(j\infty) - j(-j\infty)] = \frac{j}{\sqrt{2\pi}} \left[\int_{-j\infty+\epsilon}^{j\infty+\epsilon} F^{*}(w)e^{-jwz}dw - \int_{-j\infty-\epsilon}^{j\infty-\epsilon} F^{**}(w)e^{-jwz}dw\right] \qquad (4.11)$$

where we have replaced the condition $\mathrm{Re}(w) \geq -\lambda$ by shifting the path of integration by ϵ to the left and correspondingly the condition $\mathrm{Re}(w) \leq \mu$ by shifting it by ϵ to the right where $\epsilon > 0$ can be as small as we please. Since $f(z)$ is analytic in the strip $a < \mathrm{Re}(z) < b$, $F^{*}(w)$ and $F^{**}(w)$ cannot have any singularities other than for $\mathrm{Re}(w) = 0$, and cannot have singularities for $\mathrm{Im}(w) \neq 0$ since the integrand is analytic in the strip and finite at infinity; the only admissible singularity is a simple pole at $w = 0$ since $F(w)$ is single valued. We have for $w \neq 0$, by applying Eq. (4.3),

$$F(w) < \lim_{y \to \infty} M \int_{-jy}^{jy} e^{jwz}\, dz = \lim_{y \to \infty} \frac{e^{jwy} + e^{-jwy}}{jw} = \text{finite} \qquad (4.12)$$

The right hand side of Eq. (4.11) reduces to the integral around the pole at $w = 0$ and $F(w)$ becomes infinite for $w = 0$. The residue of $F(w)$ at this pole is given by

$$\text{residue} \cdot 2\pi j = \frac{\sqrt{2\pi}}{j} [f(j\infty) - f(-j\infty)] \qquad (4.13)$$

for all values of z. This shows that $F^{*} = F^{**}$. A more rigorous proof can be derived with the aid of the Cauchy Chilbert transform representation of the Fourier transform.

We can still improve the symmetry of the reverse transform by adding Eqs. (4.9) and (4.10) and dividing by two:

$$f(z) = \frac{1}{2}[f(j\infty) + f(-j\infty)] + \frac{j}{2\sqrt{2\pi}} \left[\int_{-j\infty-\epsilon}^{j\infty-\epsilon} F^{**}(w)e^{-jwz}\, dw + \int_{-j\infty+\epsilon}^{j\infty+\epsilon} F^{*}(w)e^{-jwz}dw\right] \qquad (4.14)$$

where $F^{*}(w)$ and $F^{**}(w)$ are given by Eqs. (4.3) and (4.4). We can drop the star and the double star. $F(w)$ is an analytic function which in the band $-\lambda < \mathrm{Re}(w) < 0$ can be represented by the integral $F^{**}(w)$ and in the band $0 < \mathrm{Re}(w) < \mu$ by the integral $F^{*}(w)$. Equation (4.14) represents a very convenient and also the most general form of the solution. But for the final evaluation, the two integrals have to be combined and written in a standard form. This can be done, for instance, by shifting the path of integration of the second integral to the left, and adding the contribution of the residue at $w = 0$ to the result (see Fig. 4.1):

$$f(z) = \frac{1}{2}\left[f(j\infty) + f(-j\infty)\right] + \frac{j}{2\sqrt{2\pi}} \int_{-\epsilon-j\infty}^{-\epsilon+j\infty} \left[F^{*}(w) + F^{**}(w)\right] e^{-jwz} dw$$

$$+ \frac{2\pi j}{\sqrt{2\pi}} \cdot \text{residue at } (w = 0) \quad , \tag{4.15}$$

or by changing w into $-w$ in the second integral of Eq. (4.14):

$$f(z) = \frac{1}{2}\left[f(j\infty) + f(-j\infty)\right] + \frac{j}{2\sqrt{2\pi}} \int_{-\epsilon-j\infty}^{-\epsilon+j\infty} \left[F^{*}(w)e^{-jwz} dw + F^{**}(-w)e^{jwz}\right] dw \tag{4.16}$$

Frequently, integration can be further simplified by discarding the odd parts of the integrals but retaining possible contributions at the pole $w = 0$.

V. THE IMPEDANCE WEDGE

(a) The Solution

In this section, wedges will be investigated whose surfaces are covered by acoustic impedances. The reflection factor for a plane incident wave at a plane surface of acoustic impedance $\bar{z}$, is given by

$$\bar{R} = \frac{\frac{\bar{z}}{\rho c}\cos\varphi - 1}{\frac{\bar{z}}{\rho c}\cos\varphi + 1} = \frac{\cos\varphi - \frac{\rho c}{\bar{z}}}{\cos\varphi + \frac{\rho c}{\bar{z}}} = \frac{\cos\varphi - \cos\bar{\vartheta}}{\cos\varphi + \cos\bar{\vartheta}} \tag{5.1}$$

where φ is the angle of incidence with the normal to the surface. For the angle given by

$$\cos\bar{\theta} = \frac{\rho c}{\bar{z}} = \frac{1}{\zeta} = \cos\left(\frac{\pi}{2} - \vartheta\right) = \sin\bar{\vartheta} \quad , \tag{5.2}$$

the reflection is zero. The angle $\vartheta = \pi/2 - \bar{\theta}$ is defined as the grazing acoustic Brewster angle, $\bar{\theta}$ as the Brewster angle with the normal to the surface. This definition applied formally also for complex impedances. In deriving the acoustic equations for wedges, it is of considerable advantage to measure angles from the central wedge plane (see Fig. 1.1). The wedge surfaces then are given by $\varphi = \pm\Phi$. The boundary conditions that have to be satisfied are: (1) For the upper surface, where $\varphi = \Phi$, $z = z_+$, $\vartheta = \vartheta_+$:

$$\tilde{v}_\varphi = \frac{\tilde{p}}{\bar{z}_+} = -\frac{j}{k\rho c}\frac{\partial\tilde{p}}{\partial(r\varphi)} \qquad \text{(time factor } e^{-j\omega t}) \quad ; \quad ; \tag{5.3}$$

or if we introduce the Brewster angle

$$jk\,\tilde{p}\,\sin\vartheta_+ = \frac{1}{r}\left(\frac{\partial\tilde{p}}{\partial\varphi}\right)_{\varphi=\Phi} \quad . \tag{5.4}$$

For the lower surface where $\varphi = -\Phi$, $z = z_-$; $\vartheta = \vartheta_-$:

$$jk\tilde{p}\,\sin\vartheta_- = -\frac{1}{r}\left(\frac{\partial p}{\partial\varphi}\right)_{\varphi=-\Phi} \quad . \tag{5.5}$$

If we apply these boundary conditions to the integral solution and using Eqs. (2.1) and (2.3), the following equations result:

$$\begin{aligned}(\sin\alpha + \sin\vartheta_+)\,S\,(\alpha+\Phi) = -(\sin\alpha - \sin\vartheta_+)\,S\,(-\alpha+\Phi) = 0\\ (\sin\alpha + \sin\vartheta_-)\,S\,(\alpha-\Phi) = -(\sin\alpha - \sin\vartheta_-)\,S\,(-\alpha-\Phi) = 0\end{aligned} \tag{5.6}$$

It is apparent from the Kirchoff theory that the impedance cover of the faces of the wedge will not displace the shadow boundary of the wedge surfaces significantly and it is obvious that it cannot effect the pole nor its residue that represents the incident wave. If, therefore, we write the solution in for form

$$S(\alpha) = \frac{\sigma(\alpha)\,\psi(\alpha)}{\psi(\varphi_o)} \quad . \tag{5.7}$$

where

$\sigma(\alpha)$ is the Sommerfeld form of the integrand of the loop integral for a pressure release wedge,

$\psi(\alpha)$ is a function that describes the effect of the impedance cover,

$\psi(\varphi_o)$ is a kind of normalizing factor,

then $\sigma(\alpha)$ will contain all the poorly behaving parts of the solution (poles describing incident and reflected waves) and $\frac{\psi(\alpha)}{\psi(\varphi_o)}$ will be a well behaving function with no poles within the range of integration (but it may have poles

at the extremes $\alpha = \pm \pi$). We shall see in section (XII) that the solution of the impedance wedge must be based on the pressure release wedge and not on the rigid wedge. The impedance wedge backscatters at all angles. The rigid straight edge does not backscatter when the wave impinges parallel to the plane of the straight edge so that $\varphi_o = 0$. The resultant solution would, therefore, break down for $\varphi_o = 0$ if $\sigma(\alpha)$ were the integrand for the rigid wedge. If we enter Eq.(5.7)into the two boundary equations above, we obtain two equations of the form of Eq.(5.6)for the function $\psi(\alpha)$, $S(\alpha)$ being replaced by $\psi(\alpha)$. The $\sigma(\alpha)$ part cancels out left and right because $\sigma(\alpha)$ satisfies the conditions (3.2) for a pressure release wedge. To solve equation (5.6), we take the logarithm left and right and differentiate. Because the logarithm of (-1) is $j\pi$, and its derivative is zero, we obtain:

$$\frac{\cos\alpha}{\sin\alpha + \sin\vartheta_+} + \frac{\psi'(\alpha+\Phi)}{\psi(\alpha+\Phi)} = \frac{\cos\alpha}{\sin\alpha - \sin\vartheta_+} - \frac{\psi'(-\alpha+\Phi}{\psi(-\alpha+\Phi)} \tag{5.8}$$

A similar equation results with ϑ_+ replaced by ϑ_- and Φ replaced by $-\Phi$. Next we introduce the new function:

$$\frac{\psi'(\alpha+\Phi)}{\psi(\alpha+\Phi)} = f(\alpha+\Phi) \tag{5.9}$$

The Malyuzhinets transform of $f(\alpha+\Phi)$ and $f(-\alpha+\Phi)$ then are given by (Eq. 4.3 and 4.4):

$$\begin{aligned} Mf(\alpha+\Phi) &= e^{-jw\Phi} F(w) \\ Mf(-\alpha+\Phi) &= e^{jw\Phi} F(-w) \end{aligned} \tag{5.10}$$

where $mf(\alpha) = F(w)$ is the Malyuzhinets transform of $f(\alpha)$ and the letter M means symbolically Malyuzhinets transform of $f(\alpha)$. Let

$$g(\alpha) = \frac{\cos\alpha}{\sin\alpha + \sin\vartheta} - \frac{\cos\alpha}{\sin\alpha - \sin\vartheta} = -\frac{2\sin\vartheta\cos\alpha}{\sin^2\alpha - \sin^2\vartheta} = \frac{4\sin\vartheta\cos\alpha}{\cos 2\alpha - \cos 2\vartheta}$$

$$= \frac{2\sin\vartheta\cos\alpha}{-\sin(\alpha+\vartheta)\sin(\alpha-\vartheta)} = \frac{1}{\sin(\alpha+\vartheta)} - \frac{1}{\sin(\alpha-\vartheta)} \qquad (5.11)$$

where ϑ is the grazing Brewster angle and θ the Brewster angle with respect to the normal to the surface. We have omitted the bars above the symbols ϑ and θ that mark them as complex quantities. The transformed equations (5.8) then are

$$g_+(w) + e^{-jw\Phi} F(w) + e^{jw\Phi} F(-w) = 0$$

$$g_-(w) + e^{jw\Phi} F(w) + e^{-jw\Phi} F(-w) = 0 \qquad (5.12)$$

where $g_+(w)$, $g_-(w)$ represent $g(w) = Mg(\alpha)$ with ϑ replaced by ϑ_+, ϑ_- respectively. Elimination of $F(-w)$ leads to:

$$F(w) = \frac{g_+(w)\, e^{-jw\Phi} - g_-(w)\, e^{jw\Phi}}{2j \sin 2w\Phi} \qquad (5.13)$$

Because $g(-j\infty)$ and $g(+j\infty)$ are zero, the inverse transform of the first term of Eq. (5.13) then is represented by

$$f(z) = \frac{-1}{4\pi} \int_{-j\infty}^{j\infty} d\alpha \left\{ \int_{-\varepsilon-j\infty}^{-\varepsilon+j\infty} + \int_{\varepsilon-j\infty}^{\varepsilon+j\infty} \right\} \left(\frac{1}{\sin(\alpha+\vartheta)} - \frac{1}{\sin(\alpha-\vartheta)} \right) \frac{e^{jw(\alpha-z-\Phi)}}{2j \sin(2\Phi w)} dw \qquad (5.14)$$

where we have written ϑ for ϑ_+. In the second integral we replace w by $-w$. The two paths then coincide, and the two contour integrals can be combined:

$$f(z) = \frac{-1}{4\pi} \int_{-j\infty}^{j\infty} \int_{-j\infty}^{j\infty} d\alpha \left[\frac{1}{\sin(\alpha + \vartheta)} - \frac{1}{\sin(\alpha - \vartheta)}\right] \frac{\sin w(\alpha - z - \Phi)}{\sin (2\Phi w)} dw \qquad (5.15)$$

Next we replace $\alpha + \vartheta$ by $\alpha + \vartheta - \frac{\pi}{2} = \alpha'$ $[\alpha = \alpha' + (\frac{\pi}{2} - \vartheta)$, in the first factor, and $\alpha - \vartheta$ by $\alpha - \vartheta + \frac{\pi}{2} = \alpha''$, $[\alpha = \alpha'' - (\frac{\pi}{2} - \vartheta)]$ in the second factor.

$$f(z) = -\frac{1}{4\pi} \int_{-j\infty}^{j\infty} \int_{-j\infty}^{j\infty} \frac{d\alpha'}{\cos \alpha'} \sin w[\alpha' - (z + \Phi + \vartheta - \tfrac{\pi}{2})] \frac{dw}{\sin 2\Phi w}$$

$$- \frac{1}{4\pi} \int_{-j\infty}^{j\infty} \int_{-j\infty}^{j\infty} \frac{d\alpha''}{\cos \alpha''} \sin w[\alpha'' - (z + \Phi - \vartheta + \tfrac{\pi}{2})] \frac{dw}{\sin 2\Phi w} \qquad (5.16)$$

Since there is no pole at $-\pi/2 > \alpha < \pi/2$, we were allowed to discard the real parts of the limits of integration. We can perform the w integration first. The following integral is of a tabulated form:

$$\int_{-j\infty}^{j\infty} \frac{\sin wa}{\sin wb} dw = 2j \int_{0}^{\infty} \frac{\sinh va}{\sin hvb} dv = j \frac{\pi}{b} \tan \frac{\pi}{2b} a \qquad (5.17)$$

Performing the w integration in the first integral Eq. (5.16) we obtain:

$$f_1(z) = -\frac{j}{8\Gamma} \int_{-j\infty}^{j\infty} \tan[\frac{\alpha - (z+\Phi+\vartheta - \pi/2)\pi}{4\Phi}] \frac{1}{\cos \alpha} d\alpha = \frac{j}{8\Phi} \int_{-j\infty}^{j\infty} \frac{\tan \nu \frac{\pi}{4\Phi}}{\cos (\nu - \mu)} d\nu \qquad (5.18)$$

where

$$\alpha - (z + \Phi + \vartheta - \frac{\pi}{2}) = - \nu$$

$$\alpha = - \nu + \mu$$

$$\mu = z + \Phi + \vartheta - \frac{\pi}{2} \tag{5.19}$$

The w integration in the second integral leads to a function $f_2(z)$ which differs only in that $\vartheta - \pi/2$ is replaced by $-(\vartheta - \pi/2)$. Two more such functions then would result for $(\Phi \rightarrow -\Phi)$, the face $\varphi = -\Phi$, which are similar in form except that $\vartheta \rightarrow \vartheta_-$.

Four integrals are of different form, they are obtained if we perform the α integration first. In this case it is expedient to combine the two integrals, Eq. (5.16) and to write $Z = z + \Phi$:

$$f(z) = - \frac{1}{4\pi} \int_{-j\infty}^{j\infty} \int_{-j\infty}^{j\infty} \frac{d\alpha}{\cos \alpha} \left[\frac{\sin w(\alpha - Z - \theta) + \sin w (\alpha - Z + \theta)}{\sin 2\Phi w} \right] dw$$

$$= - \frac{1}{2\pi} \int_{-j\infty}^{j\infty} \int_{-j\infty}^{j\infty} \frac{\sin w(\alpha - Z) \cos w\theta \, dw}{\cos \alpha \sin 2\Phi w}$$

$$= - \frac{1}{2\pi} \int_{-j\infty}^{j\infty} \int_{-j\infty}^{j\infty} \frac{(\sin w\alpha \cos w Z - \cos w\alpha \sin wZ) \cos w\theta \, dw \, d\alpha}{\cos \alpha \sin 2\Phi w}$$

$$= - \frac{1}{2\pi} \int_{-j\infty}^{j\infty} \int_{-j\infty}^{j\infty} \frac{\cos w\alpha \sin wZ \cos w\theta}{\cos \alpha \sin 2\Phi w} \, d\alpha dw \tag{5.20}$$

because only the even part of the α integral contributes to the integral. The α integration is of a tabulated form:

$$\int_{-j\infty}^{j\infty} \frac{\cos w\alpha}{\cos \alpha} \, d\alpha = 2j \int_0^{\infty} \frac{\cosh wu}{\cosh u} \, du = \frac{\pi j}{\cos \frac{w\pi}{2}} \tag{5.21}$$

and

$$f(z) = +\frac{j}{2}\int_{-j\infty}^{j\infty} \frac{\sin wZ \cos w\theta}{\cos w\frac{\pi}{2} \sin 2\Phi w}\, dw = -\int_{o}^{\infty} \frac{\sinh sZ \cosh s\theta}{\cosh s\frac{\pi}{2} \sinh 2\Phi s}\, ds \qquad (5.21)$$

$$= -\frac{1}{2}\int_{o}^{\infty} \frac{\sinh s(Z+\theta)}{\cosh (s\frac{\pi}{2}) \sinh 2\Phi s}\, ds - \frac{1}{2}\int_{o}^{\infty} \frac{\sinh s(Z-\theta)s}{\cosh (s\frac{\pi}{2}) \sinh 2\Phi s}\, ds \qquad (5.22)$$

$$= f(z_1') + f(z_2')$$

where

$$z_1' = Z + \theta = z + \Phi + \frac{\pi}{2} - \vartheta$$

$$z_2' = Z - \theta = z + \Phi - (\frac{\pi}{2} - \vartheta) \qquad (5.23)$$

and

$$f(z) = -\frac{1}{2}\int_{o}^{\infty} \frac{\sinh zsds}{\cosh s\frac{\pi}{2} \sin 2\Phi s} \qquad (5.24)$$

Again, two more terms result for the contributions of the face $\varphi = -\Phi$, which are similar in form except that Φ is replaced by $-\Phi$, and ϑ denotes ϑ_-. The logarithmic derivative of the solution thus consists of the sum of four terms

$$\frac{d \log \psi(z)}{dz} = \frac{\psi'(z)}{\psi(z)} = f(z + \Phi + \overline{\vartheta}_+) + f(z + \Phi - \overline{\vartheta}_+) + f(z - \Phi + \overline{\vartheta}_-) + f(z - \Phi - \overline{\vartheta}_-) \quad . \qquad (5.25)$$

We still have to integrate each term up to the desired value of z . We assume arbitrarily z' = 0 for the lower limit of integration. This procedure is admissible because the resultant solution is represented by $\psi(\alpha)/\psi(\varphi_o)$ so that the integration constants, which lead to identical factors in $\psi(\alpha)$ and $\psi(\varphi_o)$ cancel out in the final expressions. We thus have

$$\psi_\Phi(z'_\nu) = \exp\left\{\int_0^{z'_\nu} f(z'_\nu)dz\right\} \tag{5.26}$$

where

$$z'_1 = z + \Phi + \overline{\theta}_+, \quad z'_3 = z - \Phi + \overline{\theta}_- ,$$

$$z'_2 = z + \Phi - \overline{\theta}_+, \quad z'_4 = z - \Phi - \overline{\theta}_- ,$$

and

$$\psi(z) = \psi_\Phi(z'_1)\psi_\Phi(z'_2) \cdot \psi_\Phi(z'_3) \cdot \psi_\Phi(z'_4) \tag{5.27}$$

because of the exponential nature of the solution; the exponents add, the functions multiply. We may still write the arguments in full:

$$\psi(\alpha) = \psi_\Phi(\alpha + \Phi + \tfrac{\pi}{2} - \vartheta_+)\ \psi_\Phi(\alpha + \Phi - \tfrac{\pi}{2} + \vartheta_+)\ \psi_\Phi(\alpha - \Phi + \tfrac{\pi}{2} - \vartheta_-)\ \psi_\Phi(\alpha - \Phi - \tfrac{\pi}{2} + \vartheta_-)$$

$$= \psi_\Phi(\alpha + \Phi + \theta_+)\ \psi_\Phi(\alpha + \Phi - \theta_+)\ \psi_\Phi(\alpha - \Phi + \theta_-)\ \psi_\Phi(\alpha - \Phi - \theta_-) \tag{5.28}$$

The solution of the diffraction problem then is given by

$$P(r,\varphi,k) = \frac{1}{2\pi i}\int_\Gamma e^{-ikr\cos(\alpha - \varphi)}S(\alpha)d\alpha \tag{5.29}$$

where

$$S(\alpha) = \sigma(\alpha)\,\frac{\psi(\alpha)}{\psi(\varphi_o)}$$

$$\sigma(\alpha) = \frac{\pi}{2\Phi} \frac{\cos \frac{\pi\varphi_o}{2\Phi}}{\sin \frac{\pi\alpha}{2\Phi} - \sin \frac{\pi\varphi_o}{2\Phi}} = \left[\cot \frac{\pi}{4\Phi}(\alpha - \varphi_o) + \tan \frac{\pi(\alpha + \varphi_o)}{4\Phi}\right] \frac{\pi}{4\Phi} \qquad (5.30)$$

The exact solution is given by

$$p(r,\varphi) = \frac{1}{4\Phi i} \int_\Gamma e^{-jkr \cos \alpha} \frac{\psi(\alpha + \varphi)}{\psi(\varphi_o)} \cos \frac{\pi\varphi_o}{2\Phi} \left(\sin \frac{\pi(\alpha + \varphi)}{2\Phi} - \sin \frac{\pi\varphi_o}{2\Phi}\right)^{-1} d\alpha \quad , \qquad (5.31)$$

If, assuming $kr > 0$, we deform the integration contour Γ into two paths of steepest descent through the saddle points $\alpha = \pm \pi$.

$$p(r,\varphi) = \frac{-\pi}{2\Phi} \frac{e^{j(kr + \pi/4)}}{\sqrt{2\pi kr}} \left[M_1 \cdot \frac{\psi(\varphi - \pi)}{\psi(\varphi_o)} + M_2 \frac{\psi(\varphi + \pi)}{\psi(\varphi_o)}\right] \qquad (5.32)$$

where M_1 and M_2 are the Malyuzhinets angle factors

$$M_1 = \frac{-\cos \frac{\pi\varphi_o}{2\Phi}}{\sin \frac{\pi(\varphi - \pi)}{2\Phi} - \sin \frac{\pi\varphi_o}{2\Phi}} \qquad (5.33)$$

$$M_2 = \frac{\cos \frac{\pi\varphi_o}{2\Phi}}{\sin \frac{\pi(\varphi + \pi)}{2\Phi} - \sin \frac{\pi\varphi_o}{2\Phi}} \qquad (5.34)$$

VI. THE MALYUZHINETS $\psi_\Phi(\alpha)$ FUNCTIONS AND THEIR APPROXIMATION

The Malyuzhinets function $\psi(\alpha)$ is the solution, Eq. (5.6) without poles or zeroes in the strip $\mathrm{Re}|\alpha| < \Phi$. They are usually computed by developing the integral solution into a series up to the pole of the integrand, or by evaluating the integral directly on the computer. Beyond the pole of the integrand, the integral no longer represents the solution of the problem, and one of the extension formulae (see Appendix A) must be used to determine the functions for greater values of the agreement. Figure (6.1) shows $\psi_\Phi(z)$ for real $z = \alpha + \Phi + \theta_+$ as a function of z; Fig. (6.2) represents the same function $\psi_{0.7\pi}(z)$ and Fig. (6.3) the phase angle for complex argument as a function of the real part x_r with the imaginary part x_i of z[Jm(z) as parameter].

The ψ_Φ functions are relatively insensitive to the argument α except for argument values near their zeroes and their poles. A small imaginary part in the surface admittance increases the magnitude at the zero to a finite small value, and reduces the magnitude at the pole to a finite value; the effect on the resulting function is practically negligible if $\mathrm{Im}\ \rho c/\overline{z} \leq \frac{1}{2}$ (see Fig. 6.2). The surface then acts as if its impedance were real. If the imaginary part of the relative surface admittance $\rho c/\overline{z}$ exceeds 1, the curves become almost horizontal and the wedge acts as if it were pressure release. Because of this relatively small sensitivity of the diffraction field on the impedance on the surface, we can expect that the results also apply to boundaries that cannot be described by point impedances, such as plate boundaries.

Computations with the Malyuzhinets functions are greatly simplified by the relations that exist between them, and which are summerized in

appendix A. Furthermore, there is no need to evaluate the defining integrals. Since the Malyuzhinets functions are smooth functions, they can be approximated to a high degree of accuracy by an expression of the type

$$\psi_\Phi(\alpha) = \frac{\cos\left(\frac{\pi}{2}\frac{\alpha}{\alpha_{zero}}\right) \cdot \cos\frac{\alpha}{\beta(\Phi)}}{\cos\left(\frac{\pi}{2}\frac{\alpha}{\alpha_{pole}}\right)} \tag{6.1}$$

where α_{zero} and α_{pole} are given by Eq. (A22). This function reproduces the exact slope and magnitude of $\psi(\alpha)$ for $\alpha = 0$, and is zero at α_{zero} and infinite at the pole at α_{pole}; the second cosine factor in the numerator then is used to improve the fit in the pole region. We find the following values for $\beta(\Phi)$:

Φ	0.3π	$1/3\pi$	0.4π	$3/8\pi$	0.5π	0.7π	0.9π	π
$\beta(\Phi)$	4.63	5.04	5.87	5.56	6.98	8.6	9.72	10.49

These functions approximate $\psi_\Phi(\alpha)$ in the whole range, also beyond the pole and in the complex domain. Fig. (6.4) and (6.5) show the functions $\psi_\pi(0)$ and $\psi_{\pi/2}(\theta)$ as computed by Eq. (6.1). The exact values have been computed by Zavadskii and Sakharova which fall on the two curves.

VII. THE ANGLE FACTORS OF THE MALYUZHINETS SOLUTION

The angle factor in the Malyuzhinets integrand results by adding the two angle factors that occur in the Sommerfeld integrand for the pressure release wedge (see Eq. 3.10). The Malyuzhinets stationary phase solution then contains the angle factors

$$M_1 = \frac{-\cos\frac{\pi}{2\Phi}\varphi_o}{\sin\frac{\pi}{2\Phi}(\varphi - \pi) - \sin\frac{\pi}{2\Phi}\varphi_o}$$

and

$$M_2 = \frac{\cos\frac{\pi}{2\Phi}\varphi_o}{\sin\frac{\pi}{2\Phi}(\varphi + \pi) - \sin\frac{\pi}{2\Phi}\varphi_o} \tag{7.1}$$

We shall assume φ_o is positive. For negative φ_o, the two angle factors simply interchange. The angle factor is plotted in Fig. (7.1) for a straight edge and in Fig. (7.2) for various wedges with the angle of incident as parameter. If $\Phi \geq \pi/2$, M_1 has no poles in physical space $-\Phi \leq \varphi < \Phi$ because the first term in the denominator then is always negative. M_1 increases towards the limits $\varphi = \pm\Phi$ of the physical space without reaching a maximum (where the slope is horizontal). The two greatest values of M_1 then are given by

$$(M_1)_{\pm\Phi} = \frac{-\cos\frac{\pi}{2\Phi}\varphi_o}{\pm\cos\frac{\pi}{2\Phi}\pi - \sin\frac{\pi}{2\Phi}\varphi_o} \tag{7.2}$$

M_1 then has a minimum for $(\varphi - \pi)\pi/2\Phi = -\pi/2$ or $\varphi = \pi - \Phi$ when the diffracted ray propagates along the continuation of the face $\varphi = -\Phi$ of the wedge,

$$M_{1\ \min} = \frac{\cos \frac{\pi}{2\Phi} \varphi_o}{1 + \sin \frac{\pi}{2\Phi} \varphi_o} \leq \cos \frac{\pi}{2\Phi} \varphi_o \tag{7.3}$$

and then increases constantly towards the faces $\varphi = \pm \Phi$ of the wedge to the value

$$(M_1)_{\substack{\pm \Phi \\ \max}} = \frac{- \cos \frac{\pi}{2\Phi} \varphi_o}{\pm \cos \frac{\pi}{2\Phi} \pi - \sin \frac{\pi}{2\Phi} \varphi_o} \tag{7.4}$$

The second angle factor

$$M_2 = \frac{\cos \frac{\pi}{2\Phi} \varphi_o}{\sin \frac{\pi}{2\Phi} (\varphi + \pi) - \sin \frac{\pi}{2\Phi} \varphi_o} \tag{7.5}$$

has two poles, one at the shadow boundary of the reflected wave ($\varphi = 2\Phi - \pi - \varphi_o$) and one at the shadow boundary of the incident wave ($\varphi = -\pi + \varphi_o$). It has a true minimum between the two shadow boundaries for $\varphi = \Phi - \pi$:

$$(M_2)_{min} = \frac{\cos \frac{\varphi_o}{2\Phi} \varphi_o}{1 - \sin \frac{\pi}{2\Phi} \varphi_o} \tag{7.6}$$

and it decreases from the shadow boundaries towards the wedge at $\varphi = \pm \Phi$ to the same values as those given by Eq. (7.2) for M_1 at $\pm \Phi$.

If φ_o is negative and φ is replaced by $-\varphi$, M_1 changes into M_2 and M_2 into M_1. Fig. (7.1a) shows the basic shape of the curves $M_1(\Phi)$ and $M_2(\Phi)$ and the angular ranges in which each term is positive and negative. Figure (7.1d) to g show for comparison also the Sommerfeld and the Kirchhoff solutions for the rigid and the pressure release straight edge. We find that M_2 is not very different from the Kirchhoff or Sommerfeld solution for the pressure release straight edge. Figures (7.3) and (7.4) represent the angle factors for backscatter when $\varphi = \varphi_o$ as rectangular and polar plots. M_2 and M_1 turn out to be the exact mirror images of each other at the axis $\varphi = 0$. We can confine our attention to the space $0 \leq \varphi_o < \Phi$, because when looking at the backscattered field we can always assume we are in front of the plate ($\varphi_o > 0$). The maximum of the angle function M_2 then represents the diffraction at the shadow boundary of the reflected wave when it is coincident with the incident wave, i.e. when it impinges normal to a wedge surface. This is the case when the transducer is just at the shadow boundary of the geometrically reflected wave. In practical situations, the transducer will be within the cone of the reflected waves or it will be outside. Inside, diffraction does not contribute much to backscatter. Outside of it, the received signal is exclusively due to diffraction. The amplitude of the received signal then decreases greatly with the angular distance from the shadow boundary.

For pressure release surfaces:

$$\rho c/\bar{z} = \cos \vartheta = \cos (\vartheta_r + j\vartheta_i) = \cos \vartheta_r \cosh \vartheta_i - j \sin \vartheta_r \sin \vartheta_i \rightarrow \infty \qquad (7.7)$$

Because the real part of the impedance must be positive, $\vartheta_r \leq \frac{\pi}{2}$, we must have

$$\vartheta_i = \pm \infty$$

But as $\alpha_i \rightarrow \infty$, $\psi_\Phi(\alpha_r + j\alpha_i) \longrightarrow \psi_\Phi(j\alpha_i) \rightarrow \infty$ (see Fig. 6.2) and the ψ_Φ functions in the numerator and denominator cancel. Thus the multiplier $\psi(\alpha + \varphi)/\psi(\varphi_o) \rightarrow 1$

and the solution is given by

$$p = \frac{-\pi}{2\Phi} \frac{e^{j(kr + \frac{\pi}{4})}}{\sqrt{2\pi kr}} (M_1 + M_2) \tag{7.8}$$

The two angle factors then simply add up, and the resultant expression reduces to the classical solution for a pressure release wedge.

For a rigid wedge $\theta_+ = \theta_- = 0$, and by Eq. All

$$\psi(\alpha) = \psi_\Phi (\frac{\pi}{2})^4 \left[\cos \frac{\pi}{4\Phi} (\alpha + \Phi) \cos \frac{\pi}{4\Phi} (\alpha - \Phi)\right]$$

$$= \frac{1}{2} \psi_\Phi (\frac{\pi}{2})^4 \left[\cos \frac{\pi}{2\Phi} \alpha + \cos \frac{\pi}{2\Phi} \Phi\right] = \frac{1}{2} \psi_\Phi (\frac{\pi}{2})^4 \cos \frac{\pi}{2\Phi} \alpha \tag{7.9}$$

and

$$\frac{\psi(\alpha)}{\psi(\varphi_o)} = \frac{\cos \frac{\pi}{2\Phi} \alpha}{\cos \frac{\pi}{2\Phi} \varphi_o} \tag{7.10}$$

For a straight edge, the functions $\psi(\varphi - \pi)$ and $\psi(\varphi + \pi)$ then become proportional to sin $\varphi/2$ and to - sin $\varphi/2$, and the two terms in the Malyuzhinets solution counteract each other in the angular range $\varphi > 0$.

Thus, the solution for the rigid straight edge becomes

$$p = \frac{-\pi}{2\Phi} \frac{e^{-(jkr + \frac{\pi}{4})}}{\sqrt{2\pi kr}} \left[\frac{\sin \varphi/2 \; M_1}{\cos \varphi_o/2} - \frac{\sin \varphi/2 \; M_2}{\cos \varphi_o/2}\right] \tag{7.11}$$

Comparison with the corresponding Sommerfeld solution gives the Sommerfeld factors in terms of M_1 and M_2, (see Appendix B). The converse procedure, i.e. the expressing of the factor M_1 and M_2 in terms of the Sommerfeld

factors leads to very complex expressions that contain also the angle functions of $(\pi/2\Phi)(\alpha)$ and of $\pi^2/2\Phi$.

For an impedance matched wedge:

$$\sin \vartheta_{\pm} = 1 , \quad \vartheta_{\pm} = \pi/2 , \quad \theta_{\pm} = 0 \tag{7.12}$$

and by Eq. A13

$$\psi(\alpha) = \psi_{\Phi}(\Phi)^4 \; \psi^2_{\Phi/2}(\alpha) \tag{7.13}$$

The ψ function then is proportional to the square of the $\psi_{\Phi/2}(\alpha)$ function that is plotted in Fig. 5.1a. For a straight edge, $2\Phi/2 = \pi$ and the zero of this function occurs for $\alpha = (3/2)\pi$, and that of the solution for $\varphi + \pi = (3/2)\pi$, $\varphi = \pi/2$; i.e., there is no field reflected or diffracted normal to the surface of the straight edge.

VIII. THE MALYUZHINETS FUNCTION AND THE CLASSICAL REFLECTION FACTOR AND THE EXIT FACTOR

The second term in the Malyuzhinets stationary phase solution (Eq. 5.32) is closely related to the classical reflexion factor. If φ_o is the angle of incidence with respect to the plane of symmetry of the wedge, the angle φ_{No} of the incident wave with the normal of the wedge surface($\varphi = \Phi - \pi/2$) is given by (see Fig. 8.1):

$$\varphi_{No} = \Phi - \pi/2 - \varphi_o \tag{8.1}$$

and the angle of the reflected wave with the $\varphi = 0$ axis by

$$\varphi_R = \Phi - \pi/2 + \varphi_{No} = 2\Phi - \pi - \varphi_o \tag{8.2}$$

For this angle, the angle factor M_2 (Eq. 5.34), in the Malyuzhinets solution Eq. (5.32) has a pole which determines the field at the shadow boundary. To evaluate the solution for the shadow boundary, the integral (5.31) is written in the form

$$p = \int_\Gamma \frac{h(z)}{z - z_o}\, e^{rg(z)}dz \tag{8.3}$$

The stationary phase solution then, when z_o coincides with the stationary phase point, is given by

$$p = j\pi\, h(z_o)\, e^{rg(z_o)} \tag{8.4}$$

(see Jones, The Theory of Electromagnetism, Pergamon Press 1964, New York, p. 690). Thus we find from (5.31) for the contribution of the saddle point $Re(z) = +\pi$:

$$p(r,\varphi) = j\pi \frac{1}{4\Phi j} \frac{e^{jkr}}{\psi(\varphi_o)} \frac{\psi(\pi + \varphi)}{\frac{\pi}{2\Phi} \cos \frac{\pi}{2\Phi} (\pi + \varphi)} \frac{\cos(\pi\varphi_o/2\Phi)}{\Big|_{\varphi_R}} \tag{8.5}$$

$$= 1/2 \quad e^{jkr} \quad \frac{\psi(2\Phi - \varphi_o)}{\psi(\varphi_o)}$$

It is shown in the classical theory of diffraction* that this term should be equal to half the amplitude of and of opposite signs as that of the reflected wave.

Thus, we are justified to interpret the ratio

$$\frac{-\psi(2\Phi - \varphi_o)}{\psi(\varphi_o)} = R(\varphi_o) \tag{8.6}$$

as the reflection factor of the wedge surface for a wave incident under an angle $(\Phi - \varphi_o)$ with respect to the plane of the reflecting surface. To prove this conclusion, let us assume for reasons of simplicity that both wedge surfaces are covered with the same material so that $\overline{\theta}_+ = \overline{\theta}_- = \overline{\theta}$. We then have (see Eqs. 5.28 and A13):

$$\frac{\psi(\alpha)}{\psi(\varphi_o)} = \frac{\psi_{\Phi/2}(\alpha + \overline{\theta})\ \psi_{\Phi/2}(\alpha - \overline{\theta})}{\psi_{\Phi/2}(\varphi_o + \overline{\theta})\ \psi_{\Phi/2}(\varphi_o - \overline{\theta})} \tag{8.7}$$

and using Equation A15:

---

*Skudrzyk: Foundations of Acoustics, page 570-571, Springer Verlag, New York and Vienna, 1972.

$$\frac{\psi(2\Phi - \varphi_o)}{\psi(\varphi_o)} = \frac{\psi_{\Phi/2}(2\Phi - \varphi_o + \overline{\theta})\ \psi_{\Phi/2}(2\Phi - \varphi_o - \overline{\theta})}{\psi_{\Phi/2}(-\varphi_o + \overline{\theta})\ \psi_{\Phi/2}(-\varphi_o - \overline{\theta})}$$

$$= \cot\ 1/2(-\varphi_o + \overline{\theta} + \pi/2 + \Phi)\ \cot\ 1/2(-\varphi_o - \overline{\theta} + \pi/2 + \Phi)$$

$$= \frac{\cos\theta - \sin(-\varphi_o + \Phi)}{\cos\theta + \sin(-\varphi_o + \Phi)} = -R(\varphi_o) \qquad (8.8)$$

But $\Phi - \varphi_o$ is the grazing angle of the incident wave with the reflecting surface of the wedge. If we replaced $\Phi - \varphi_o$ by the angle with respect to the normal of the surface, the sine would be replaced by the cosine of that angle. Thus, $R(\varphi_o)$ is identical with the classical reflection factor of the impedance covered infinite surface. This classical reflection factor, therefore, describes the effect of diffraction at the shadow boundary.

The impedance covers of the wedge surfaces modify the diffraction phenomenon. This modification, relative to the diffraction of a pressure release wedge, is described by the functions

$$\frac{\psi(\varphi + \pi)}{\psi(\varphi_o)} \quad \text{and} \quad \frac{\psi(\varphi - \pi)}{\psi(\varphi_o)} \qquad (8.9)$$

Because $\psi(\varphi_o)$ is a function that varies very little with the angle of incidence, the above two functions are practically independent of the angle of incidence.* This conclusion is the most remarkable result derived from the exact theory. It is the angle φ of exit of the diffracted rays that determines the influence of the impedance, regardless of the angle of the incident radiation (see Fig. 8.2).

*The factor $\cos \pi\varphi_o/2\Phi$ occurs also in the classical theory if the field is formulated in the Malyuzhinets form.

For an arbitrary exit angle φ, we express the angle of exit by what would be the angle φ_o' of incidence for φ as an angle of exit in the second term in the solution; i.e. $\varphi = 2\Phi - \pi - \varphi_o$. The second term of the solution then takes the form

$$\frac{\psi(\varphi + \pi)}{\psi(\varphi_o)} = \frac{\psi(2\Phi - \varphi_o')}{\psi(\varphi_o')} \frac{\psi(\varphi_o')}{\psi(\varphi_o)} = R(\varphi_o') \left[\frac{\psi(\varphi_o')}{\psi(\varphi_o)} \right] \tag{8.10}$$

It is proportional to the factor $R(\varphi_o')$ which we shall define as the exit factor. The factor in the rectangular bracket is very nearly unity as long as the angle of incidence φ_o and the angle of incidence φ_o' (if the diffracted ray were a reflected ray) are somewhat different from $\pm \Phi$.

Figures 8.3 show a comparison of the classical exit factor $R(\varphi_o')$ with the Malyuzhinets function $\psi(\varphi + \pi)$. If we divided $\psi(\varphi + \pi)$ by $\psi(\varphi_o)$ it becomes exactly equal to $R(\varphi_o')$. If we move the Malyuzhinets curve up or down in the logarithmic plot, the two curves coincide for $\varphi = \varphi_o'$, and then the difference between the two curves will give us the error that results if we replace $\psi(\varphi + \pi)/\psi(\varphi_o')$ by $R(\varphi_o')$. The curves prove that this error is practically negligible everywhere except in the region near $\varphi = 0$. We thus obtain a very good approximation to the second term by replacing

$$M_2 \psi(\varphi + \pi)/\psi(\varphi_o) \rightarrow M_2 R(\varphi_o')$$

in the range $\varphi > 0$, $\varphi_o > 0$. The impedance cover reduces the diffracted ray by the exact factor which is the same as the reflection factor for a plane wave that makes the same angle with the impedance surface of the wedge as the exit angle φ .

For negative φ, $\psi(-|\varphi| + \pi)/\psi(\varphi_o) = \psi(|\varphi| - \pi)/\psi(-\varphi_o)$ is no longer equivalent to the reflection factor, but is similar to the first factor $\psi(\varphi - \pi)$ for positive φ. At the shadow boundary of the incident wave, $\varphi = -(\pi - \varphi_o)$, $\varphi + \pi = \varphi_o$ and $\psi(\varphi + \pi)/\psi(\varphi_o) = \psi(\varphi_o)/\psi(\varphi_o)$ becomes equal to unity. The first factor

$$\frac{\psi(-|\varphi| - \pi)}{\psi(\varphi_o)} = R_-(\varphi_o') \frac{\psi(\varphi_o')}{\psi(\varphi_o)} \tag{8.11}$$

where $R_-(\varphi_o')$ is the exit factor for the second surface ($\vartheta = \vartheta_-$), then represents the reflection from the second surface.

It is convenient to call the factor M_2 the shadow boundary factor. It reduces to $R(\varphi_o)$ at the shadow boundary of the reflected wave, and to unity at the shadow boundary of the incident wave.

IX. ZEROES AND POLES OF THE ψ_Φ FUNCTIONS AND THE VARIATION OF THE ψ FACTORS IN THE MALYUZHINETS SOLUTION

The properties of the wedge surface are represented by the ψ_Φ functions. The zeroes and poles of the ψ_Φ functions follow from the mathematical derivation. They can, however, be derived directly on the basis of the physics of the problem. Since the Brewster angle adds additively to the argument of the ψ_Φ functions, we can assume the simplest possible situation, e.g. matching for normal incidence for the front surface impedance ($\theta_+ = 0$, $\varphi_o = \Phi - \pi/2$), and pressure release behavior for the rear surface. The pressure release part then is very large and independent of φ and φ_o and cancels out in the ratio $\psi(\alpha)/\psi(\varphi_o)$. Thus we have

$$\frac{\psi(\alpha)}{\psi(\varphi_o)} \to \frac{\psi_\Phi(\alpha + \Phi)\psi_\Phi(\alpha - \Phi)}{\psi_\Phi(\varphi_o + \Phi)\psi_\Phi(\varphi_o - \Phi)} = \frac{-\psi_{\Phi/2}(\alpha)}{\psi_{\Phi/2}(\varphi_o)} \tag{9.1}$$

The reflected wave in the solution is proportional to $\psi(\pi + \varphi)$. Since reflection must vanish for normal incidence when $\varphi = \varphi_o = \Phi - \pi/2$, we must have

$$\psi_{\Phi/2}(\varphi + \pi)\Big|_{\varphi = \Phi - \pi/2} = \psi_{\Phi/2}[\pi + (\Phi - \pi/2)] = 0 \tag{9.2}$$

Hence the zeroes closest to $\alpha = 0$ of the functions $\psi_\Phi(\alpha)$ are given by

$$\pm \alpha_o = \pi/2 + 2\Phi \tag{9.3}$$

The wedge solution contains the factor $\cos(\pi\varphi_o/2\Phi)$, which vanishes for grazing incidence unless ψ part becomes infinite. For a rigid surface, $\theta_+ = \pi/2$, and the reflected wave never vanishes, not even at grazing incidence when $\varphi_o = -\Phi$ and $\varphi = \Phi$. Thus $(\pi + \Phi)$ must become infinite.

Thus we have with $\theta_+ = \pi/2$

$$\psi(\alpha) \rightarrow \psi_\Phi(\alpha + \Phi + \pi/2)\psi_\Phi(\alpha - \Phi - \pi/2) \quad , \tag{9.4}$$

hence at $\varphi = \Phi$

$$\psi(\Phi + \pi) \rightarrow \psi_\Phi(2\Phi + \frac{3\pi}{2})\ \psi_\Phi(\pi/2) \rightarrow \infty \tag{9.5}$$

and the poles must be given by

$$\pm\, \alpha_p = 2\Phi + 3\pi/2 \tag{9.6}$$

The ψ functions have poles and zeroes also for $|\alpha| > 3\pi/2 + 2\Phi$, i.e. outside the basic α - range. But these poles and zeroes are of interest only for the product and series developments of the ψ_Φ functions (see, for instance, Eq. A31).

The terms $\psi(\varphi - \pi)$ and $\psi(\varphi + \pi)$ of the stationary phase solution are made up of the product of four ψ_Φ functions. Each term is zero, when one of the arguments of the ψ_Φ functions reduces to $\alpha_o = \pm\,[2\Phi + \frac{\pi}{2}]$. The zeroes of the $\psi(\pi + \varphi)$ and $\psi(\pi - \varphi)$ terms of the Malyuzhinets solution then depend on the θ_+ and θ_- of the impedance of the wedge surfaces. Let us first consider the term $\psi(\pi + \varphi)$ which in the space $0 < \varphi < \Phi$ is similar to the reflection factor of the surface z_+. The argument of the factors

$$\psi_\Phi(\varphi + \pi + \Phi \pm \theta_+) = \psi_\Phi\,[(\varphi + \frac{\pi}{2} - \Phi \pm \theta_+) + (2\Phi + \frac{\pi}{2})] \tag{9.7}$$

reduce to $\alpha_o = 2\Phi + \pi/2$, and consequently vanishes, iff

$$\varphi = \Phi - \frac{\pi}{2} \pm \theta_+ = \begin{cases} \Phi - \vartheta_+ \\ \Phi - \pi + \vartheta_+ \end{cases} \tag{9.8}$$

i.e. when the exit angle is equal to one of the two Brewster angles θ_+ of an impedance covered infinite surface.

Similarly, the factors

$$\psi_\Phi(\varphi + \pi - \Phi \pm \theta_-) = \psi_\Phi[\varphi + \Phi + 3\pi/2 - (2\Phi + \pi/2) + \theta_-]$$

or

$$= \psi_\Phi[\varphi + \frac{\pi}{2} - 3\Phi + (2\Phi + \frac{\pi}{2}) + \theta_-]$$

or due to the 4Φ periodicity of ψ_Φ

$$= \psi_\Phi[\varphi + \frac{\pi}{2} + \Phi \pm \theta_- + (2\Phi + \frac{\pi}{2})] \tag{9.9}$$

vanishes iff

$$\varphi = -\Phi - 3\pi/2 \pm \theta_-$$

which is not in physical space, or if

$$\varphi = -\Phi - \pi/2 \pm \theta_- \leq -\Phi \tag{9.10}$$

The last value lies in physical space if $\mathrm{Re}(\theta_-) = \pi/2$, i.e. if the z_- surface is rigid and the wedge is degenerated to a semi-infinite plane.

The first term in the Malyuzhinets solution is proportional to $\psi(\varphi - \pi)$. The zero values are given by

$$\psi_\Phi(\varphi - \pi + \Phi \pm \theta_+) = \psi_\Phi[\varphi - \pi - \Phi + (2\Phi + \pi/2) - \pi/2 + \theta_+] \tag{9.11}$$

Thus, due to the 4Φ periodicity of ψ_Φ,

$$\varphi = 3\pi/2 + \Phi \pm \theta_+ - 4n\Phi$$

or

$$-\Phi < 3\Phi \pm \theta_+ - \frac{3\pi}{2} < \Phi$$

Thus zeroes in the first factor can occur only if $\Phi < 3\pi/4 + \theta_+/2$. It is convenient to consider the space $\varphi > 0$ only and to define for this space the factor that proportional to $\psi(\varphi + \pi)$ as the generalized shadow boundary (and reflection) factor, and the factor that is proportional to $\psi(\varphi - \pi)$ and which is usually much smaller than the scattering factor.

The term $\psi(\varphi - \pi)$ of the solution then is practically independent of the impedance covers of the wedge as long as $\varphi > 0$. We have

$$\psi(\varphi - \pi) = \psi_\Phi(\varphi - \pi + \Phi + \theta_+)\, \psi_\Phi(\varphi - \pi + \Phi - \theta_+)\, \psi_\Phi(\varphi - \pi - \Phi + \theta_-)$$

$$\psi_\Phi(\varphi - \pi - \Phi - \theta_-) \quad ; \tag{9.13}$$

all the factors have arguments that are within the limits

$$2\Phi + \theta_+ - \pi \approx \Phi + \theta_+ \tag{9.14}$$

and

$$- \pi - \Phi - \theta_- \approx - 2\Phi - \theta_- \tag{9.15}$$

Their product therefore is practically independent of θ_+, and depends on θ_- only as φ approaches zero. The term $\psi(\varphi + \pi)$ is taken as

$$\psi(\varphi + \pi) = \psi_\Phi(\varphi + \pi + \Phi + \theta_+)\, \psi_\Phi(\varphi + \pi + \Phi - \theta_+)$$

$$\cdot\, \psi_\Phi(\varphi - \pi - \Phi + \theta_-)\, \psi_\Phi(\varphi + \pi - \Phi - \theta_-) \tag{9.16}$$

The first two factors depend greatly on θ_+ because their zeroes are in the range of positive φ. The arguments of the third and fourth terms then are relatively small so that their product differs only little from unity. Thus for positive φ, $\psi(\varphi - \pi)$ is independent of θ_+ and depends on θ_- only in the neighborhood of $\varphi = 0$. In contrast, $\psi(\varphi + \pi)$ depends strongly on θ_+ and is practically independent of θ_-. For negative values of $\varphi = - |\varphi|$

$$\psi(\varphi + \pi) = \psi(-|\varphi| + \pi) = \psi(|\varphi| - \pi)$$

$$\psi(\varphi - \pi) = \psi(-|\varphi| - \pi) = \psi(|\varphi| + \pi) \qquad (9.17)$$

Changing the sign of φ interchanges the two terms of the solution, and the second term in the space $\varphi < 0$ becomes similar to the first term in the space $\varphi > 0$ except that θ_+ and θ_- are interchanged. But, we have, however to keep in mind that these two terms are not independent of each other and that strictly speaking, we cannot seperate the solution into reflection and scattering effects. Figure 9.1 shows the two ψ functions as a function of the scattering angle. These curves have been computed on the assumption that the two surfaces of the wedge have the same acoustic impedance. The functions $\psi_1 = \psi(\varphi - \pi)$ and $\psi_2 = \psi(\varphi + \pi)$ then are completely symmetric with respect to the angle $\varphi = 0$, i.e. $\psi(-\varphi - \pi) = \psi(\varphi + \pi)$, and $\psi(\varphi - \pi) = \psi(-\varphi + \pi)$. The term $M_2\psi_2$ is zero for the two Brewster angles of exit for $\varphi > 0$ and the scatter term $M_1\psi_1$ is zero for the Brewster angles of exit with respect to the second wedge surface $\varphi = -\Phi$ when $\varphi < 0$.

Figure (9.2)shows the ψ functions for a straight edge whose faces have different acoustic impedances. In Fig. 9.2a, the straight edge is matched to the medium for normal incidence. The shadow boundary factor $\psi(\varphi + \pi)$ then is very similar to that for a straight edge. The scattering factor is similar, too, on the side of the incident wave. In the half space opposite to that of the incident wave, the scattering factor is modulated by the exit factor of the impedance that faces the shadow space. Fig. (9.3) shows the same as some of the $\psi(\varphi + \pi)$ and $\psi(\varphi - \pi)$ functions as polar graphs.

X. THE EFFECT OF THE IMPEDANCE OF THE WEDGE SURFACES ON THE DIFFRACTION FIELD

(a) The Backscattered Field

The analysis of backscatter is simpler than that of diffraction since we restrict ourselves to the half space in front of the scatterer. The dominant term, also in the backscattered field, is the second term of the solution. It is obtained by multiplying the angle factor M_2 with the Malyuzhinetz function $\psi(\varphi + \pi)/\psi(\varphi_o)$. This function reduces to the reflection factor for normal incidence and, except for angles near $\varphi = 0$, approaches closely the exit factor of the reflecting surface. It is practically independent of the material on the other side of the straight edge. The backscattered $M_2\psi(\pi + \varphi_o)/\psi(\varphi_o)$ field is thus modulated by the exit factor of the wedge material; it vanishes for the two Brewster angles. But in addition to this field, there is the field described by the first term of the solution $M_1\psi(\varphi_o - \pi)$ [see Eq. (9.14) and Figs. 10.1 and 10.2). In contrast to the field $M_2\psi(\pi + \varphi_o)/\psi(\varphi_o)$, this field does not depend on the impedance of the illuminated side of the straight edge, and depends on the impedance of the face in the shadow side only for small angles φ_o. We would feel tempted to interpret the M_2 term as the field generated by the shadow boundary of the reflected wave, and the M_1 term as that due to the shadow boundary of the incident wave. However, this interpretation of the Malyuzhinets solution is not permissible.

For backscatter in the direction $\varphi = 0$, the two Malyuzhinets components always have the same sign and add up; this follows by considering the sign of the components $M_1\psi(\varphi - \pi)$ and $M_2\psi(\varphi + \pi)$ in Figs. 10.1 and 10.2. Thus there is always a maximum of backscatter for $\varphi_o = 0$ like in the case of the ideally pressure release straight edge or wedge (see Fig. 10.2). The width of this maximum decreases as the surface impedances increase for a close to rigid surface; all that is left is a needle shaped loop and for a rigid straight

edge, the width of this needle decreases to zero. The rigid edge does not backscatter for $\varphi_o = 0$. The term $M_2\psi(\varphi_o + \pi)$ has zeroes at the two Brewster angles and changes its sign between thin lines. The term $M_1\psi(\varphi_o - \pi)$ is always positive from $\varphi_o = 0$ up to the first Brewster angle. Both terms then are positive and the field is represented by their sum. Beyond the first Brewster angle up to 90°, the second term becomes negative and stays negative until φ reaches 90°. In this angular range, the two terms substract. At the first Brewster angle, the resultant field is finite. But above the first Brewster angle, the two terms eventually become equal in magnitude and the resultant field is zero. A computation based on the formulae given in Appendix A shows that this zero for a straight edge is given by $\cos\theta + \cos\varphi_o = 1$. In the example shown in Fig. 10.3, the zero in the Brewster angle is shifted by about 27 degrees towards the normal of the surface. At and above the second Brewster angle, both terms are again of the same sign and their sum decreases drastically towards grazing exit; the second Brewster angle therefore does not seem to generate another zero in the resultant solution.

(b) The Diffracted Field

In considering diffraction, we also have to consider the solution for negative values of φ. In the half space behind the diffracting plane, at the shadow boundary of the incident wave, the $\psi(\varphi + \pi)/\psi(\varphi_o)$ term then reduces to unity since the field near the shadow boundary of the incident wave is not influenced by the material of the reflector. Away from the shadow boundary towards the positive half space, this field shows a very slight dependence on θ_+. In contrast, the $M_1[\psi(\varphi - \pi)/\psi(\varphi_o)]$ term turns out to be modulated by the exit factor of the θ_- surface (see Fig. 9.1). Thus, the term which at first sight we would have expected to be generated by the shadow boundary of the reflected wave is modulated not with the

reflection factor of the reflecting surface, but with the exit factor of the surface in the shadow region. We are compelled to assume that this term is generated exclusively by the surface in the shadow space.

We thus arrive at the conclusion that the diffraction field of a rigid or pressure release diffractor can be basically attributed to the shadow boundaries. But the diffraction field of an impedance covered surface is no longer generated by the shadow boundaries alone, but is strongly modulated with the exit factors of the diffracting surfaces. It exhibits minima in the direction of the Brewster angles. Thus, the orinetation of the diffracting surface is a significant factor in the exact theory in addition to the location of the shadow boundaries.

XI. COMPARISON OF THE MALYUZHINETZ THEORY WITH THE KIRCHHOFF AND SOMMERFELD THEORY

In the calssical Kirchhoff theory of diffraction, the diffracting screens are black screens. The screens act as if they were the openings of infinitely long ducts. Any radiation that hits the screen disappears in it without the slightest reflection. Radiation that propagates grazing to a screen is neither attenuated nor diffracted into the screen; and radiation that has been diffracted once is no longer affected by the screen. The field at the aperture is assumed to be that of the incident wave and diffracted fields that propagate across the aperture are neglected in setting up the solution, as a consequence of these assumptions. The diffracted field spreads mostly in the direction of the incident wave, and there is no backscatter in this direction. This conclusion follows also directly from the classical Kirchhoff integral. This integral on the velocity potential U contains a source and a dipole term as follows:

$$U\partial \frac{e^{-jkr}/4\pi r}{\partial n} - \frac{e^{-jkr}}{4\pi r} \frac{\partial U}{\partial n} = -\frac{1}{\rho c}(\rho c j\, kU \cos\theta - \rho c v_n)\frac{e^{-jkr}}{4\pi r}$$

$$= -\frac{1}{\rho c}(p\cos\theta - \rho c v_n)\frac{e^{-jkr}}{4\pi r} \qquad (11.1)$$

where

$$p = \rho \frac{\partial U}{\partial z}, \quad v_n = \frac{-\partial U}{\partial n}, \qquad (11.2)$$

and the term proportional to $1/r$ has been neglected here. For a plane wave such as the field that is assumed in the aperture in the Kirchhoff theory, these two terms can be combined to a term of cardioid characteristics. Because for a plane wave $\rho c v_n = p$, the Kirchhoff integrand reduces to

$$- p (\cos \theta - 1) \frac{e^{-jkr}}{\rho c r} \tag{11.3}$$

Thus the radiation is zero in the backward direction ($\theta = 0$).

The diffraction field in the Kirchhoff theory can be attributed to the discontinuity of the field at the shadow boundary. This shadow boundary acts like a semi-infinite plate that vibrates infinitely slightly below its coincidence frequency. The regions of positive and negative volume flow counteract each other except for a region of about half a wave length width along the aperture. This region then generates the so called edge wave. Edge radiation and radiation from the shadow boundary are thus equinatural interpretations of the diffraction that is generated by a Kirchhoff diffractor. It turns out that for a straight edge the Kirchhoff diffraction is a maximum in the direction of propagation of the incident wave, and exactly zero opposite. It is crudely inversely proportional to the angular distance from the shadow boundary and hence decreases monotonically.

The Sommerfeld edge-wedge theory applies for rigid or pressure release straight edges and wedges. The first term of the Sommerfeld solution

$$u(r,\Phi) = - \frac{e^{j(kr + \frac{\pi}{4})}}{\sqrt{2\pi kr}} \frac{1}{\cos \frac{\varphi - \varphi_o}{2}} \tag{11.4}$$

is independent on whether the diffracting surface is rigid or is a pressure release surface. It satisfies the wave equation and satisfies exactly the same conditions at the screens as the Kirchhoff solution. In the Sommerfeld language, the screens represent the branch surfaces (the two-dimensional branch cuts) that connect the physical space with the Riemann spaces (the ducts that represent the Kirchhoff screens). It satisfies the continuity conditions at the shadow boundary of the incident wave. But the Sommerfeld

term does represent the exact field in the apertures as it would correspond to Kirchhoff screens if they could be realized. Because of this field, backscatter is quite considerable.

The corresponding Malyuzhinets solution is obtained by assuming the impedance matched for the angle of incidence $\varphi_o = \pi/2$:

$$R = 0 = \frac{\cos \varphi_o - \cos \overline{\theta}}{\cos \varphi_o + \cos \overline{\theta}} \tag{11.5}$$

Hence $0 = \pm \varphi_o = \frac{\pi}{2}$; the negative sign is unacceptable because the impedance must have a positive real part. This angle φ_o has been introduced in Section 5 as the acoustic Brewster angle.

Figure 11.1 and 11.2 show a comparison for normal incidence of the Kirchhoff solution with the first term of the Sommerfeld solution and with the Malyuzhinets solution for impedance match. The Kirchhoff solution shows no backscatter, but otherwise agrees better with the exact solution than the first term of the Sommerfeld solution. The zero of the Malyuzhinets solution at $\varphi = \pi$, i.e. at the impedance matched surface is obvious. Since we have used a stationary phase evaluation, the distance from the edge of the wedge is assumed to be very large, as a consequence, all the field energy is impedance matched at and near the impedance matched surfaces. For finite wedges and edges, the zero will usually be replaced by a minimum. It is very likely that the Kirchhoff solution then will lead to still a much better agreement with the exact solution that it does for the infinitely extended wedge.

Figure 11.3 shows the two terms of the Malyuzhinets solution plotted separately and their sum, for impedance match at normal incidence. The first term I is negative and reduces the resultant amplitude to zero for rays that propogate grazing to the impedance matched surface.

In the Kirchhoff theory, diffraction is exclusively a phenomenon of the shadow boundaries or waves. We therefore obtain the Kirchhoff solution by simply adding the field generated by the incident wave and that generated by the reflected wave, assuming that the reflected amplitude is $R(\varphi_o)$ times that of the incident wave. This solution then approaches closely the exact Malyuzhinets solution on the whole angular range except for two regions: (1) the Malyuzhinets solution vanishes along the impedance covered surface because we have derived it by a stationary phase method, assuming that the field point is very far away from the diffracting edge. In contrast, the Kirchhoff surfaces do not affect grazing rays. The Kirchhoff and the exact solution therefore must differ for $\varphi = \pm \Phi$; and (2) the Kirchhoff terms always lead to zero backscatter. The two solutions with, therefore, also differ for $\varphi = \mp \varphi_o$.

The Malyuzhinets solution shows that the exit factor should be used rather than the reflexion factor. For the exit angle equal to the angle of incidence, the two factors are the same. But for other angles, the results differ slightly. The exit factor usually leads to a better approximation of the position of the minima of the diffracted field; but in general, the deviations are not great because, also in the view of the exact theories, diffraction is basically a phenomenon of the shadow boundaries. It is the angle of incidence and that of reflection that determines the bulk of the diffraction phenomenon. Figures 11.4, 11.5 and 11.6 show a comparison of the exact solution with the Kirchhoff and Sommerfeld solution, the second terms weighted both with $R(\varphi_o)$ and $R(\varphi)$. Agreement between the exact solution and the Kirchhoff result is excellent for

the regions pointed out above i.e. grazing exit, backscatter in direction of incidence and reflected waves.

Tinally, we are very interested in wedges where one surface is rigid, the other pressure release. The ψ function for this case reduces to

$$\psi(\alpha) = \psi_\Phi(\alpha + \Phi + \frac{\pi}{2})\psi_\Phi(\alpha + \Phi - \frac{\pi}{2}) = \psi_\Phi^2(\frac{\pi}{2}) \cos(\alpha + \Phi) \frac{\pi}{4\Phi} = \psi_\Phi^2(\frac{\pi}{2}) \cos(\frac{\pi\alpha}{4\Phi} + \frac{\pi}{4}) \tag{11.6}$$

where we have assumed the $+\Phi$ surface rigid, the $-\Phi$ surface pressure release. The functions $\psi_\varphi(\alpha + j\infty)$ have been dropped since they are constant and occur in similar form in $\psi(\varphi_o)$. The results are shown in Figure 11.7. If the wave impinges on the pressure release surface, and if the second surface is rigid, the solution is similar except that the term $\pi/4$ is replaced by $-\pi/4$. The result of the computation is also plotted in Figure 11.7.

For normal incidence, the curves are practically independent of the impedance of the material in the shadow space. It follows from the derivatiion in section (IX), that the solution near the shadow boundary is entirely independent of the surface properties, and that it does slightly depend on the impedance of the surface in the shadow space as the field point moves towards the diffracting plane. As a consequence of this dependency, the zero in the diffracted field which for $\varphi_o = \pi/2$ occurs at exactly zero degrees for the rigid-rigid straight edge is shifted to about 3° for the rigid-pressure release straight edge. Figure 11.8a shows the exact solution for the rigid-rigid straight edge, Fig. 11.8b that for the pressure release-release straight edge. Figure 11.9 shows for comparison the Kirchhoff approximation, which as would be expected, leads to very good agreement in most of the angular range.

Figure 11.10 shows the exact solution for a 90° pressure release-rigid rigid, and a rigid-pressure release wedge. For comparison, the diffraction at similar rigid-rigid and pressure release - pressure-release wedges are also entered. Again, the Kirchhoff theory would lead to a very good approximation of the exact curves. For instance, if the incident wave impinges on the pressure release surface at $\varphi_o = 120^\circ$, its shadow boundary occurs at $\varphi = -60^\circ$. The shadow boundary of the reflected wave which now is reflected in antiphase, occurs at $\varphi = -30^\circ$. The results for an incident angle of 135° are not included. This position lies along the face of the wedge. The solution for this case does not exist. As stated previously, the stationary phase method assumes that the field point is very far from the diffracting edge, and since the angle of incidence lies along the surface of the wedge, all the incident energy is absorbent for these rays propagating at grazing.

XII. THE PHYSICAL INTERPRETATION OF THE MALYUZHINETS SOLUTION

The exact solution for a straight edge with non rigid surfaces is based on the solution for the straight edge with pressure release surfaces. There is a good reason for using the pressure release solution as a starting point and to modify this solution for impedance covered surfaces. A wave propagating in the direction of the plane of the edge towards the edge of a pressure release straight edge is backscattered, i.e. the diffracted field is not zero for $\varphi_o = 0$. It is physically obvious that an impedance covered straight edge will also backscatter, whereas a rigid straight edge will have no effect at all on a wave that propagates parallel to its plane, φ_o being zero. The wave passes left and right along it without generating a diffraction field. Thus a solution based on the field scattered by a rigid straight edge would break down for $\varphi_o = 0$. The solution is finite for $\varphi = \pm \Phi$ for the pressure release wedge, and for all wedges whose faces have finite impedances regardless of how small their impedance may be. The vanishing of the basic solution for $\varphi = \pm \Phi$ is therefore of no consequence.

The solution for the pressure release wedge then is given by the sum of the two Sommerfeld terms, or by the sum of the two Malyuzhinets terms. The Sommerfeld and the Malyuzhinets terms represent different partial fraction representation of the exact solution for the pressure release straight edge. The Sommerfeld solution is equivalent to superposing the fields generated by a source and by an image source located behind the complementary straight edge.

However, the image concept breaks down when the surfaces are impedance covered. An infinite number of image sources of strength R, R^2, R^3, etc. would then be needed where R is the reflection factor of each of the two surfaces, and the Sommerfeld representation becomes useless.

The Malyuzhinets term $M_2\psi(\varphi + \pi)/\psi(\varphi_o)$ depends almost only on θ_+; and it depends only to a small extent on the impedance of the surface on the shadow side of the straight edge* in the angular range near zero. It reduces to the amplitude of the reflected wave at the shadow boundary of this wave, and to unity at the shadow boundary of the incident wave. For other angles on the positive side of the straight edge, this field is proportional to the exit factor of the reflecting (upper) surface. The field described by this term is not very different from the Kirchhoff fields generated by the shadow boundaries of the reflected and the incident wave. But as we penetrate into the shadow region, the contribution of the shadow boundary of the reflected wave practically disappears.

In the region around $\varphi = 0$, the Malyuzhinets term $\psi(\varphi + \pi)M_2/\psi(\varphi_o)$ describes a field that is stronger than the Kirchhoff field. Because of the impedance cover, the surfaces of the straight edge move in and out like the surfaces of a transducer; they are forced to vibrate by the incident wave. If there were no edge region, the impedance covered surface would reemit the incident wave in form of the reflected wave and would simply act like a reflector. However, the wave that passes the edge represents a reservoir of energy. Some of the energy is also sucked into the edge region, a wave is always bent into an impedance surface, and remitted as an edge wave. The

---

* $\psi(\varphi - \pi) = \psi_\pi(\varphi + \theta_+)\psi_\pi(\varphi - \theta_+)\psi_\pi(\varphi - 2\pi + \theta_-)\psi_\pi(\varphi - 2\pi \pm \theta_-)$

$\cong \psi_\pi(\varphi - 2\pi + \theta_-)\psi_\pi(\varphi - 2\pi - \theta_-)$ for $\varphi > 0$,

because $\psi_\pi \approx 1$ if $|\alpha| \leq \pi$.

and

$\psi(\varphi - \pi) = \psi(-|\varphi| - \pi) \cong \psi_\pi(|\varphi| + 2\pi + \theta_-)\psi_\pi(|\varphi| + 2\pi - \theta_-)$ for $\varphi \leq 0$

also

$\psi(\varphi + \pi) = \psi_\pi(\varphi + 2\pi + \theta_+)\psi_\pi(\varphi + 2\pi - \theta_+)\psi_\pi(\varphi + \theta_-)\ \pi(\varphi + \theta_-)$

$\cong \psi_\pi(\varphi + 2\pi + \theta_+)\psi_\pi(\varphi + 2\pi - \theta_+)$

first term of the Malyuzhinets solution then seems dominantly to represent two fields. The function $\psi(\varphi - \pi)$ depends almost exclusively on θ_-. In the front space, $\psi(\varphi - \pi)$ depends very weekly on θ_- and is practically independent of θ_+. This field can therefore be interpreted as a further contribution of the shadow boundary of the incident wave to the diffraction field. In the space $\varphi < 0$, this term becomes proportional to the exit factor of the surface θ_-. The term $M_\perp \psi(\varphi - \pi)/\psi(\varphi_o)$ can then be interpreted as the field that is reemitted by the vibrating edge region. Figure (11.5) shows a schematic representation of the nature of the two terms of the solutions on the two sides of the diffracting semi-infinite plane.

The exact solution proves that the Kirchhoff concept of the diffraction phenomenon being solely generated by the shadow boundaries is only a first approximation for impedance covered surfaces. According to the exact theory, some of the incident energy is scattered at the edge because of the discontinuity of the acoustic properties of the medium due to the impedance cover. Because of its finite impedance, the edge region is compressible and scatters sound like a chain of air bubbles, located at the edge, scatter sound in water. This scattering effect seems to be greater the smaller the surface impedance. A pc matched edge thus scatters almost as much sound as a pressure release wedge; for instance, when the wave propagates into the edge parallel to an impedance covered plane. In addition, the edge region and the whole surface of the straight edge reemits the incident energy that is not scattered according to the exit law. The amplitude reemitted ray is proportional to the exit factor of the surface. The diffracted Brewster angles of the impedance covered surfaces, regardless of the position of the shadow boundaries. If the

Kirchhoff concept would apply, then the diffraction field would be proportional to the reflection factor for the angle of incidence of the radiation and would not show any Brewster angle dependence.

The curves presented in this report show the variations of backscatter and diffraction in those instances that might be of practical interest. The various approximations are of considerable interest since they help to understand the physics of diffraction. But on the basis of the cosine representation of the Malyuzhinets functions, practically exact computations can be performed with the same case as Sommerfeld or Kirchhoff approximations. There is thus no need to investigate wedge or edge diffraction with the aid of approximate theories.

APPENDIX A

Representation of the ψ_Φ Functions

The following representations of the $\psi_\Phi(\alpha)$ functions have been derived in the above Section V.

$$\psi_\Phi(\alpha) = \exp\left[\frac{i}{8\Phi}\int_0^{\alpha}\int_{-i\infty}^{i\infty} \operatorname{tg}\frac{\pi\nu}{4\Phi}\,\frac{d\nu d\mu}{\cos(\nu-\mu)}\right]; \tag{A1}$$

$$\psi_\Phi(\alpha) = \sqrt{\cos\frac{\pi\alpha}{4\Phi}}\,\exp\left[\frac{1}{2\pi}\int_{-\infty}^{\infty}\ln\left(1 - i\operatorname{tg}\frac{\pi\alpha}{4\Phi}\operatorname{th}\frac{\pi\nu}{4\Phi}\right)\frac{d\nu}{\operatorname{ch}\nu}\right] \tag{A2}$$

$$\Psi_\Phi(\alpha) = \prod_{n=1}^{\infty}\prod_{m=1}^{\infty}\left[1 - \left(\frac{\alpha}{2\Phi(2n-1) + (\pi/2)(2m-1)}\right)^2\right]^{(-1)^{m+1}} \tag{A3}$$

The form A1 is derived in very much the same manner as Eq.(5.18) except that the ν integration is performed first in Equation (A2). By deforming the path of integration from infinity above the real axis to zero and back to infinity below the real axis, and determining the residues, the following forms are obtained for the rational ratio $4\Phi/\pi = n/m$ and $\alpha(k,\ell) = \frac{\pi}{2}\left(\frac{2\ell-1}{n} - \frac{2k-1}{m}\right)$ we have for odd and even n, respectively:

$$\Psi_{\pi n/4m}(\alpha) = \prod_{k=1}^{m}\prod_{\ell=1}^{n}\left(\frac{\cos 1/2\,\alpha(k,\ell)}{\cos 1/2\,[\alpha/n + \alpha(k,\ell)]}\right)^{(-1)^{\ell}}; \tag{A4}$$

$$\Psi_{\pi n/4m}(\alpha) = \prod_{k-1}^{m}\prod_{\ell-1}^{n}\exp\left[(-1)^{\alpha(k,\ell)+\alpha/n}\int_{\alpha(k,\ell)} u\operatorname{ctg} u\,du\right]. \tag{A5}$$

Examples:

$$\Psi_{\pi/4}(\alpha) = \cos\frac{\alpha}{2}\ ;\quad \Psi_{\pi/2}(\alpha) = \exp\left[\frac{1}{4\pi}\int_0^{\alpha}\frac{2u - \pi\sin u}{\cos u}\,du\right]\ ; \tag{A6}$$

$$\Psi_{3\pi/4}(\alpha) = \frac{\cos 1/6\ (\alpha - \pi)\cos 1/6\ (\alpha + \pi)}{\cos^2(\pi/6)\cos 1/6\ \alpha}\ ; \tag{A7}$$

$$\psi_{\pi}(\alpha) = \exp\left[\frac{1}{8\pi}\int_0^{\alpha}\frac{-\pi\sin\nu + 4\pi\cos\frac{\pi}{4}\sin\frac{\nu}{2} - 2\nu}{\cos\nu}\,d\nu\right] \tag{A8}$$

For large values of Im(z):

$$\psi(z)\to 0\left\{e^{\pi|\mathrm{Im}z/8\Phi|}\right\} \cong \sqrt{\cos\frac{\pi z}{4\Phi}}\exp\left[-\frac{1}{2\pi}\int_{-\infty}^{\infty}\frac{\ell n\cosh(\pi s/4\Phi)}{\cosh s}\,ds\right] \tag{A9}$$

and

$$\frac{\psi(z)}{\psi(\varphi_o)} \to 1 \tag{A10}$$

The following relations can be derived for the Malyuzhinetz functions either from their integral representation or residue evaluation of the contour integral or from the basic properties of these functions (meromorphic in strip, poles and zeroes known).

$$\psi_\Phi(\alpha + \tfrac{\pi}{2})\ \psi_\Phi(\alpha - \tfrac{\pi}{2}) = \psi_\Phi^2\ (\tfrac{\pi}{2})\ \cos\tfrac{\pi\alpha}{4\Phi} \tag{A11}$$

$$\psi_\Phi(\alpha)\ \psi_\Phi(\alpha + \pi) = \psi_\Phi^2(\tfrac{\pi}{2})\ \cos\tfrac{\pi}{4\Phi}\ (\alpha + \tfrac{\pi}{2}) \tag{A12}$$

$$\psi_\Phi(\alpha + \Phi)\ \psi_\Phi(\alpha - \Phi) = \psi_\Phi(\Phi)^2\ \psi_{\Phi/2}(\alpha) \tag{A13}$$

$$\psi_\Phi(\alpha + 2\Phi)\ \psi_\Phi(\alpha) = \psi_\Phi(\Phi)^2\ \psi_{\Phi/2}(\alpha + \Phi) \quad . \tag{A14}$$

$$\frac{\psi_\Phi(\alpha + 2\Phi)}{\psi_\Phi(\alpha - 2\Phi)} = \cot\tfrac{1}{2}\ (\alpha + \tfrac{\pi}{2}) \quad , \tag{A15}$$

$$\frac{\psi_\Phi(\alpha + 4\Phi)}{\psi_\Phi(\alpha)} = \cot\tfrac{1}{2}\ (\alpha + \tfrac{\pi}{2} + 2\Phi) \quad , \tag{A16}$$

$$\frac{\psi_\Phi(\alpha)}{\psi_\Phi(\alpha - 4\Phi)} = \tan\tfrac{1}{2}\ (\alpha + \tfrac{\pi}{2} - 2\Phi) \tag{A17}$$

$$\psi_\Phi(\alpha + \tfrac{\pi}{2})\ \psi_\Phi(\alpha - \tfrac{\pi}{2}) = \psi_\Phi^2(\tfrac{\pi}{2})\ \cos\tfrac{\pi\alpha}{4\Phi} \quad , \tag{A18}$$

$$\psi_\Phi(\alpha + \pi)\ \psi_\Phi(\alpha) = \psi_\Phi^2(\tfrac{\pi}{2})\ \cos\tfrac{\pi}{4\Phi}\ (\alpha + \tfrac{\pi}{2}) \tag{A19}$$

$$\psi_\Phi(\alpha)\ \psi_\Phi(\alpha - \pi) = \psi_\Phi^2(\tfrac{\pi}{2})\ \cos\tfrac{\pi}{4\Phi}\ (\alpha - \tfrac{\pi}{2}) \tag{A20}$$

$$\psi_\Phi[z \pm (2\Phi + \tfrac{3\pi}{2})] = \pm \sin\frac{\pi(\pi + z)}{4\Phi}\ \operatorname{cosec}\frac{\pi z}{4\Phi}\ (2\Phi - \tfrac{\pi}{2} \pm z) \tag{A21}$$

$$z_p = \pm\ (2\Phi + \tfrac{3\pi}{2}) \ , \qquad z_o = \pm\ (2\Phi + \tfrac{\pi}{2}) \tag{A22}$$

where z_p are the values of z for the poles of $\psi_\Phi(z)$ and z_o those for the zeroes.

The residues $r_{\pm}$ at the poles $\alpha_{\pm}$ are easily determined by means of the relation

$$\Psi_{\Phi}[z \pm (2\Phi + \frac{3\pi}{2})] = \pm \sin \frac{\pi(\pi + z)}{4\Phi} \operatorname{cosec} \frac{\pi z}{4\Phi} \psi_{\Phi}(2\Phi - \frac{\pi}{2} \pm z) \quad , \tag{A23}$$

which puts the poles into a trigonometric factor.

Two more forms for the complex $\psi(\alpha)$ function are of interest. They are derived with the aid of the relations that apply for the $\psi_{\Phi}(\alpha)$ functions.

$$\begin{aligned}\psi(\alpha) &= \psi_{\Phi}(\alpha + \Phi + \theta_{+})\ \psi_{\Phi}(\alpha + \Phi - \theta_{+})\ \psi_{\Phi}(\alpha - \Phi + \theta_{-})\ \psi_{\Phi}(\alpha - \Phi - \theta_{-}) \\ &= [\psi_{\Phi}(\tfrac{\pi}{2})]^{4}\ [\cos \tfrac{\pi}{4\Phi}(\alpha + \Phi - \vartheta_{+}) \cos \tfrac{\pi}{4\Phi}(\alpha - \Phi + \vartheta_{-})] \\ &\quad \times \frac{\psi_{\Phi}(\alpha + \Phi - \frac{1}{2}\pi + \vartheta_{+})}{\psi_{\Phi}(\alpha + \Phi - \frac{1}{2}\pi - \vartheta_{+})} \frac{\psi_{\Phi}(\alpha - \Phi + \frac{1}{2}\pi - \vartheta_{-})}{\psi_{\Phi}(\alpha - \Phi + \frac{1}{2}\pi + \vartheta_{-})}\end{aligned} \tag{A24}$$

also if $\theta_{+} = \theta_{-}$

$$\begin{aligned}\psi(\alpha) &= \psi_{\Phi}(\alpha + \Phi + \theta)\ \psi_{\Phi}(\alpha - \Phi + \theta)\ \psi_{\Phi}(\alpha + \Phi - \theta)\ \psi_{\Phi}(\alpha - \Phi - \theta) \\ &= [\psi_{\Phi}(\Phi)]^{4}\ \psi_{\Phi/2}(\alpha + \theta)\ \psi_{\Phi/2}(\alpha - \theta)\end{aligned} \tag{A25}$$

If

$$\vartheta_{+} = \vartheta_{-} = 0 \quad \text{(rigid wedge)}$$

$$\begin{aligned}\psi(\alpha) &= \psi_{\Phi}(\alpha + \Phi + \tfrac{\pi}{2})\psi_{\Phi}(\alpha + \Phi - \tfrac{\pi}{2})\psi_{\Phi}(\alpha - \Phi + \tfrac{\pi}{2})\psi_{\Phi}(\alpha - \Phi - \tfrac{\pi}{2}) \\ &= \psi_{\Phi}^{4}(\Phi)\psi_{\Phi/2}^{2}(\tfrac{\pi}{2}) \cos \frac{\pi\alpha}{2\Phi} = \psi_{\Phi}^{4}(\tfrac{\pi}{2}) \cos \frac{\pi\alpha}{2\Phi}\end{aligned}$$

Hence

$$\psi(\varphi - \pi) = \cos \frac{\pi}{2\Phi} (\varphi - \pi)$$

$$\psi(\varphi + \pi) = \cos \frac{\pi}{2\Phi} (\varphi + \pi)$$

and for $\Phi = \pi$:

$$\psi(\varphi - \pi) = \text{const. } \sin \varphi/2$$

$$\psi(\varphi + \pi) = \text{const. } \sin \varphi/2$$

If

$$\vartheta_+ = \vartheta_- = \frac{\pi}{2} + j\infty \quad ,$$

$$\frac{\psi(\alpha)}{\psi(\varphi_o)} = 1 \quad \text{regardless of} \quad \alpha \quad \text{and} \quad \varphi_o$$

If one surface is pressure release

$$\overline{\theta} = \frac{\pi}{2} + j\infty \quad , \quad \psi_\Phi(\alpha + \overline{\theta}) \rightarrow \psi_\Phi(\overline{\theta}) \rightarrow \infty \tag{A26}$$

and the two ψ_Φ factors that contain $\overline{\theta}$ drop out of the solution

$$\frac{\psi(\varphi + \pi)}{\psi(\varphi_o)}$$

If a surface is rigid, $\overline{\theta} = \pi/2$, then

$$\psi_\Phi(\alpha + \Phi + \frac{\pi}{2})\psi_\Phi(\alpha + \Phi - \frac{\pi}{2}) = \psi_\Phi^2 (\frac{\pi}{2}) \cos \frac{\pi\alpha}{4\Phi} \tag{A27}$$

and the two terms in the solution $\psi(\varphi \pm \pi)/\psi(\varphi_o)$ can be replaced by the two terms $\cos \frac{\pi(\varphi \pm \pi)}{4\Phi}$ respectively.

If the front surface is impedance matched ($z_+ = \rho c$), then $\theta_+ = 0$, and:

$$\psi(\alpha) = \psi_\Phi(\alpha + \Phi)\psi_\Phi(\alpha - \Phi)\psi_\Phi(\alpha - \Phi + \theta_-)\psi_\Phi(\alpha - \Phi - \theta_-)$$

$$= \psi_\Phi^2(\Phi)\psi_{\Phi/2}(\alpha)\psi_\Phi(\alpha - \Phi + \theta_-)\psi_\Phi(\alpha - \Phi - \theta_-)$$

APPENDIX B

Comparison of the Malyuzhinets and the Sommerfeld Solution

The Sommerfeld solution applies only to the rigid and the pressure release wedges. It consists of two terms, one of which represents the field of the incident wave, the other the field generated by an image source (hidden in a Riemann space). It is of interest to force the Malyuzhinets solution into a similar form, to investigate whether in the general case a simple analysis is possible in terms of fields generated by a real source and an image source.

The Malyuzhinets solution is given by

$$u(r,\varphi,k) = \frac{-\pi}{2\Phi}\left(\frac{\cos\frac{\pi\varphi_o}{2\Phi}}{\psi(\varphi_o)}\right)\left[\frac{-\psi(\varphi-\pi)}{\sin\frac{\pi}{2\Phi}(\varphi-\pi)-\sin\frac{\pi\varphi_o}{2\Phi}}+\frac{\psi(\varphi+\pi)}{\sin\frac{\pi}{2\Phi}(\varphi+\pi)-\sin\frac{\pi\varphi_o}{2\Phi}}\right]\frac{e^{jk(r+\frac{\pi}{4})}}{\sqrt{2\pi kr}} \tag{B1}$$

and the Sommerfeld solution is

$$u(r,\varphi,k) = \frac{-\pi}{2\sqrt{2\pi\,kr}}\sin\frac{\pi}{\nu}\left[\frac{-1}{\cos\frac{\pi}{\nu}-\cos\frac{\varphi-\varphi_o}{\nu}}\pm\frac{1}{\cos\frac{\pi}{\nu}+\cos\frac{\varphi+\varphi_o}{\nu}}\right]e^{jk(r+\frac{\pi}{4})} \tag{B2}$$

where

$$\nu = \frac{2\Phi}{\pi} \tag{B3}$$

For the straight edge, $\nu = 2$. The two angular functions in (B2) can be written as follows:

$$\frac{-1}{\cos\frac{\pi}{\nu}-\cos\frac{\varphi-\varphi_o}{\nu}}\pm\frac{1}{\cos\frac{\pi}{\nu}+\cos\frac{\varphi+\varphi_o}{\nu}} = S_1 \pm S_2 \tag{B4}$$

Let us write their sum with a common denominator.

For the minus sign we have the numerator

$$\cos\frac{\pi}{\nu}+\cos\frac{\varphi+\varphi_o}{\nu}-\cos\frac{\pi}{\nu}+\cos\frac{\varphi-\varphi_o}{\nu}=\cos\frac{\varphi+\varphi_o}{\nu}+\cos\frac{\varphi-\varphi_o}{\nu}=2\cos\frac{\varphi}{\nu}\cos\frac{\varphi_o}{\nu} \tag{B5}$$

For the plus sign we get

$$\cos\frac{\pi}{\nu}+\cos\frac{\varphi+\varphi_o}{\nu}+\cos\frac{\pi}{\nu}-\cos\frac{\varphi-\varphi_o}{\nu}=2(\cos\frac{\pi}{\nu}-\sin\frac{\varphi_o}{\nu}\sin\frac{\varphi}{\nu}) \tag{B6}$$

Thus we have

$$S_1-S_2=\frac{2\cos\frac{\varphi}{\nu}\cos\frac{\varphi_o}{\nu}}{(\cos\frac{\pi}{\nu}-\cos\frac{\varphi-\varphi_o}{\nu})(\cos\frac{\pi}{\nu}+\cos\frac{\varphi+\varphi_o}{\nu})} \tag{B7}$$

and

$$S_1+S_2=\frac{2(\cos\frac{\pi}{\nu}-\sin\frac{\varphi_o}{\nu}\sin\frac{\varphi}{\nu})}{(\cos\frac{\pi}{\nu}-\cos\frac{\varphi-\varphi_o}{\nu})(\cos\frac{\pi}{\nu}+\cos\frac{\varphi+\varphi_o}{\nu})} \tag{B8}$$

The Malyuzhinets solution contains the terms $\frac{1}{\alpha_M}$ and $\frac{1}{\beta_M}$ where

$$\frac{1}{\alpha_M}-\frac{1}{\beta_M}=\frac{1}{\sin\frac{\varphi-\pi}{\nu}-\sin\frac{\varphi_o}{\nu}}-\frac{1}{\sin\frac{\varphi+\pi}{\nu}-\sin\frac{\varphi_o}{\nu}}$$

$$=\frac{1}{2\sin\frac{\varphi-\pi-\varphi_o}{2\nu}\cos\frac{\varphi-\pi+\varphi_o}{2\nu}}-\frac{1}{2\sin\frac{\varphi+\pi-\varphi_o}{2\nu}\cos\frac{\varphi+\pi+\varphi_o}{2\nu}} \tag{B9}$$

$$=\frac{\sin(\frac{\varphi+\pi}{\nu})-\sin(\frac{\varphi_o}{\nu})-[\sin\frac{\varphi-\pi}{\nu}-\sin\frac{\varphi_o}{\nu}]}{2\sin\frac{\varphi-\pi-\varphi_o}{2\nu}\sin\frac{\varphi+\pi-\varphi_o}{2\nu}\cdot 2\cos\frac{\varphi-\pi+\varphi_o}{2\nu}\cos\frac{\varphi+\pi+\varphi_o}{2\nu}} \tag{B10}$$

$$\frac{\left[\sin\frac{\varphi+\pi}{\nu}-\sin\frac{\varphi_o}{\nu}\right]-\left[\sin\frac{\varphi-\pi}{\nu}-\sin\frac{\varphi_o}{\nu}\right]}{\left[\cos\frac{\pi}{\nu}-\cos\frac{\varphi-\varphi_o}{\nu}\right]\left[\cos\frac{\pi}{\nu}+\cos\frac{\varphi+\varphi_o}{\nu}\right]}=$$

$$\frac{\left[\sin\frac{\varphi+\pi}{\nu}-\sin\frac{\varphi-\pi}{\nu}\right]}{\left[\cos\frac{\pi}{\nu}-\cos\frac{\varphi-\varphi_o}{\nu}\right]\left[\cos\frac{\pi}{\nu}+\cos\frac{\varphi+\varphi_o}{\nu}\right]}=\frac{2\sin\frac{\pi}{\nu}\cos\frac{\varphi}{\nu}}{\left(\cos\frac{\pi}{\nu}-\cos\frac{\varphi-\varphi_o}{\nu}\right)\left(\cos\frac{\pi}{\nu}+\cos\frac{\varphi+\varphi_o}{\nu}\right)} \tag{B11}$$

Similarly we have

$$\frac{1}{\alpha_M}+\frac{1}{\beta_M}=\frac{1}{\sin\frac{\varphi-\pi}{\nu}-\sin\varphi_o}+\frac{1}{\sin\frac{\varphi+\pi}{\nu}-\sin\frac{\varphi_o}{\nu}}=$$

$$\frac{\left[\sin\frac{\varphi+\pi}{\nu}-\sin\frac{\varphi_o}{\nu}\right]+\left[\sin\frac{\varphi-\pi}{\nu}-\sin\frac{\varphi_o}{\nu}\right]}{\left(\cos\frac{\pi}{\nu}-\cos\frac{\varphi-\varphi_o}{\nu}\right)\left(\cos\frac{\pi}{\nu}+\cos\frac{\varphi+\varphi_o}{\nu}\right)}=$$

$$\frac{2\left[-\sin\frac{\varphi_o}{\nu}+\sin\frac{\varphi}{\nu}\cos\frac{\pi}{\nu}\right]}{\left(\cos\frac{\pi}{\nu}-\cos\frac{\varphi-\varphi_o}{\nu}\right)\left(\cos\frac{\pi}{\nu}+\cos\frac{\varphi-\varphi_o}{\nu}\right)} \tag{B12}$$

We can express the Malyuzhinets terms in terms of the Sommerfeld terms as follows:

$$\frac{1}{\alpha_M}-\frac{1}{\beta_M}=\frac{2\sin\frac{\pi}{\nu}\cos\frac{\varphi}{\nu}}{\left(\cos\frac{\pi}{\nu}-\cos\frac{\varphi-\varphi_o}{\nu}\right)\left(\cos\frac{\pi}{\nu}+\cos\frac{\varphi+\varphi_o}{\nu}\right)}$$

$$=\frac{2\sin\frac{\pi}{\nu}\cos\frac{\varphi}{\nu}}{2\cos\frac{\varphi}{\nu}\cos\frac{\varphi_o}{\nu}}(S_1-S_2)=\frac{\sin\frac{\pi}{\nu}}{\cos\frac{\varphi_o}{\nu}}(S_1-S_2) \tag{B13}$$

$$\frac{1}{\alpha_M} + \frac{1}{\beta_M} = \frac{2\left[-\sin\frac{\varphi_o}{\nu} + \sin\frac{\varphi}{\nu}\cos\frac{\pi}{\nu}\right]}{\left(\cos\frac{\pi}{\nu} - \cos\frac{\varphi-\varphi_o}{\nu}\right)\left(\cos\frac{\pi}{\nu} + \cos\frac{\varphi+\varphi_o}{\nu}\right)}$$

$$= + \frac{\left(-\sin\frac{\varphi_o}{\nu} + \sin\frac{\varphi}{\nu}\cos\frac{\pi}{\nu}\right)}{\left(\cos\frac{\pi}{\nu} - \sin\frac{\varphi_o}{\nu}\sin\frac{\varphi}{\nu}\right)}\left(S_1 + S_2\right) \qquad (B14)$$

The Malyuzhinets solution can now be written as follows

$$\psi(\varphi - \pi) + \psi(\varphi + \pi) = A \qquad (B15)$$

$$\psi(\varphi - \pi) - \psi(\varphi + \pi) = B \qquad (B16)$$

$$\left[\frac{\psi(\varphi-\pi)}{\alpha_M} - \frac{\psi(\varphi+\pi)}{\beta_M}\right] = \frac{A}{2}\left(\frac{1}{\alpha_M} - \frac{1}{\beta_M}\right) + \frac{B}{2}\left(\frac{1}{\alpha_M} + \frac{1}{\beta_M}\right) \qquad (B17)$$

$$u(r,\varphi) = \frac{1}{4\nu\psi(\varphi_o)}\left\{\left[A\sin\frac{\pi}{\nu}\left(S_1 - S_2\right) + B\cos\frac{\varphi_o}{\nu}\frac{\left(-\sin\frac{\varphi_o}{\nu} + \sin\frac{\varphi}{\nu}\cos\frac{\pi}{\nu}\right)}{\left(\cos\frac{\pi}{\nu} - \sin\frac{\varphi_o}{\nu}\sin\frac{\varphi}{\nu}\right)}\left(S_1 + S_2\right)\right\} \qquad (B18)$$

$$= \frac{1}{4\nu\psi(\varphi_o)}\left\{\left[\left(A\sin\frac{\pi}{\nu} + B\cos\frac{\varphi_o}{\nu}\frac{\left(-\sin\frac{\varphi_o}{\nu} + \sin\frac{\varphi}{\nu}\cos\frac{\pi}{\nu}\right)}{\cos\frac{\pi}{\nu} - \sin\frac{\varphi_o}{\nu}\sin\frac{\varphi}{\nu}}\right] S_1\right.$$

$$\left. + \left[-A\sin\frac{\pi}{\nu} + \frac{B\cos\left(\frac{\varphi_o}{\nu}\right)\left(-\sin\frac{\varphi_o}{\nu} + \sin\frac{\varphi}{\nu}\cos\frac{\pi}{\nu}\right)}{\cos\frac{\pi}{\nu} - \sin\frac{\varphi_o}{\nu}\sin\frac{\varphi}{\nu}}\right] S_2\right\} \qquad (B19)$$

For the pressure release wedge, $A/\psi(\varphi_o) = 1$, $B/\psi(\varphi_o) = 0$, and the solution becomes identical with that given by Sommerfeld. For the straight edge, this Eq. 19 reduces to

$$u(r,\varphi) = \frac{1}{4\psi(\varphi_o)}\left\{\left[A + B\frac{\cos(\varphi_o/2)}{\sin(\varphi/2)}\right] S_1 + \left[-A + B\frac{\cos(\varphi_o/2)}{\sin(\varphi/2)}\right] S_2\right\}$$

$$= \frac{1}{4\psi(\varphi_o)}\left\{[\psi(\varphi - \pi) + \psi(\varphi + \pi) + [\psi(\varphi - \pi) - \psi(\varphi + \pi)] \frac{\cos \varphi_o/2}{\sin \varphi/2}\right\} \frac{1}{-\cos \frac{\varphi - \varphi_o}{2}}$$

$$+ \frac{1}{4\psi(\varphi_o)} [-\psi(\varphi - \pi) - \psi(\varphi + \pi) + [\psi(\varphi - \pi) \quad \psi(\varphi + \pi)] \frac{\cos \varphi_o/2}{\sin \varphi/2}] \frac{1}{\cos \frac{\varphi + \varphi_o}{2}} \tag{B20}$$

The first factor

$$S_1 = \frac{-1}{\cos \frac{\varphi - \varphi_o}{2}} \tag{B21}$$

has a pole at $\varphi = -\pi + \varphi_o$; this pole occurs at the shadow boundary of the transmitted wave. The second factor

$$S_2 = \frac{1}{\cos \frac{\varphi + \varphi_o}{2}} \tag{B22}$$

has a pole at $\varphi = \pi - \varphi_o$ at the shadow boundary of the reflected wave.

For the shadow boundary of the incident wave, $\varphi = -\pi + \varphi_o$. The first bracket with the factor in front reduces to the Sommerfeld first term; the second bracket with the factor in front reduces to the shadow boundary of the reflected wave to the classical reflection factor $(1/2\ \psi(2\pi - \varphi_o)/\psi(\varphi_o)$ times the second Sommerfeld term. But the term differs from the Sommerfeld terms in the range between the two shadow boundaries. This all means that the impedance surfaces generate some interaction between the two fields and that the exact solution therefore cannot be obtained by the method of simple image sources. The results show that the Malyuzhinets form of the solution is considerably simpler. Forcing it into the Sommerfeld form helps in no way.

ACKNOWLEDGMENTS

The author wishes to express his appreciation to Dr. E. J. McKinney and Mr. E. G. Liszka of the Naval Sea Systems Command for encouragement, support, and their valuable comments. The author is also greatly obligated to Dr. S. I. Hayek for many helpful suggestions and for checking the validity of the mathematical derivations, and to Dr. A. D. Stuart for many stimulating discussions. Particular thanks are due to Mrs. Susan M. Cohick for computing the many curves and for her valuable help in the preparation of this report. The work has been supported by Code 034-A of the U. S. Naval Sea Systems Command.

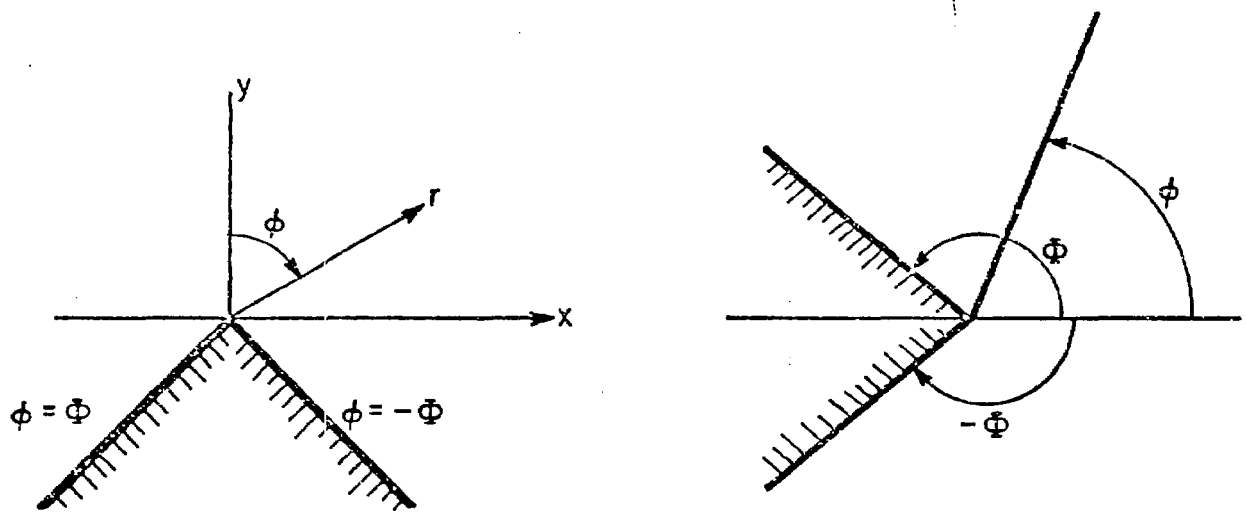

Figure 1.1 Coordinates used in describing the wedge.

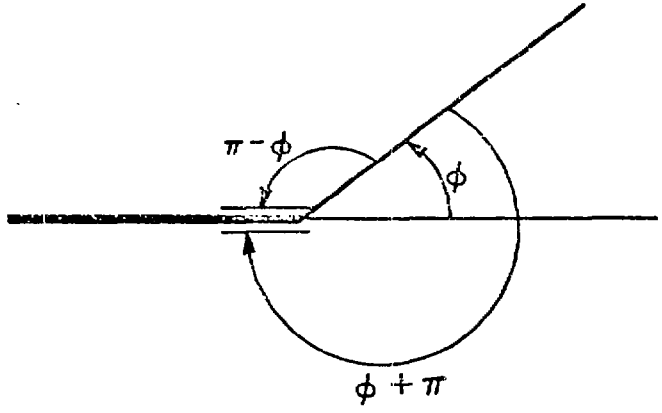

Figure 1.2 Coordinates used in describing the straight edge.

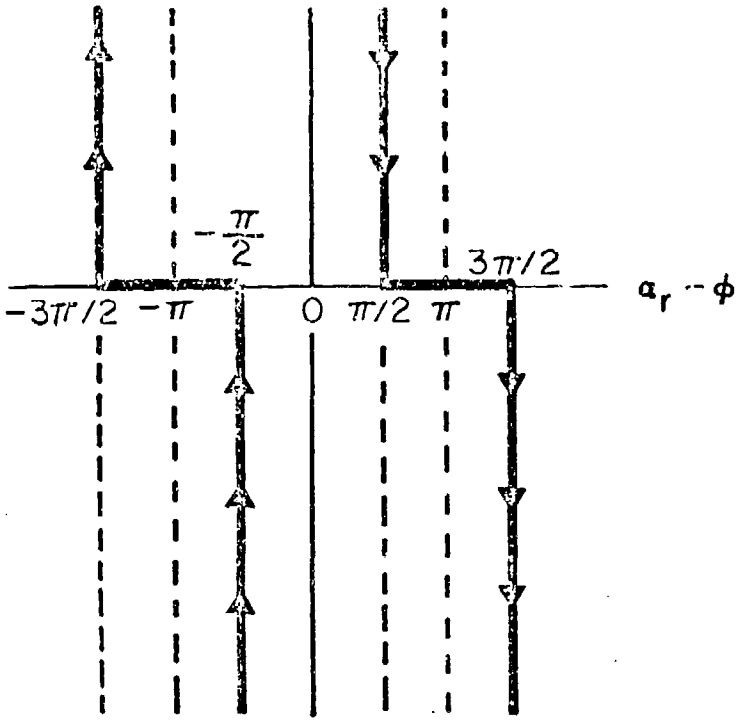

FIG. I.3a PATHS OF INTEGRATION

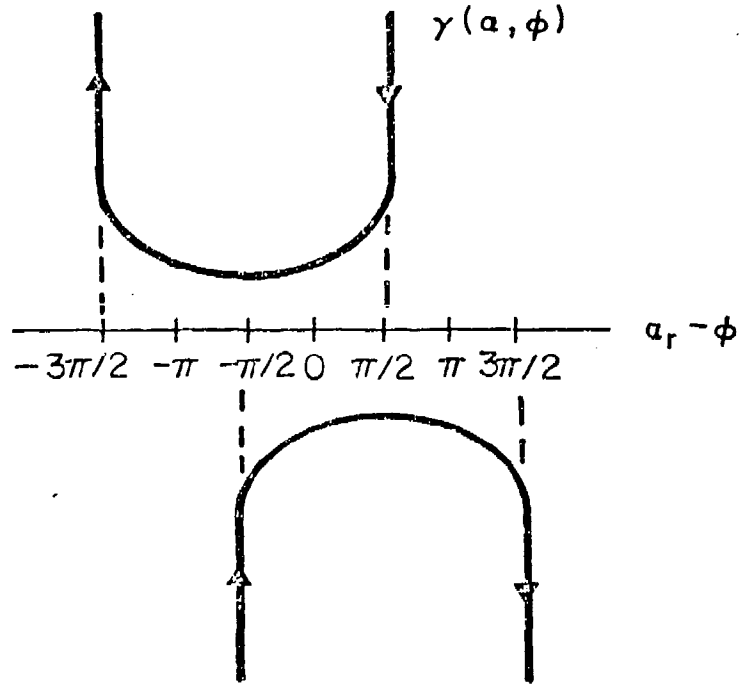

FIG. I.3b THE STRAIGHT LINE PATHS OF FIG. I.3a DEFORMED INTO TWO LOOPS

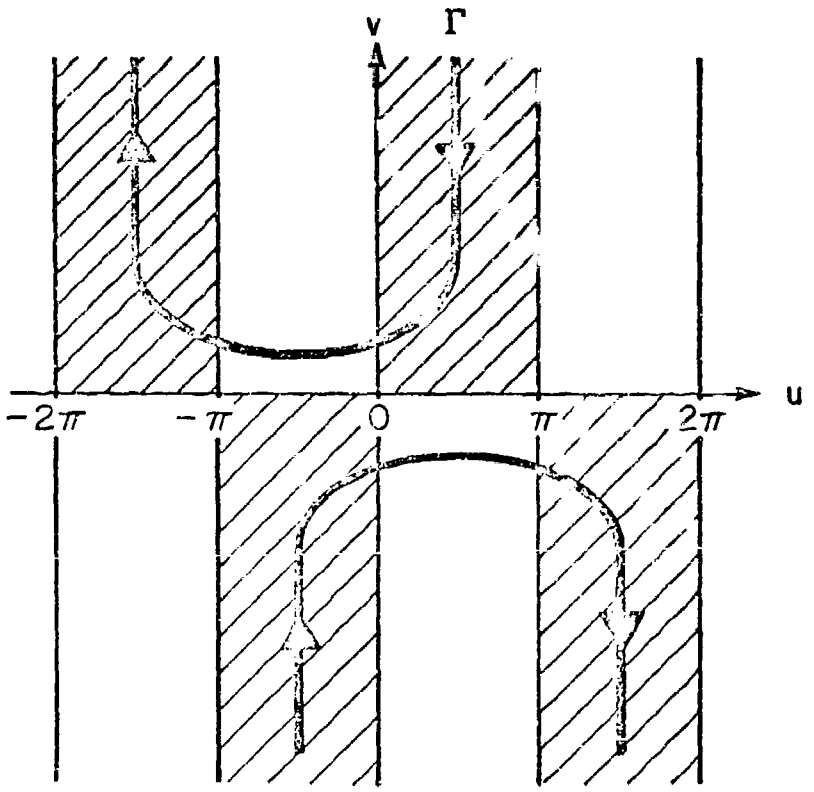

Figure 1.4 The path Γ of integration can be deformed arbitrarily within the regions of convergence shown shaded in the diagram.

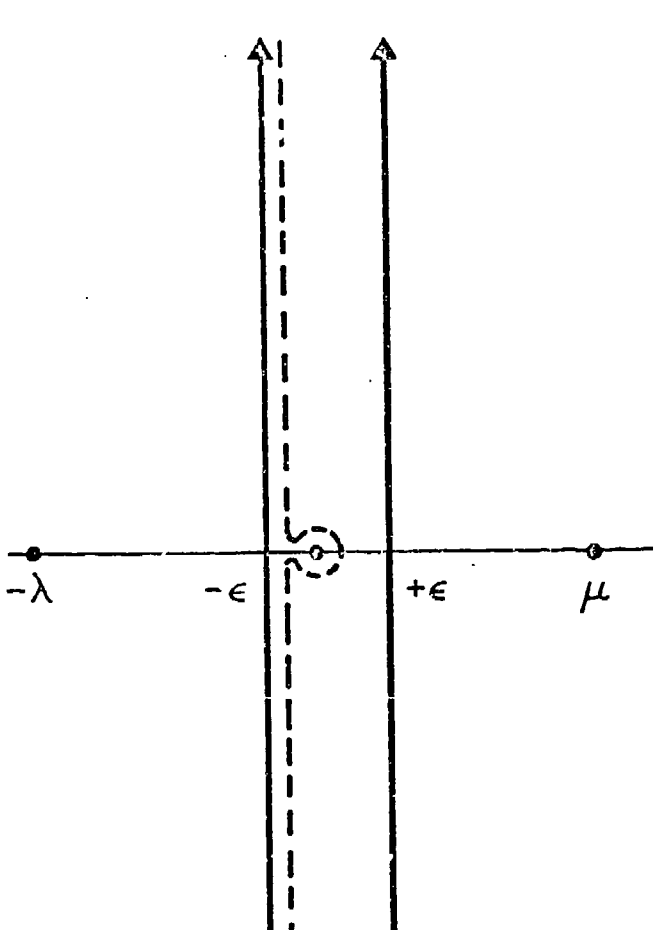

Figure 4.1 Deformation of the path C_2 into C_2' to transform the integrals to have the same path of integration.

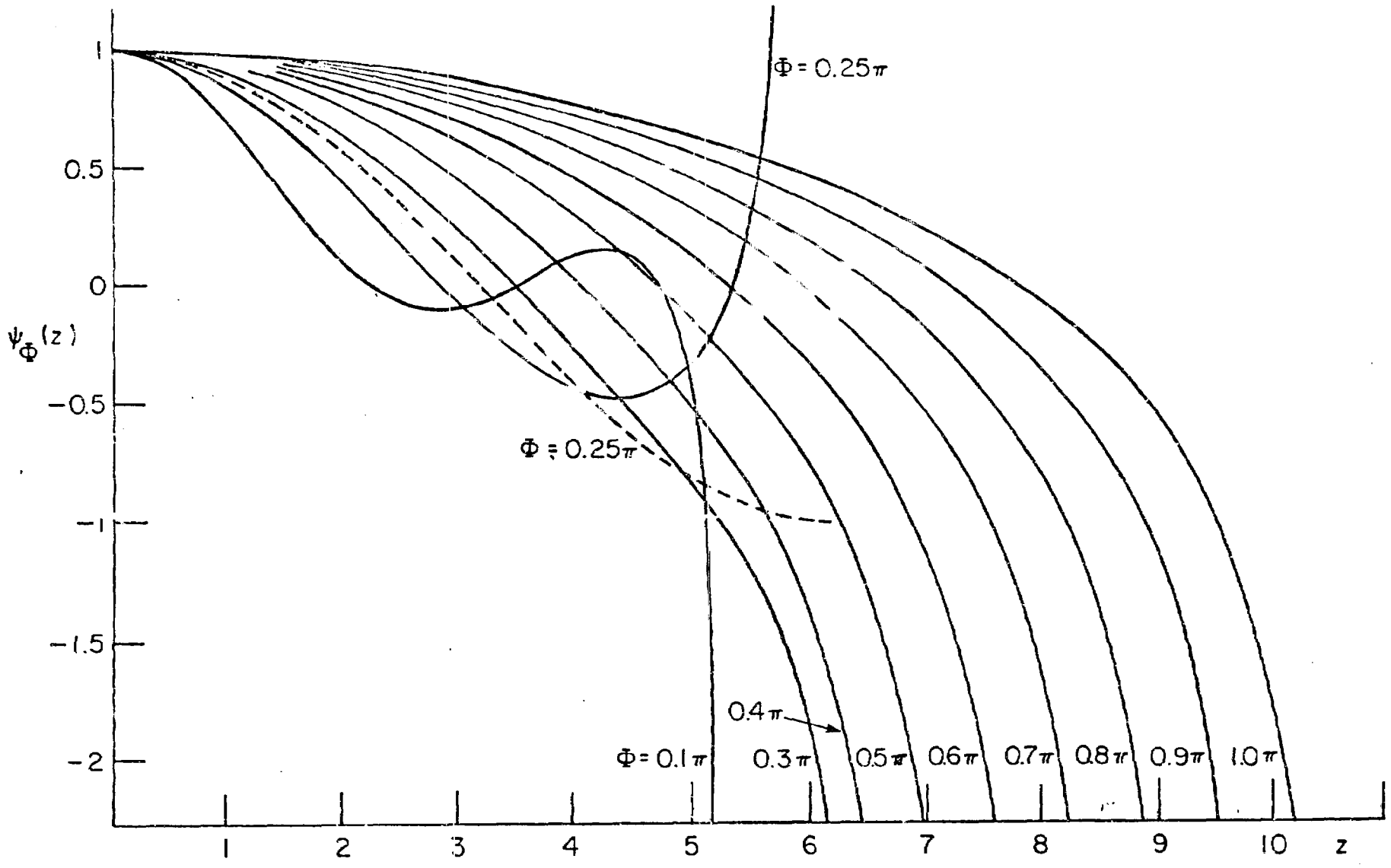

Figure 6.1 The Malyuzhinets function $\Psi_\Phi(z)$ for real argument.

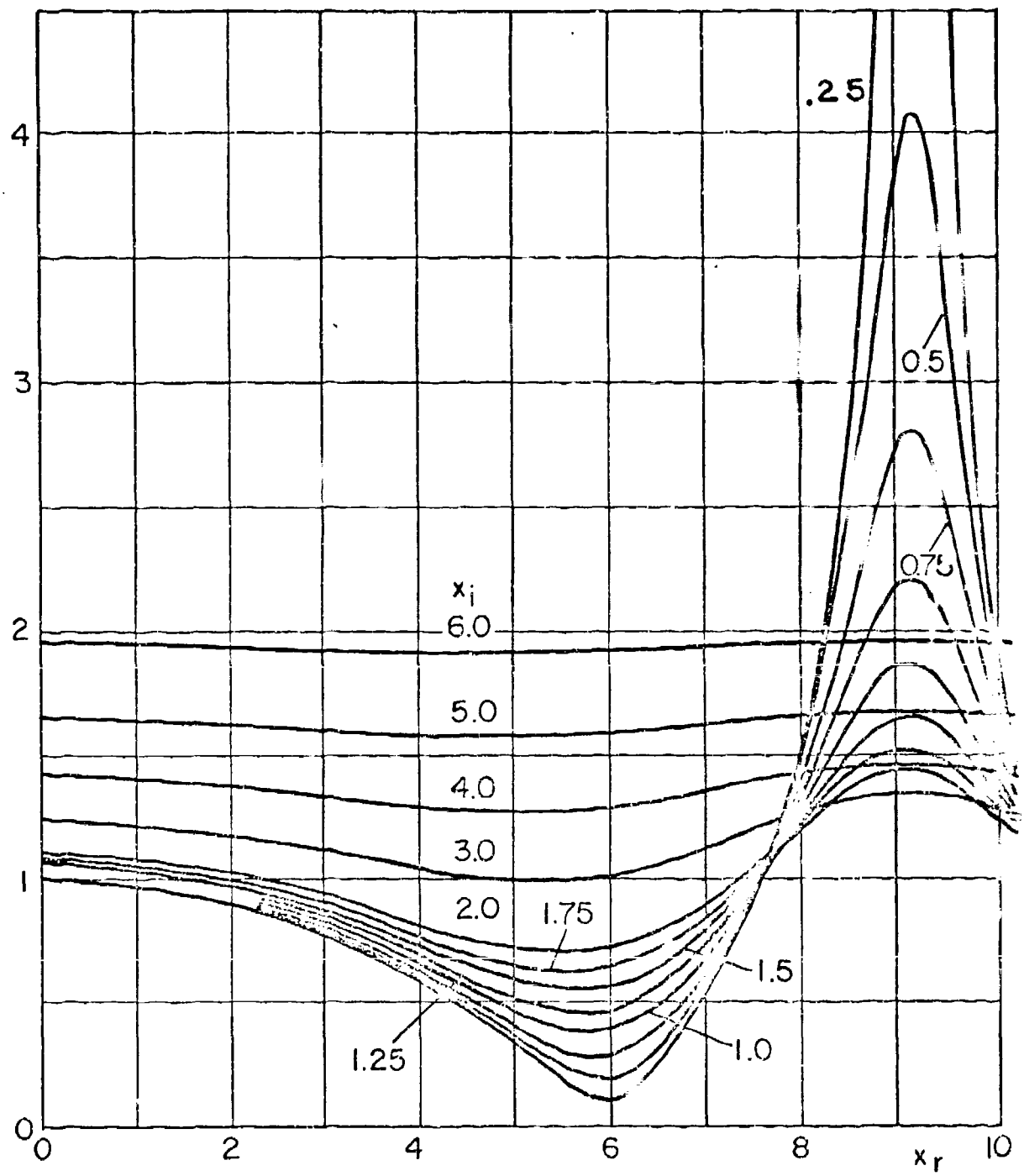

Figure 6.2 The absolute value of the Malyuzhinets function for argument $Z = x_r + jx_i$.

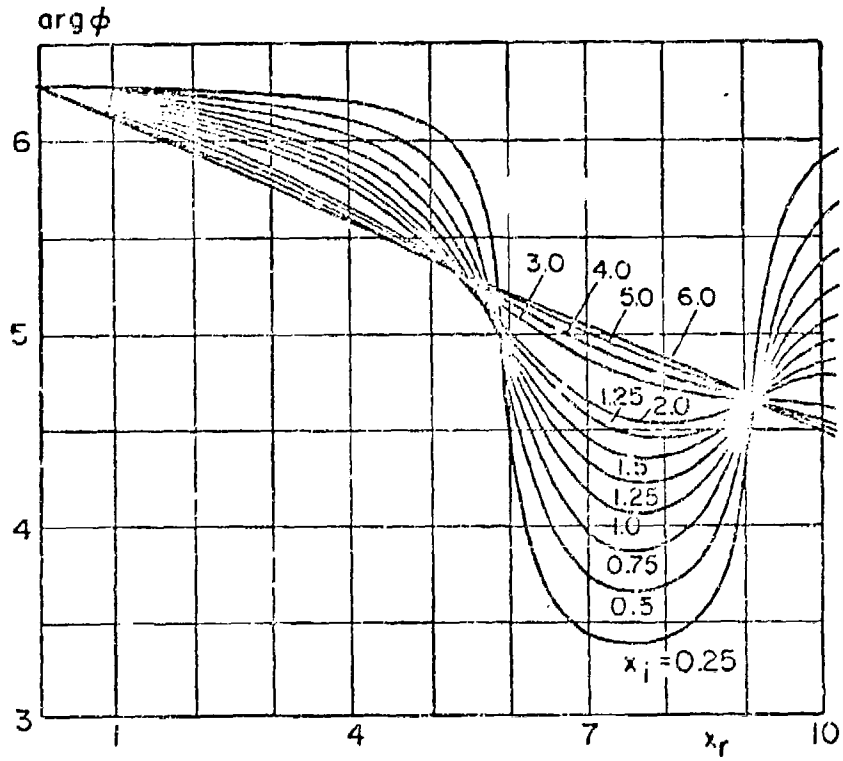

Figure 6.3 The phase angle of the Malyuzhinets function.

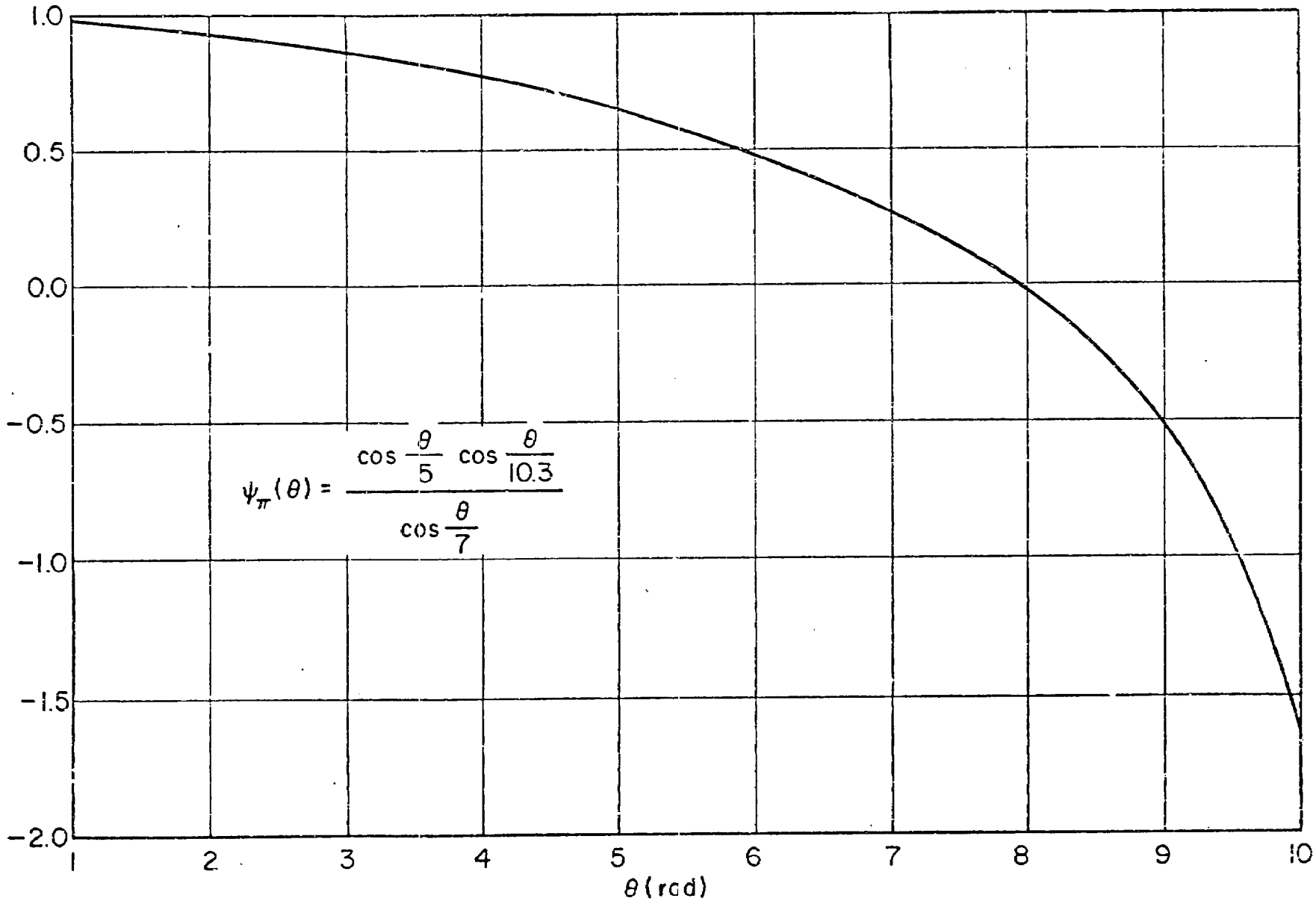

Figure 6.4 Approximation to the Malyuzhinets function $\psi_\pi(\theta)$. The exactly computed points lie on the same curve.

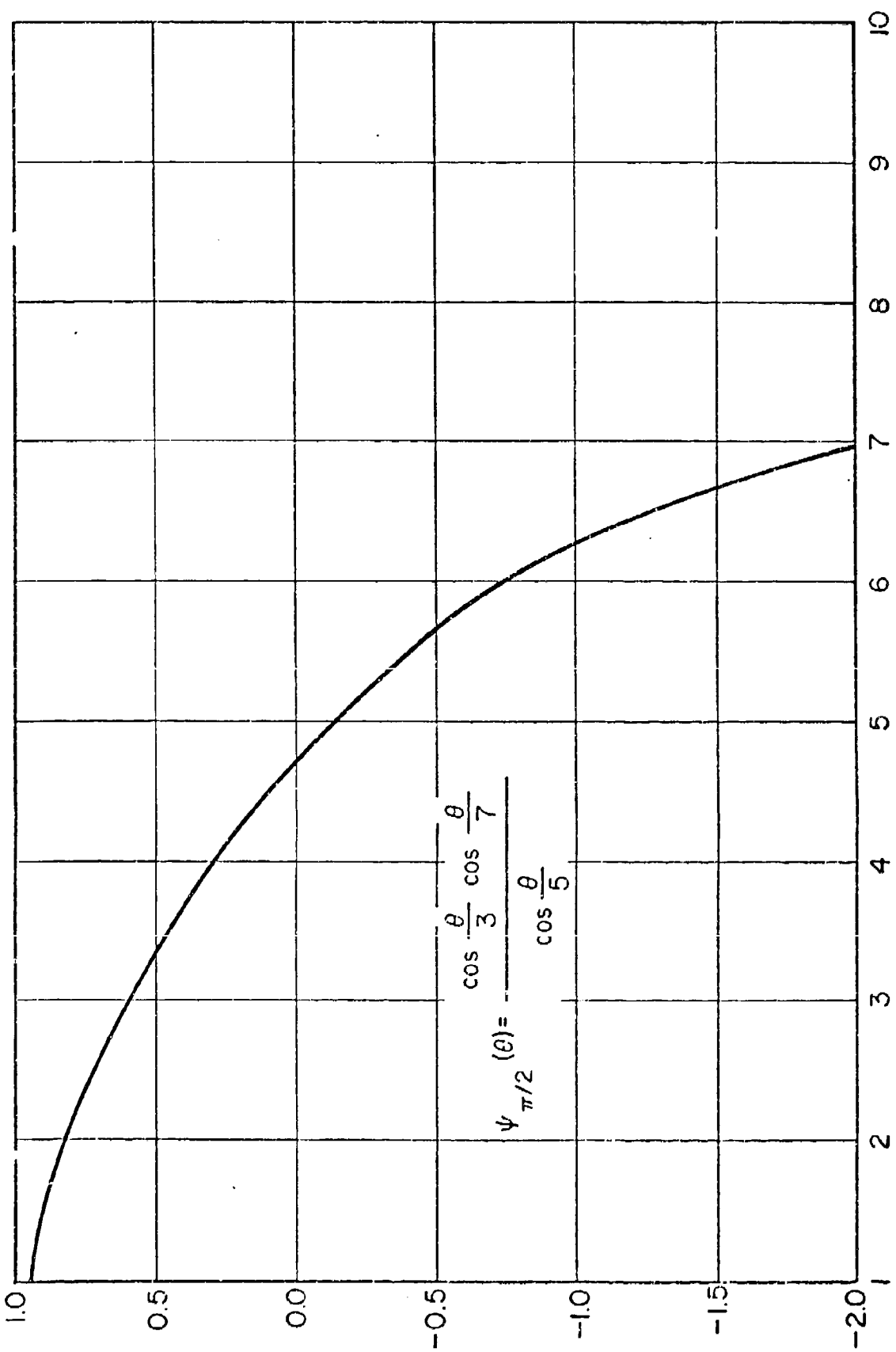

Figure 6.5 Approximation to the Malyuzhinets function $\psi_{\pi/2}(\theta)$. The exactly computed points lie on the same curve.

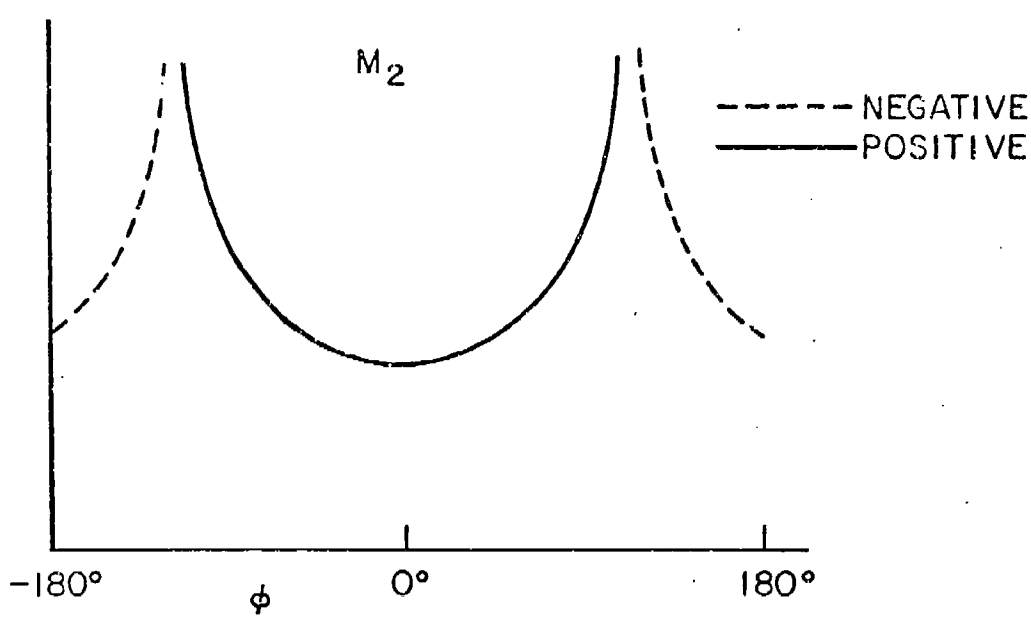

$$M_2 = \frac{\cos \frac{\pi}{2\Phi} \phi_0}{\sin \frac{\pi}{2\Phi} (\phi + \pi) - \sin \frac{\pi}{2\Phi} \phi_0}$$

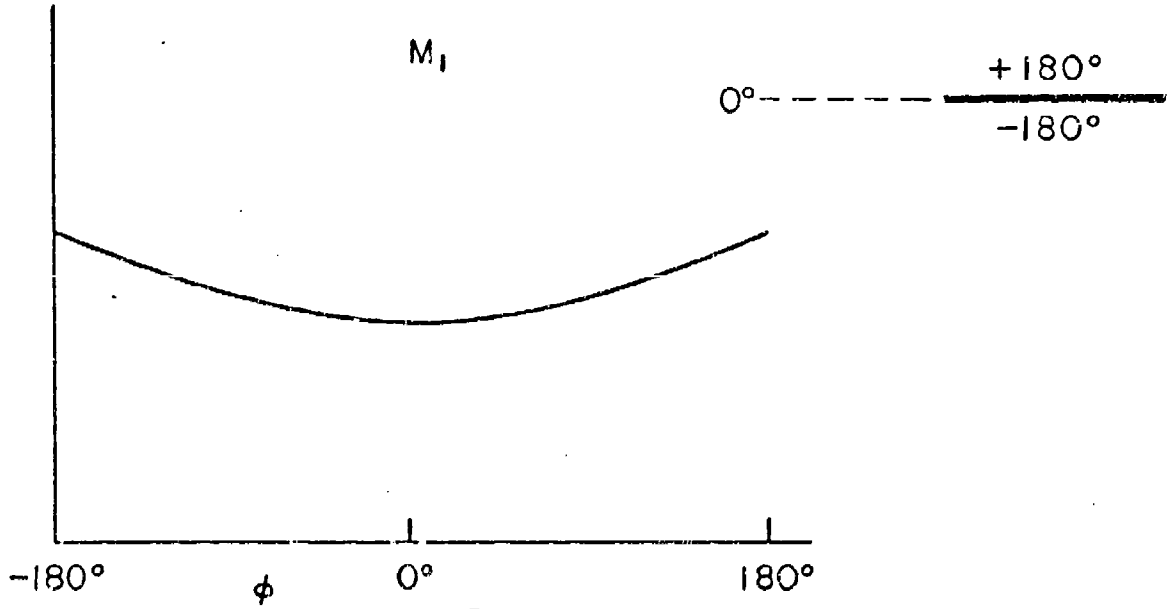

$$M_1 = \frac{-\cos \frac{\pi}{2\Phi} \phi_0}{\sin \frac{\pi}{2\Phi} (\phi - \pi) - \sin \frac{\pi}{2\Phi} \phi_0}$$

Figure 7.1a M_1 and M_2 the angle functions of the Malyuzhinets solution for an edge ($\Phi = \pi$).

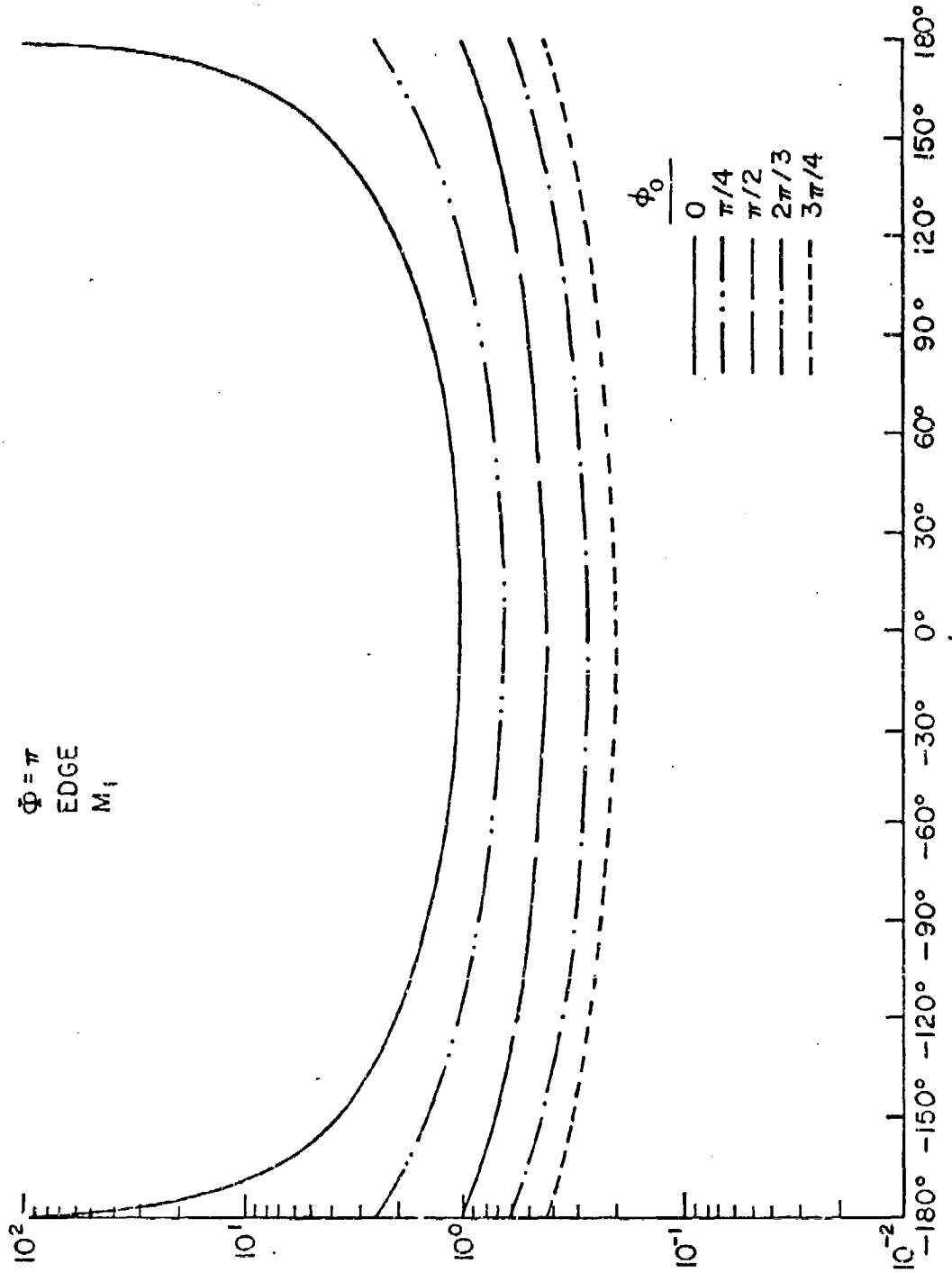

Figure 7.1b The Malyuzhinets angle function M_1 for an edge.

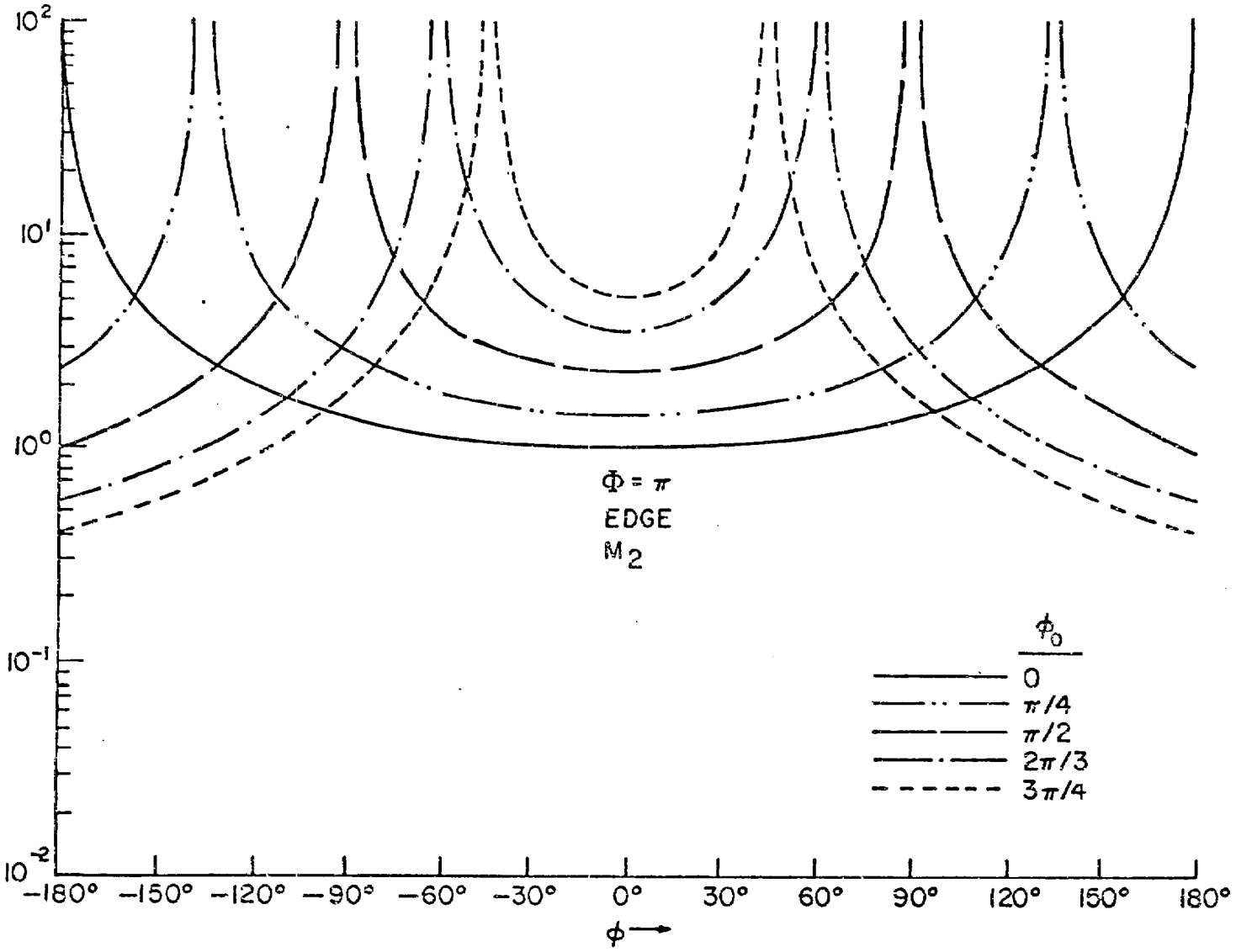

Figure 7.1c The Malyuzhinets angle function M_2 for an edge.

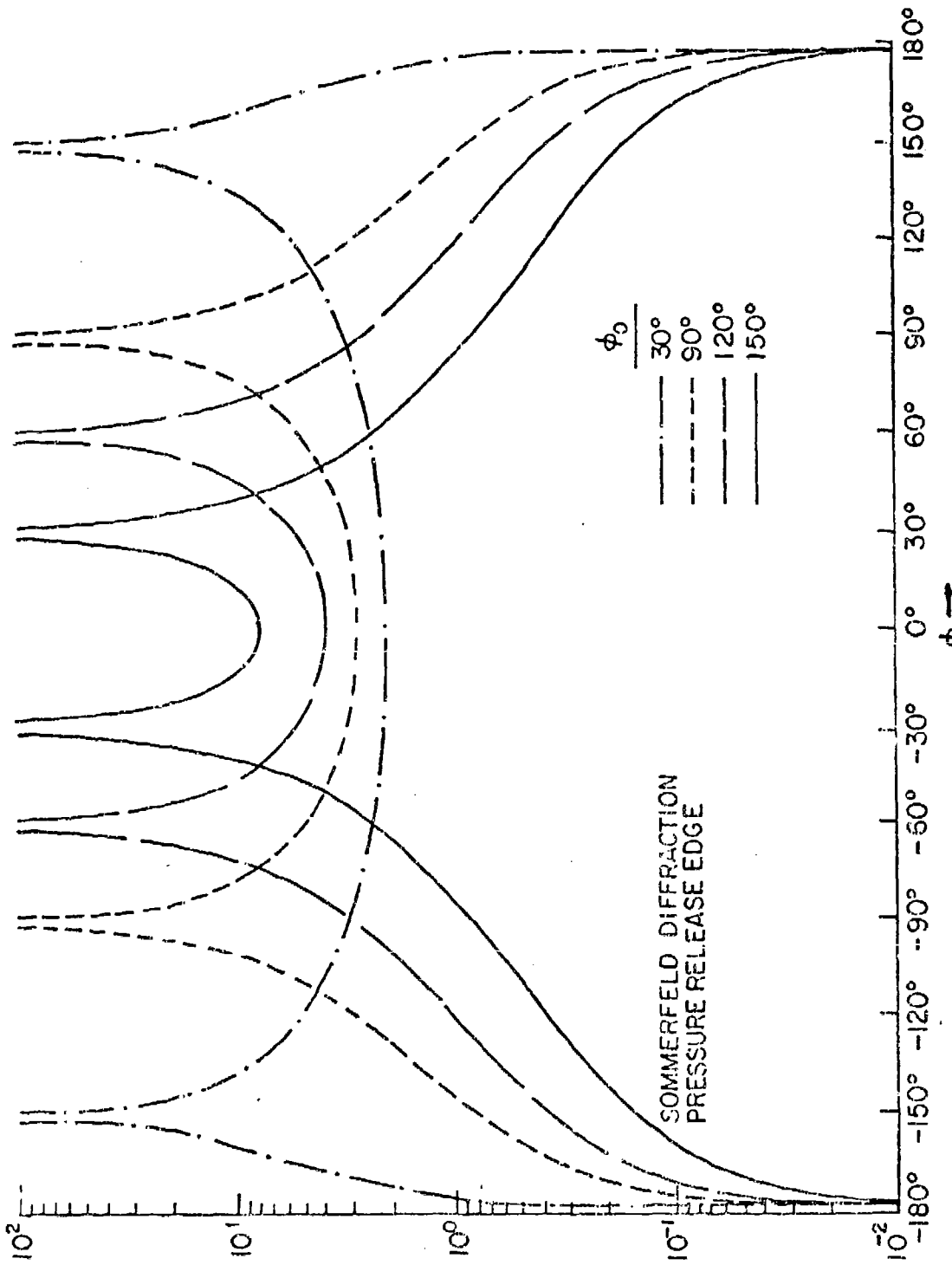

Figure 7.1d The Sommerfeld solution for a pressure release edge.

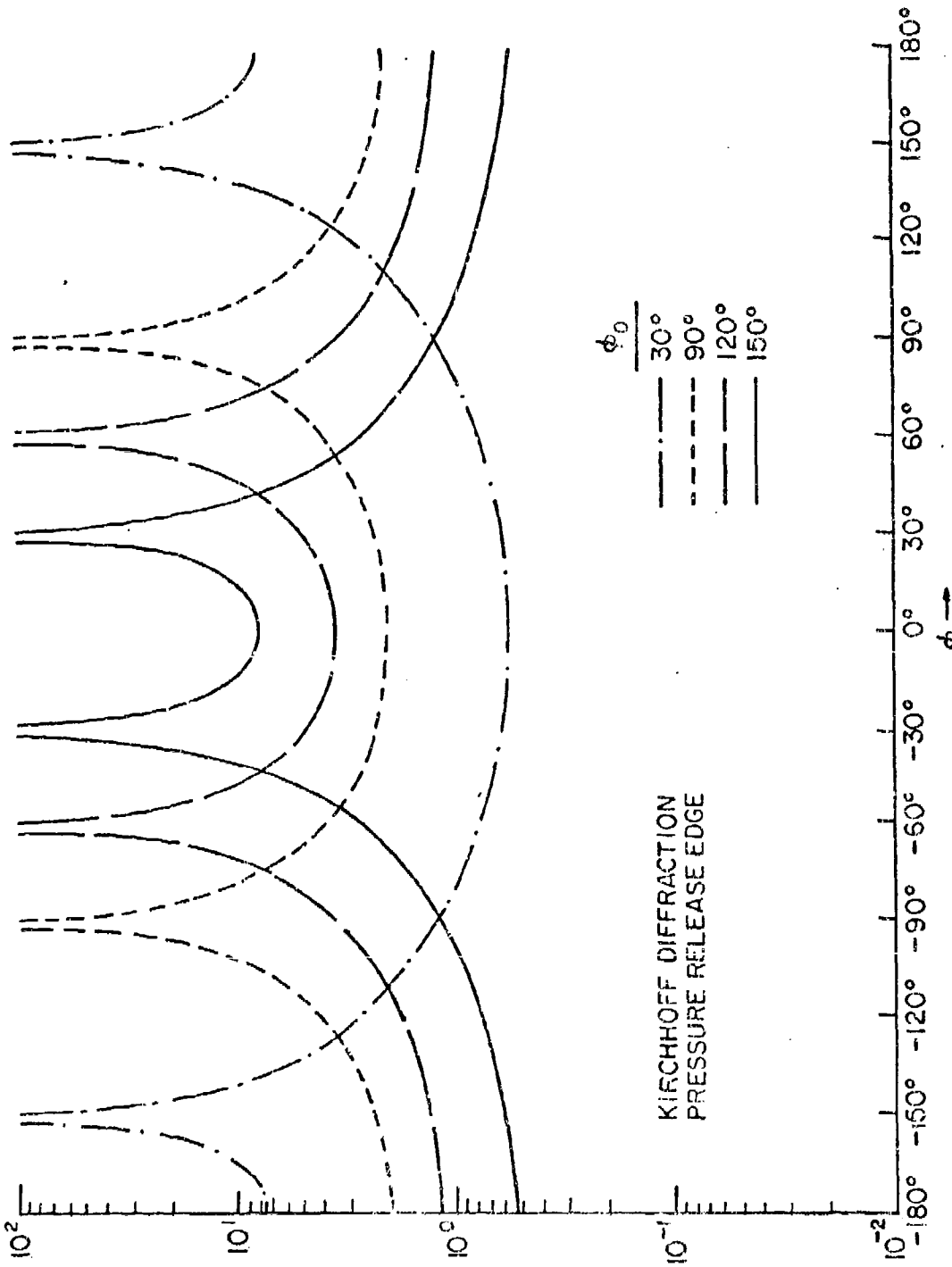

Figure 7.1e The Kirchhoff solution for a pressure release edge.

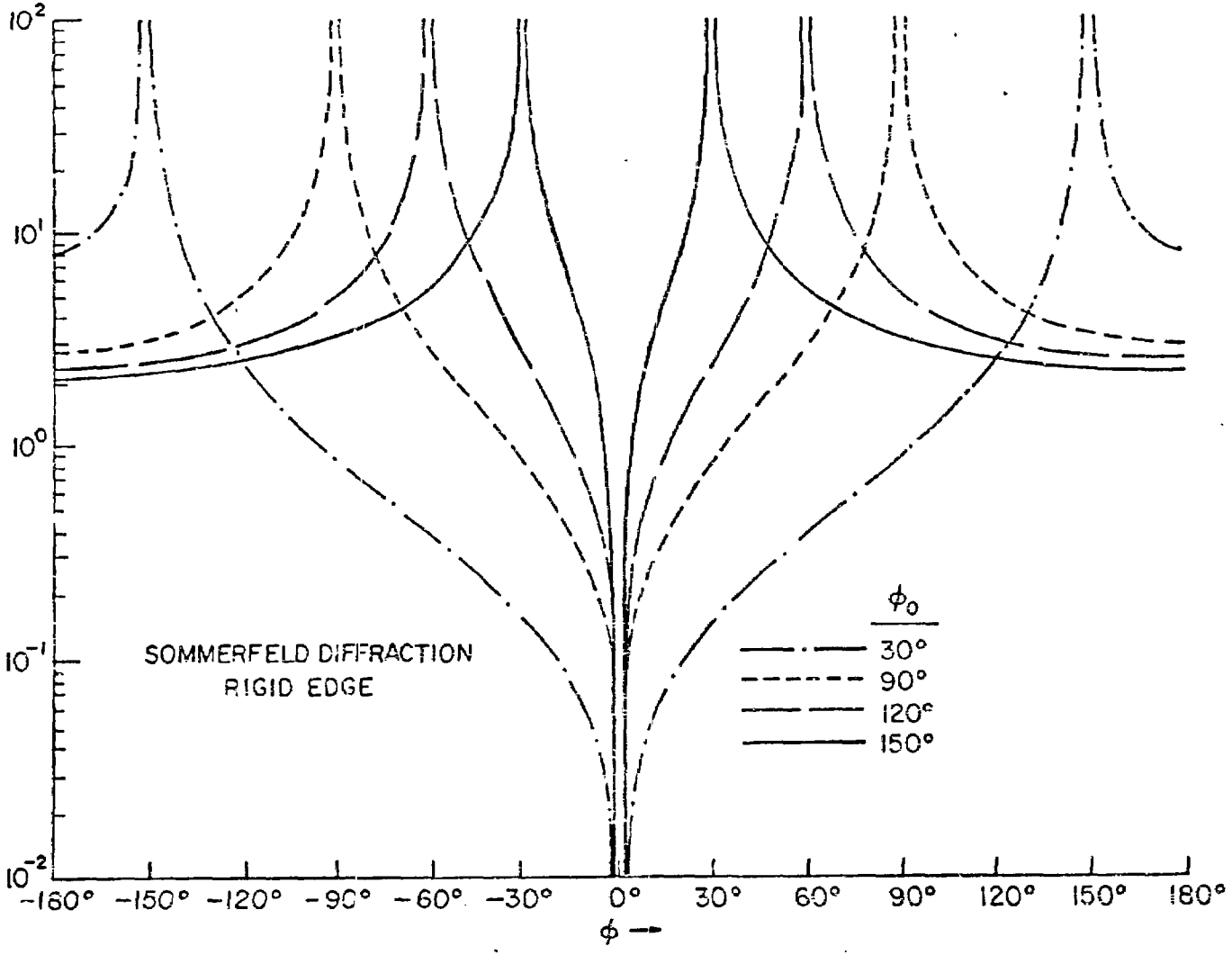

Figure 7.1f The Sommerfeld solution for a rigid edge.

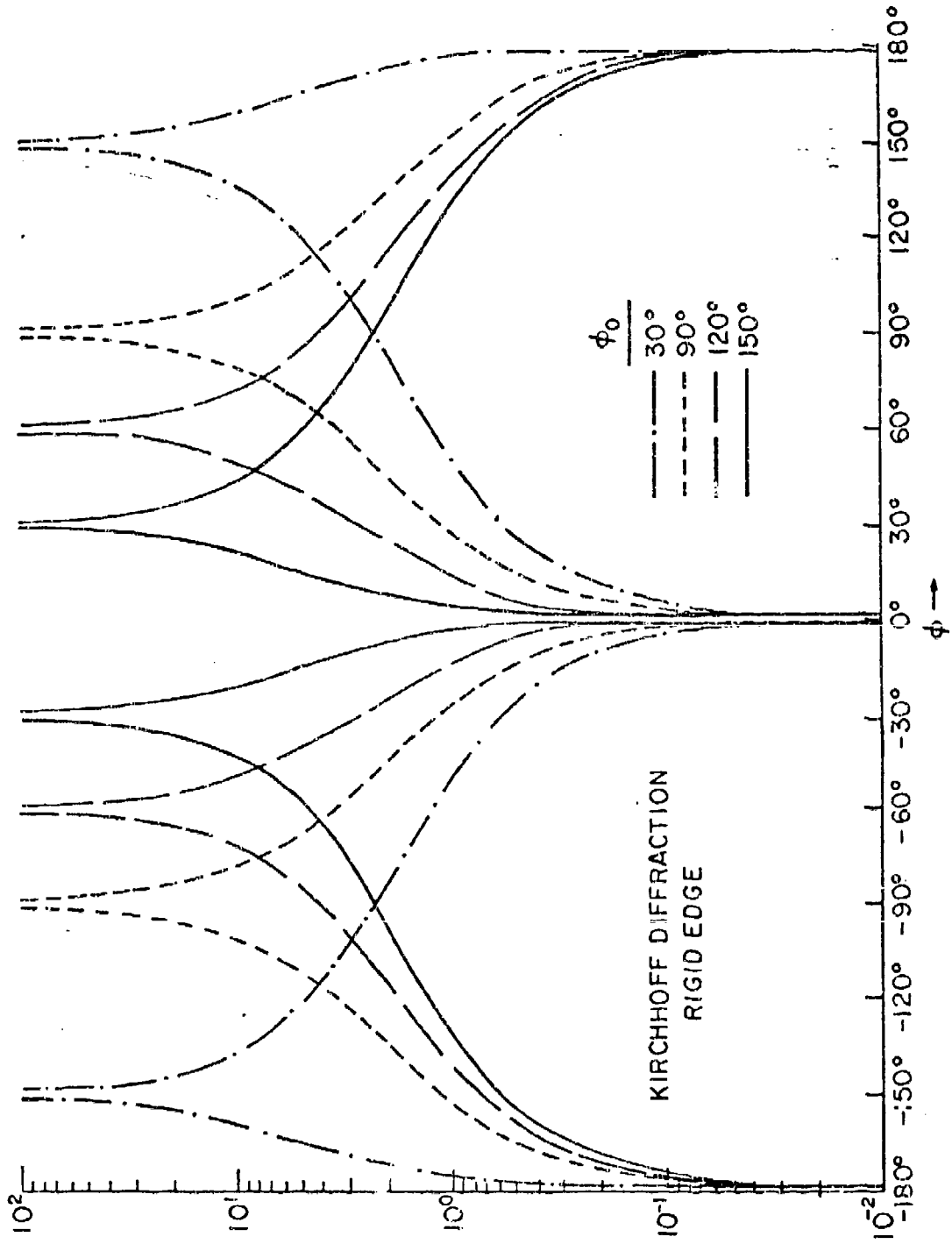

Figure 7.1g The Kirchhoff solution for a rigid edge.

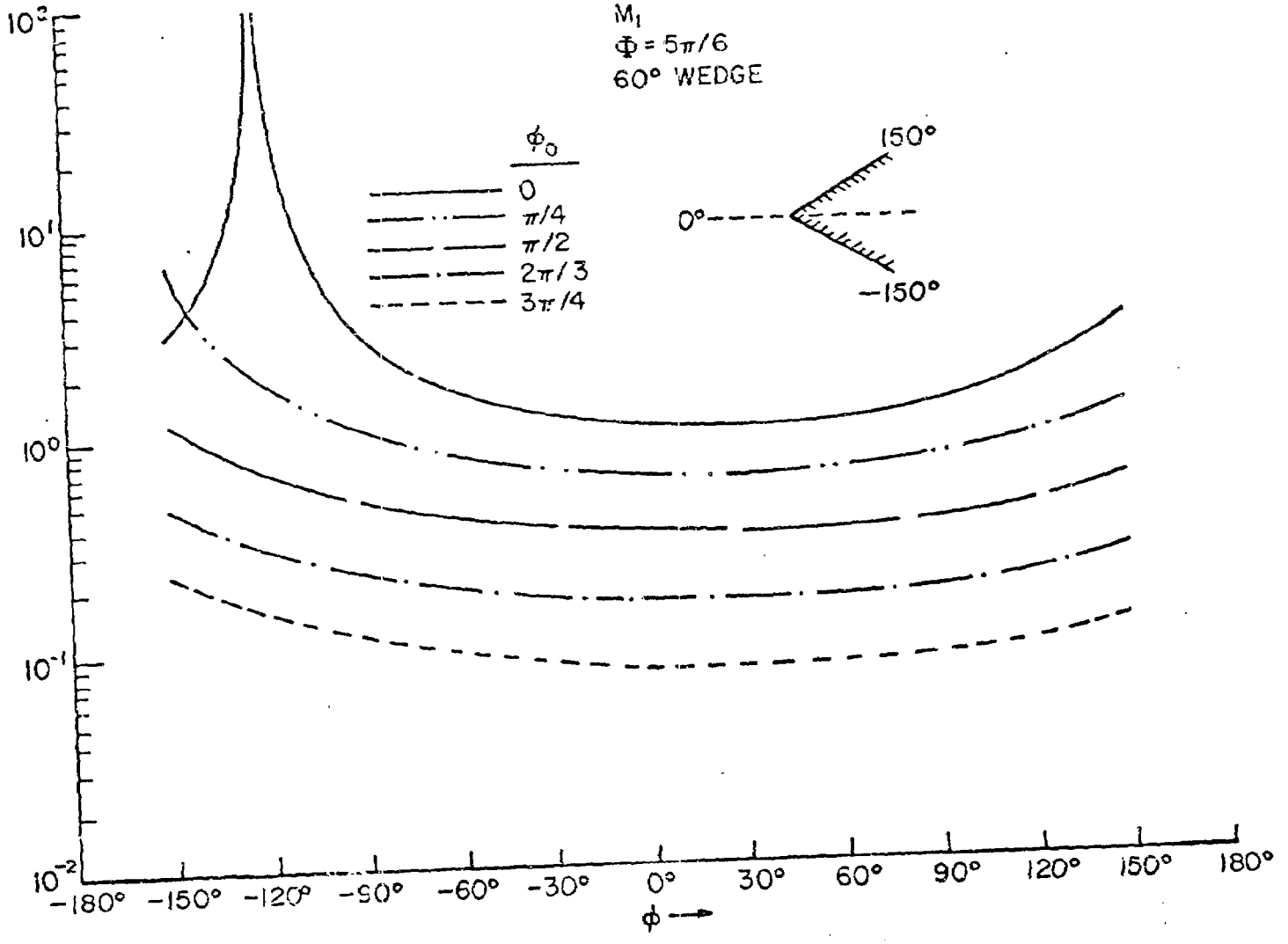

Figure 7.2a The Malyuzhinets angle function M_1 for a 60° wedge.

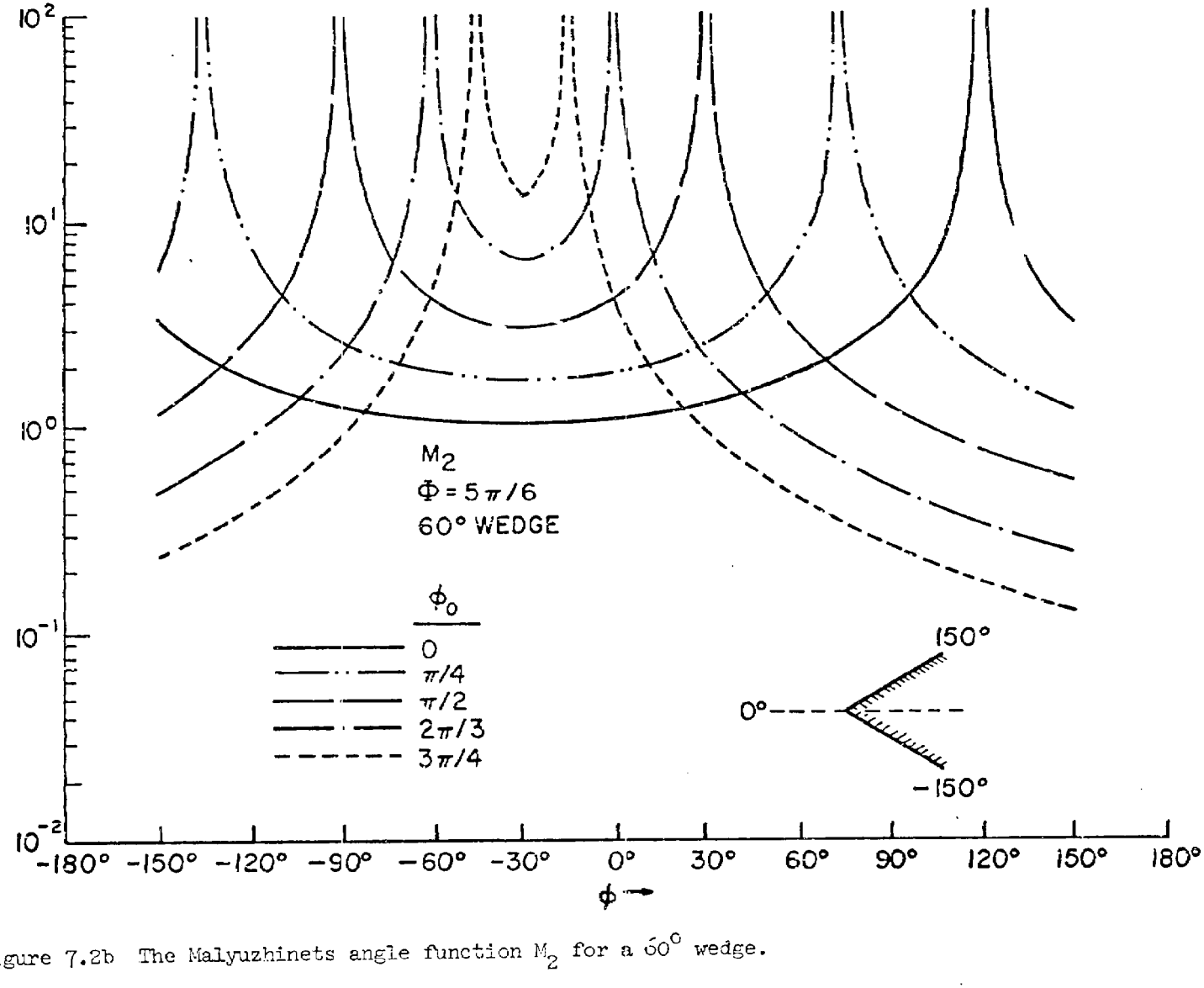

Figure 7.2b The Malyuzhinets angle function M_2 for a 60° wedge.

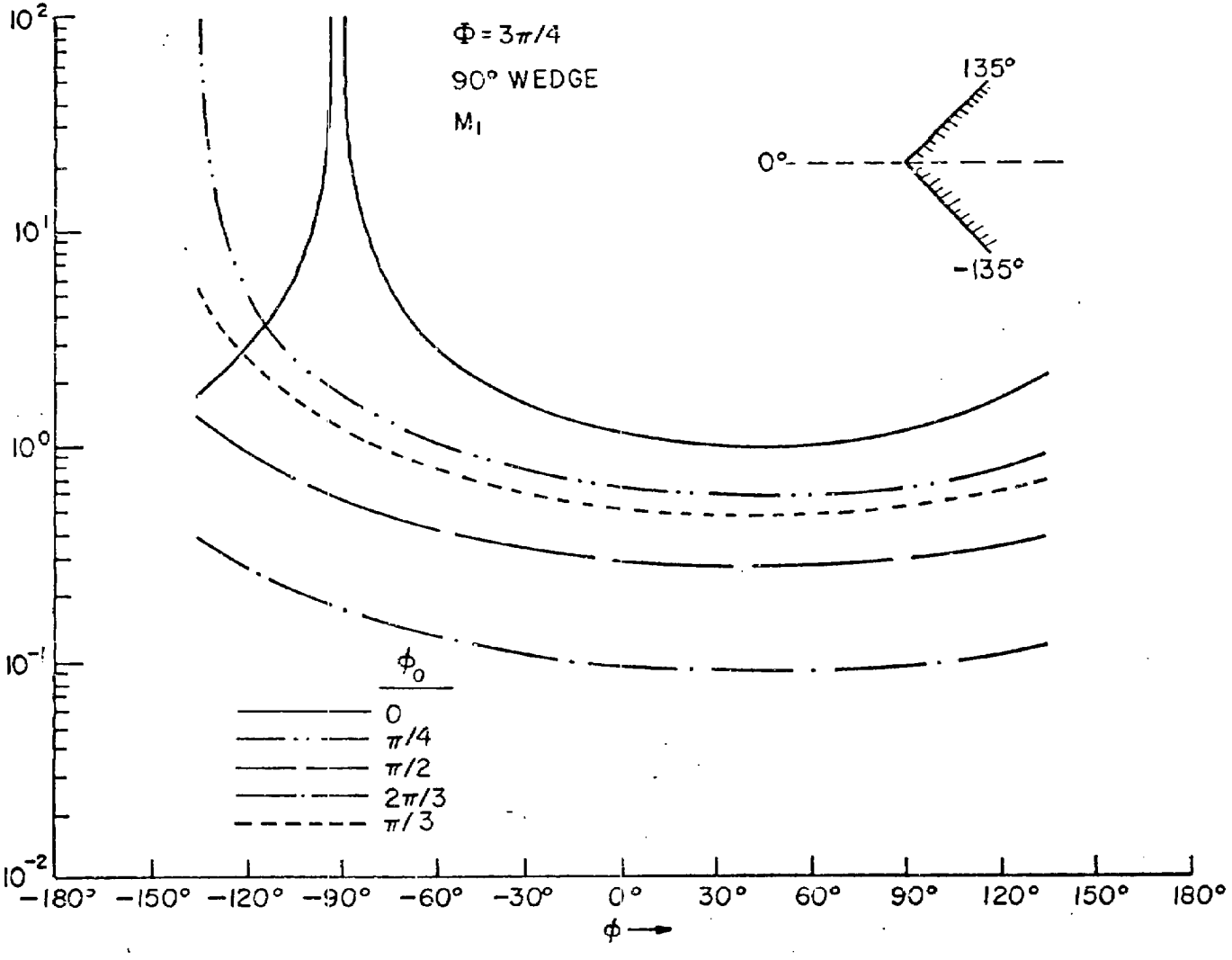

Figure 7.2c The Malyuzhinets angle function M_1 for a 90° wedge.

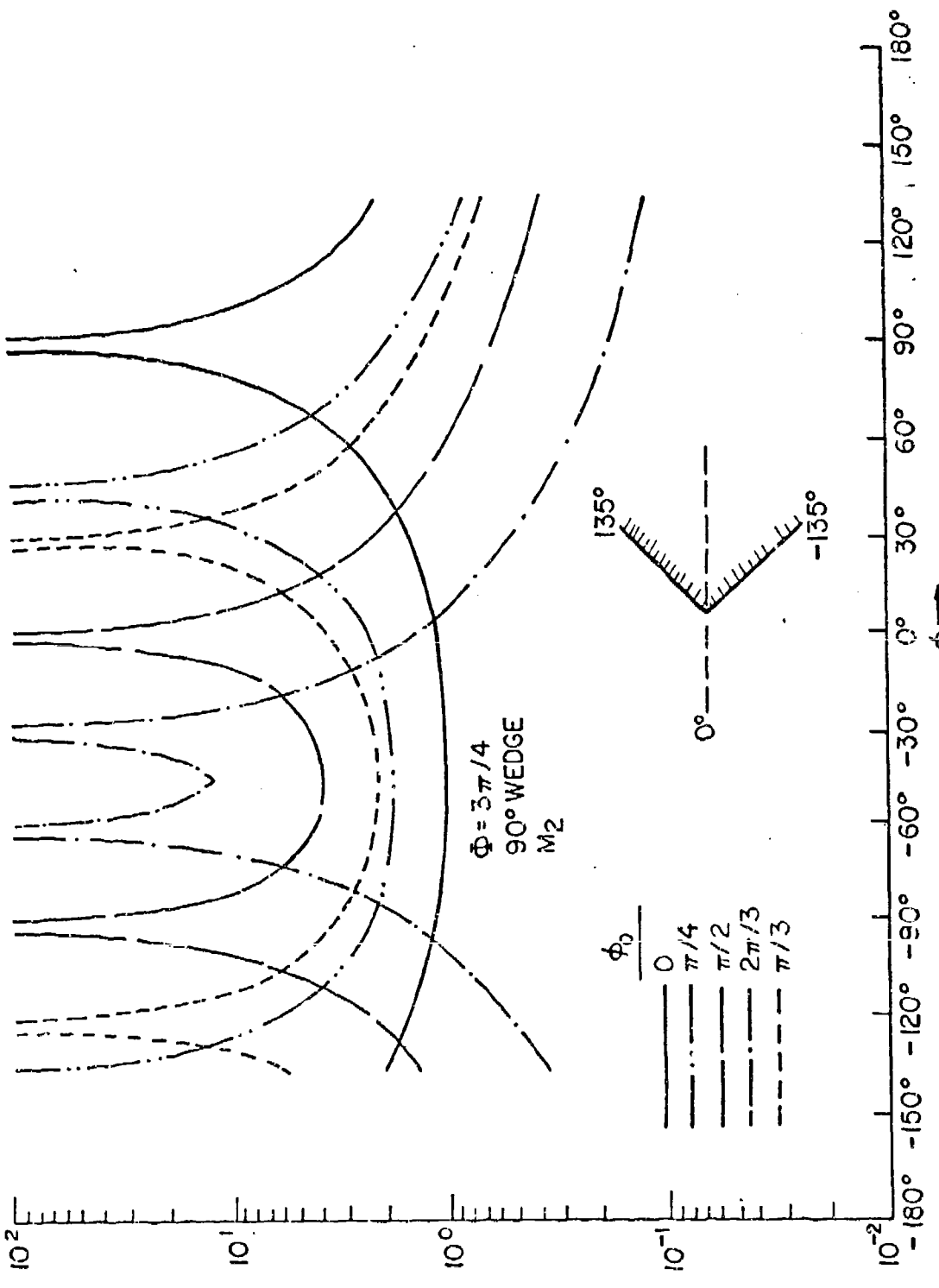

Figure 7.2d The Malyuzhinets angle function M_2 for a 90° wedge.

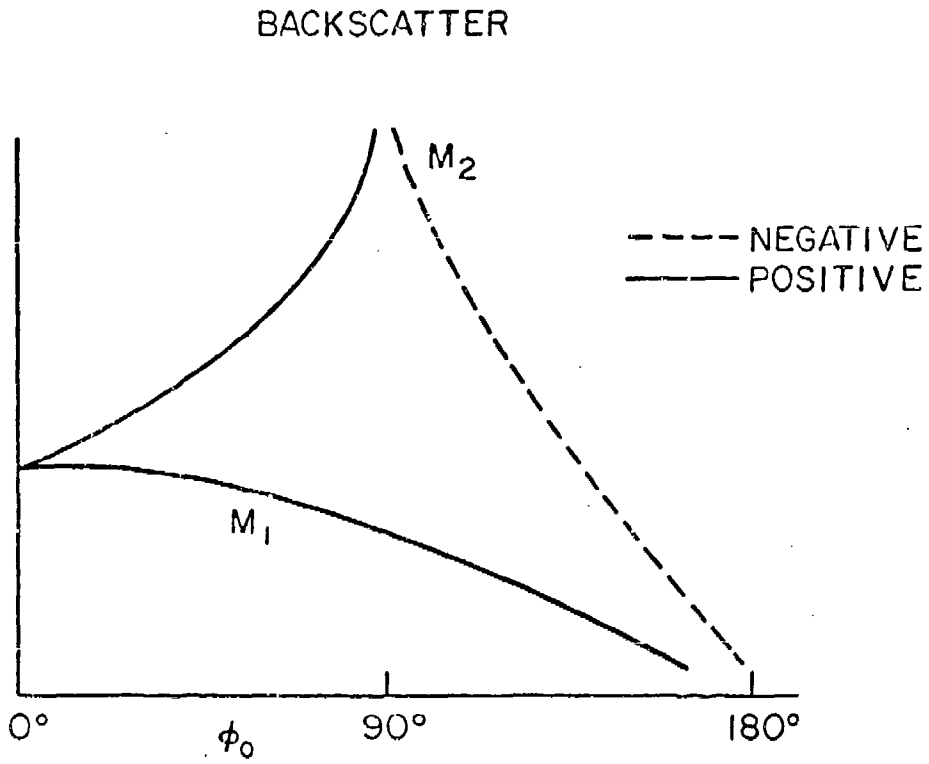

$$M_1 = \frac{-\cos\frac{\pi}{2\Phi}\,\phi_0}{\sin\frac{\pi}{2\Phi}\,(\phi_0-\pi) - \sin\frac{\pi}{2\Phi}\,\phi_0}$$

$$M_2 = \frac{\cos\frac{\pi}{2\Phi}\,\phi_0}{\sin\frac{\pi}{2\Phi}\,(\phi_0+\pi) - \sin\frac{\pi}{2\Phi}\,\phi_0}$$

Figure 7.3a M_1 and M_2, the angle factors for backscatter.

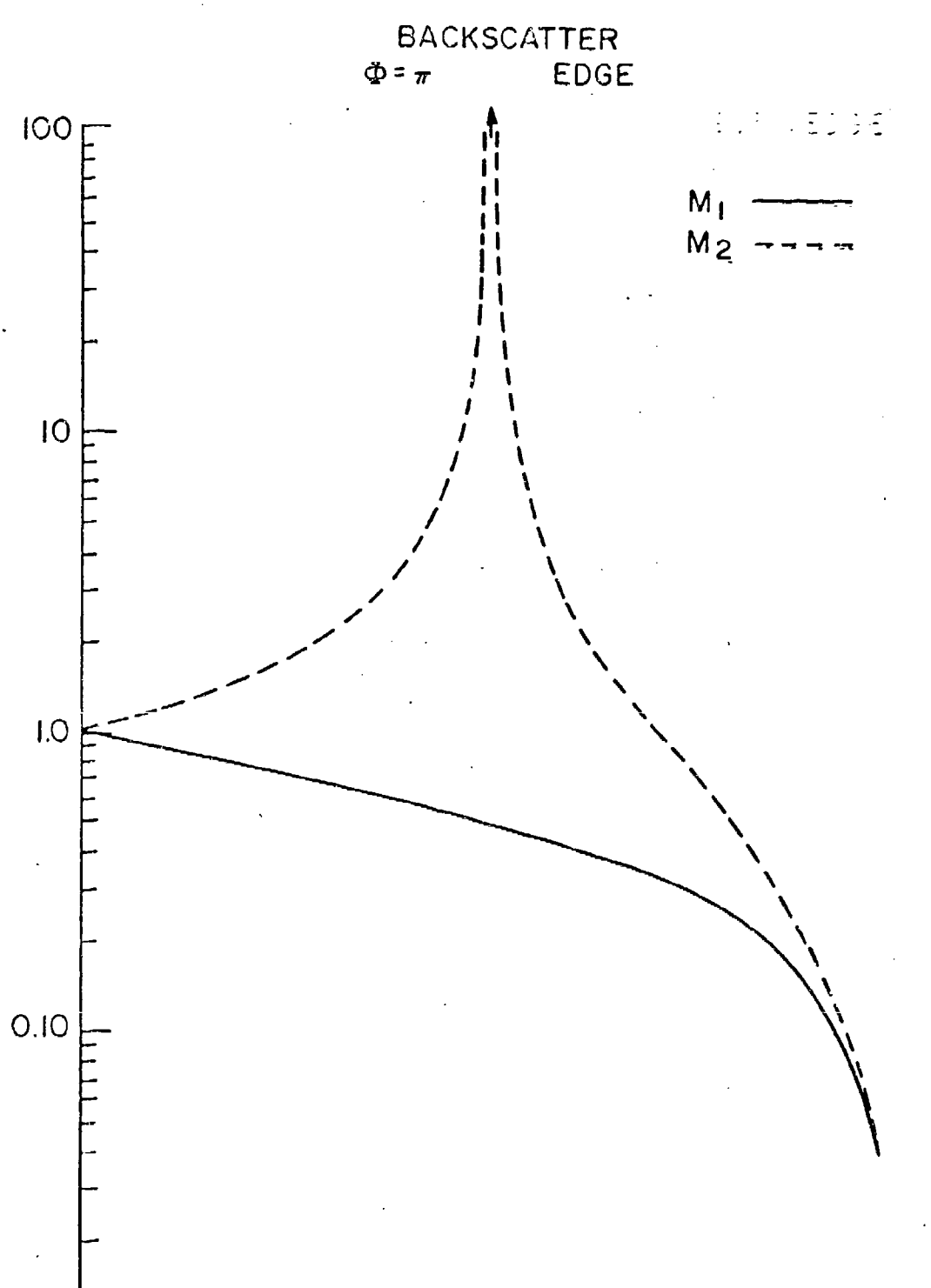

Figure 7.3b M_1 and M_2, the angle factors for backscatter from an edge.

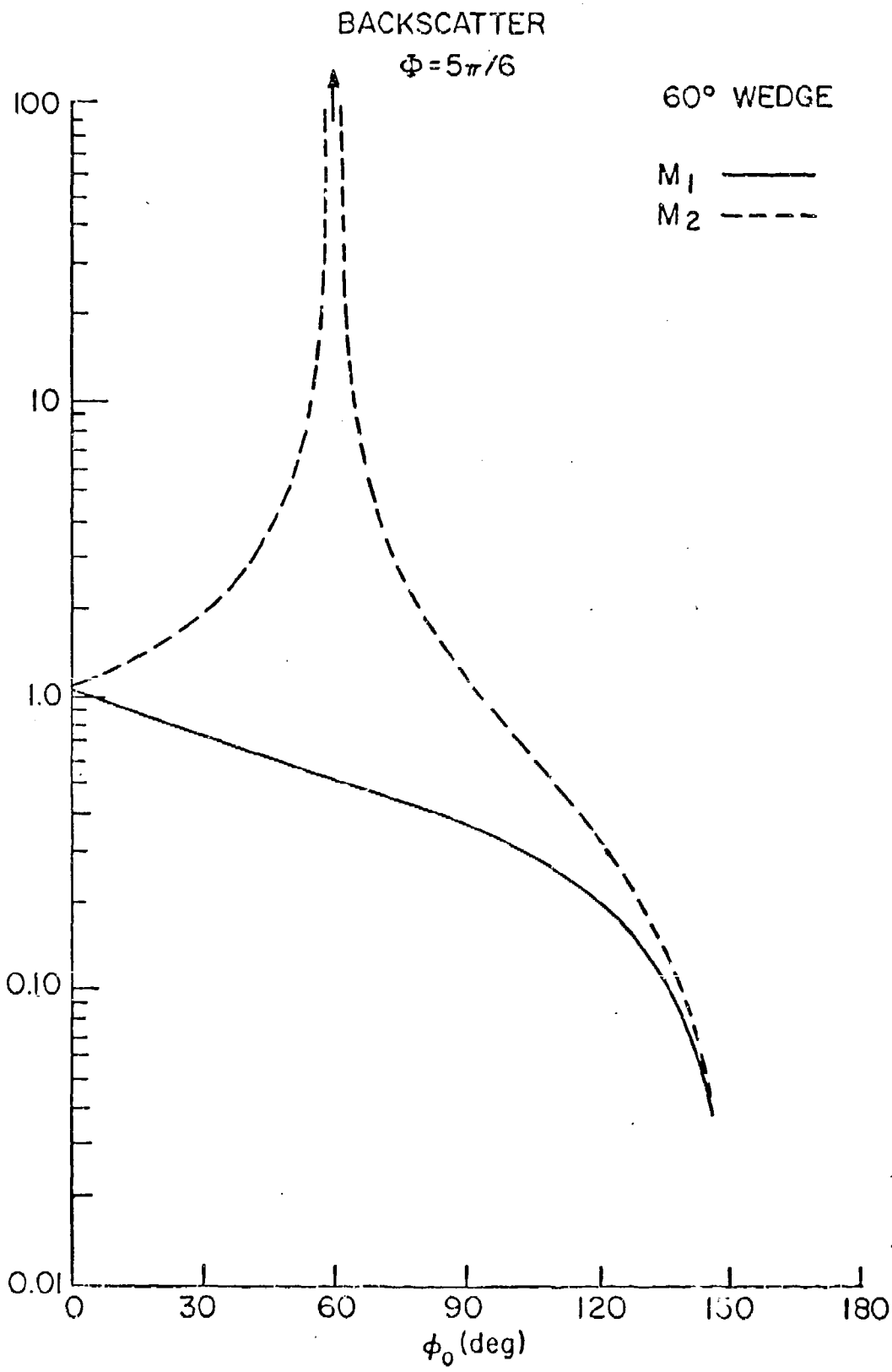

Figure 7.3c M_1 and M_2, the angle factors for backscatter from a 60° wedge.

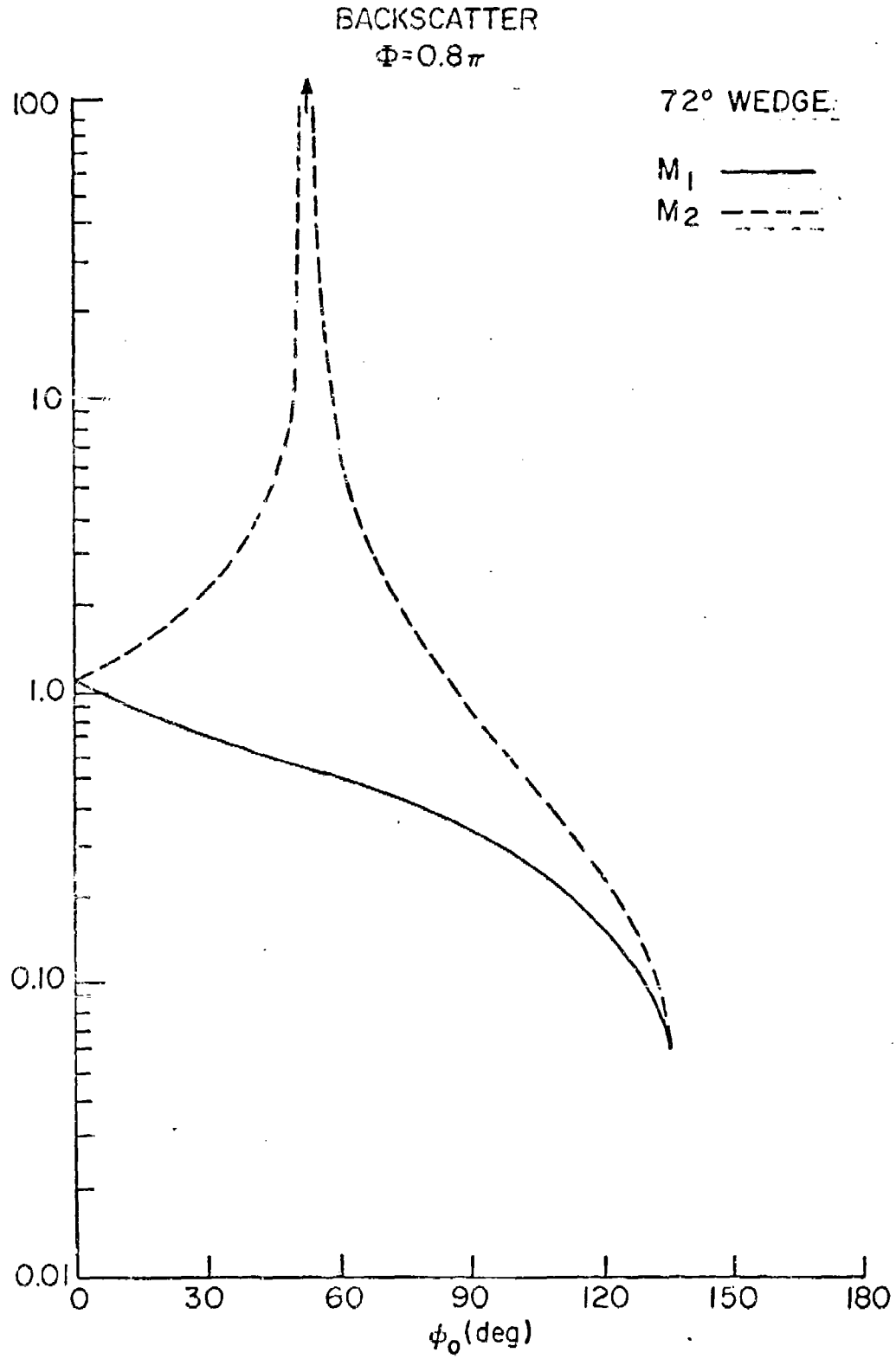

Figure 7.3d M_1 and M_2, the angle factors for backscatter from a 72° wedge.

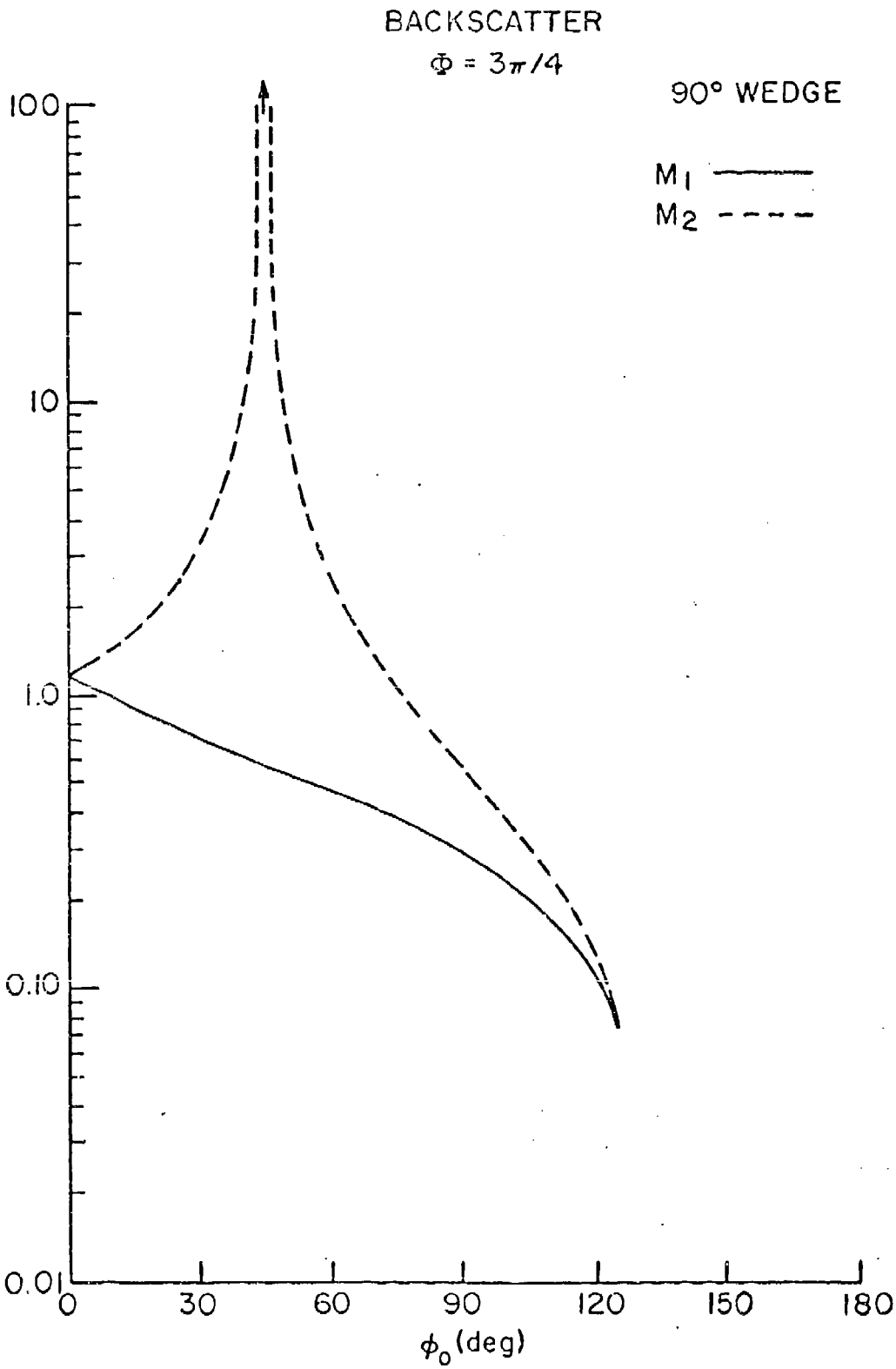

Figure 7.3e M_1 and M_2, the angle factors for backscatter from a 90° wedge.

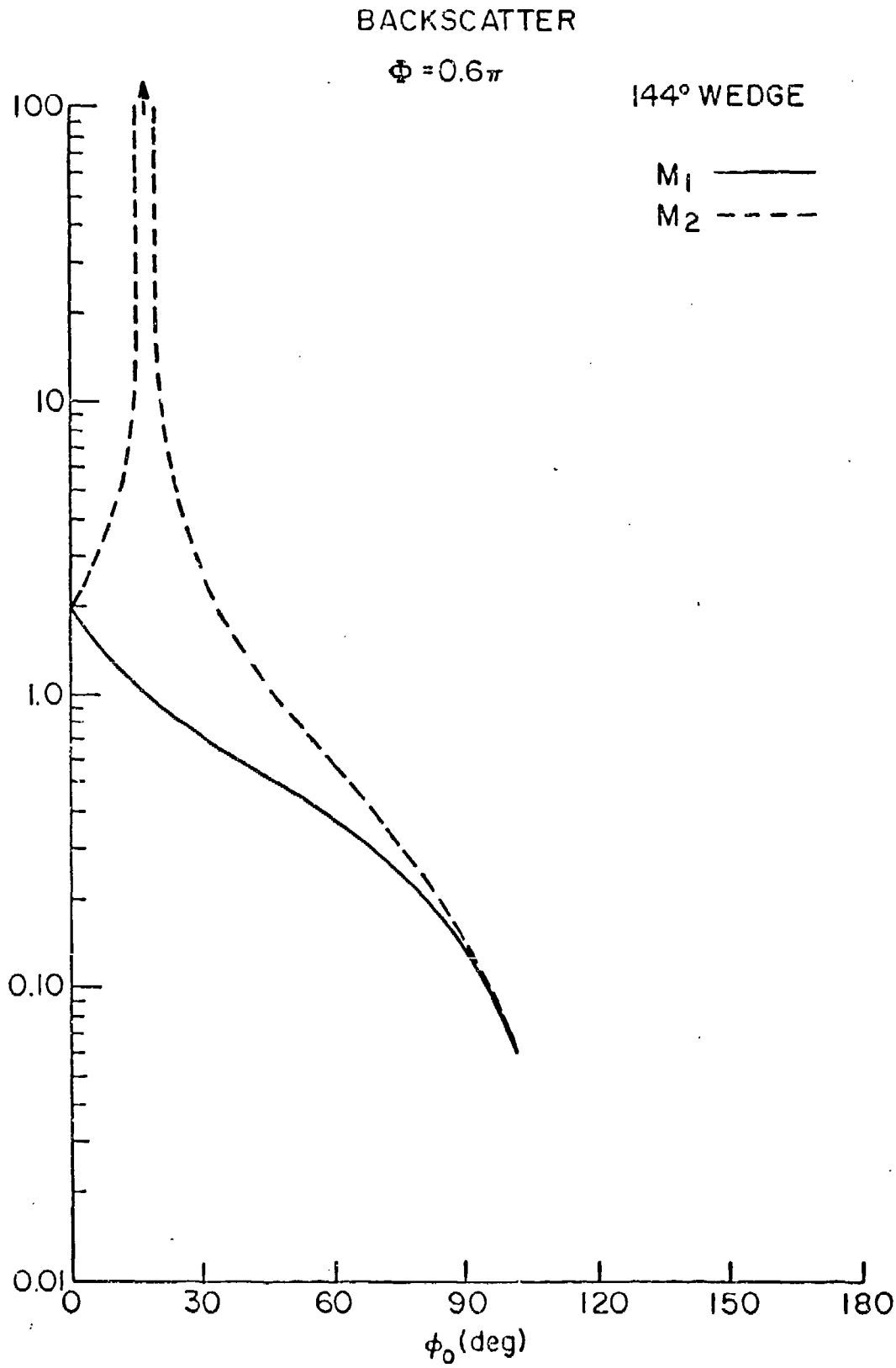

Figure 7.3f M_1 and M_2, the angle factors for backscatter from a 144° wedge.

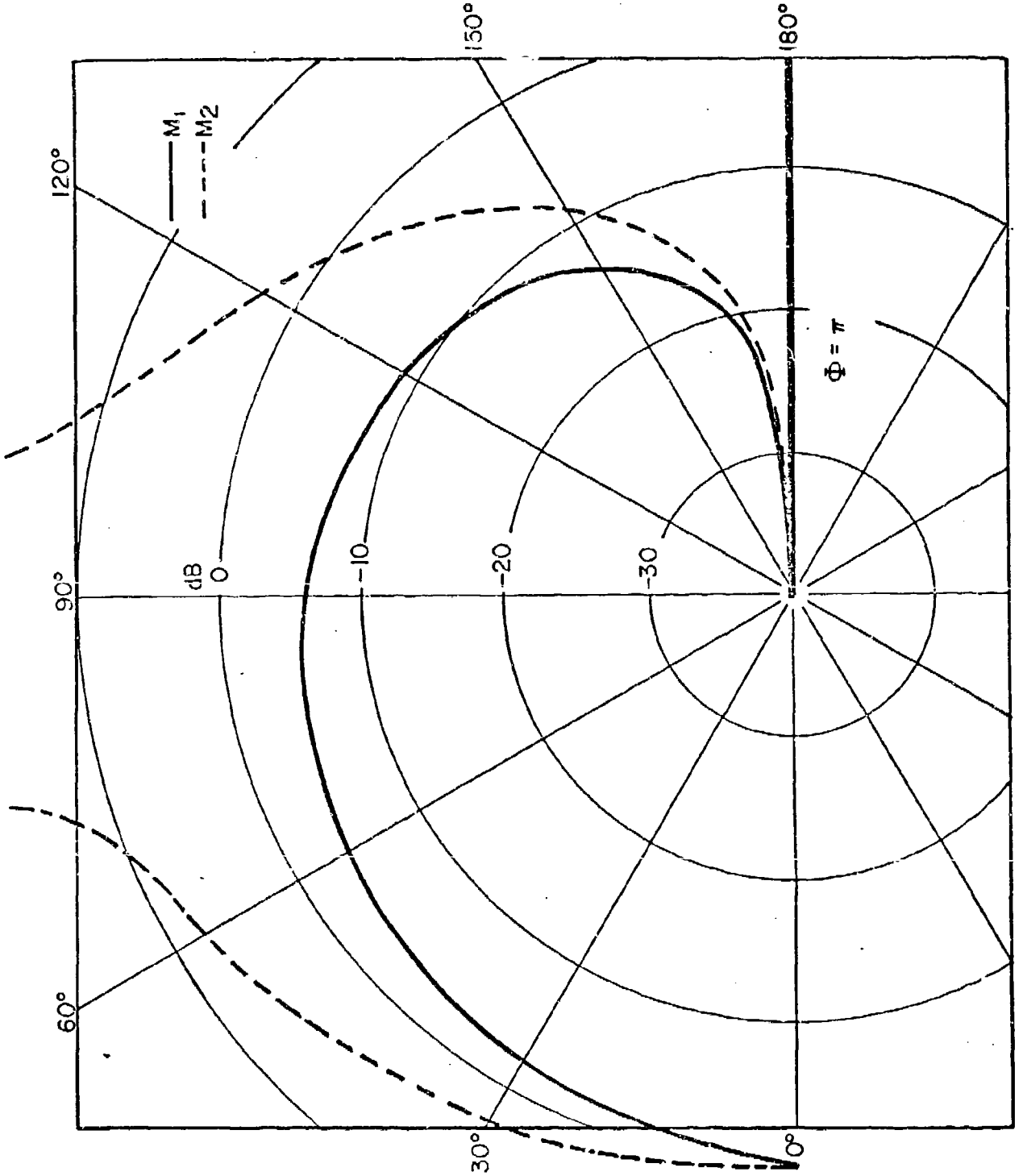

Figure 7.4a M_1 and M_2, the angle factors for backscatter from an edge, in polar form.

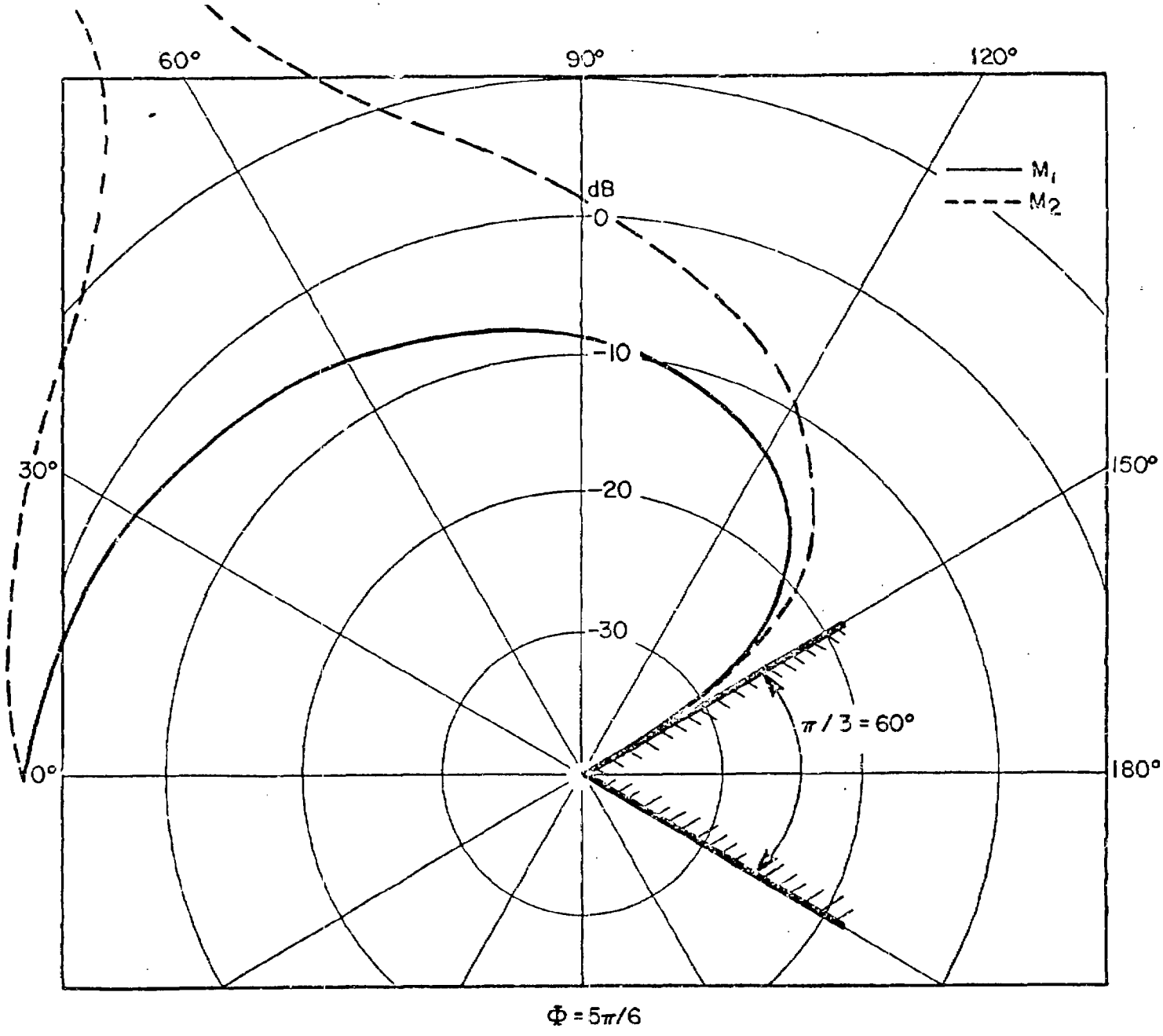

Figure 7.4b M_1 and M_2, the angle factors for backscatter from a 60° wedge, in polar form.

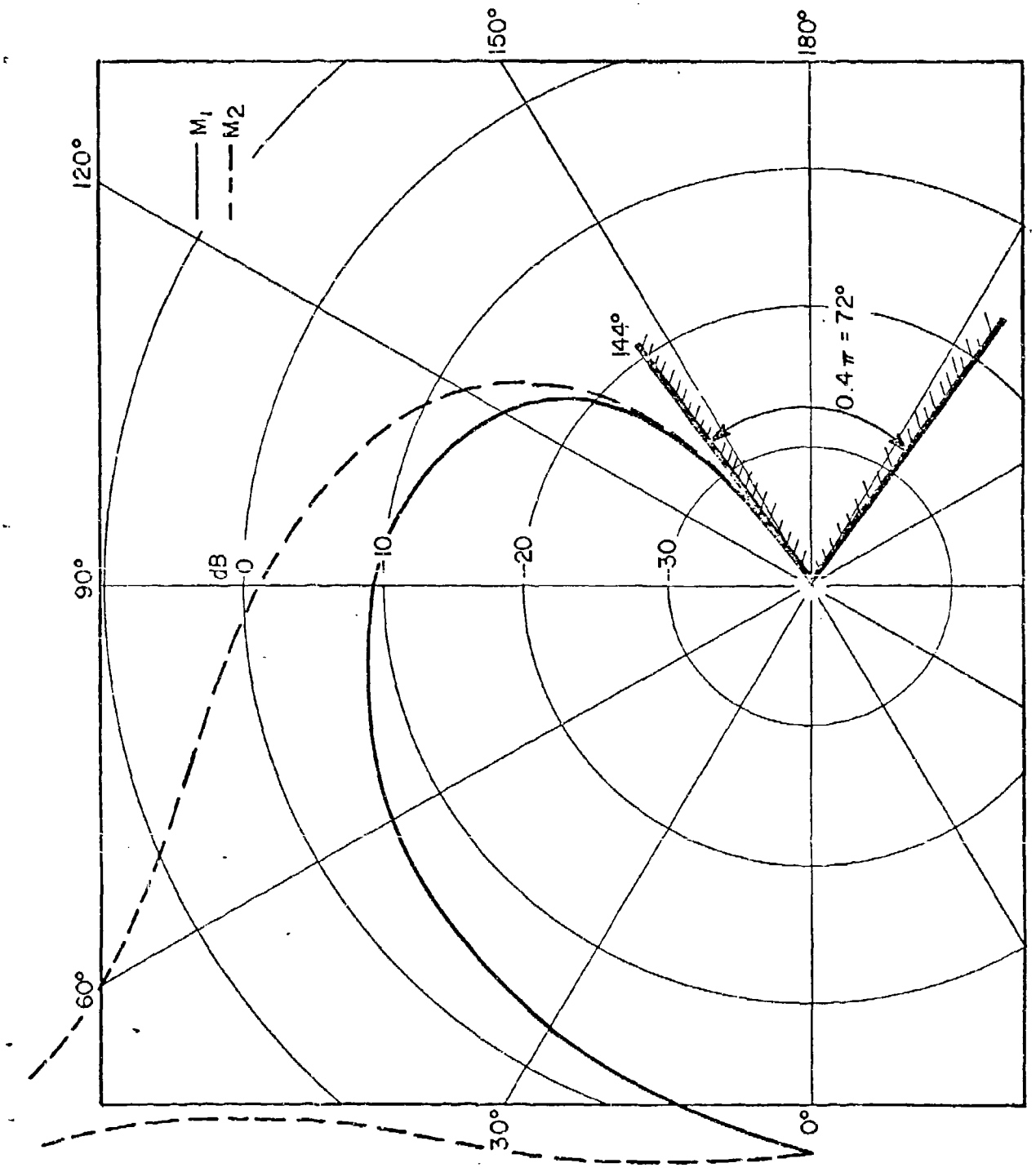

Figure 7.4c M_1 and M_2, the angle factors for backscatter from a 72° wedge, in polar form.

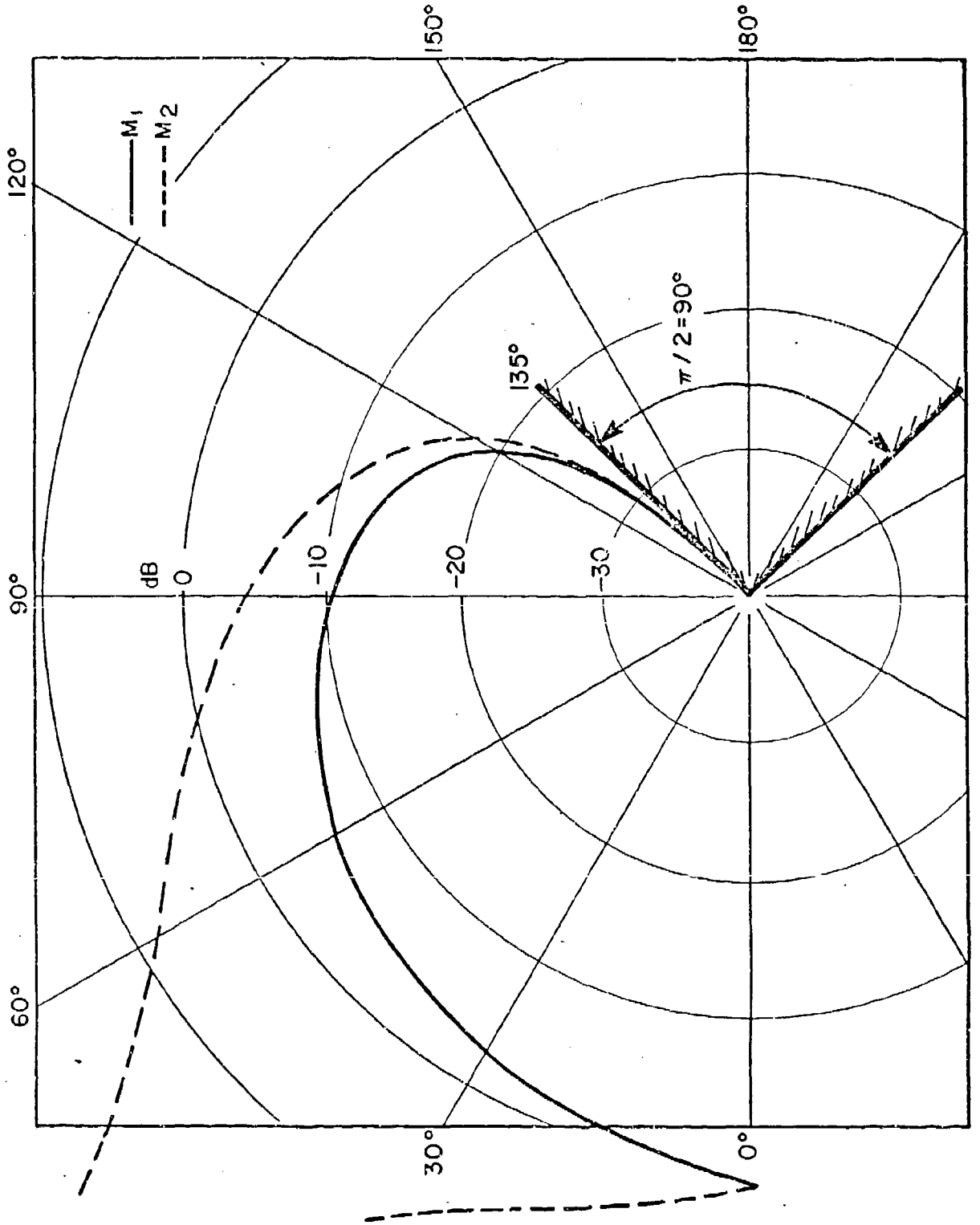

Figure 7.4d M_1 and M_2, the angle facotrs for backscatter from a 90° wedge, in polar form.

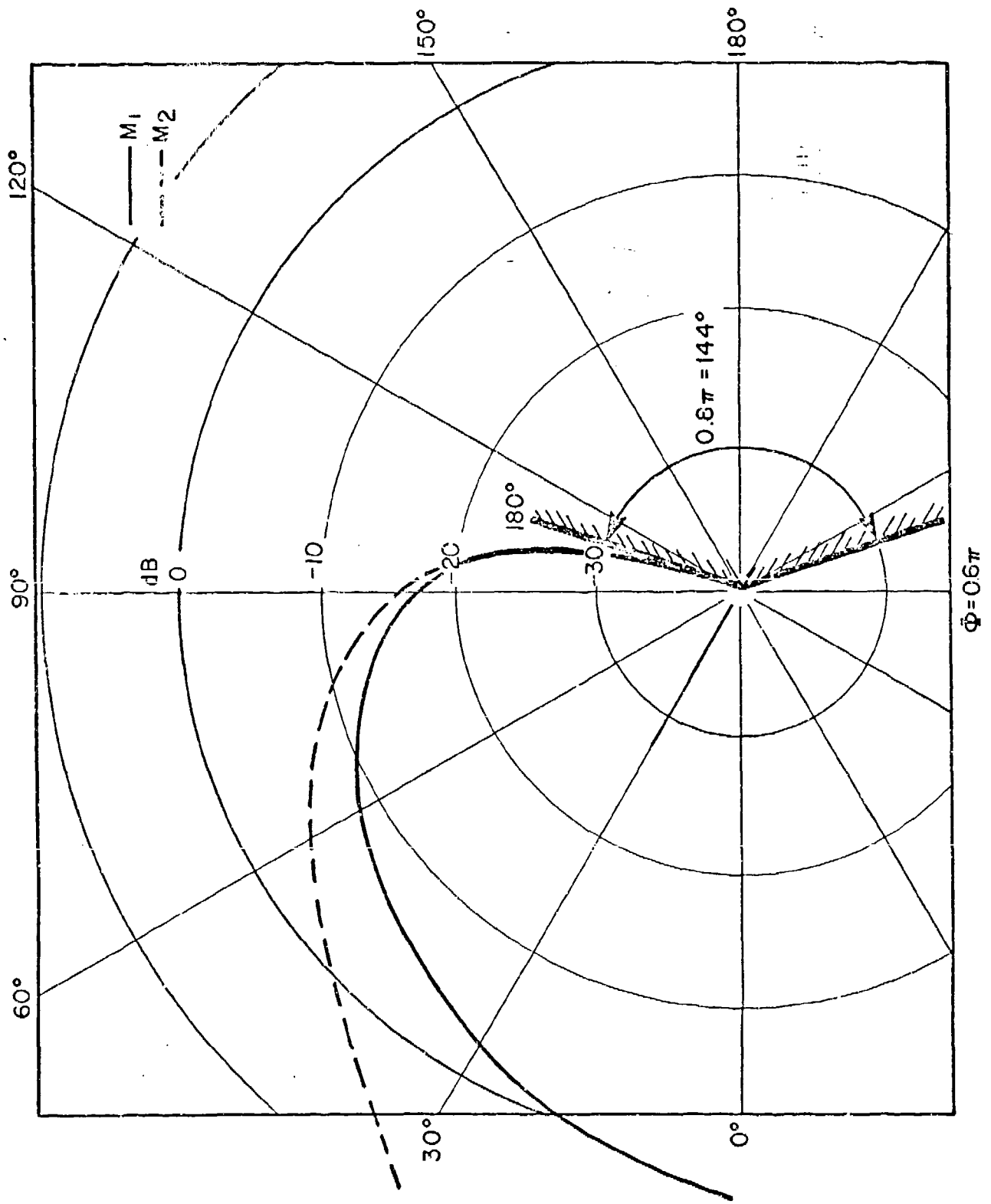

Figure 7.4e M_1 and M_2, the angle factors for backscatter from a 144° wedge, in polar form.

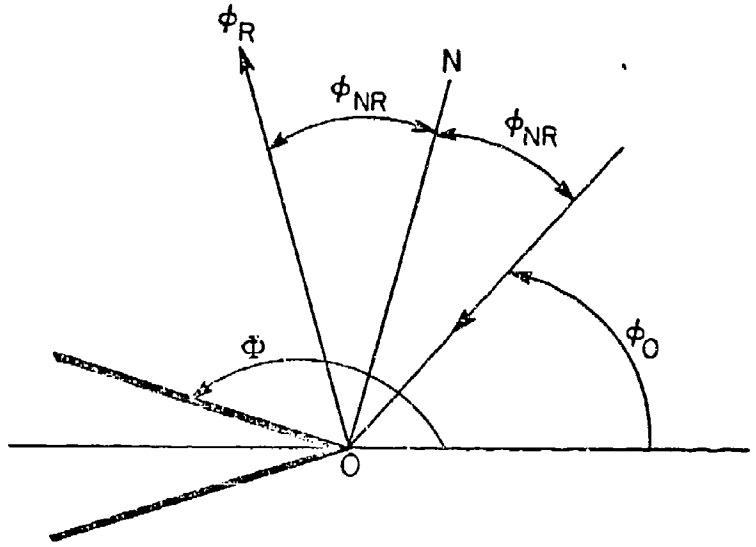

Figure 8.1 Reflection at the wedge surface Φ.

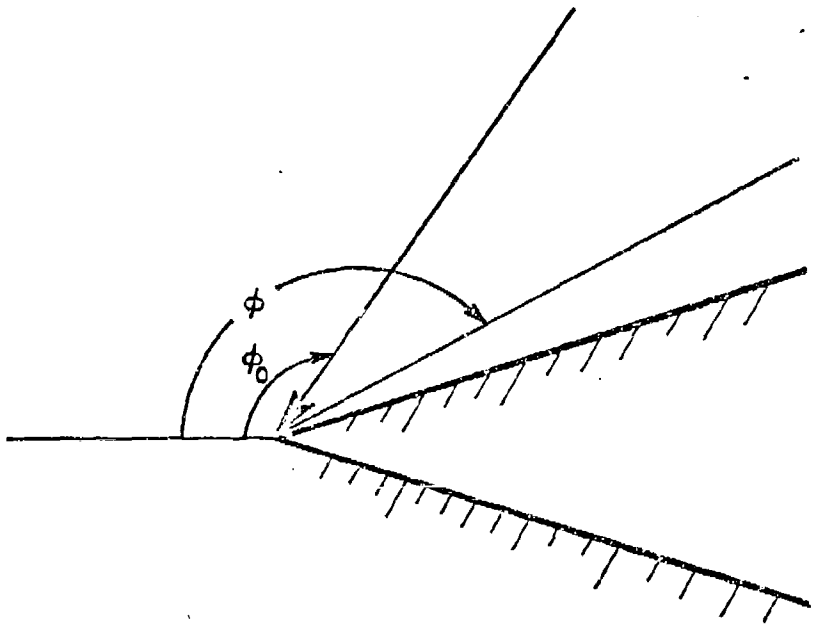

Figure 8,2 The angle of incidence ϕ_0 and the angle of exit ϕ for a wedge.

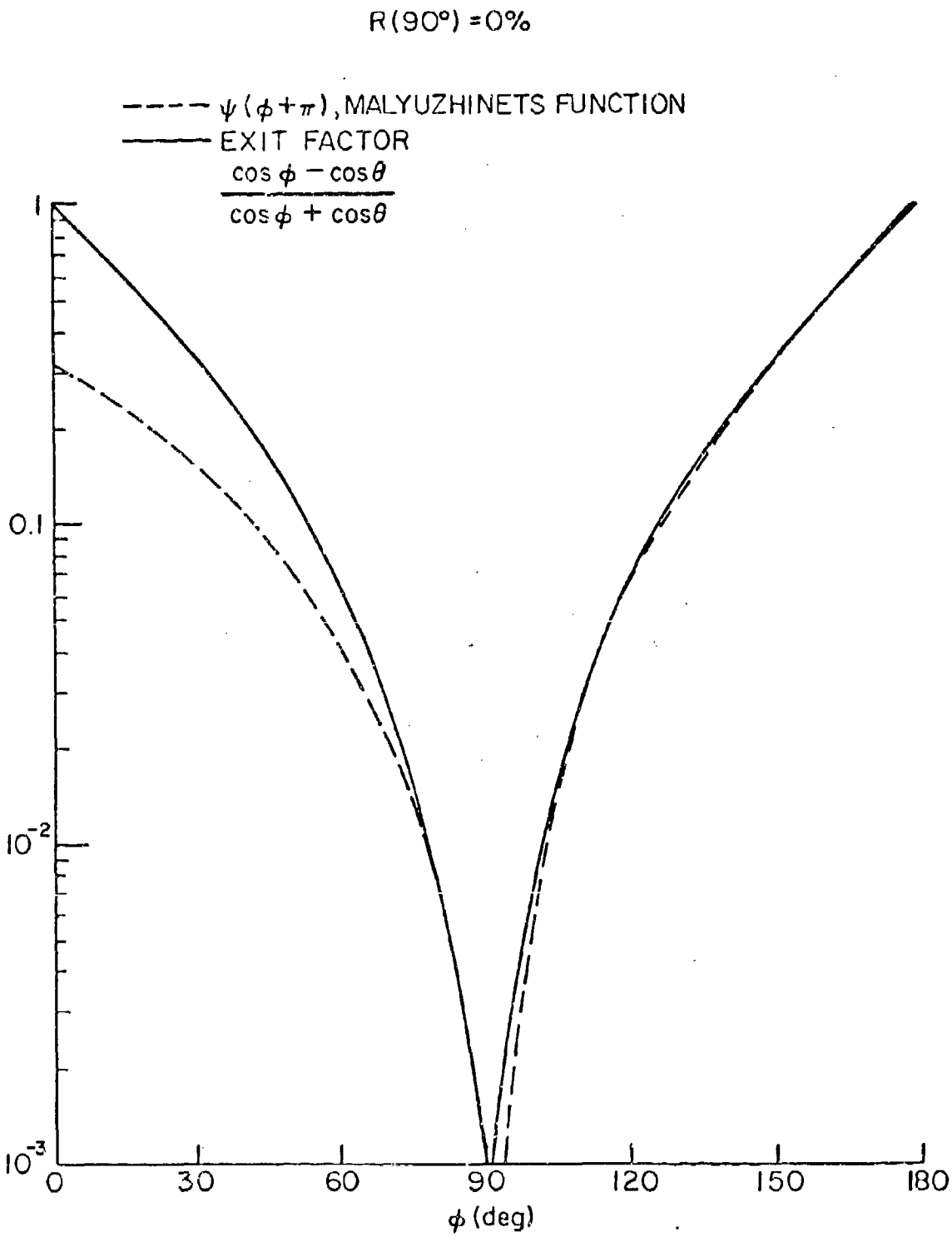

Figure 8.3a Comparison of the exit factor with the Malyuzhinets function. A constant multiplying the Malyuzhinets function is determined by having the two curves coincide for $\varphi = \pi - \varphi_0$.

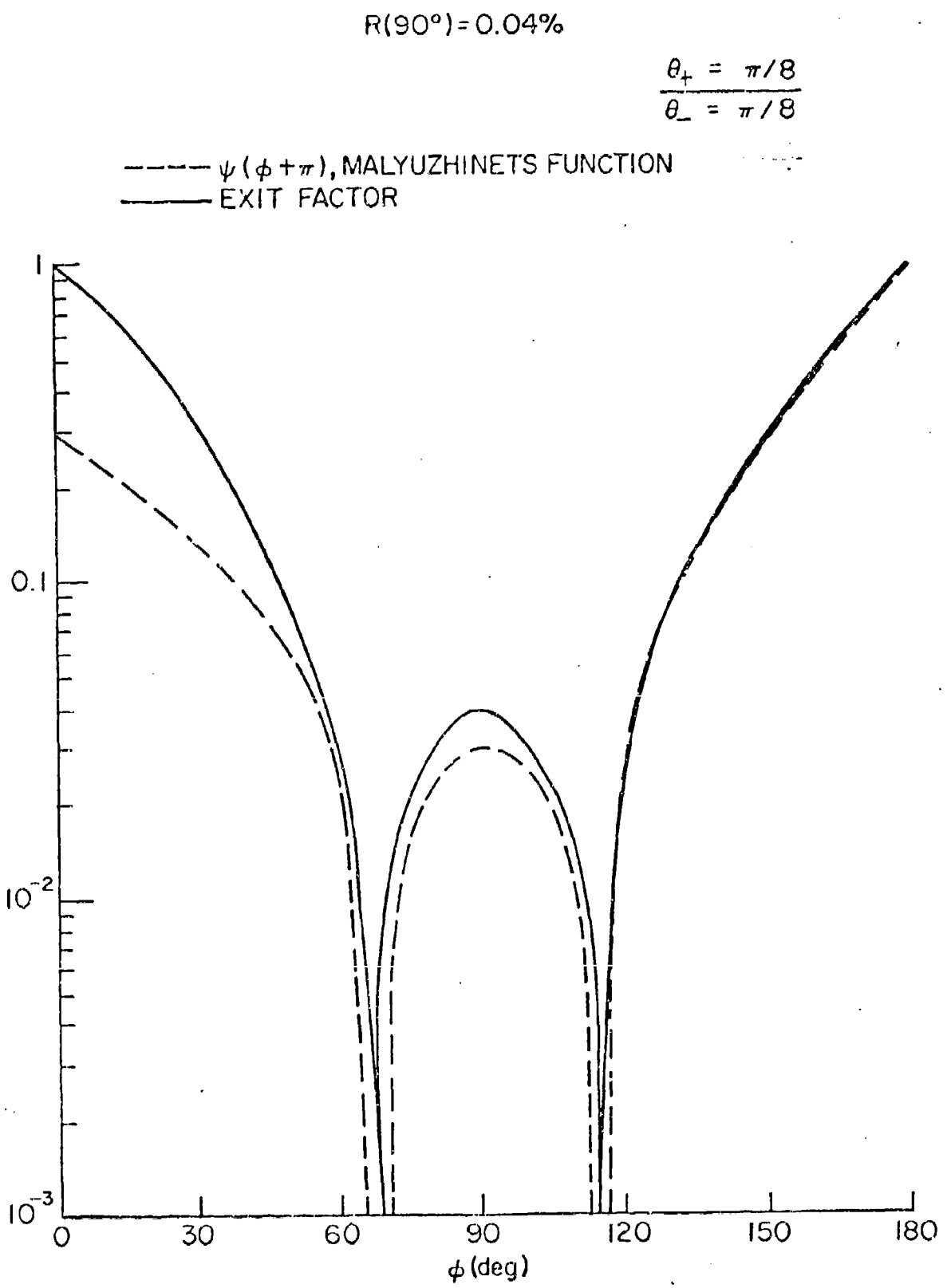

Figure 8.3b Comparison of the exit factor with the Malyuzhinets function. A constant multiplying the Malyuzhinets function is determined by having the two curves coincide for $\varphi = \pi - \varphi_0$.

$R(90°) = 17.2\%$

$\theta_+ = \pi/4$

$\theta_- = \pi/4$

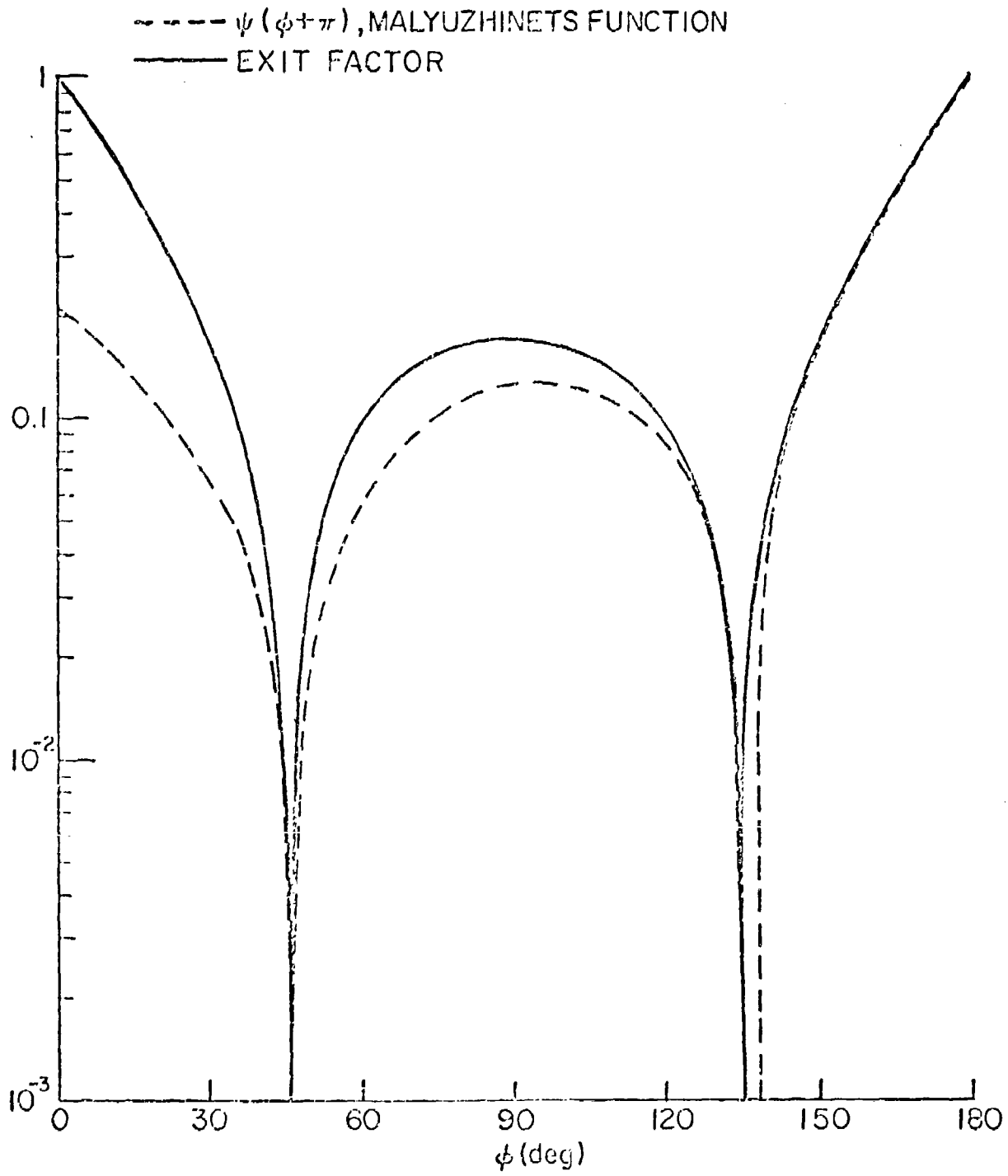

Figure 8.3c Comparison of the exit factor with the Malyuzhinets function. A constant multiplying the Malyuzhinets function is determined by having the two curves coincide for $\varphi = \pi - \varphi_o$.

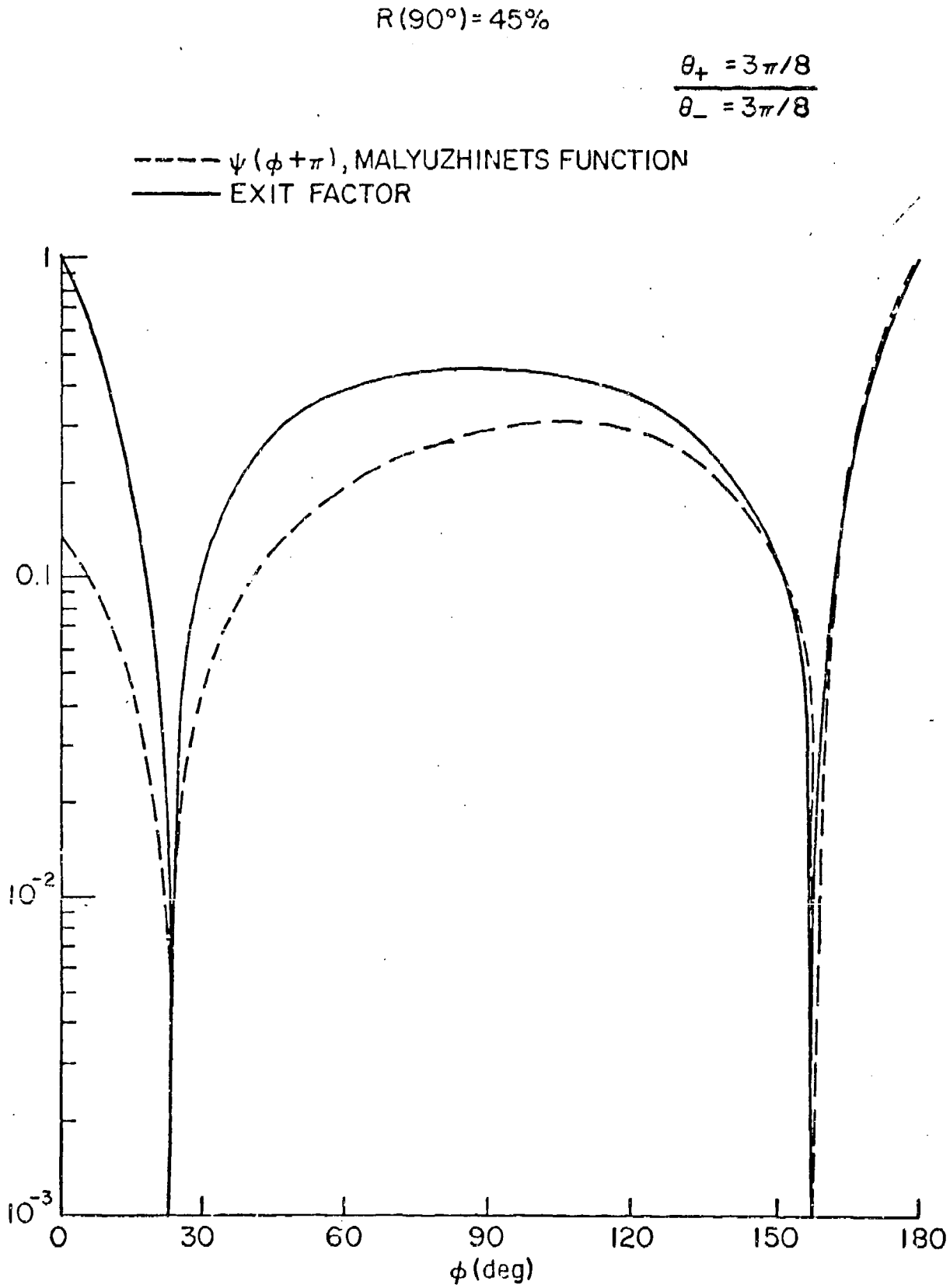

Figure 8.3d Comparison of the exit factor with the Malyuzhinets function. A constant multiplying the Malyuzhinets function is determined by having the two curves coincide for $\varphi = \pi - \varphi_o$.

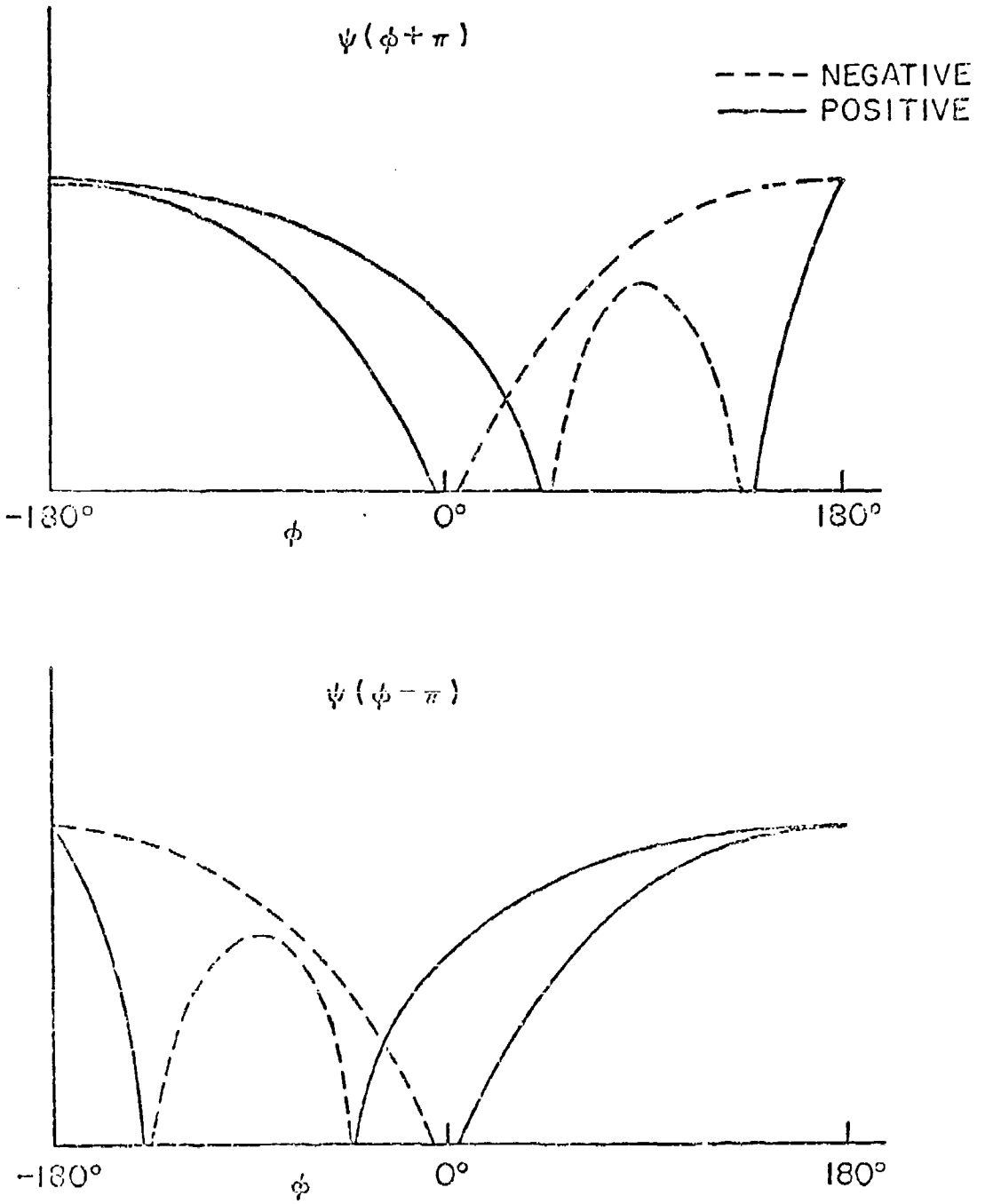

Figure 9.1a The basic shapes and the signs of the functions $\psi(\varphi - \pi)$ and $\psi(\varphi + \pi)$.

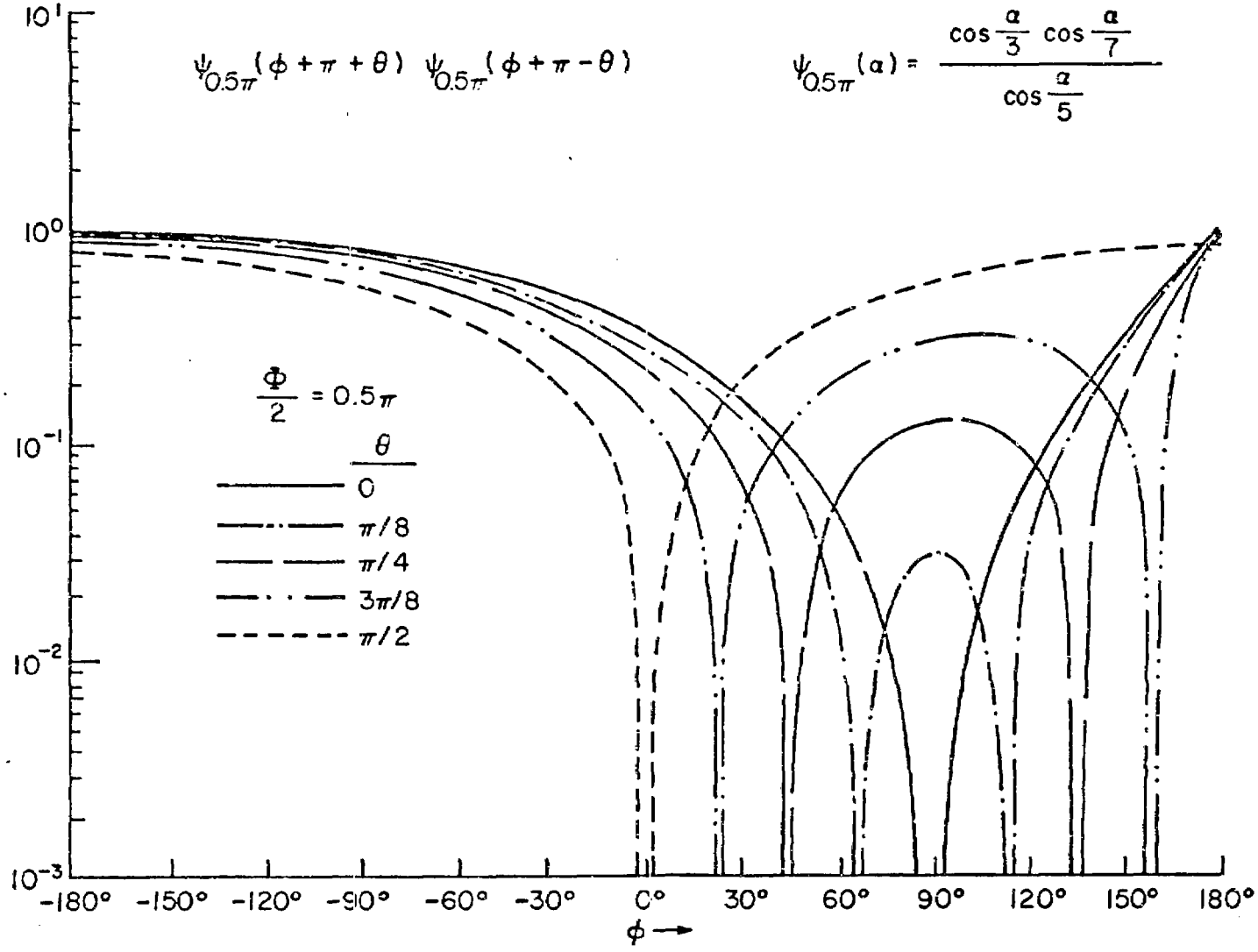

Figure 9.1b$_1$ The product of the $\psi(\varphi + \pi)$ functions for a straight edge for various Brewster angles θ.

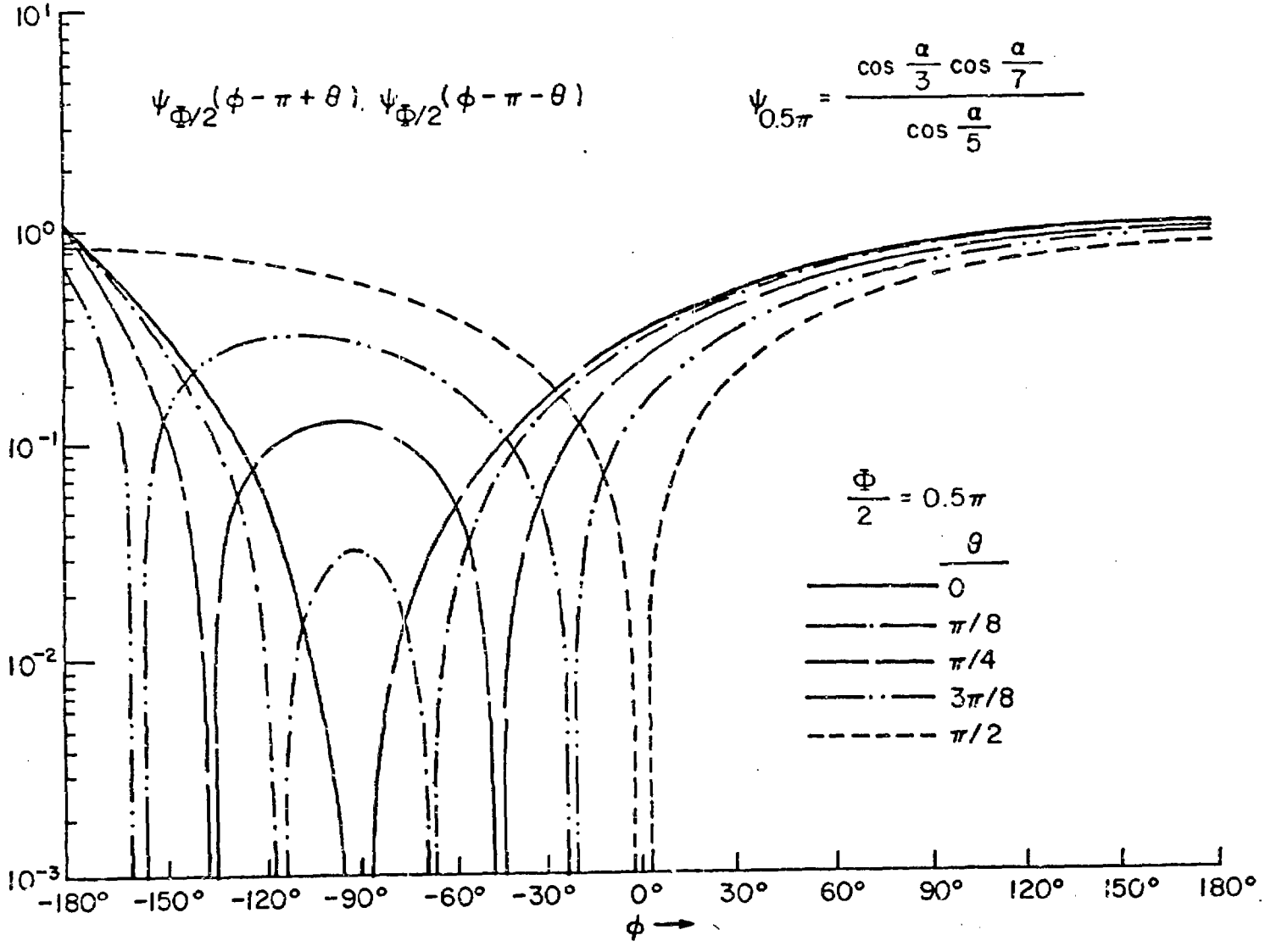

Fig. $9.1b_2$ The product of the $\psi(\varphi - \pi)$ functions for a straight edge for various Brewster angles θ.

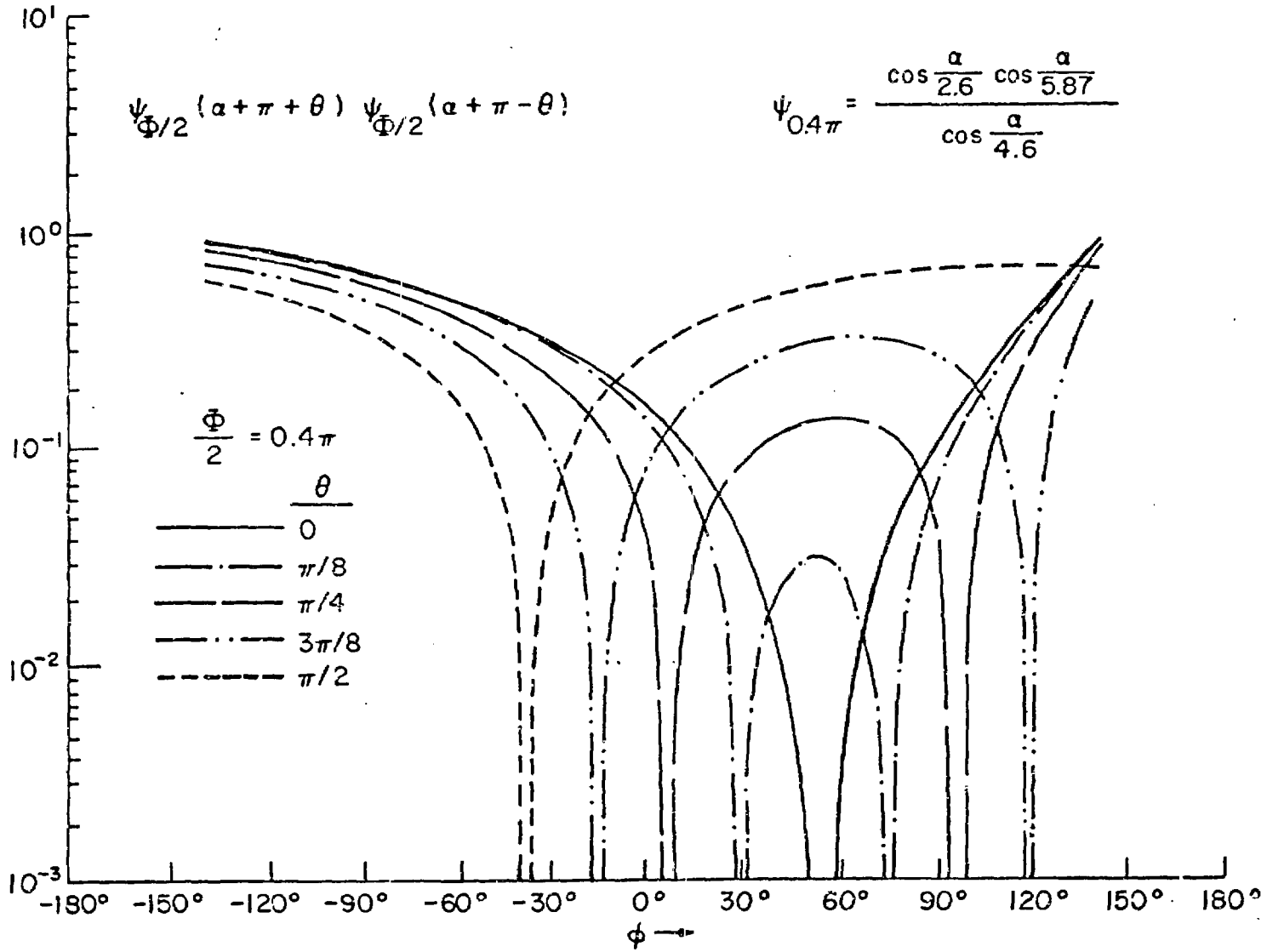

Figure 9.1c$_1$ The product of the $\psi(\varphi + \pi)$ functions for a wedge of solid angle 0.8π for various Brewster angles θ.

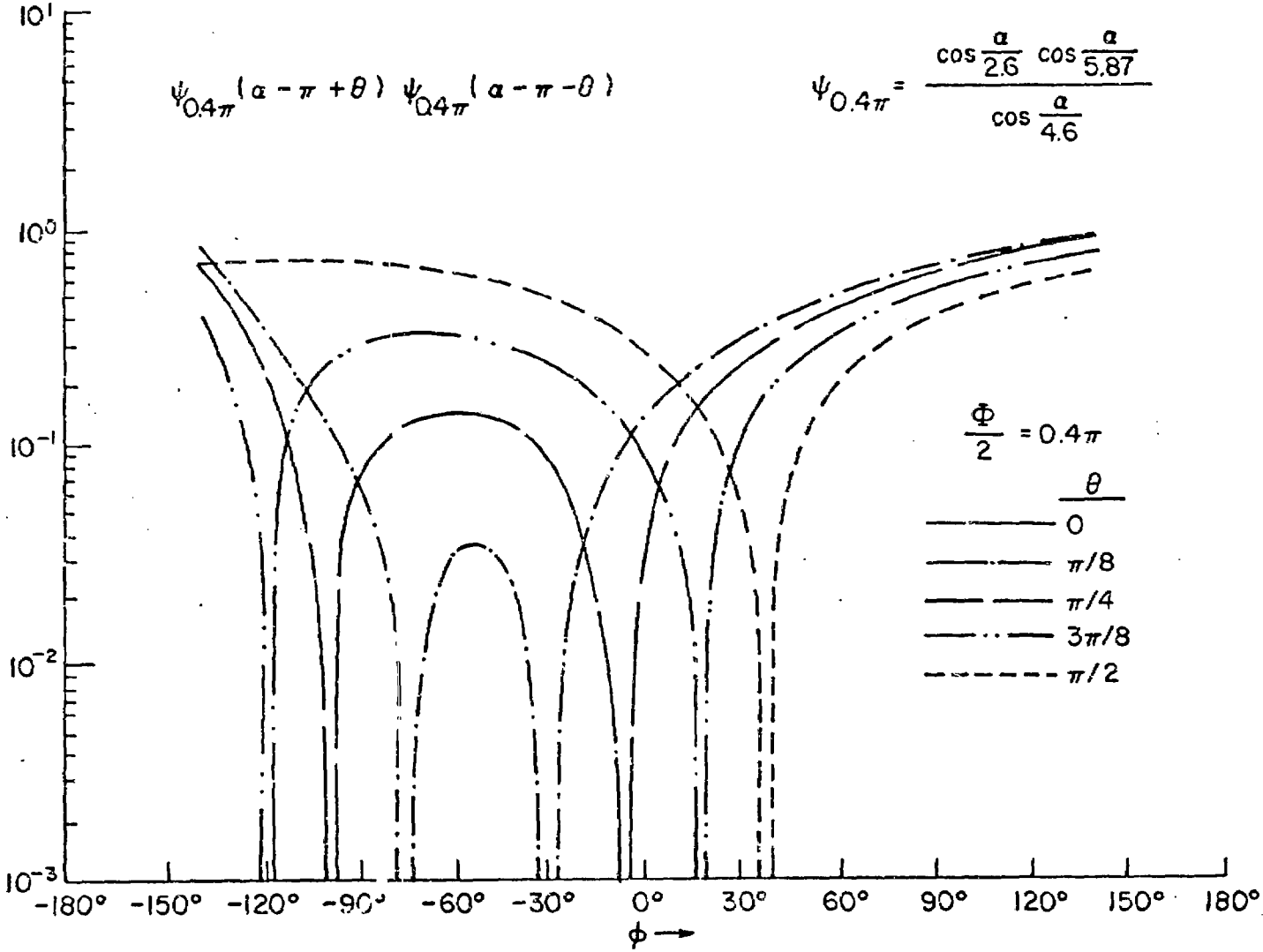

Figure 9.1c$_2$ The product of the $\psi(\varphi - \pi)$ functions for a wedge of solid angle 0.8π for various Brewster angles θ.

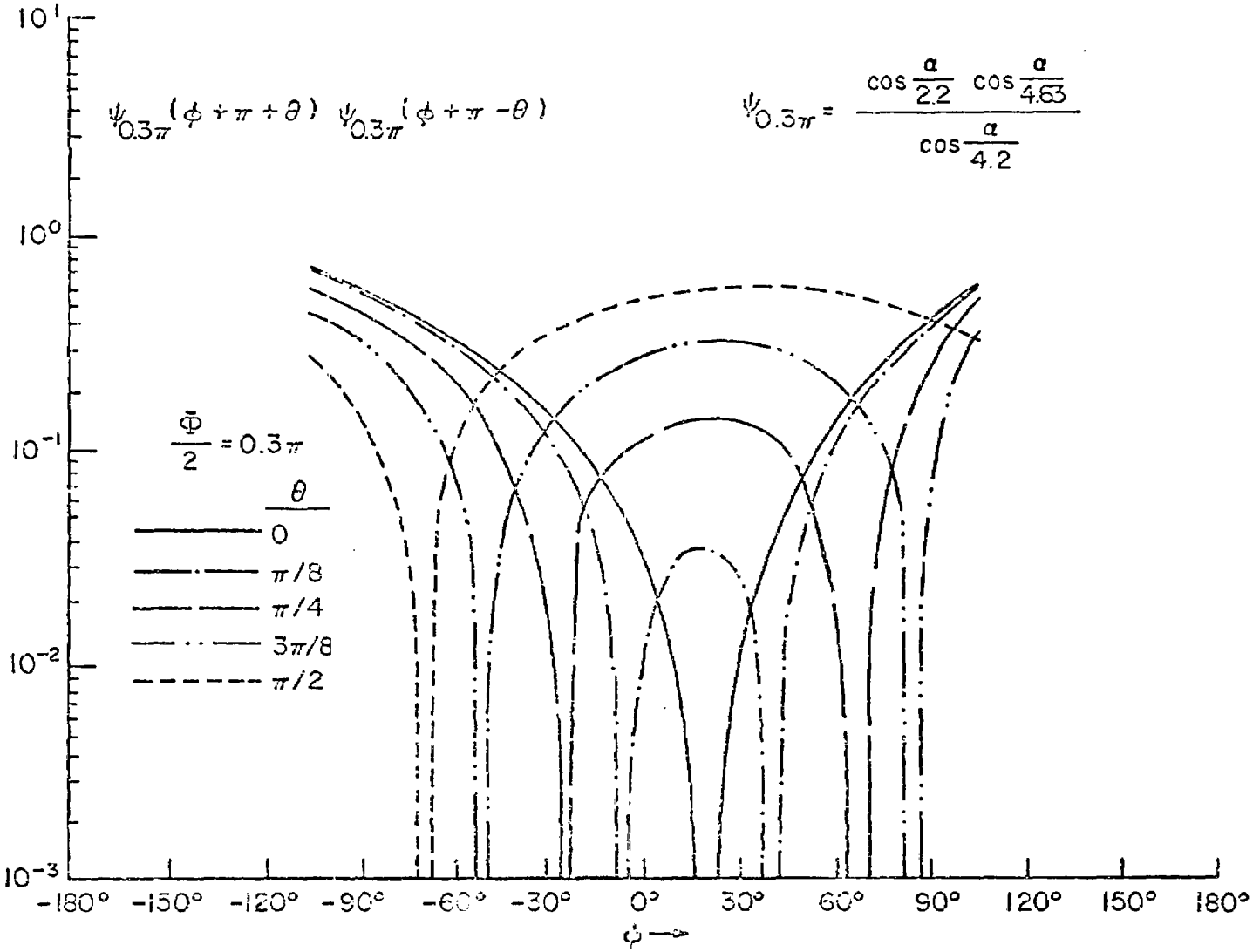

Figure 9.1d$_1$ The product of the $\psi(\varphi + \pi)$ functions for a wedge of solid angle 0.6π for various Brewster angles θ.

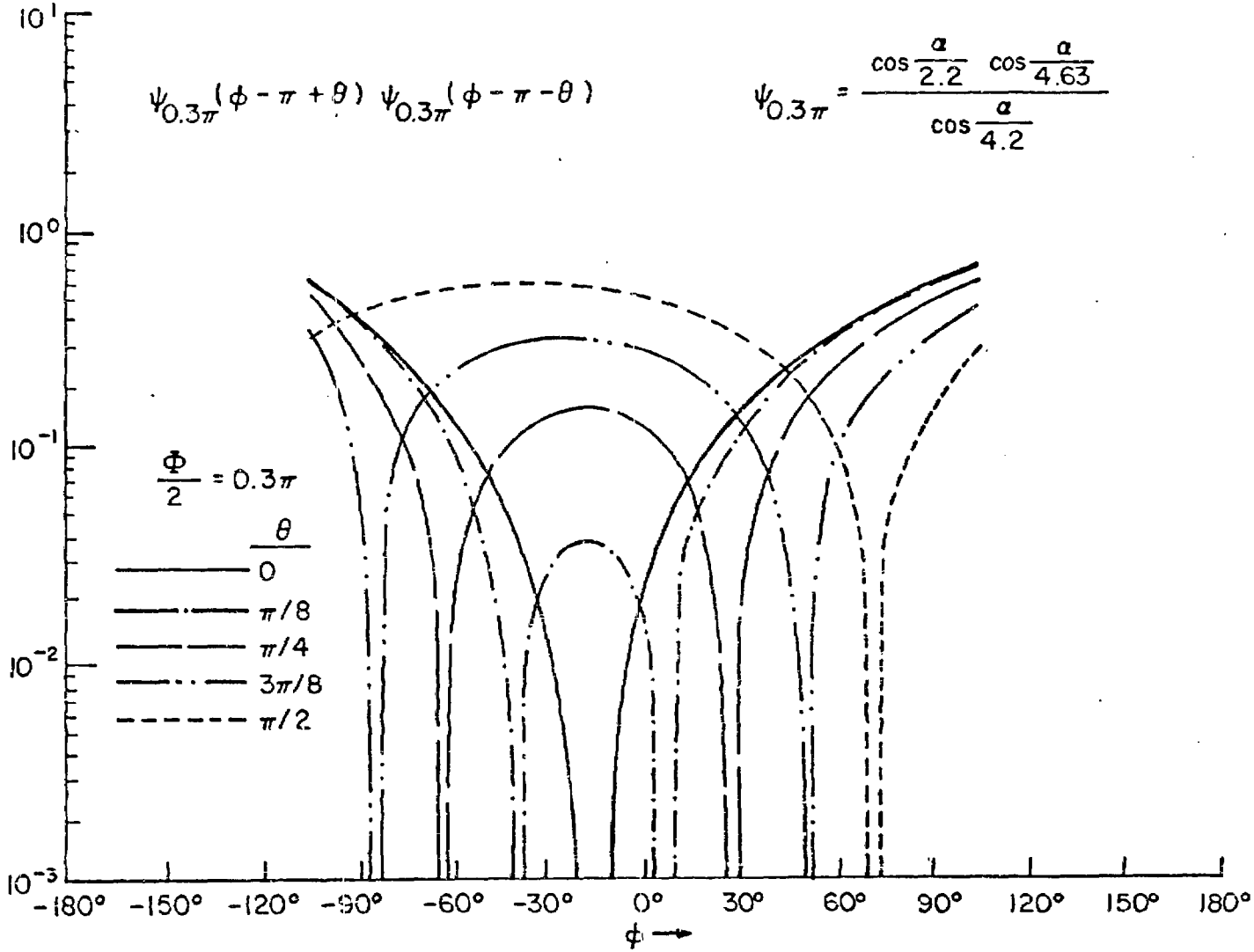

Figure $9.1d_2$ The product of the $\psi(\varphi - \pi)$ functions for a wedge of solid angle 0.6π for various Brewster angles θ.

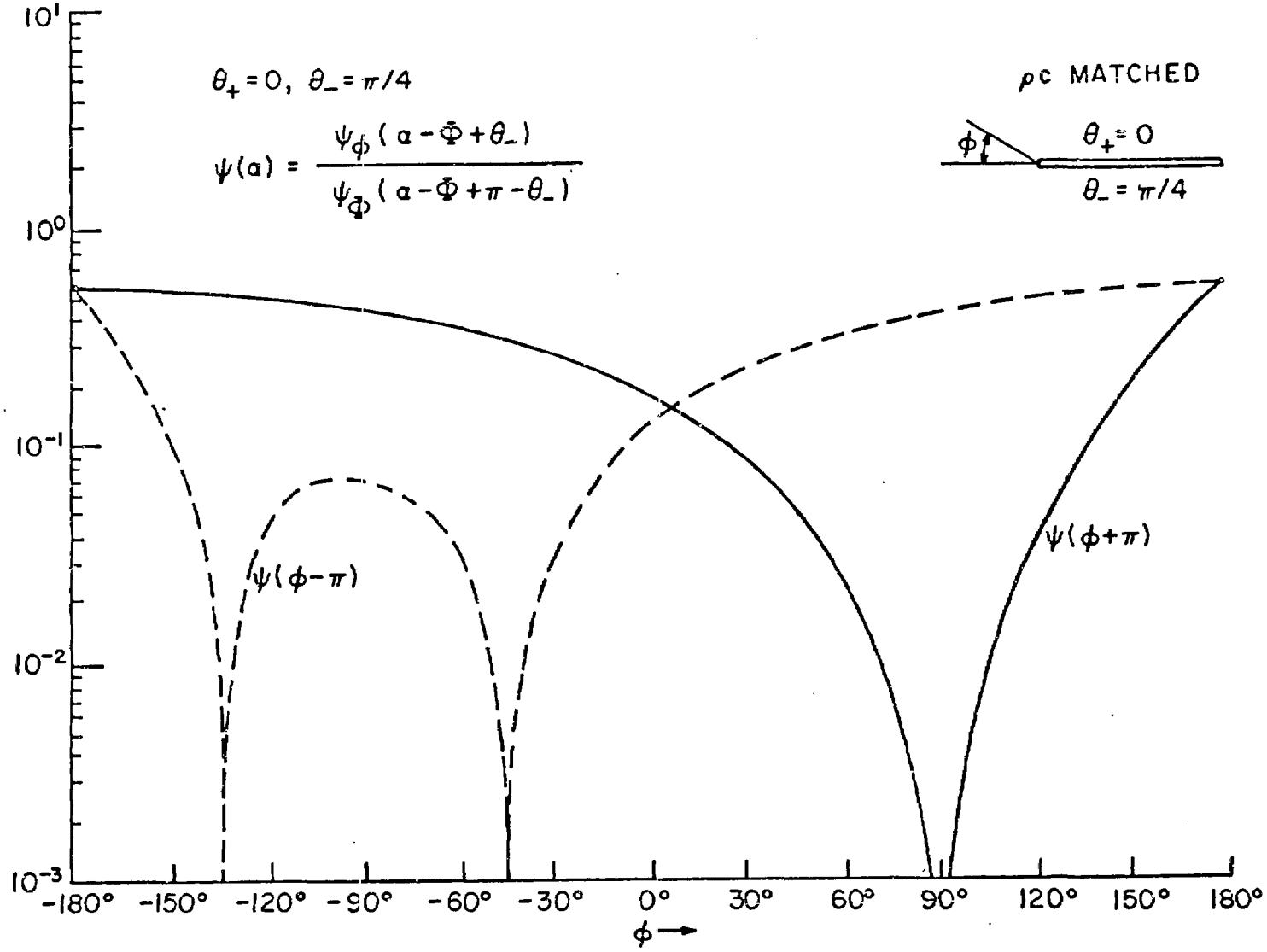

Figure 9.2a The ψ functions for a straight edge with different impedances on its two surfaces. A multiplicative constant has been omitted.

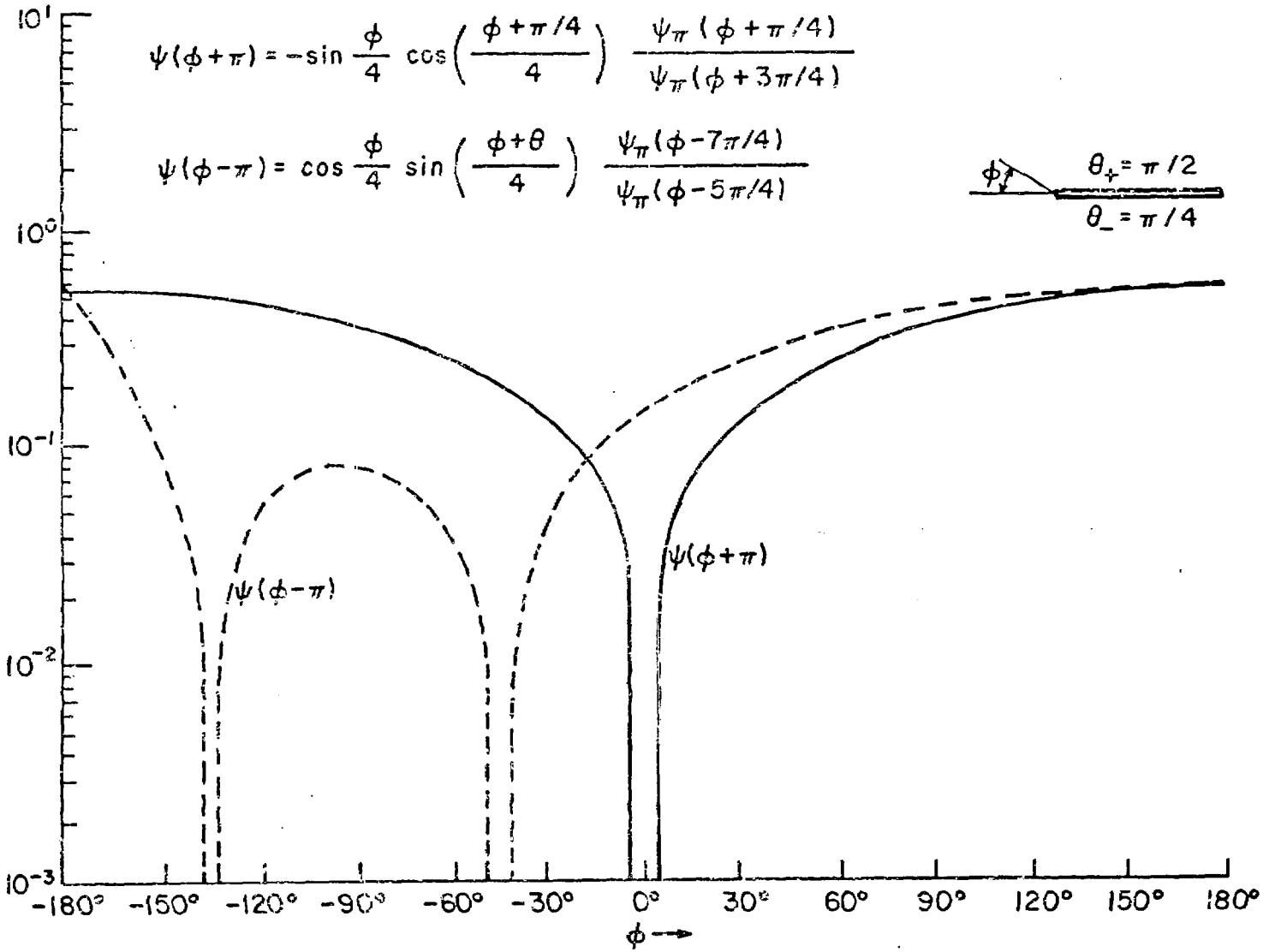

Figure 9.2b The ψ functions for a straight edge with different impedances on its two faces.

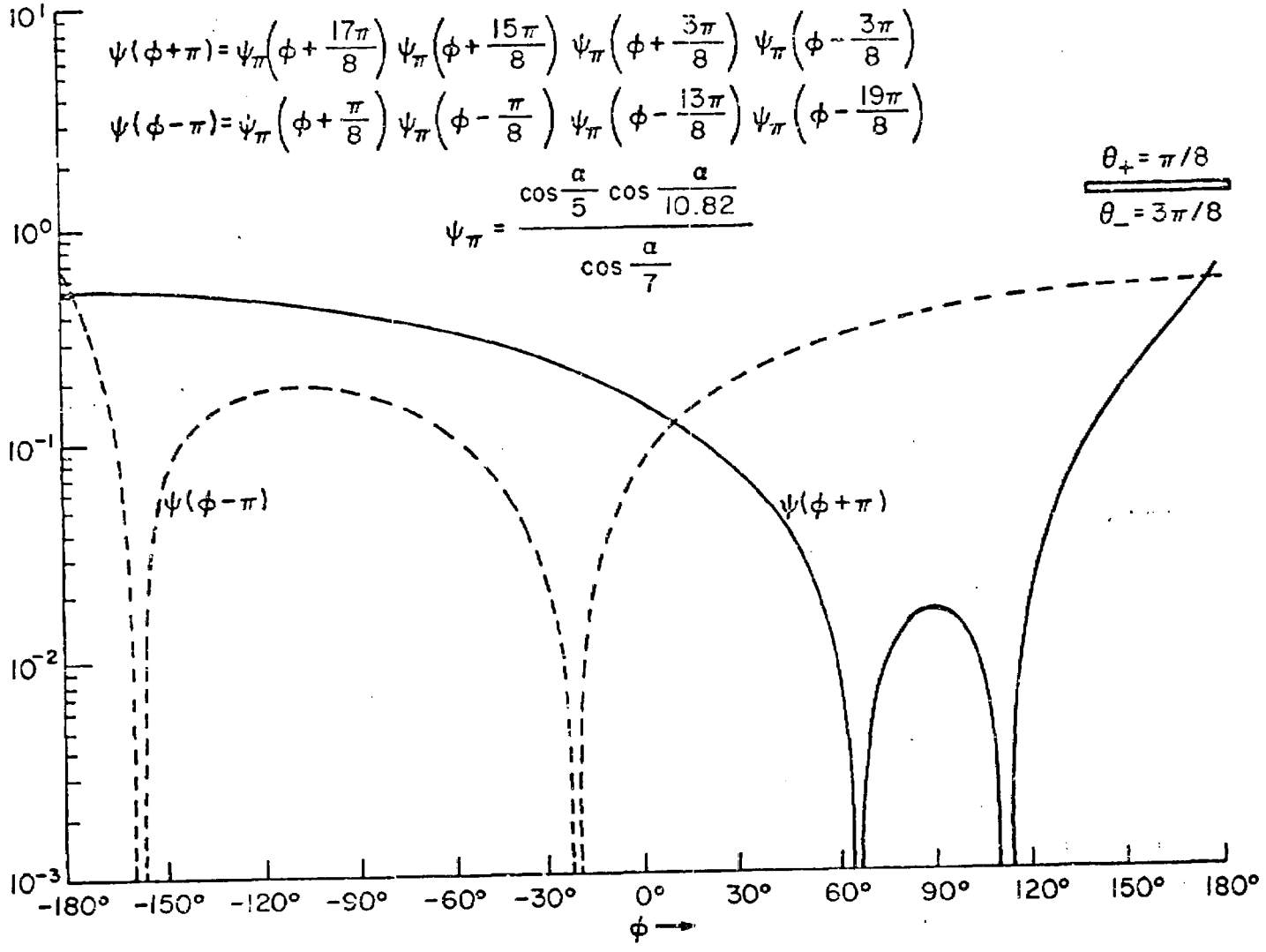

Figure 9.2c The ψ functions for a straight edge with different impedances on its two faces.

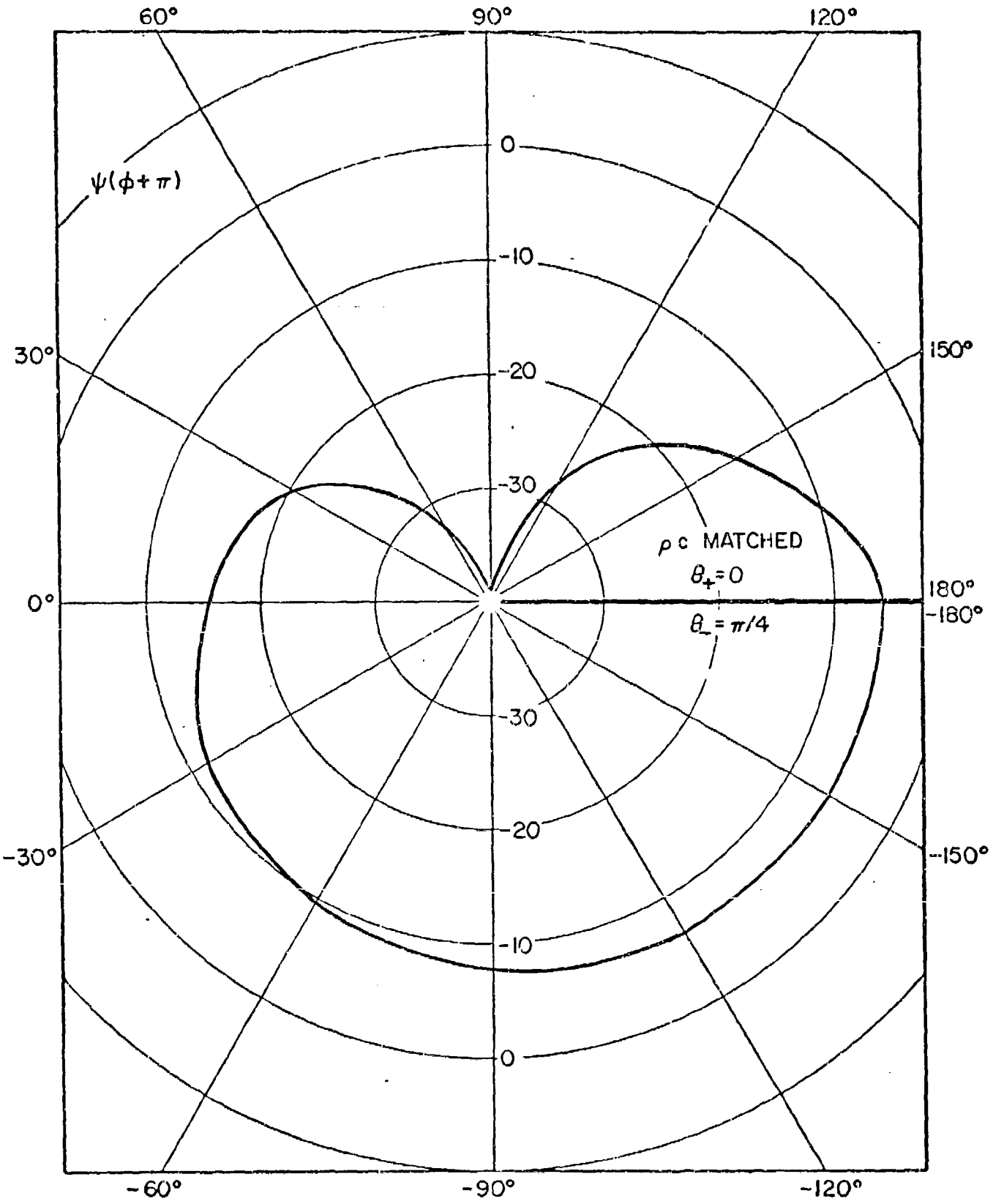

Figure 9.3a$_1$ The $\psi(\varphi + \pi)$ and $\psi(\varphi - \pi)$ functions in polar coordinates.

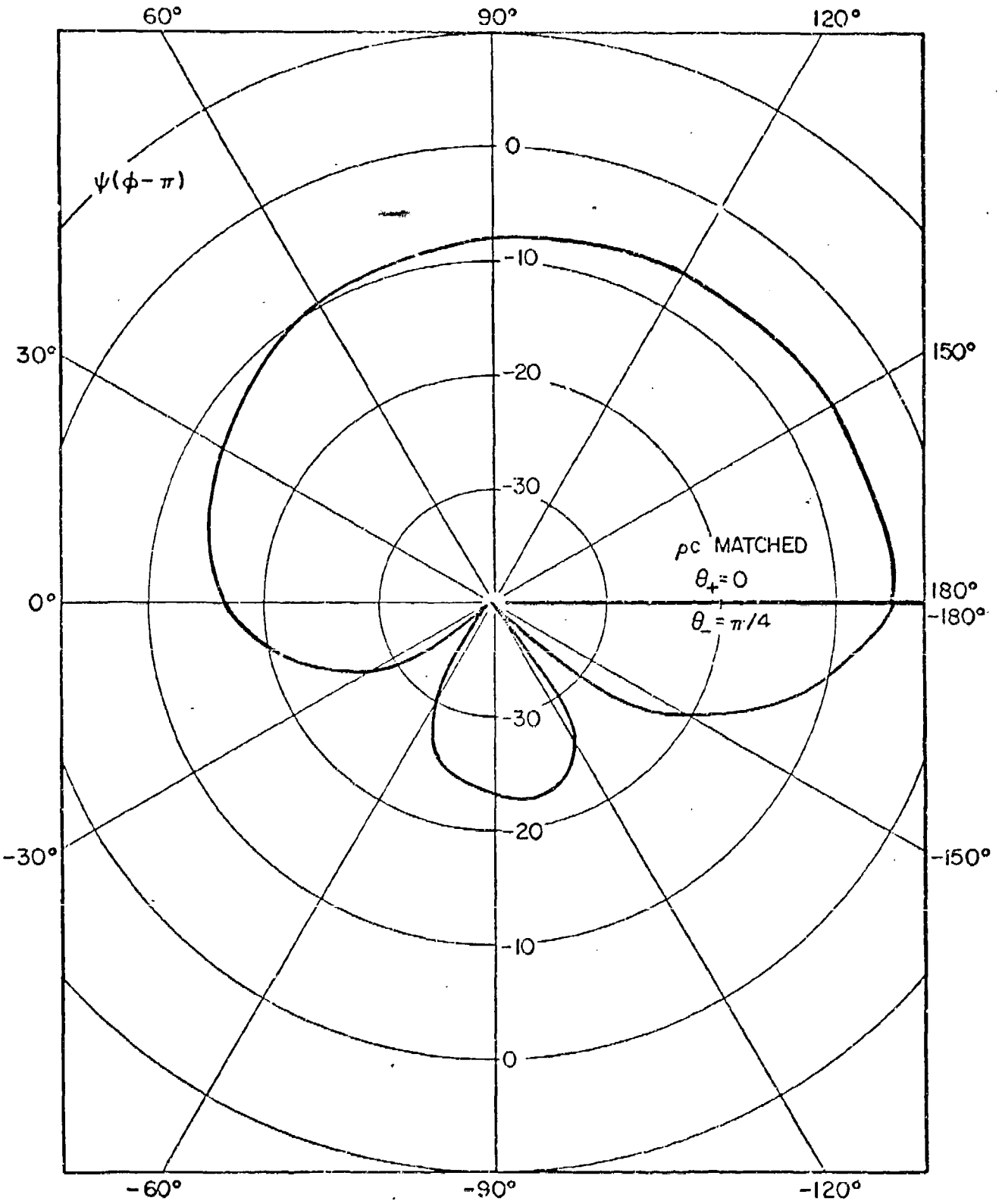

Figure $9.3a_2$ The $\psi(\varphi + \pi)$ and $\psi(\varphi - \pi)$ functions in polar coordinates.

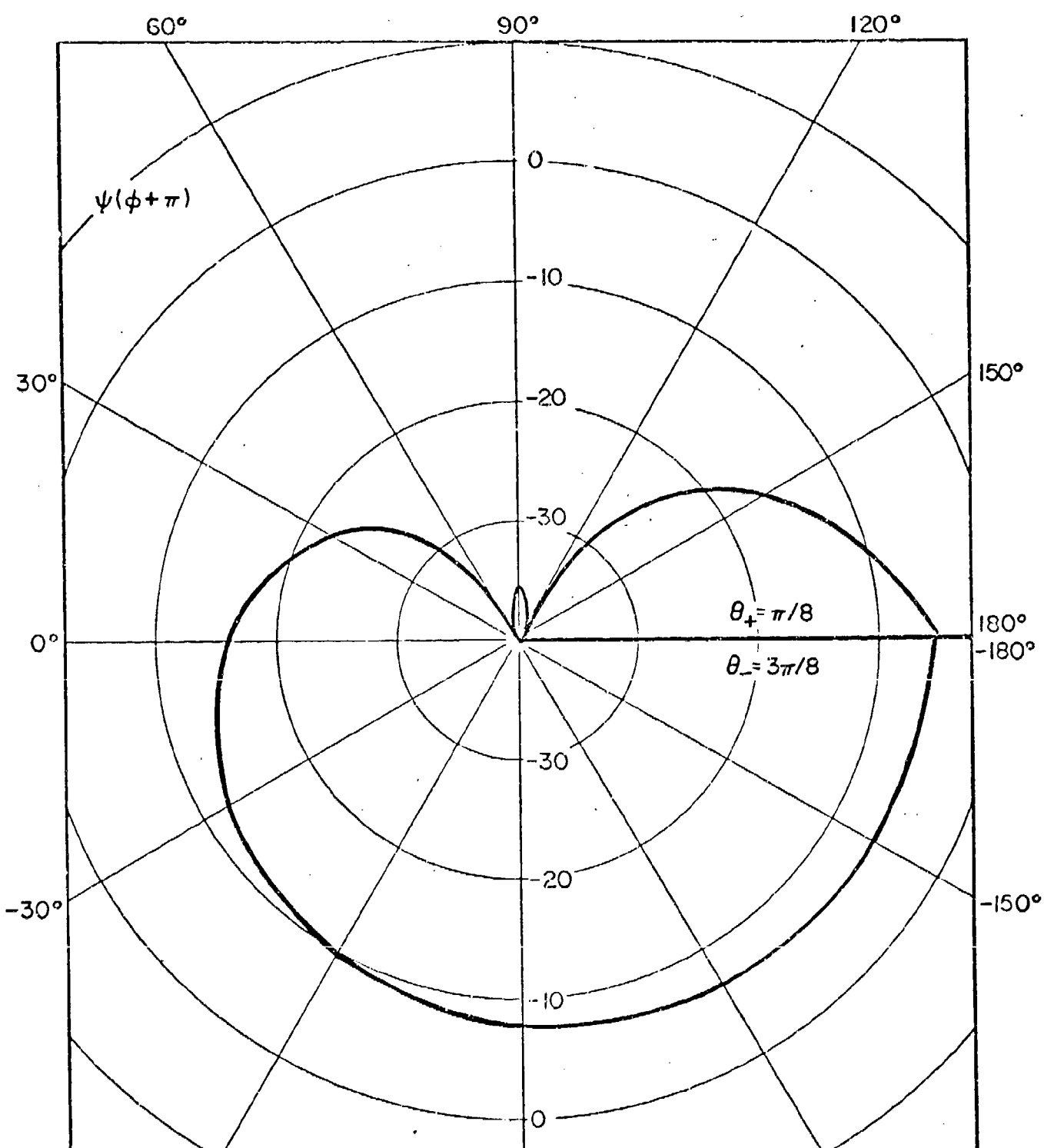

Figure 9.3b$_1$ The $\psi(\varphi + \pi)$ and $\psi(\varphi - \pi)$ functions in polar coordinates.

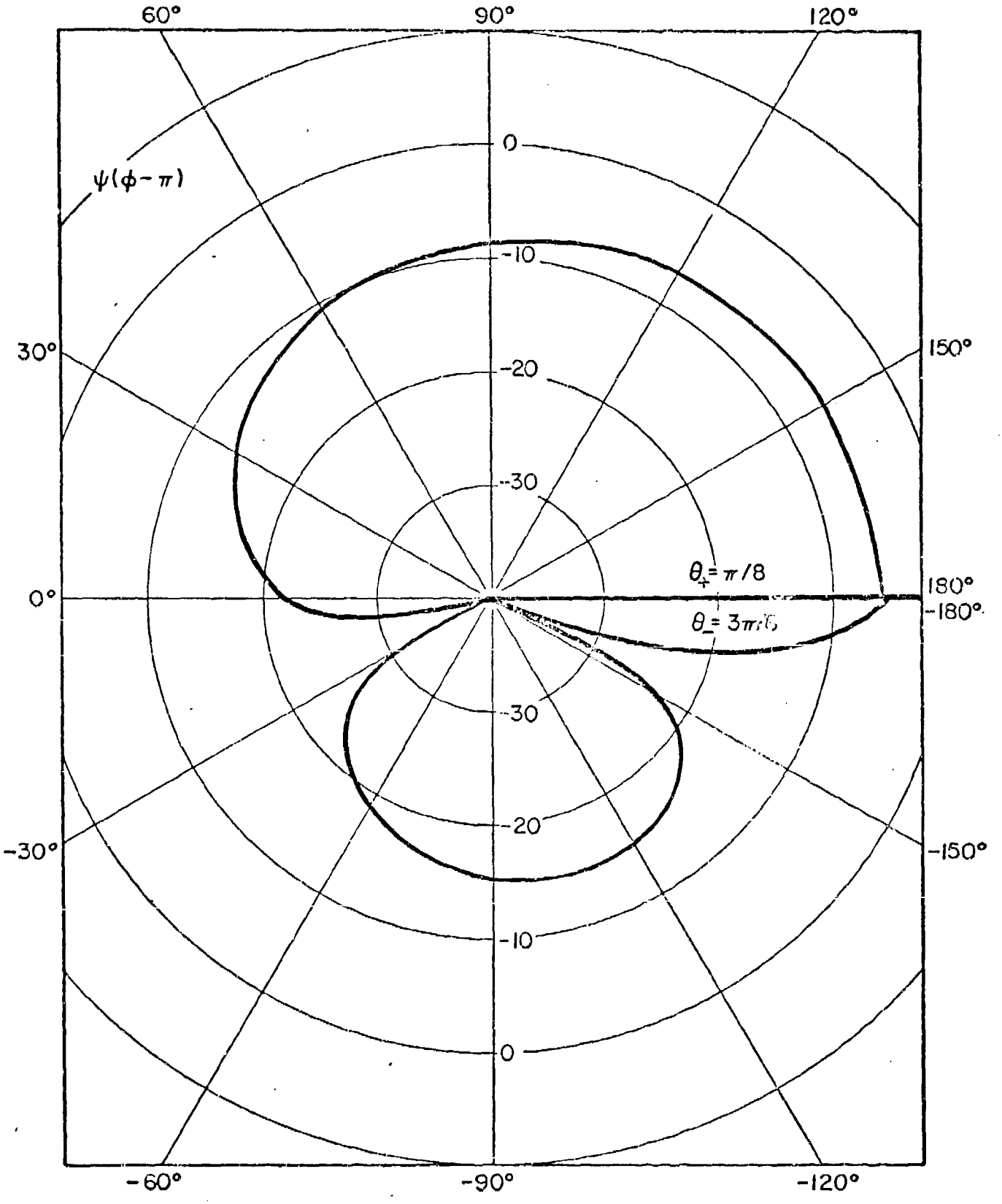

Figure 9.3b. The $\psi(\varphi + \pi)$ and $\psi(\varphi - \pi)$ functions in polar coordinates.

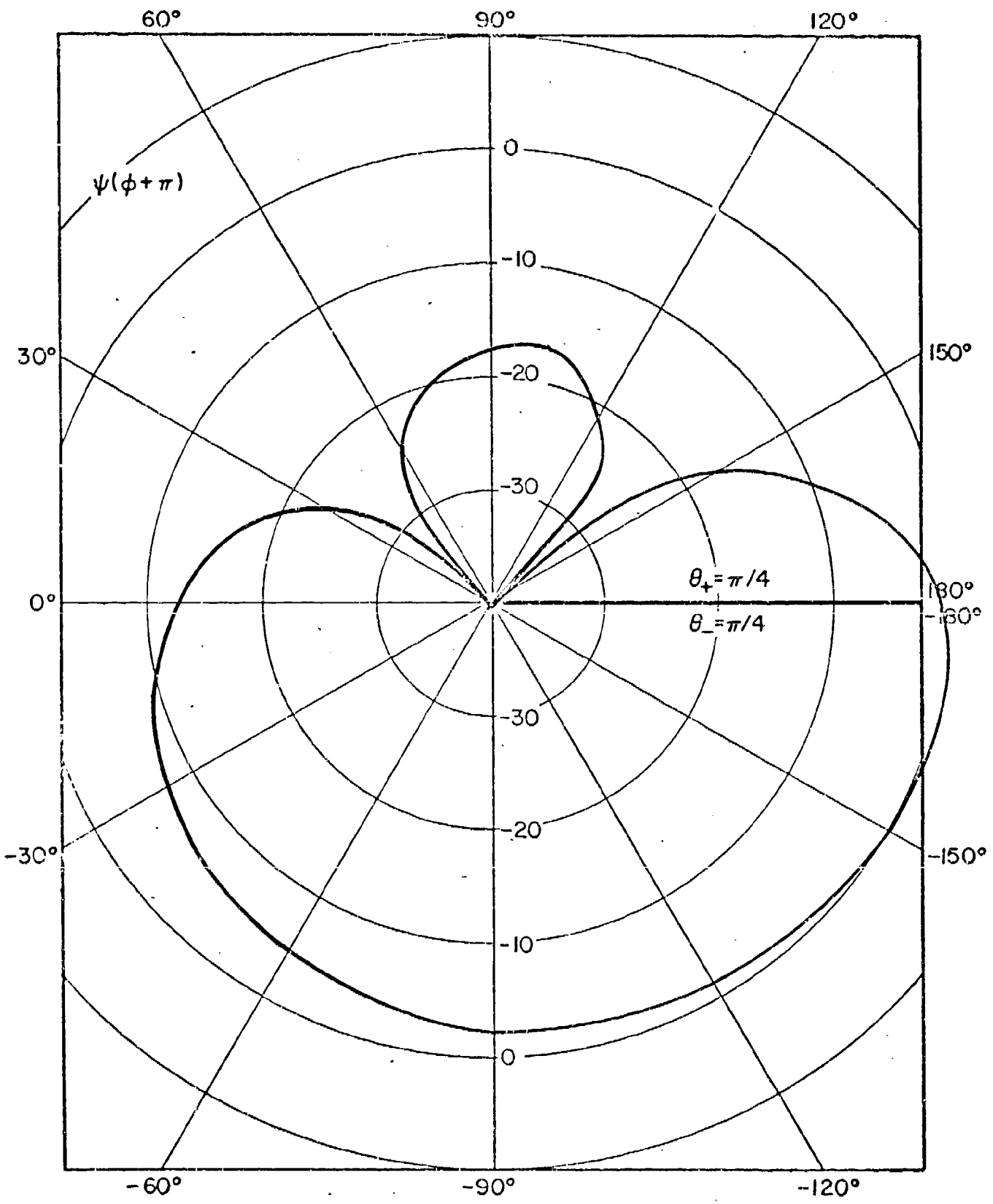

Figure 9.3c$_1$ The $\psi(\varphi + \pi)$ and $\psi(\varphi - \pi)$ functions in polar coordinates.

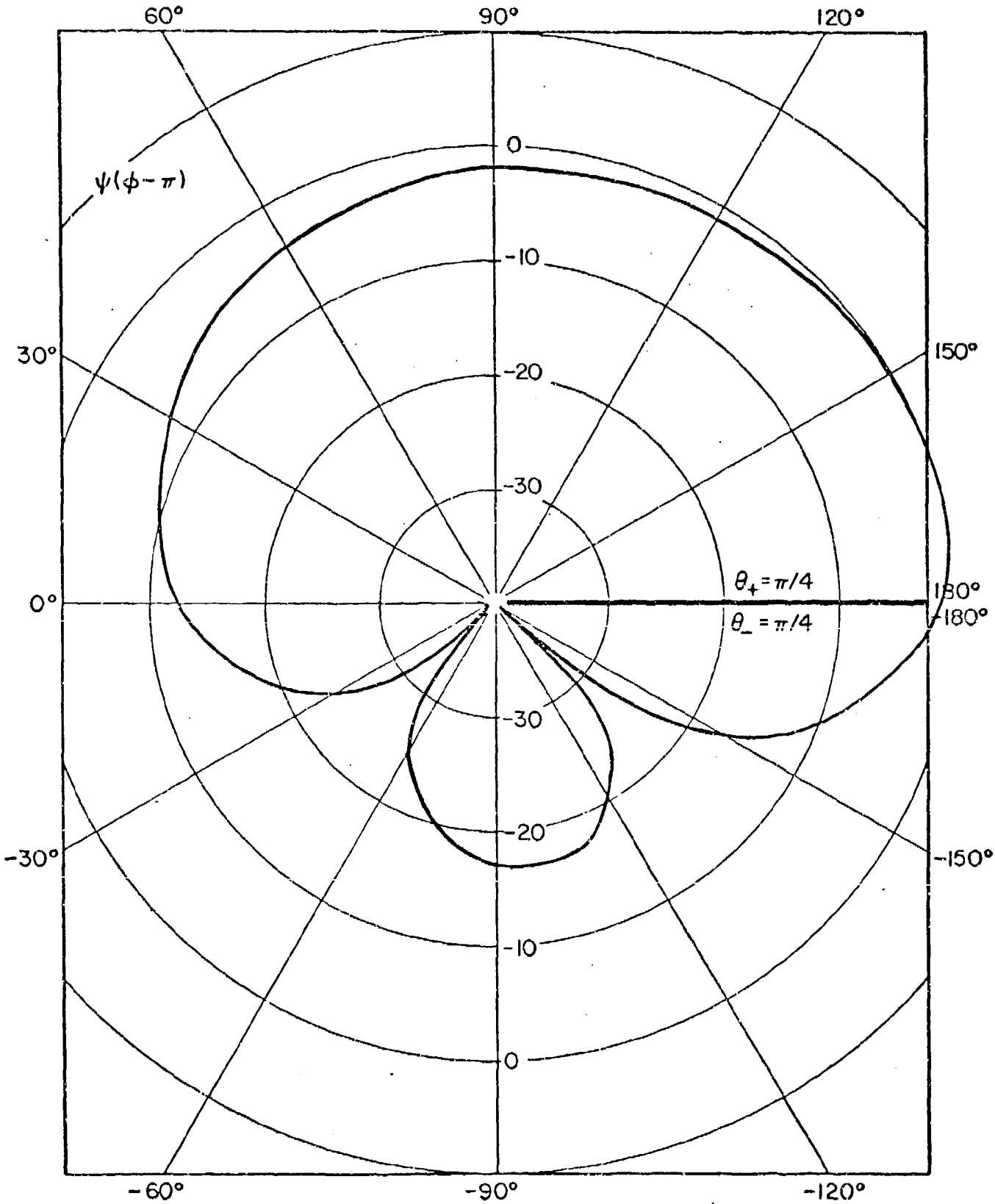

Figure 9.3c$_2$ The $\psi(\varphi + \pi)$ and $\psi(\varphi - \pi)$ functions in polar coordinates.

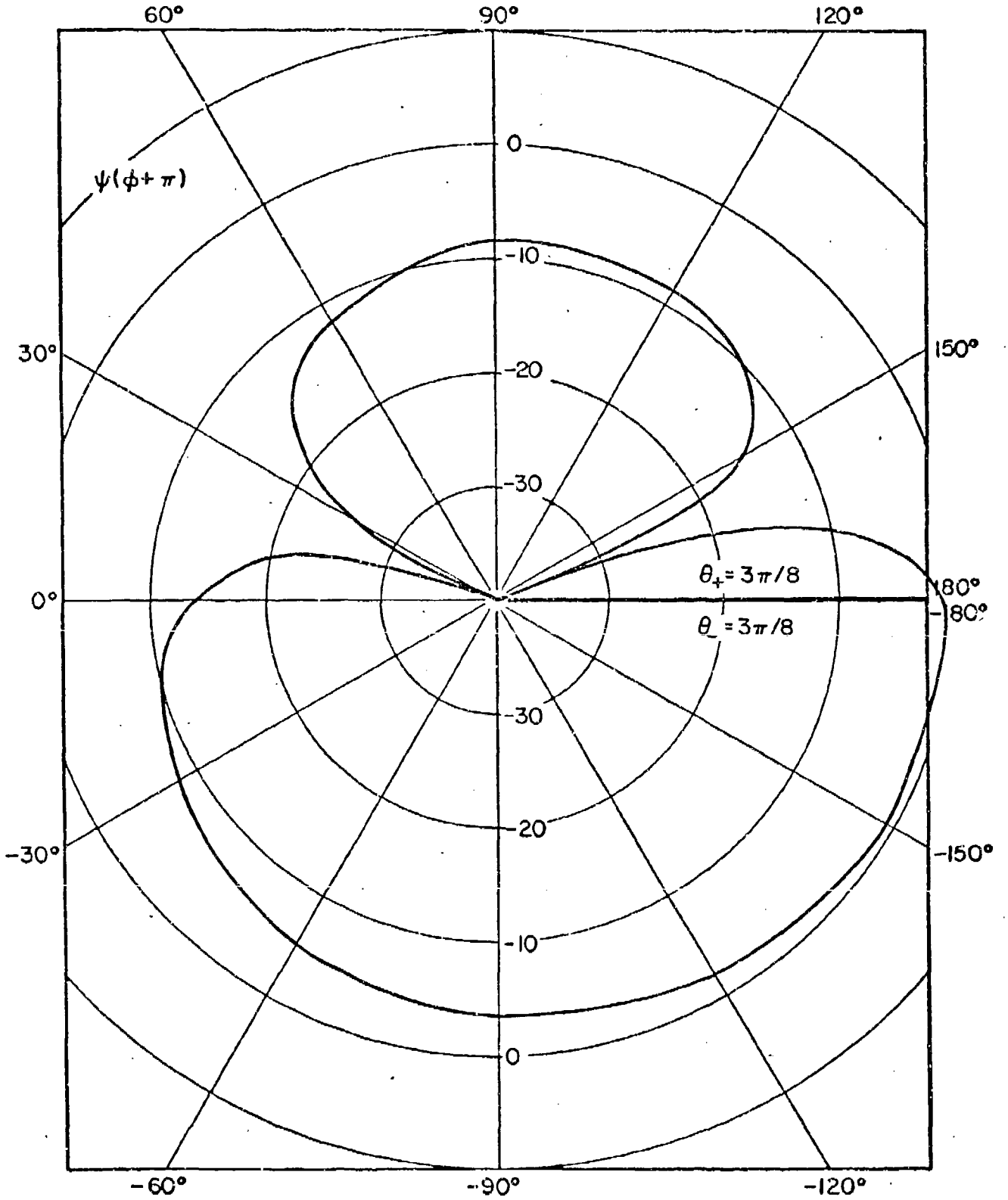

Figure 9.3d$_1$ The $\psi(\varphi + \pi)$ and $\psi(\varphi - \pi)$ functions in polar coordinates.

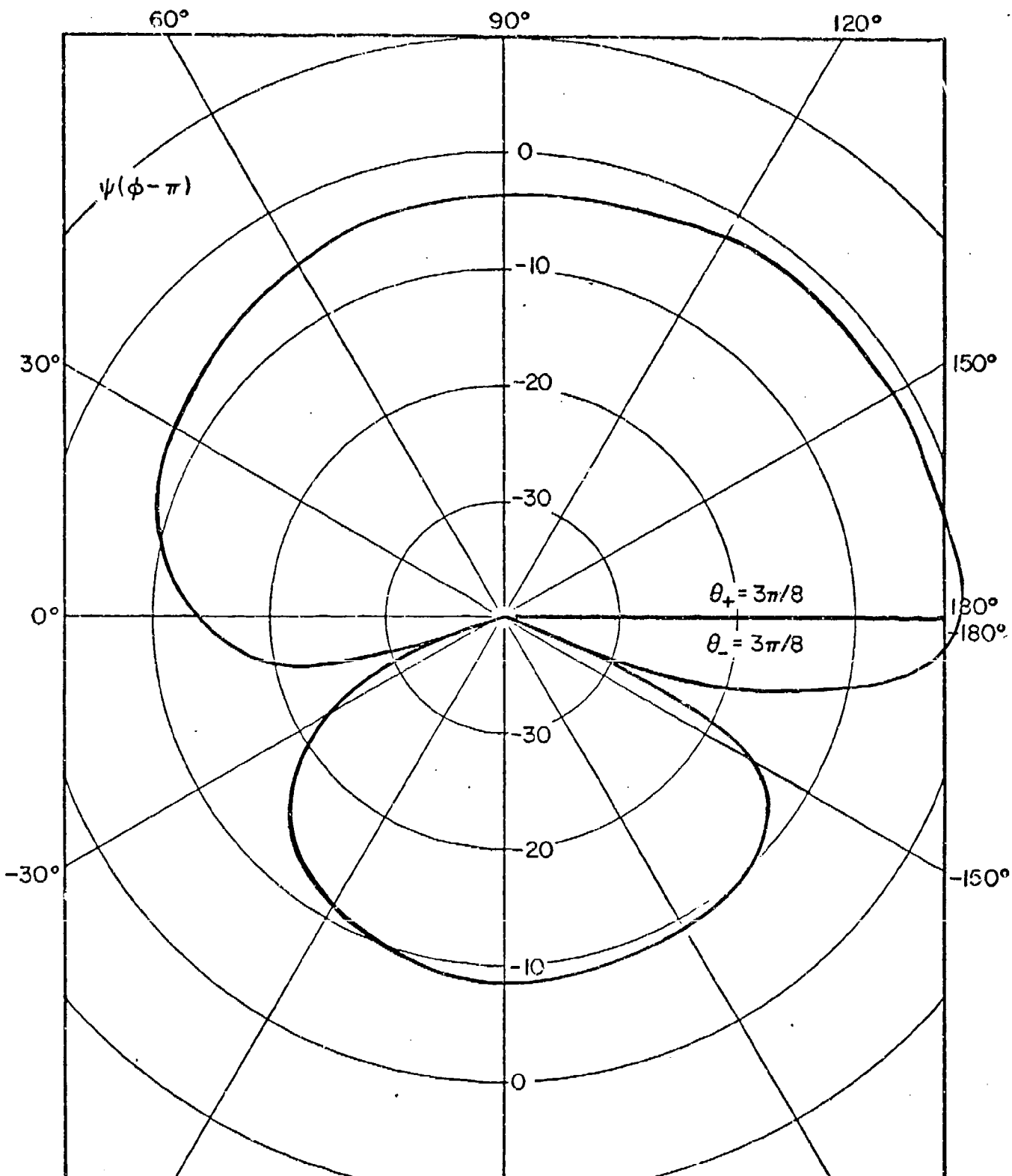

Figure 9.3d$_2$ The $\psi(\varphi + \pi)$ and $\psi(\varphi - \pi)$ functions in polar coordinates.

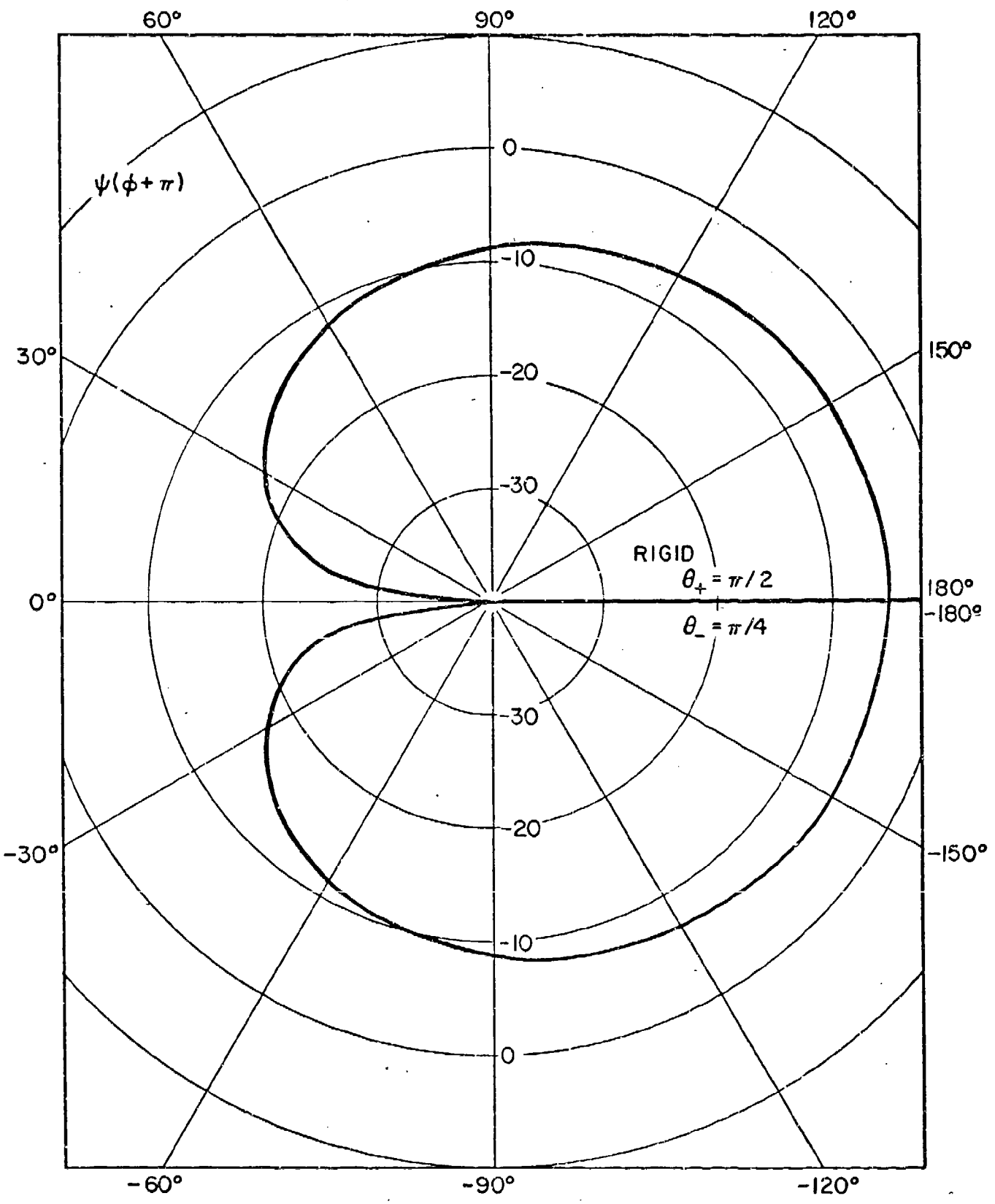

Figure 9.3e$_1$ The $\psi(\varphi + \pi)$ and $\psi(\varphi - \pi)$ functions in polar coordinates.

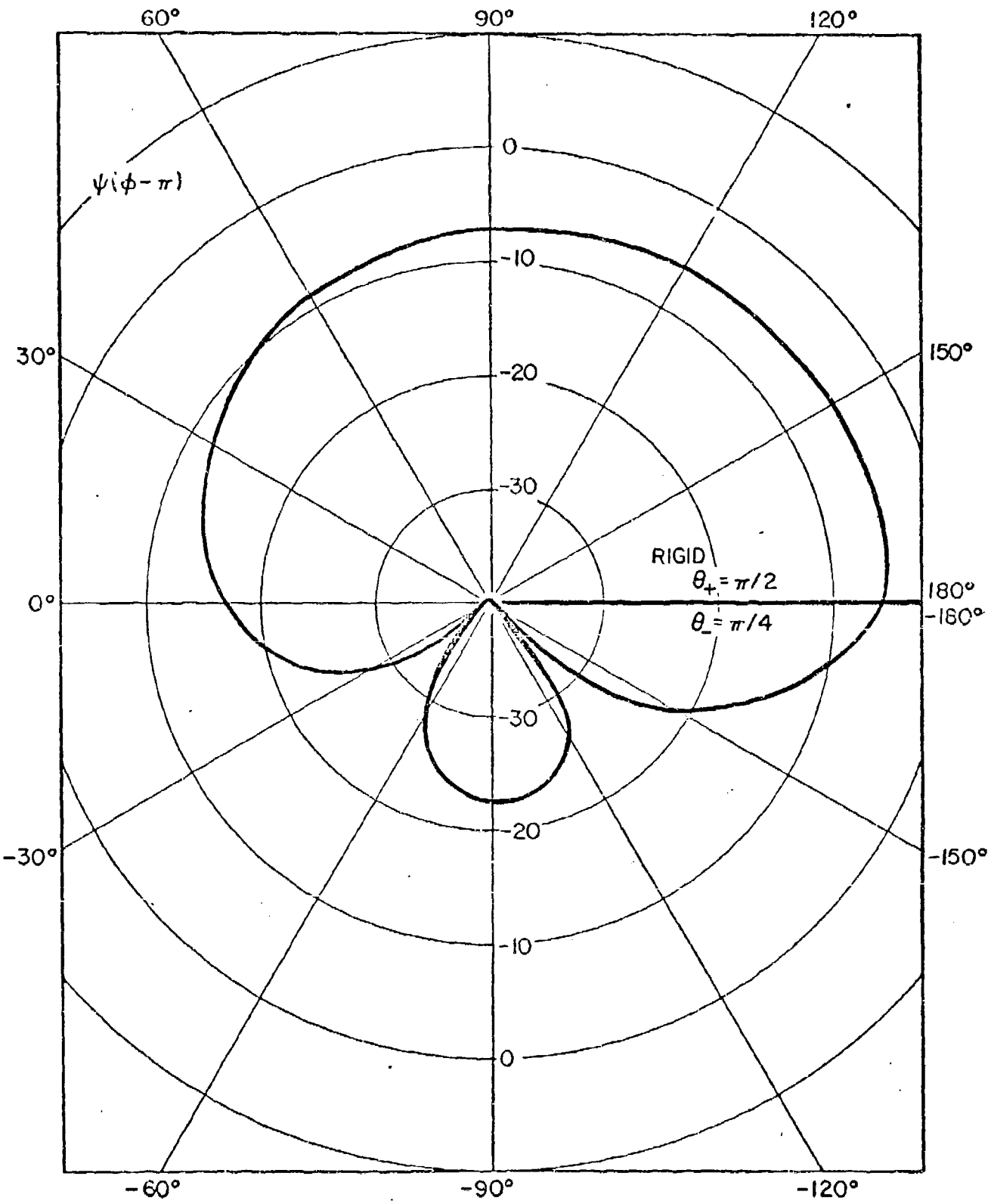

Figure 9.3e$_2$ The $\psi(\varphi + \pi)$ and $\psi(\varphi - \pi)$ functions in polar coordinates.

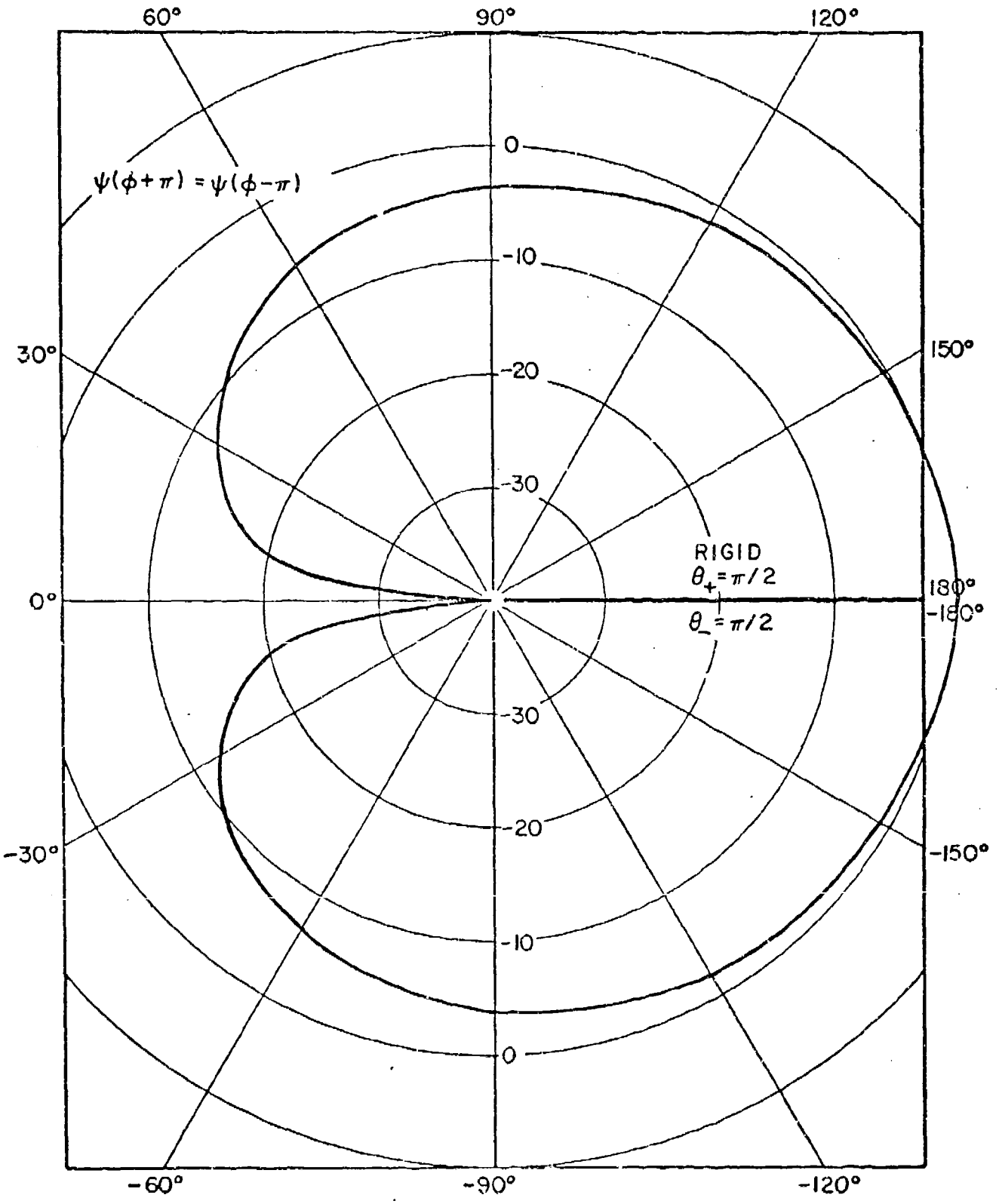

Figure 9.3f The $\psi(\varphi + \pi)$ and $\psi(\varphi - \pi)$ functions in polar coordinates.

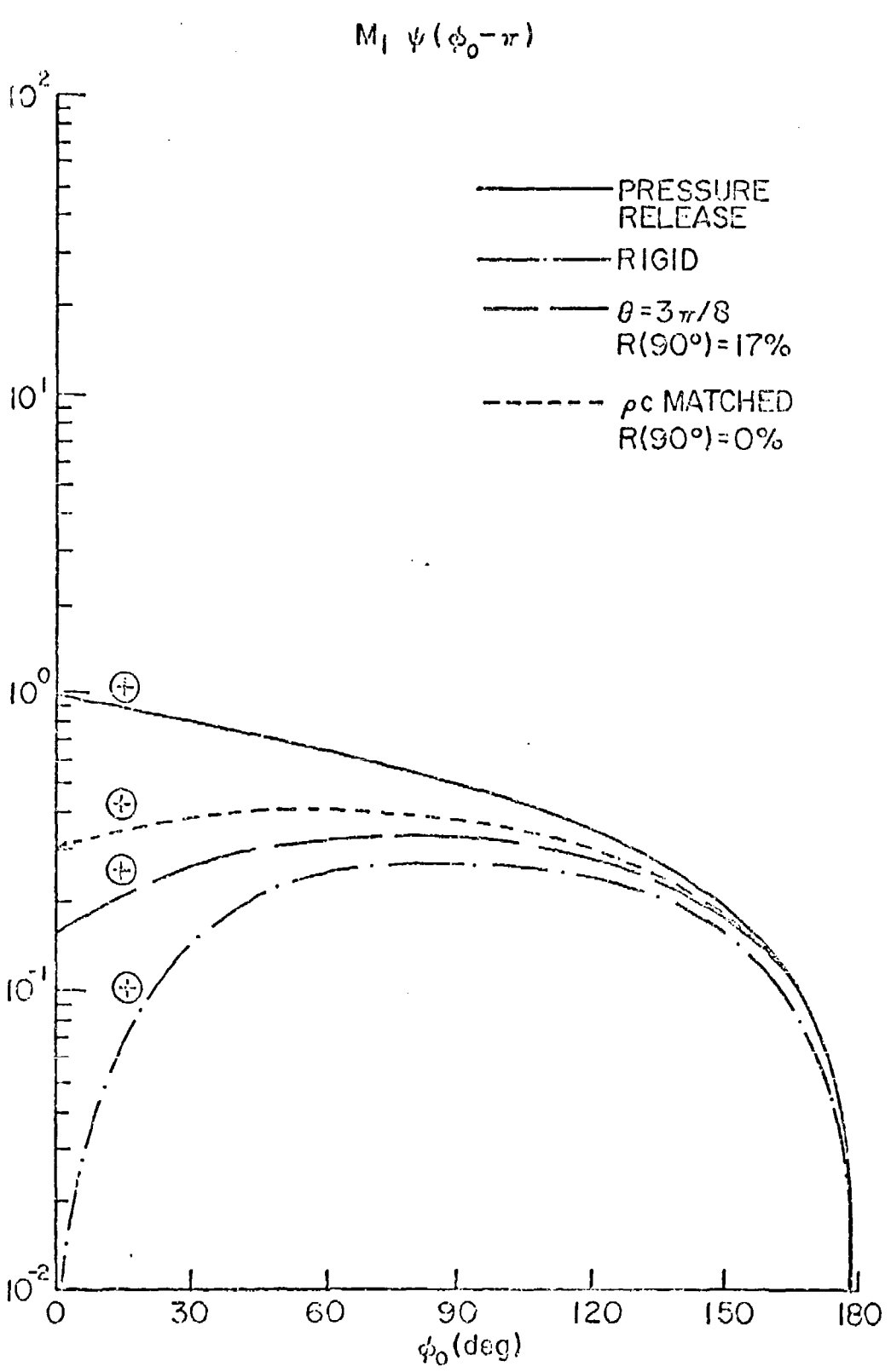

Figure 10.1a$_1$ The term $M_1\psi(\varphi_o - \pi)$ of the Malyuzhinets solution for edges of various impedances.

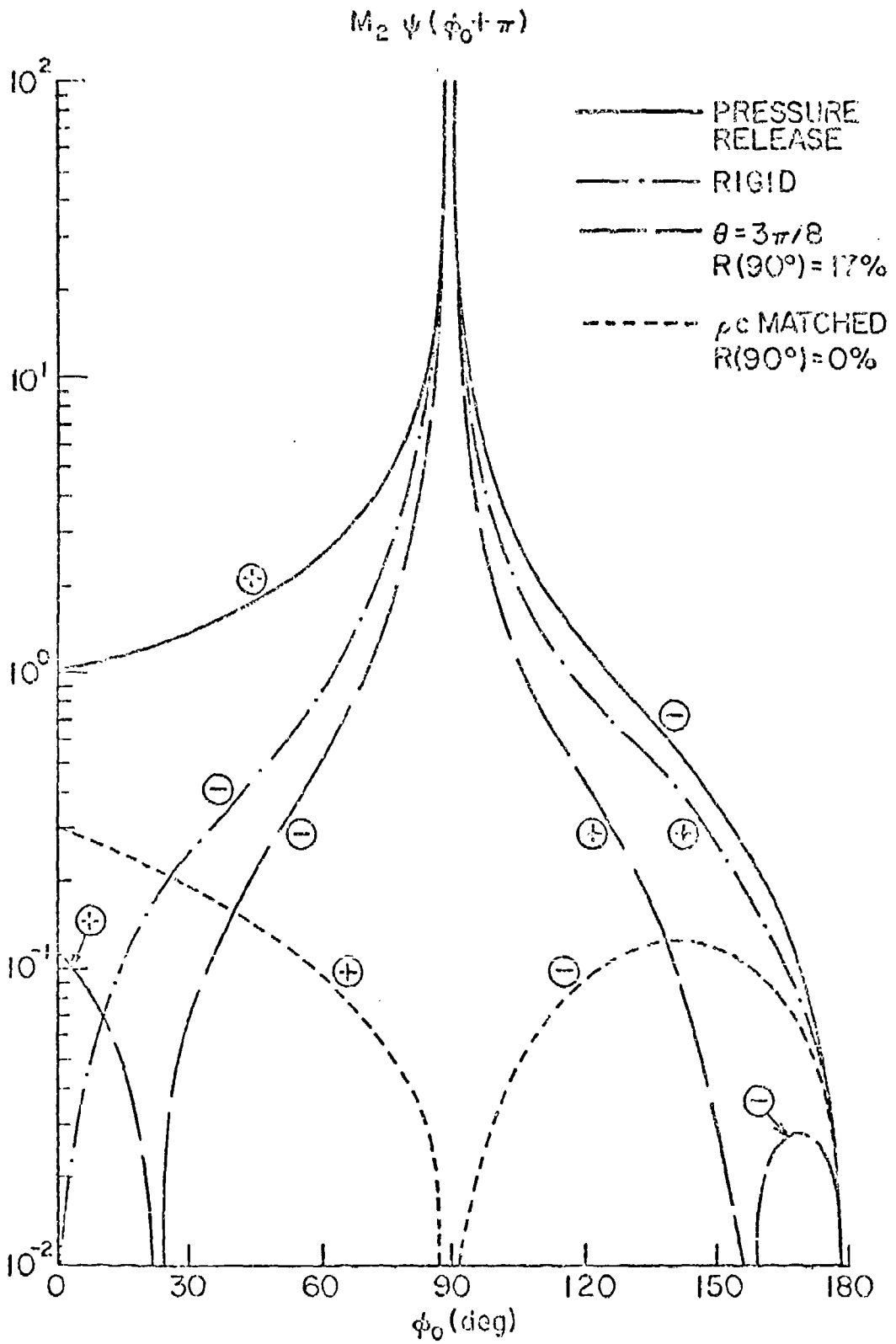

Figure 10.1a$_2$ The term $M_2\psi(\varphi_o + \pi)$ of the Malyuzhinets solution for edges of various impedances.

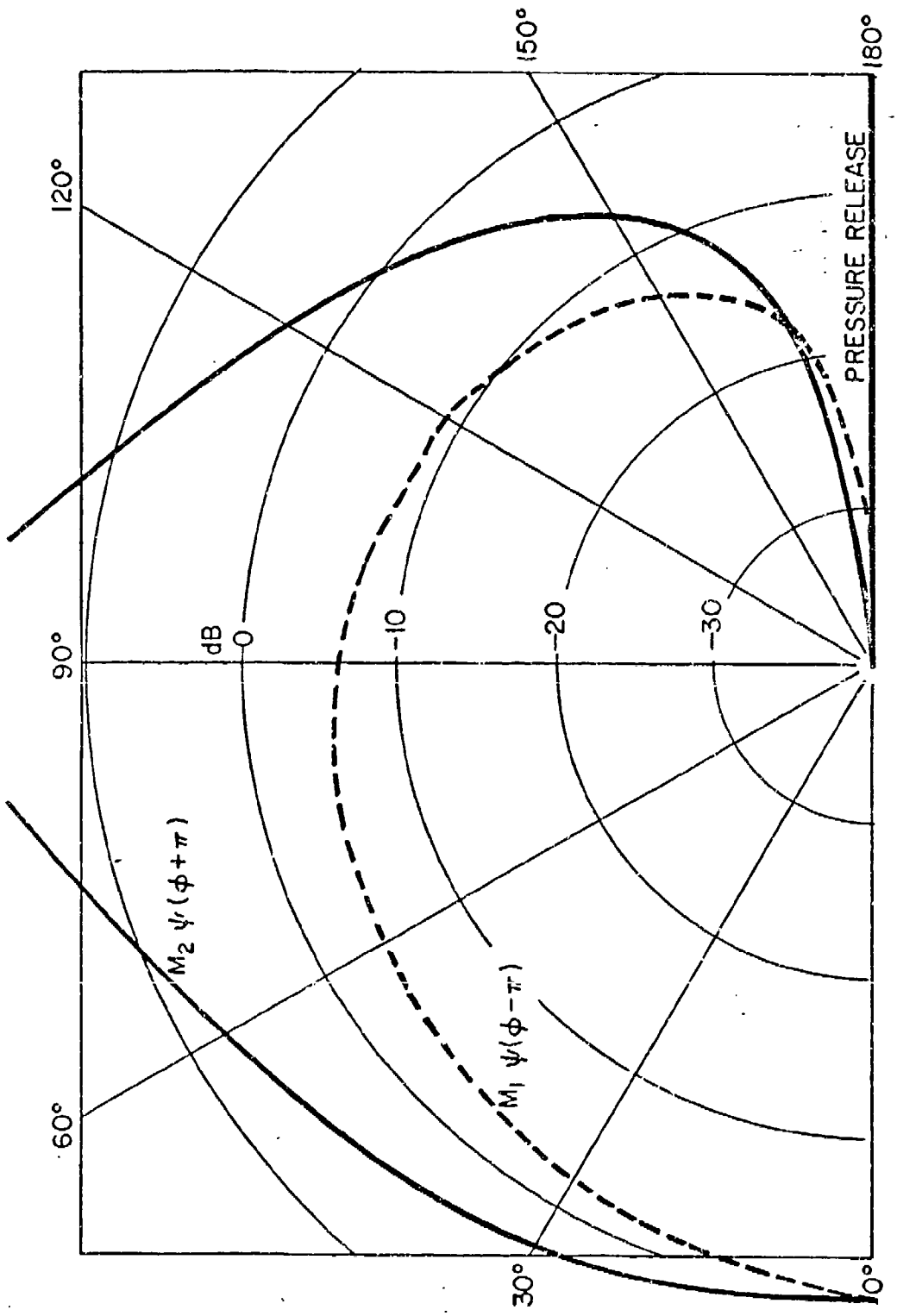

Figure 10.2a The polar diagram of the Malyuzhinets terms for backscatter from a pressure release edge.

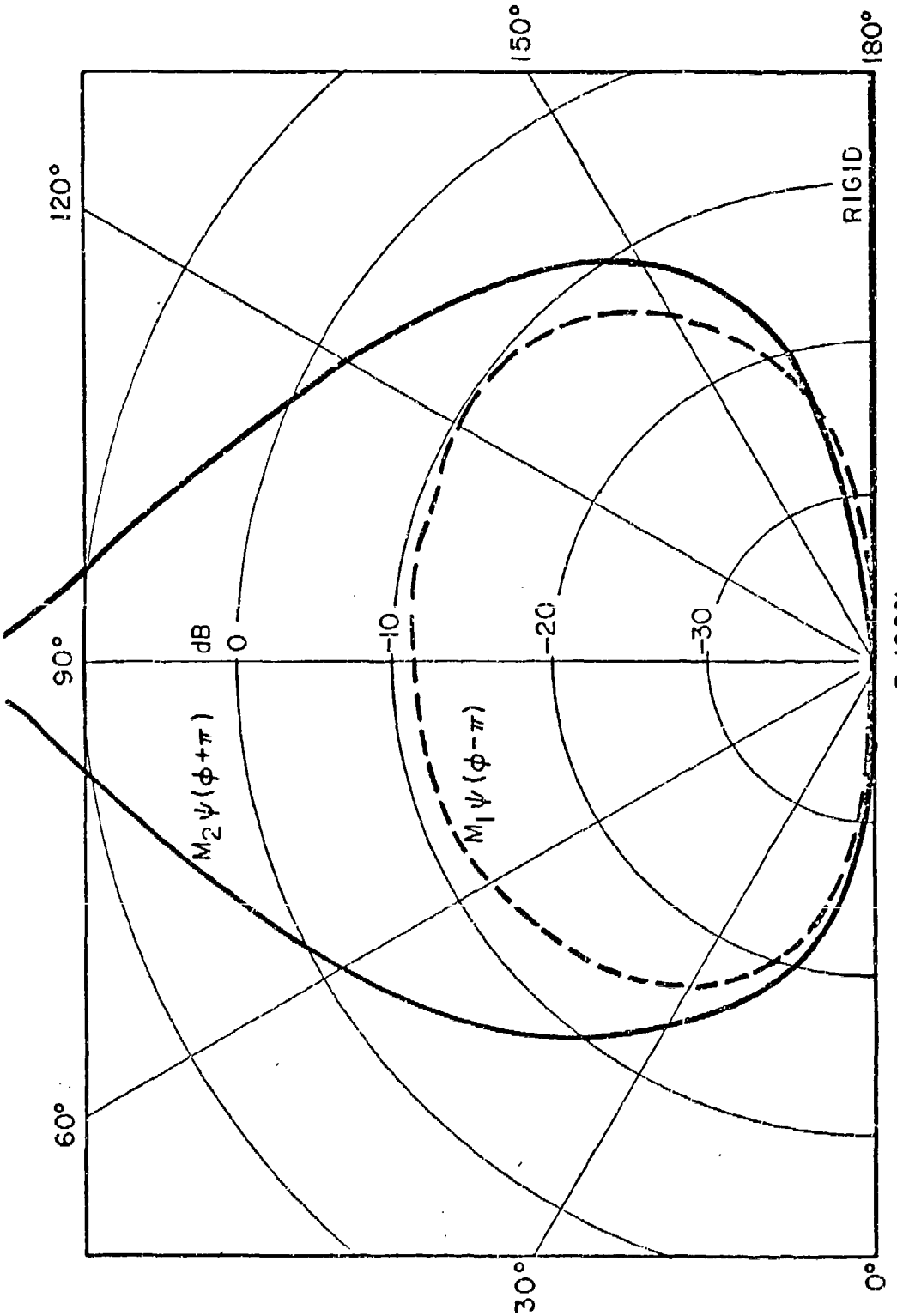

Figure 10.2b The polar diagram of the Malyuzhinets terms for backscatter from a rigid edge.

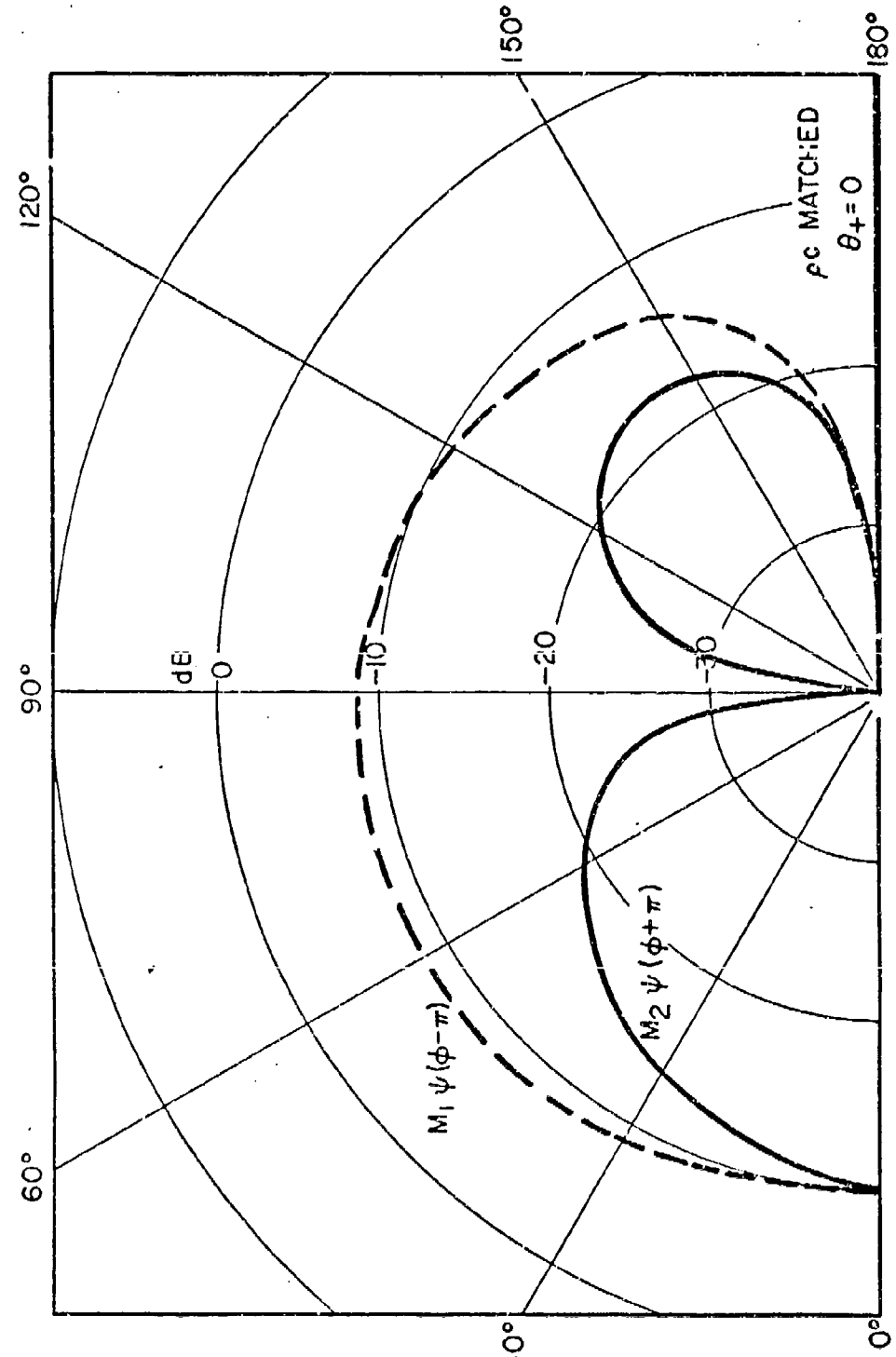

Figure 10.2c The polar diagram of the Malyuzhinets terms for backscatter from a ρc matched edge.

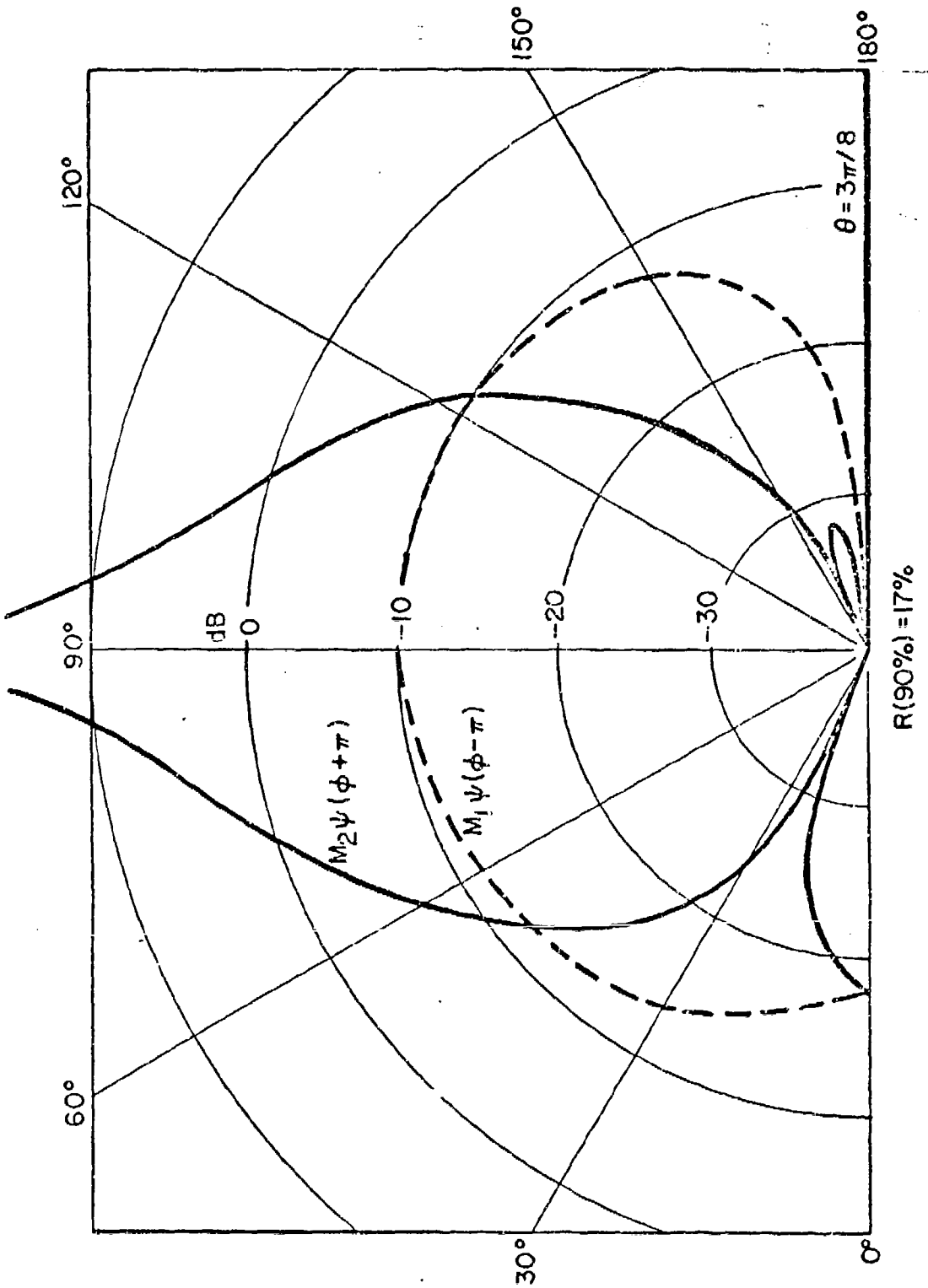

Figure 10.2d The polar diagram of the Malyuzhinets terms for backscatter from an edge with $\theta = 3\pi/8$.

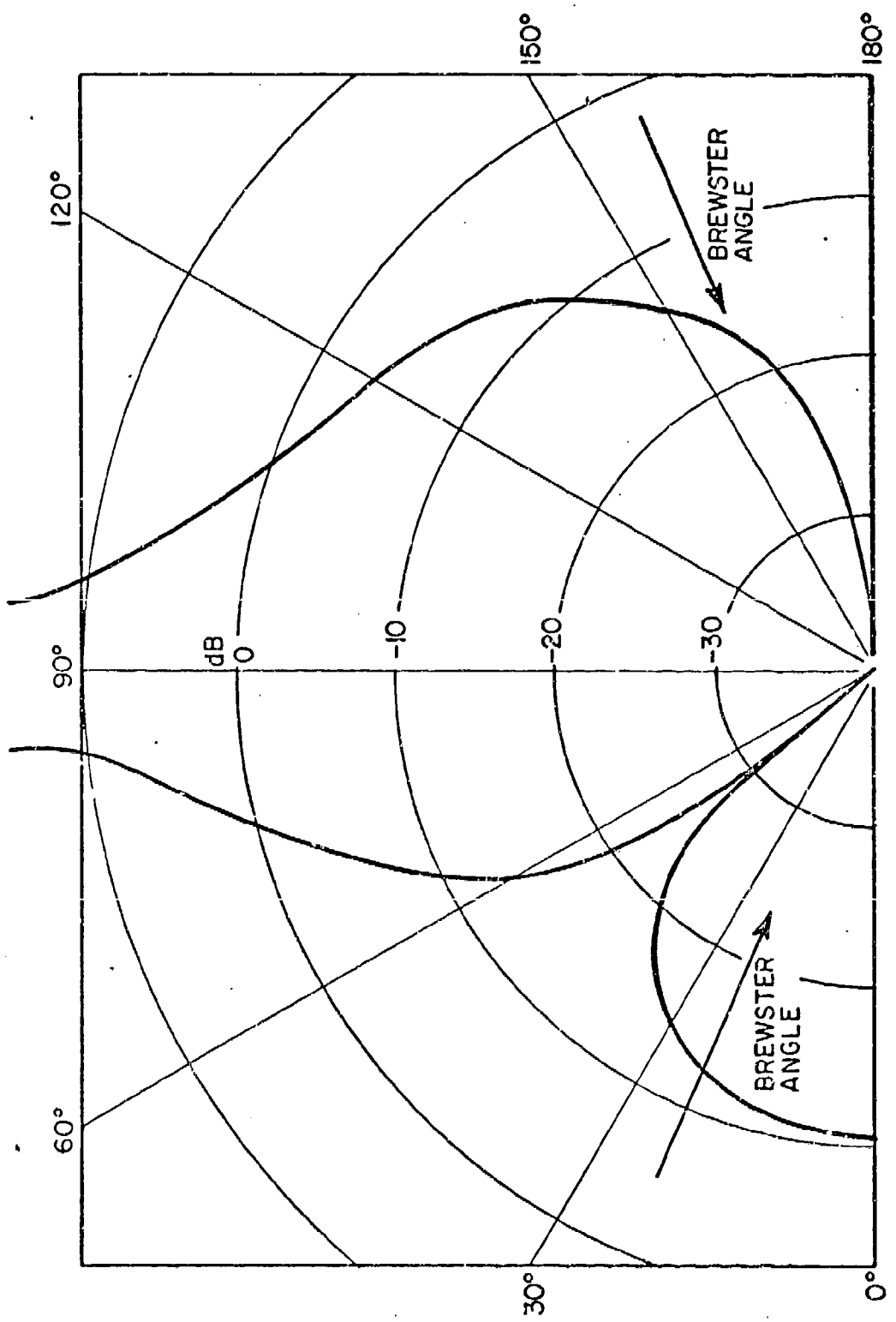

Figure 10.3 Only one Brewster angle displaced by 27° shows up in the resultant backscattered field.

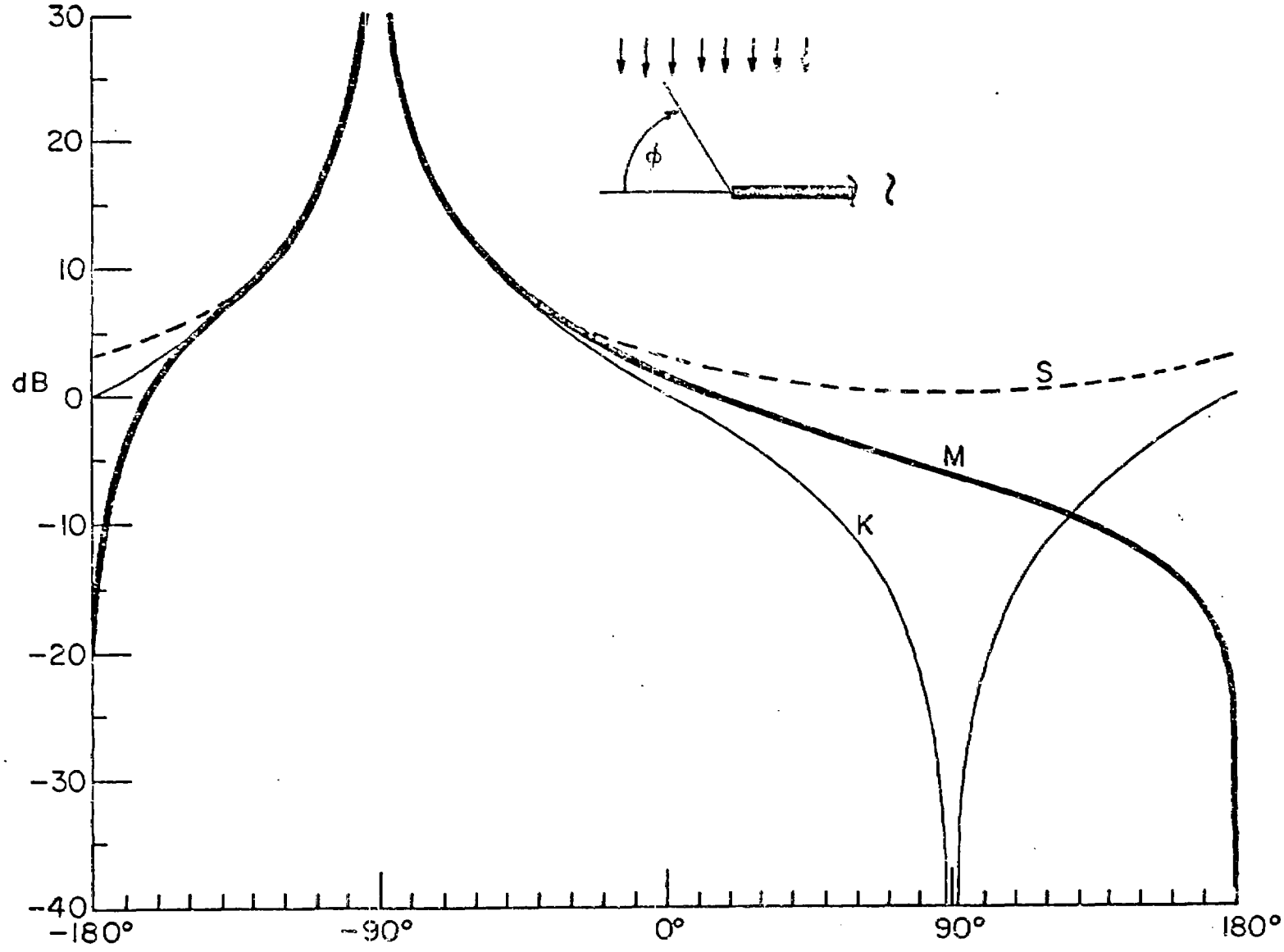

Figure 11.1 Comparison of the exact solution M for normal incidence and impedance match for normal incidence with the first term of the Sommerfeld solution S and with the Kirchhoff solution K as a function of the angle of exit.

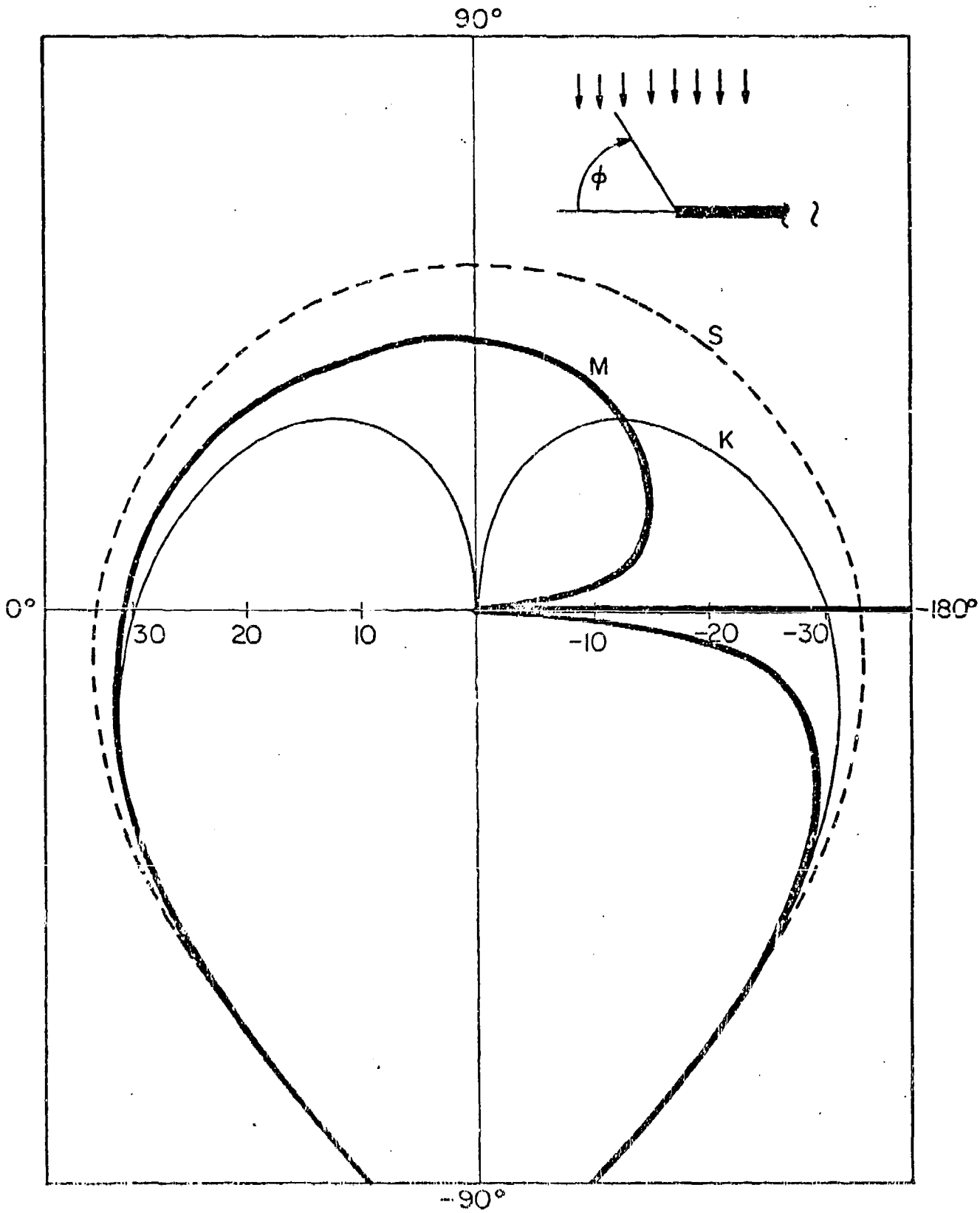

Figure 11.2 Comparison of the exact solution M for normal incidence and impedance match for normal incidence with the first term of the Sommerfeld solution S and with the Kirchhoff solution K as a function of the angle of exit in polar form.

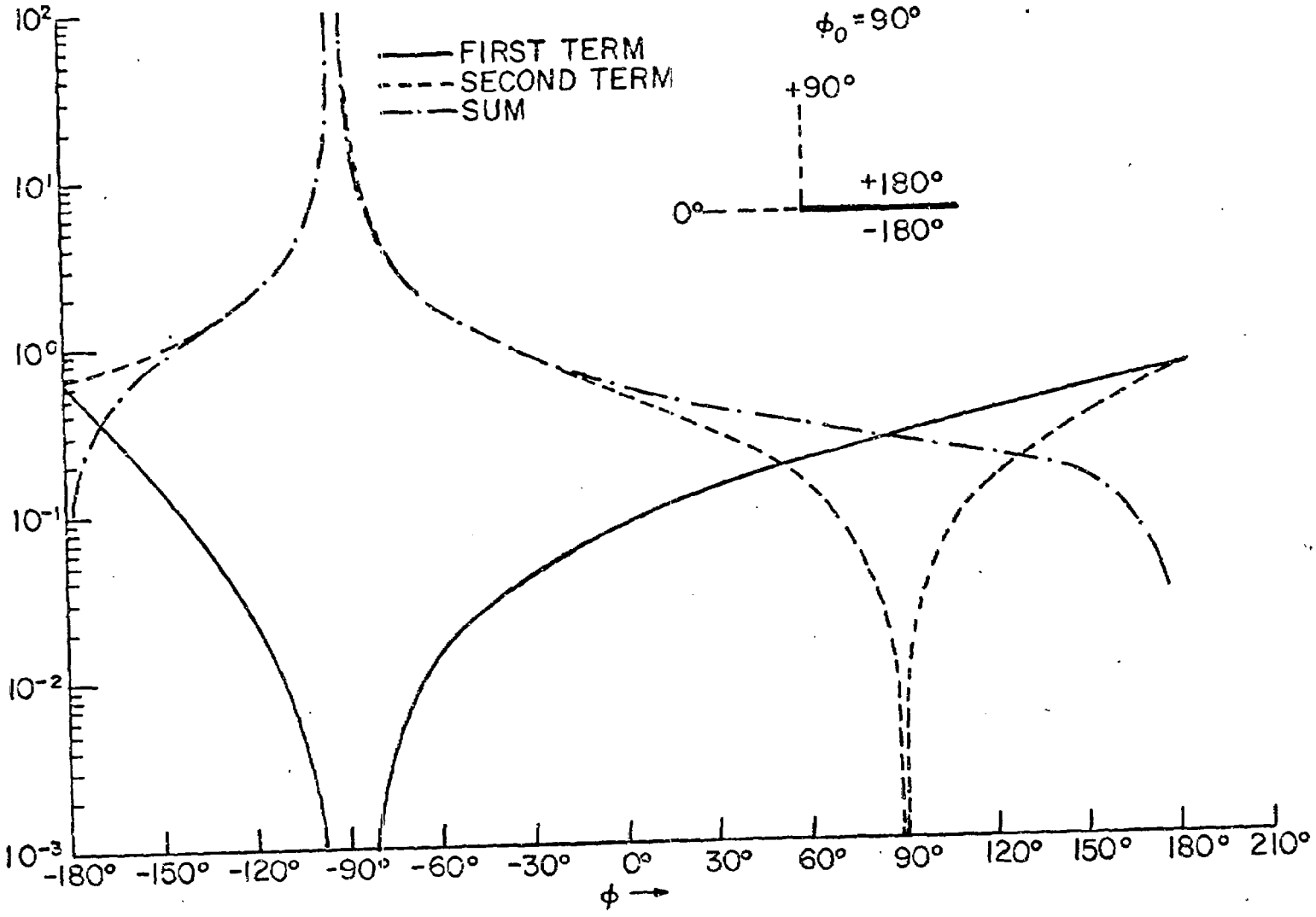

Figure 11.3 The two terms of the Malyuzhinets (exact) solution and the resultant solution (SUM) for normal incidence and impedance match for normal incidence.

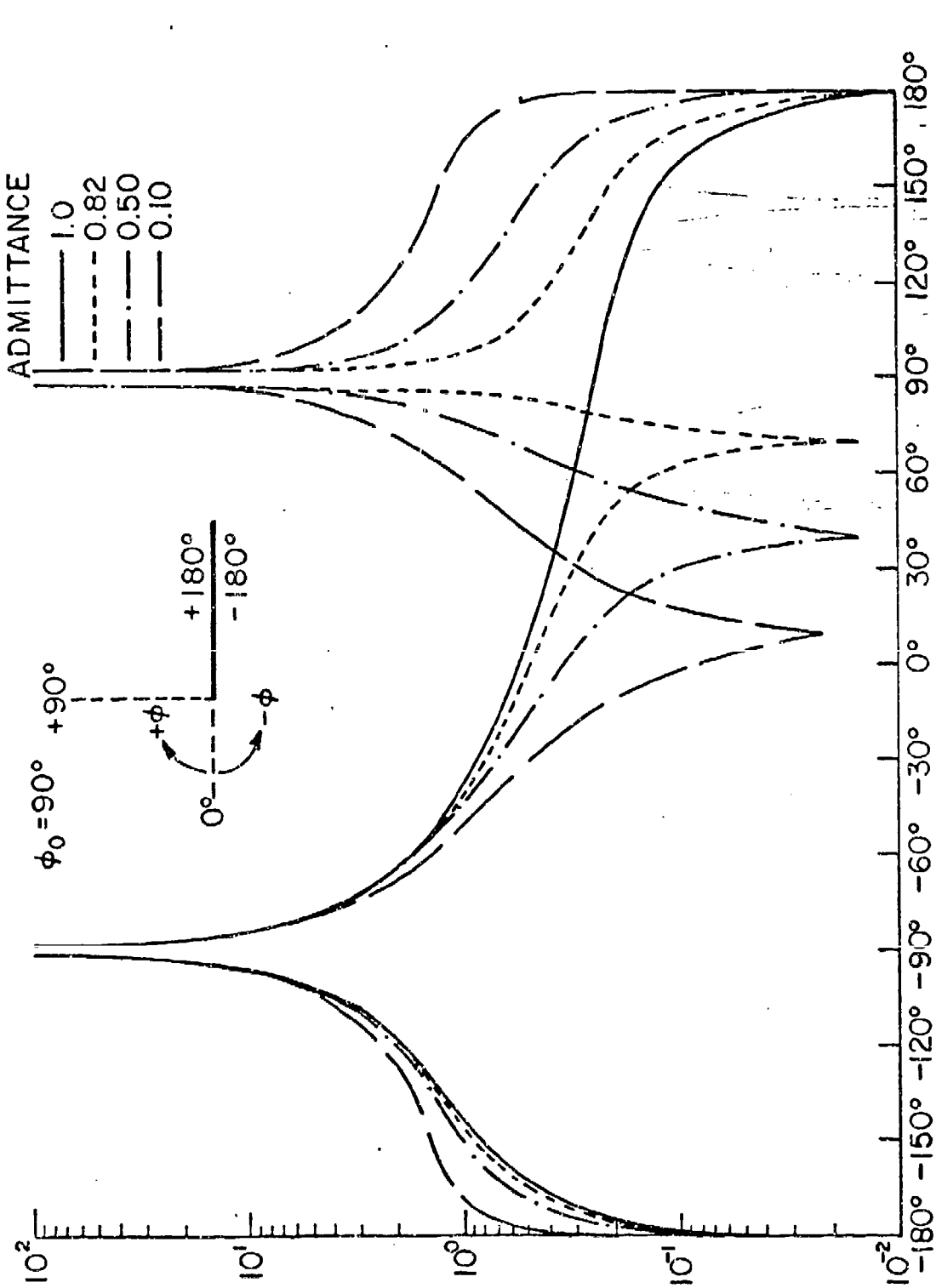

Figure 11.4a The exact solution for a straight edge for $\phi_0 = 90^0$. In contrast to the Sommerfeld approximation, the exact solution depends on the surface admittance also for grazing incidence.

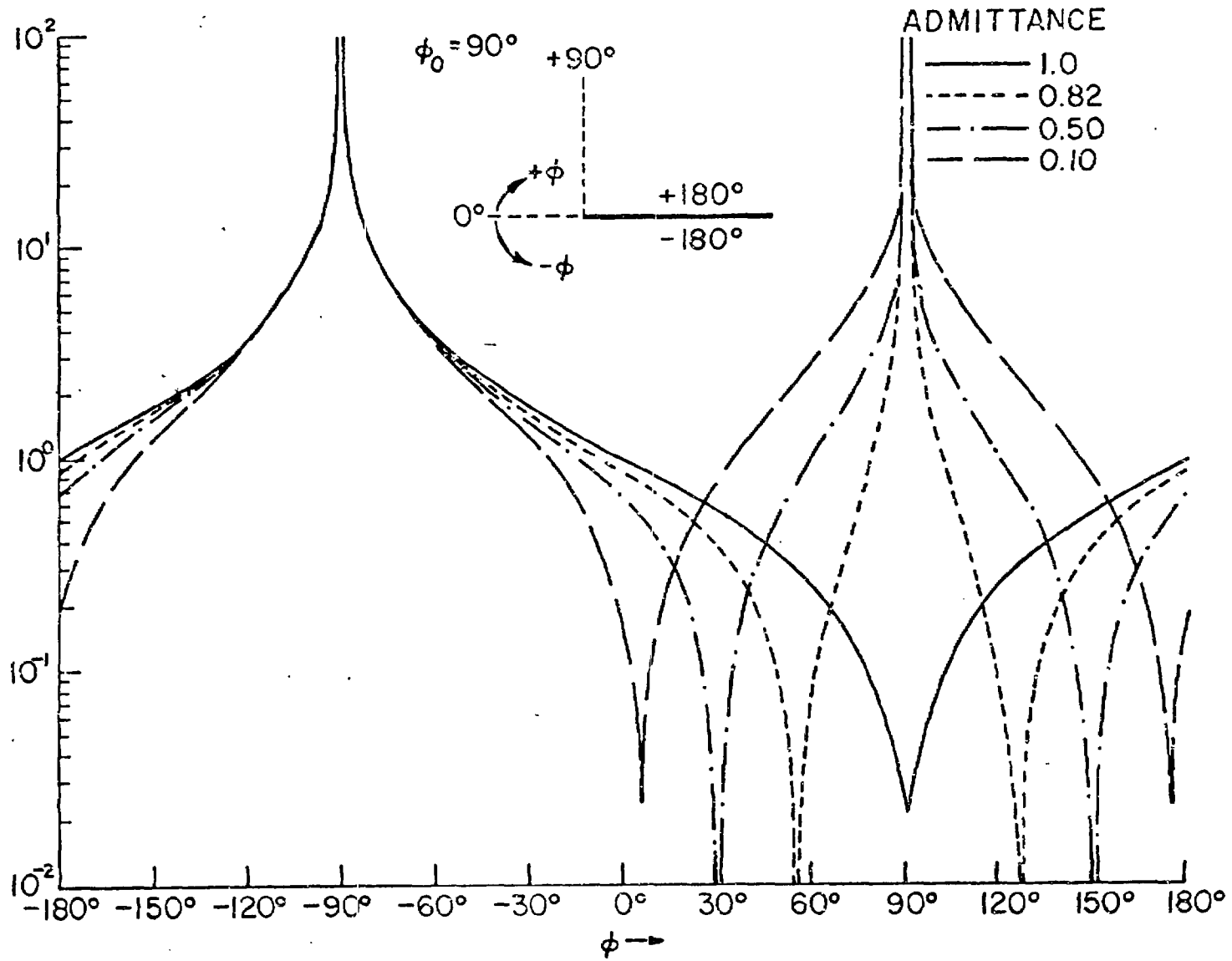

Figure 11.4b The Kirchhoff solution for a straight edge with $R=R(\phi_0)$ for $\phi_0 = 90^\circ$. This represents a good approximation to the exact solution.

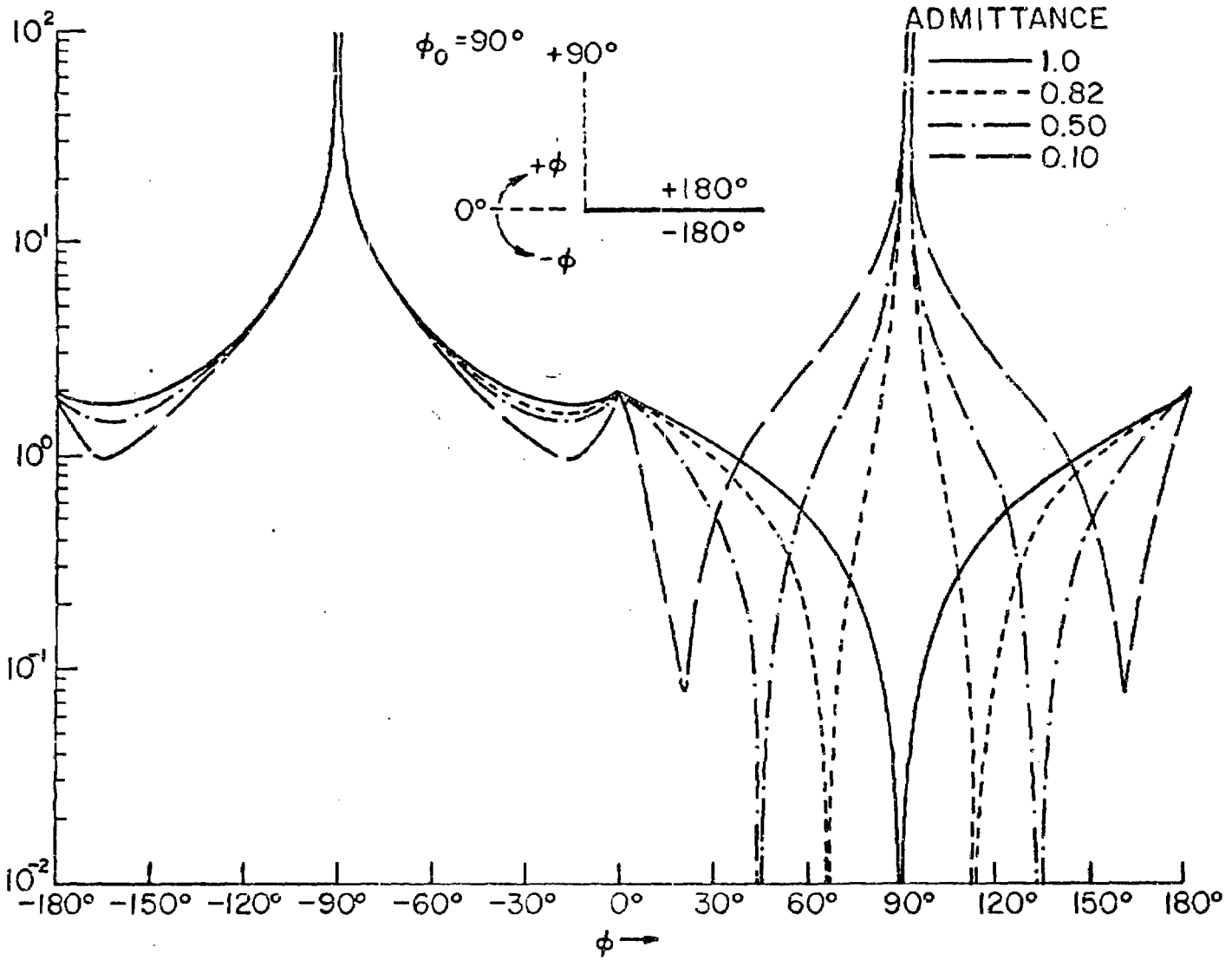

Figure 11.4c The Kirchhoff solution for a straight edge with R=R(ϕ) for $\phi_0 = 90^\circ$. Using the exit factor the zeroes agree with those of the exact solution. But the Kirchhoff solution also has a small peak near $\phi = 0$ that is not found in the exact solution.

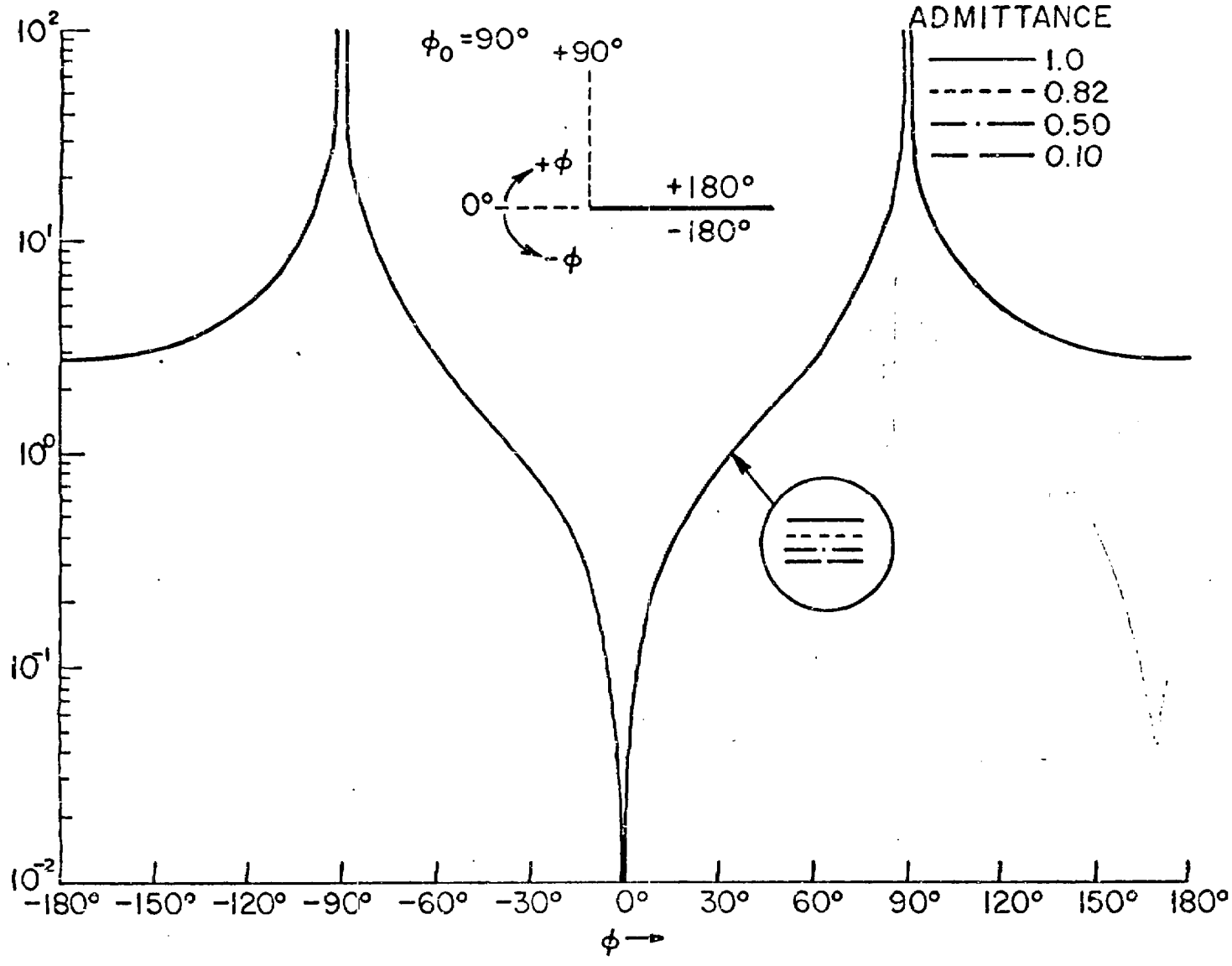

Figure 11.4d The Sommerfeld solution for a straight edge with $R=R(\phi_o)$ for $\phi_o = 90^o$. Because all surfaces act like pressure release surfaces for grazing incidence, the curves are independent of the surface admittance.

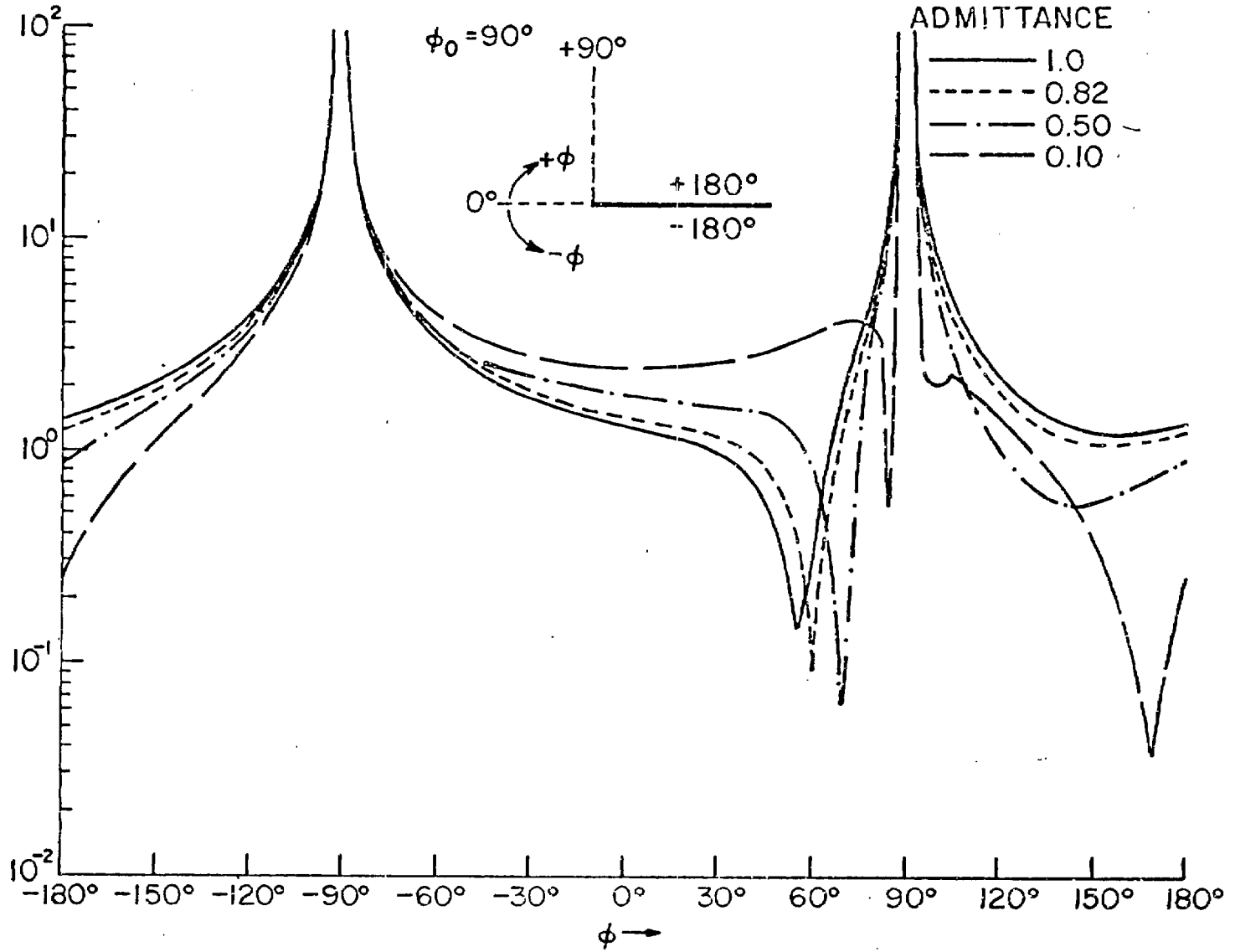

Figure 11.4e The Sommerfeld solution for a straight edge with $R=R(\phi)$ for $\phi_0 = 90^\circ$. This is a poor approximation to the exact solution.

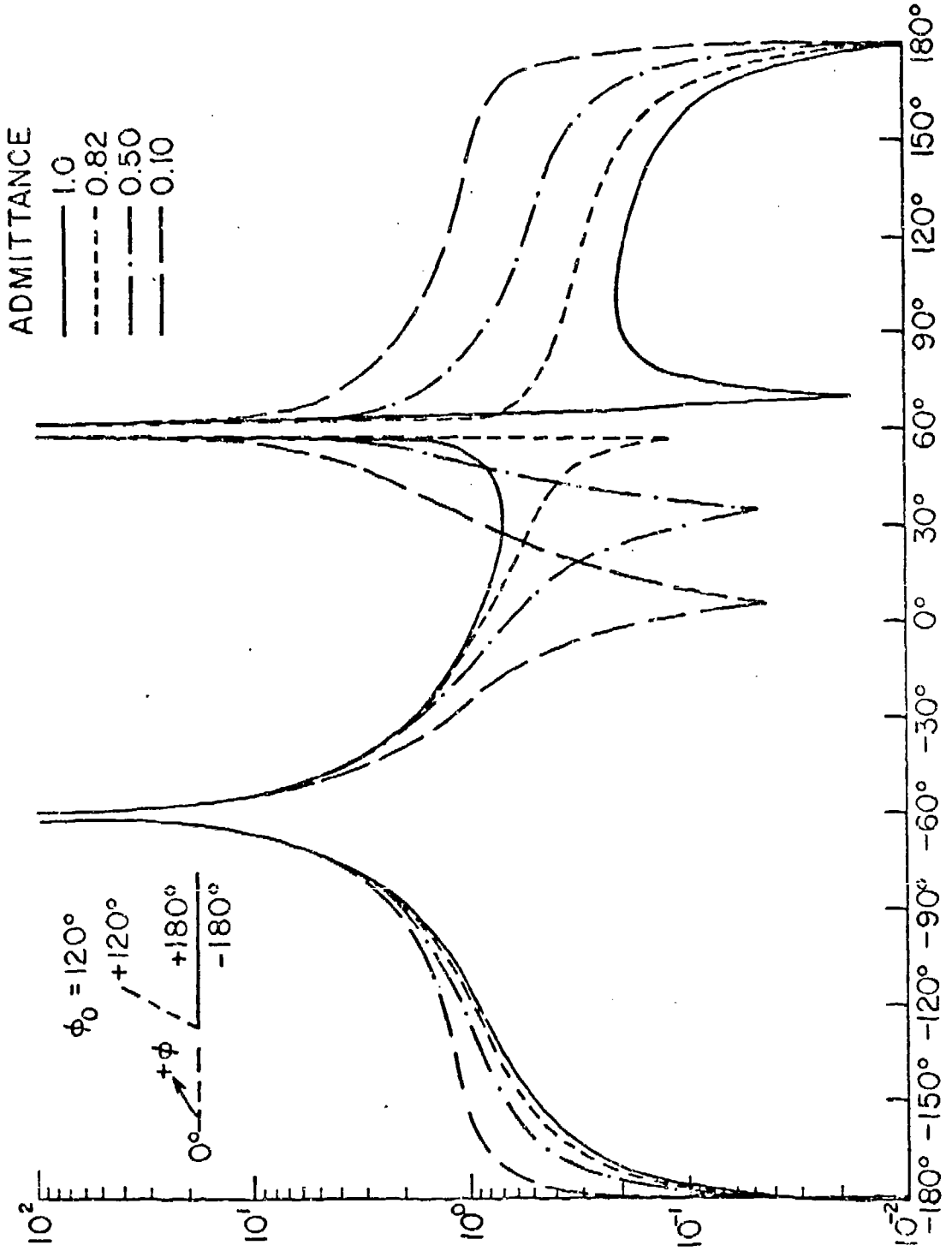

Figure 11.5a The exact solution for a straight edge for $\phi_o = 120^o$.

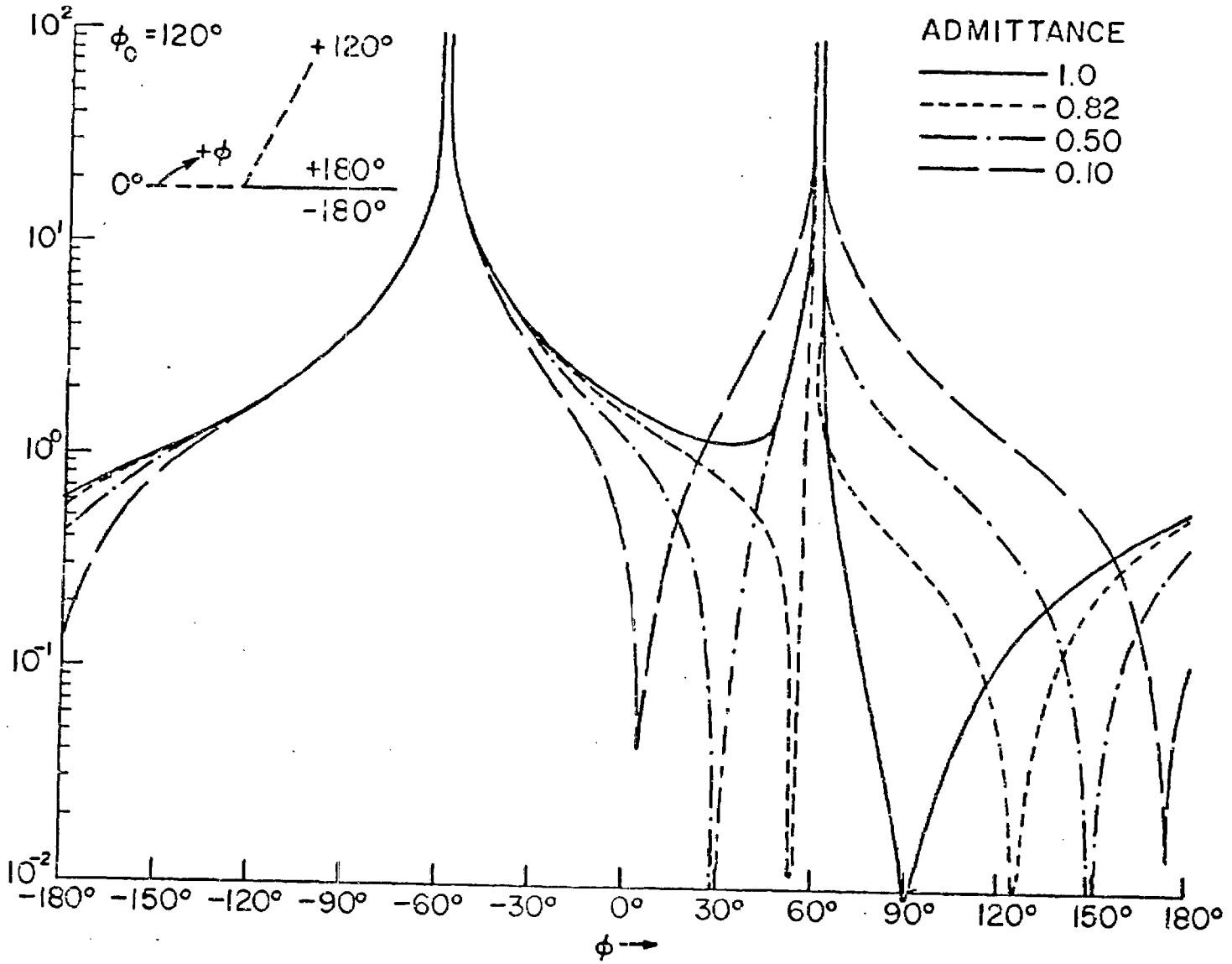

Figure 11.5b The Kirchhoff solution for a straight edge with $R=R(\phi_0)$ for $\phi_0 = 120^\circ$.

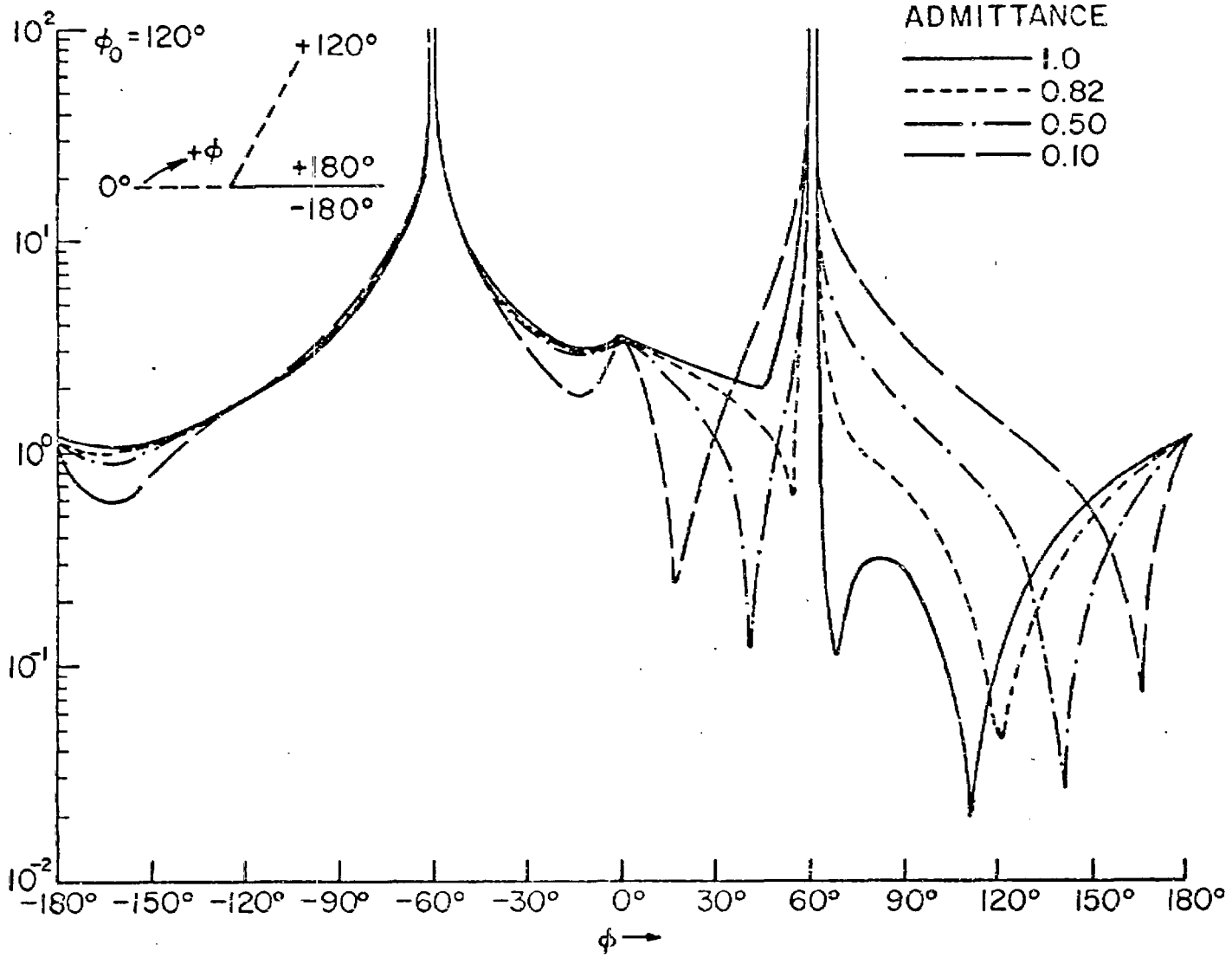

Figure 11.5c The Kirchhoff solution for a straight edge with R=R(φ) for $\phi_0 = 120^\circ$.

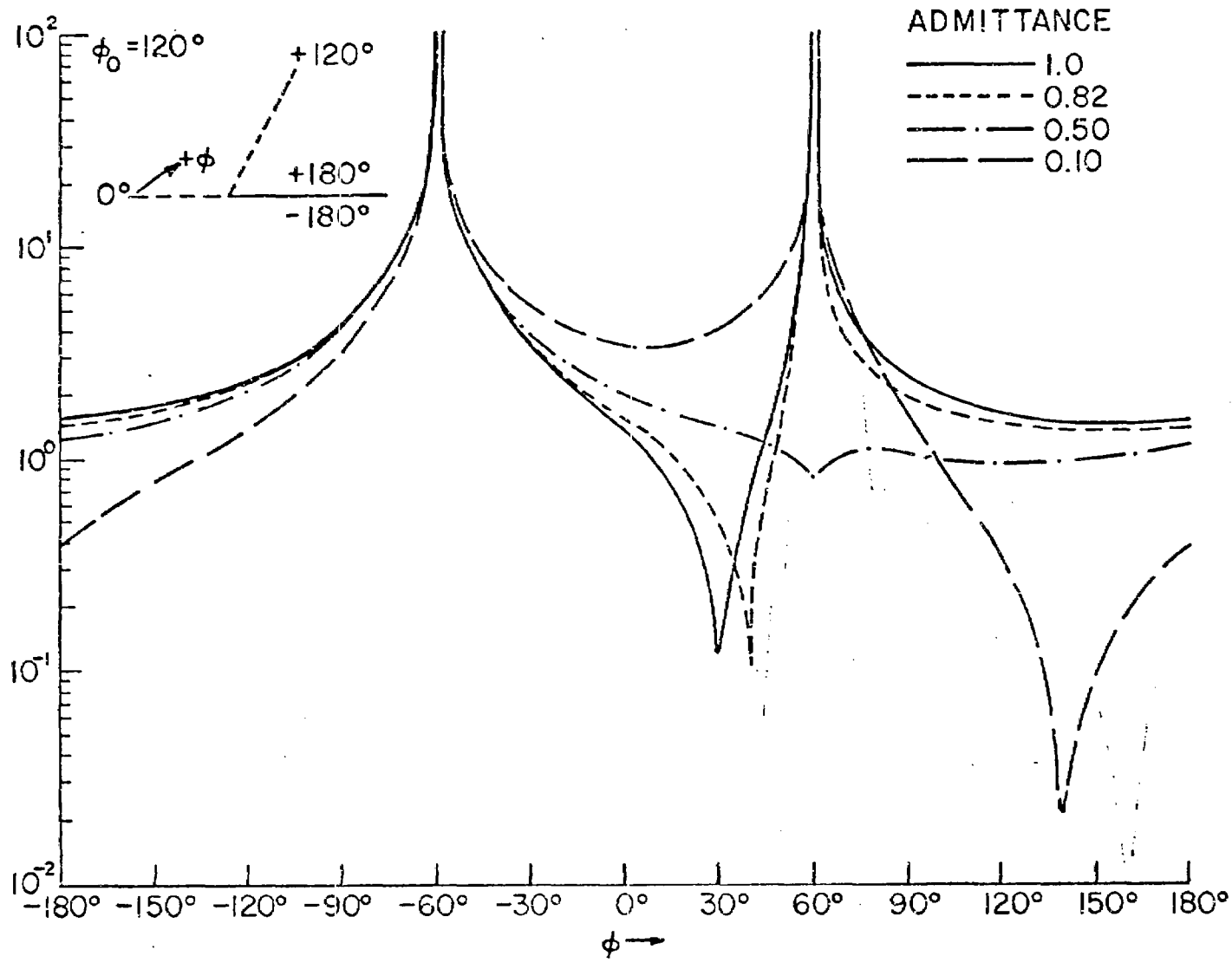

Figure 11.5d The Sommerfeld solution for a straight edge with $R=R(\phi_o)$ for $\phi_o = 120^\circ$.

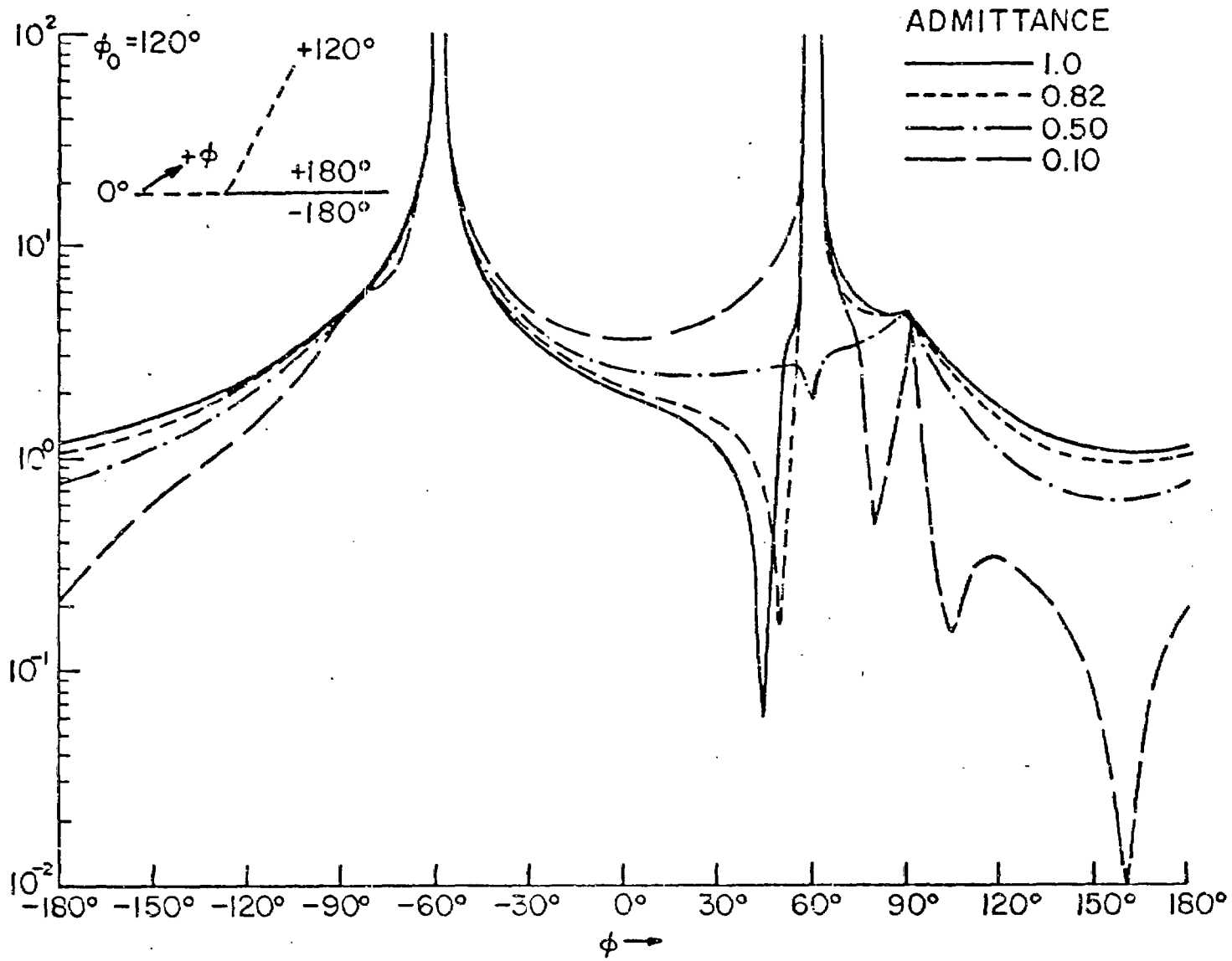

Figure 11.5e The Sommerfeld solution for a straight edge with $R=R(\phi)$ for $\phi_0 = 120^\circ$.

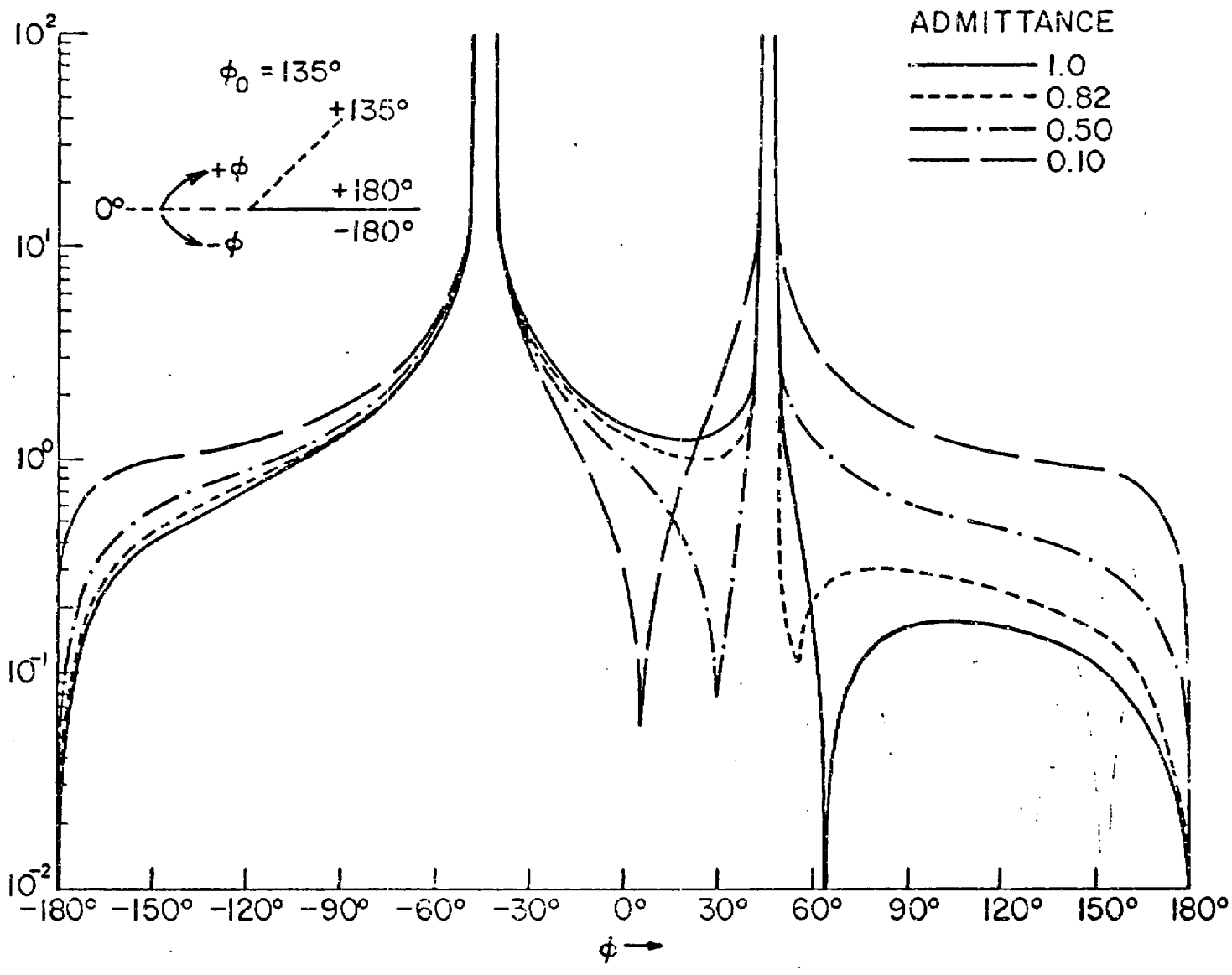

Figure 11.6a The exact solution for a straight edge for $\phi_0 = 135^\circ$.

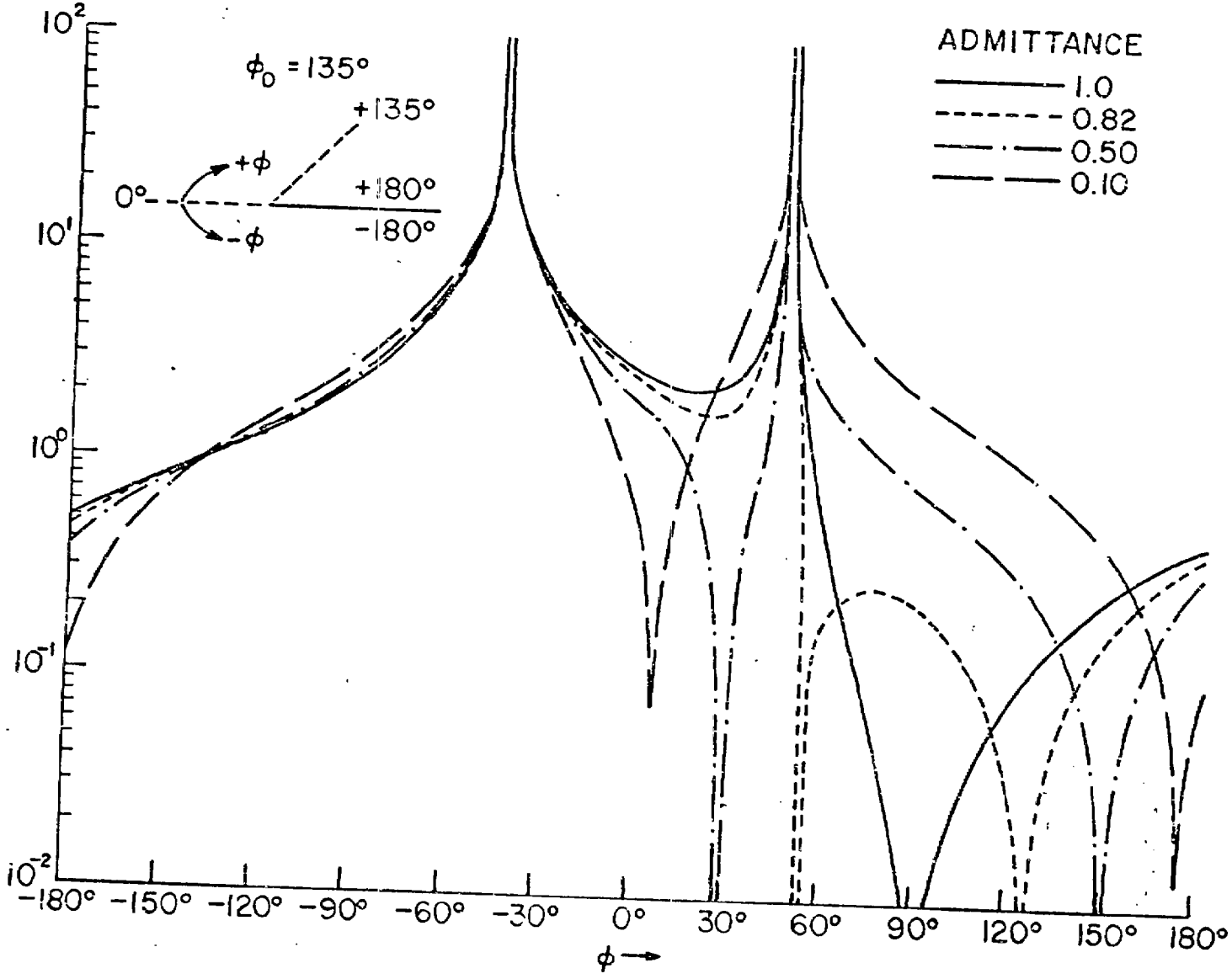

Figure 11.6b The Kirchhoff solution for a straight edge with $R=R(\phi_0)$ for $\phi_0 = 135°$.

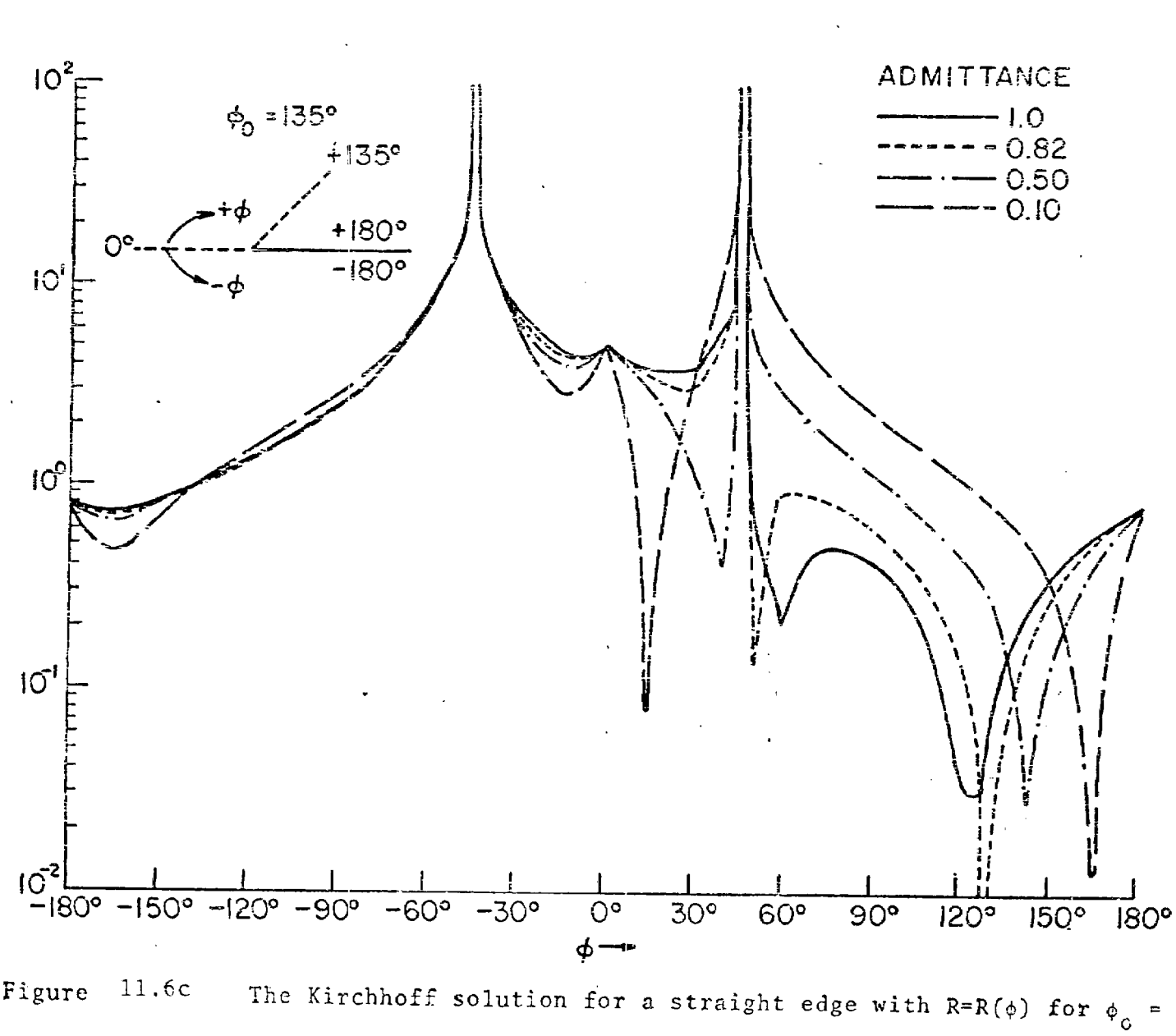

Figure 11.6c The Kirchhoff solution for a straight edge with $R=R(\phi)$ for $\phi_0 = 135^\circ$.

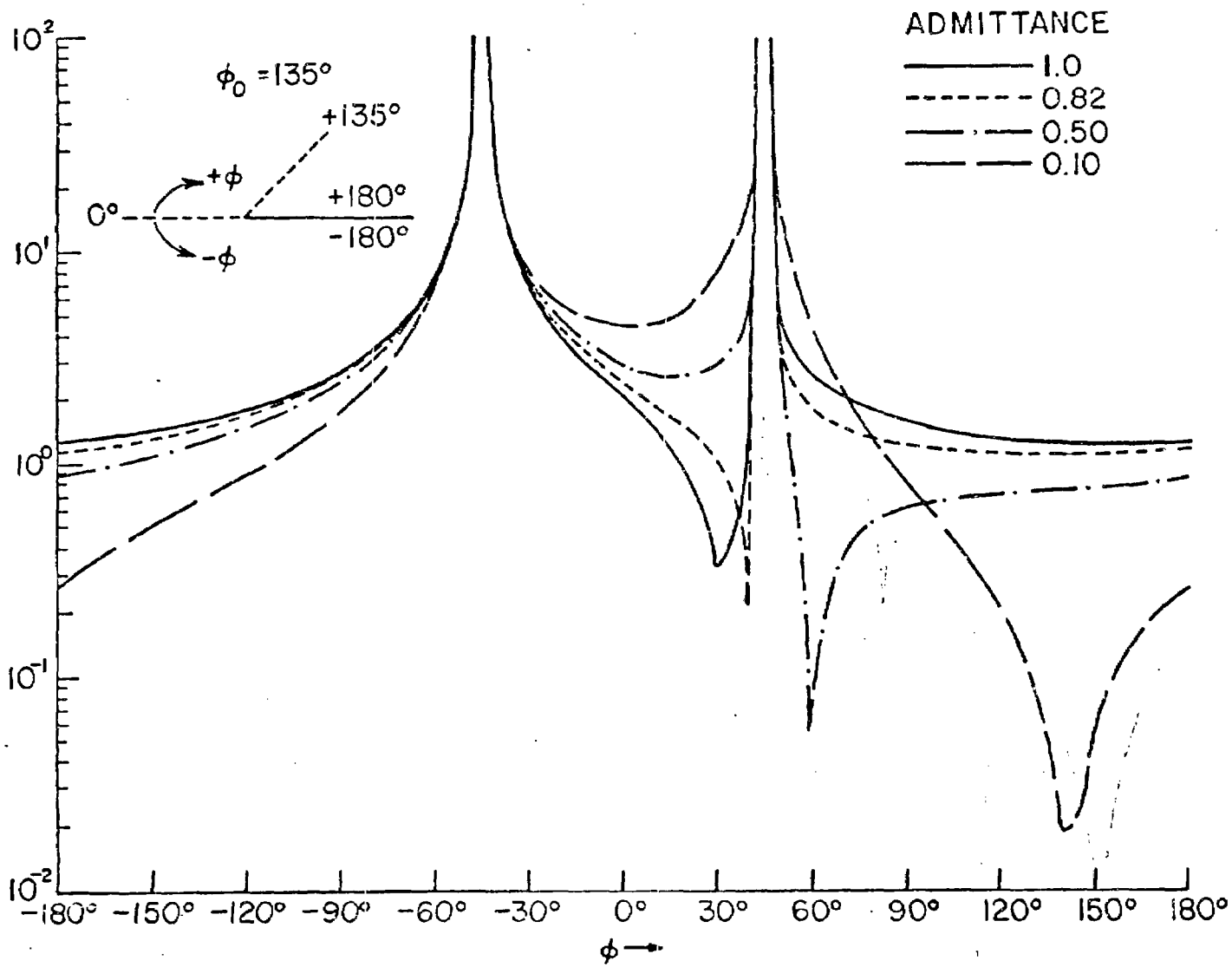

Figure 11.6d The Sommerfeld solution for a straight edge with $R=R(\phi_0)$ for $\phi_0 = 135^\circ$.

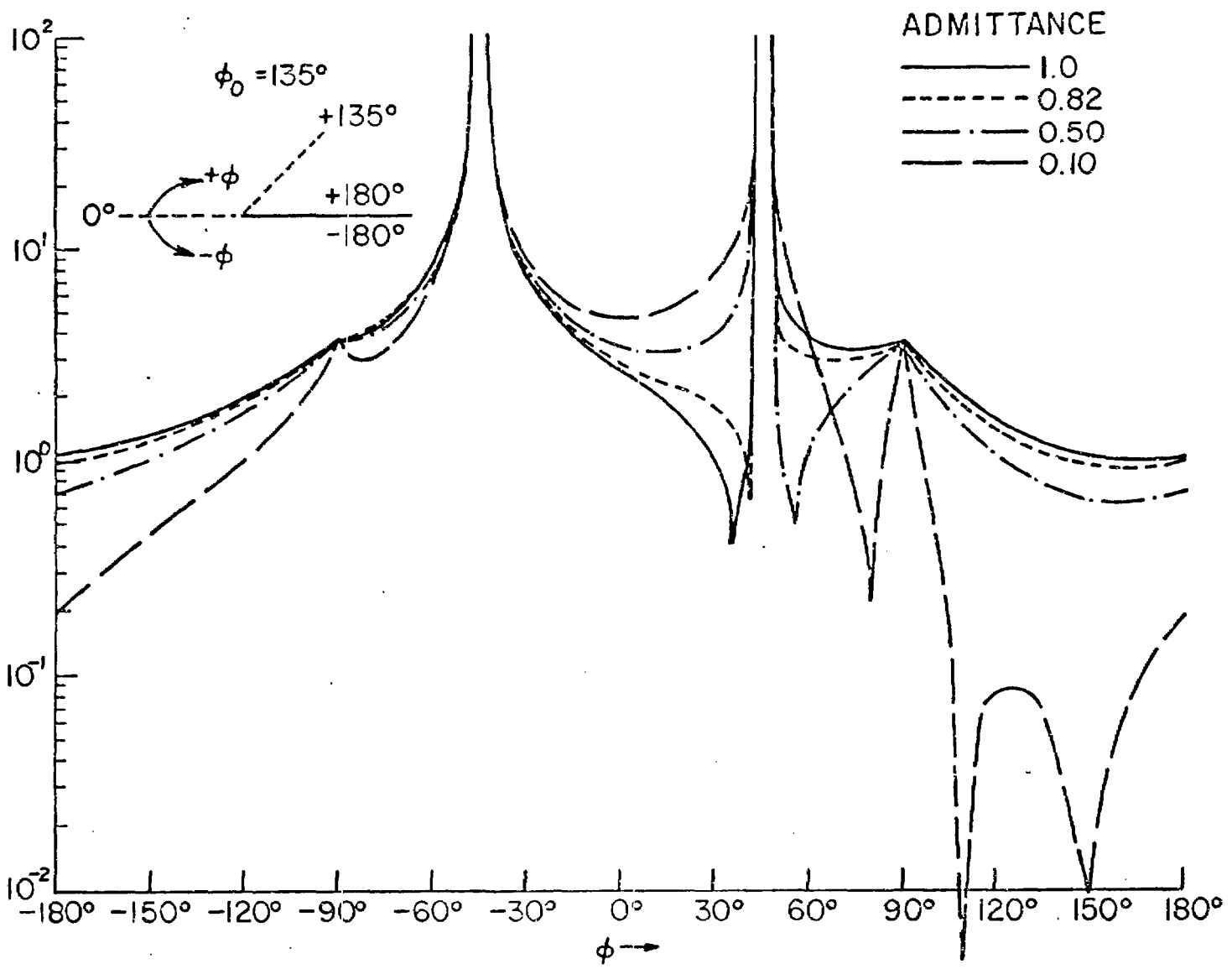

Figure 11.6e The Sommerfeld solution for a straight edge with R=R(φ) for $\phi_0 = 135^\circ$.

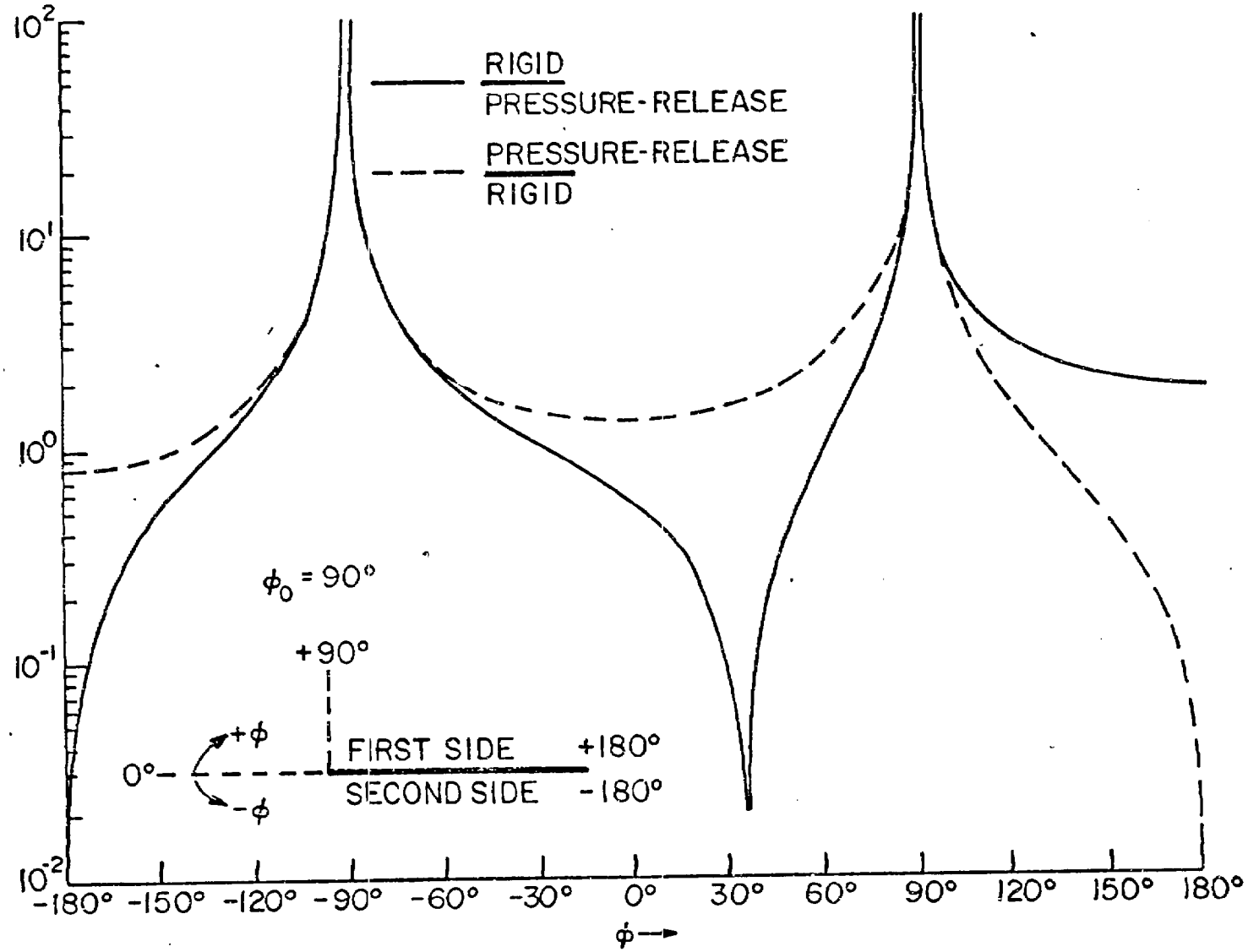

Figure 11.7a The diffracted field for a straight edge, one surface rigid, the other pressure release, for $\phi_0 = 90°$. The field is dominated by the impedance of the surface in the insonified space. But for a rigid surface the field generated by the pressure release surface dominates near $\phi = 0$ and the zero is shifted to positive values of ϕ.

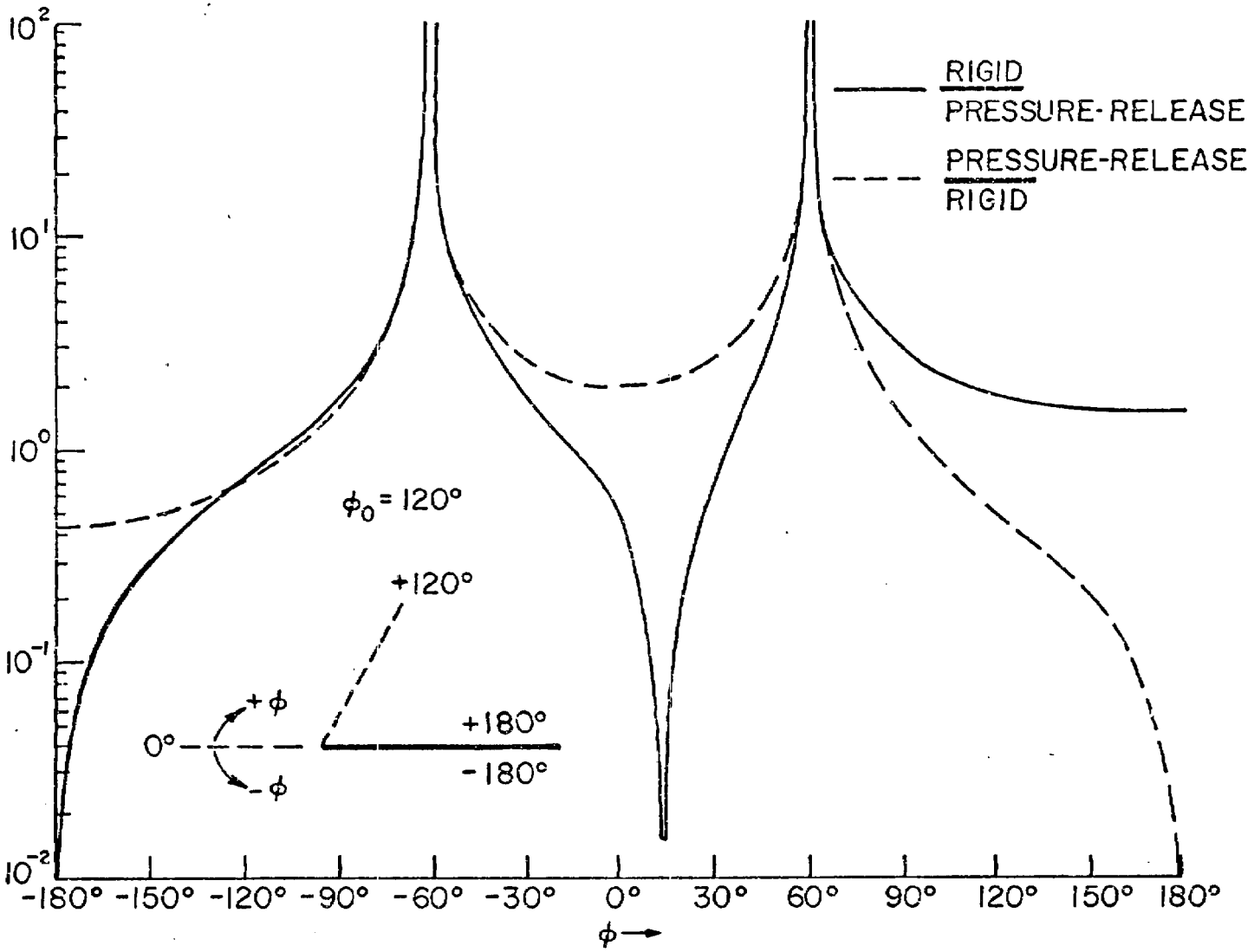

Figure 11.7b The diffracted field for a straight edge, one surface rigid, the other pressure release, for $\phi_0 = 120°$. The field is similar to that of the preceding figure.

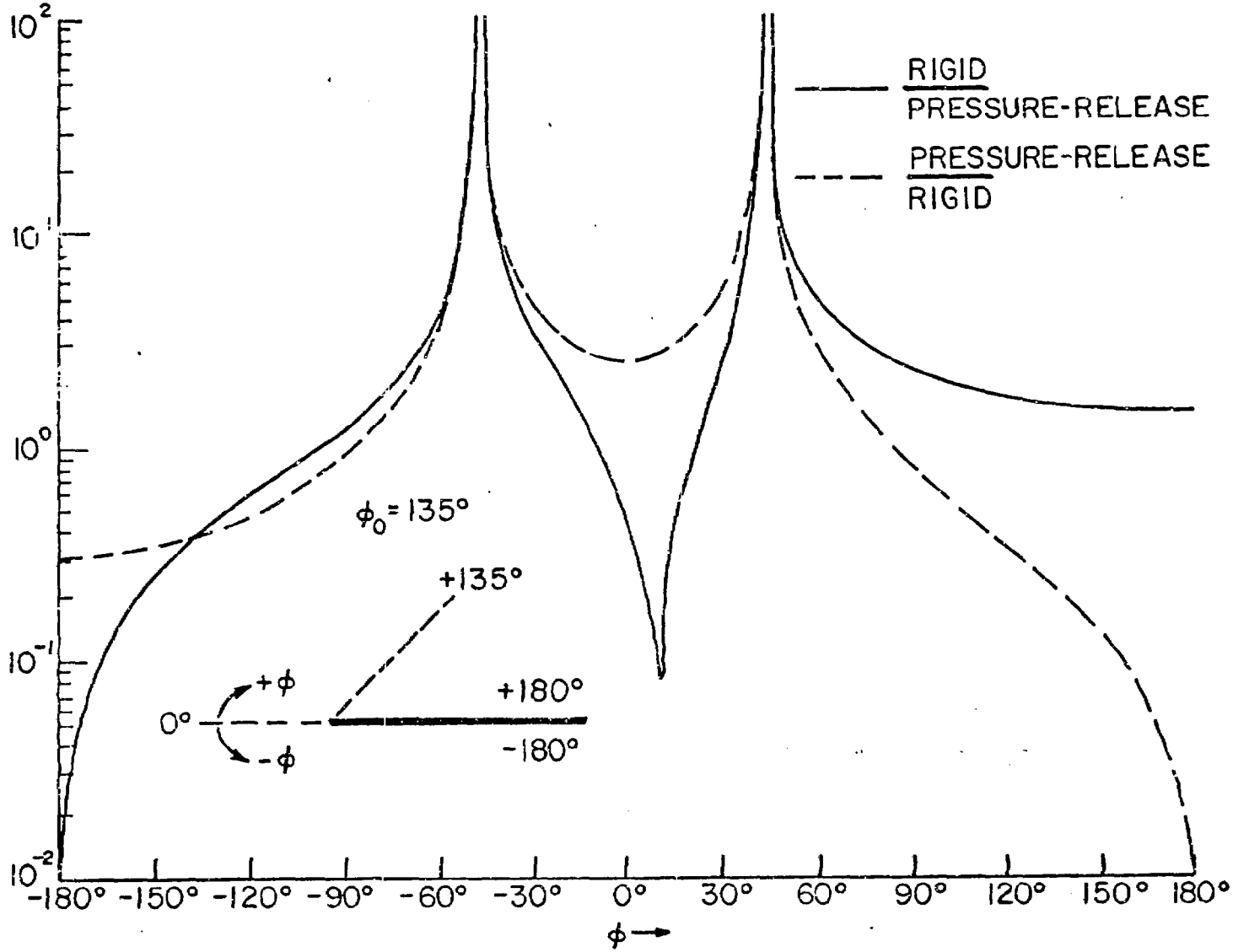

Figure 11.7c The diffracted field for a straight edge, one surface rigid, the other pressure release, for $\phi_0 = 135^\circ$.

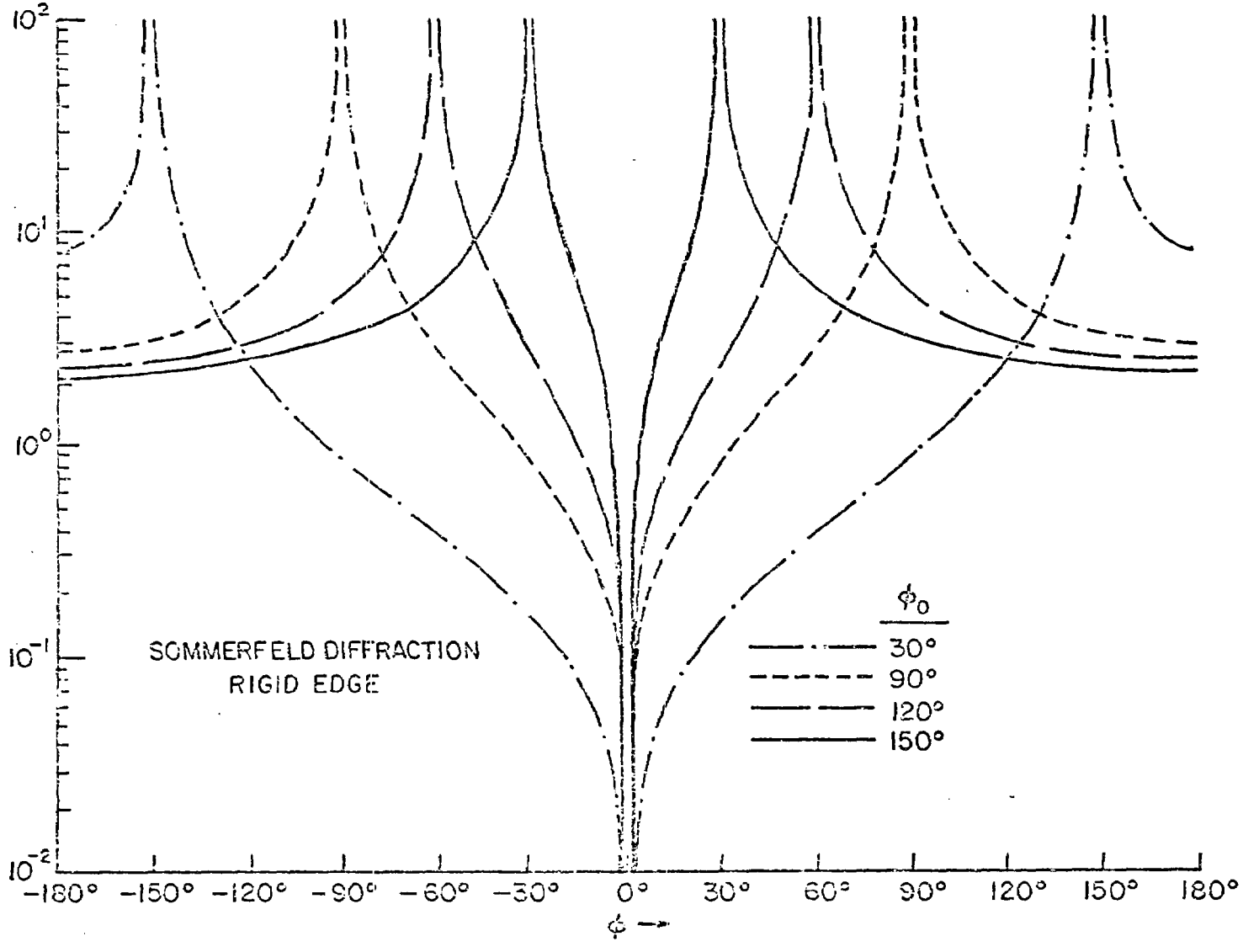

Figure 11.8a The Sommerfeld solution for diffraction from a rigid edge is identical with the case for both surfaces rigid.

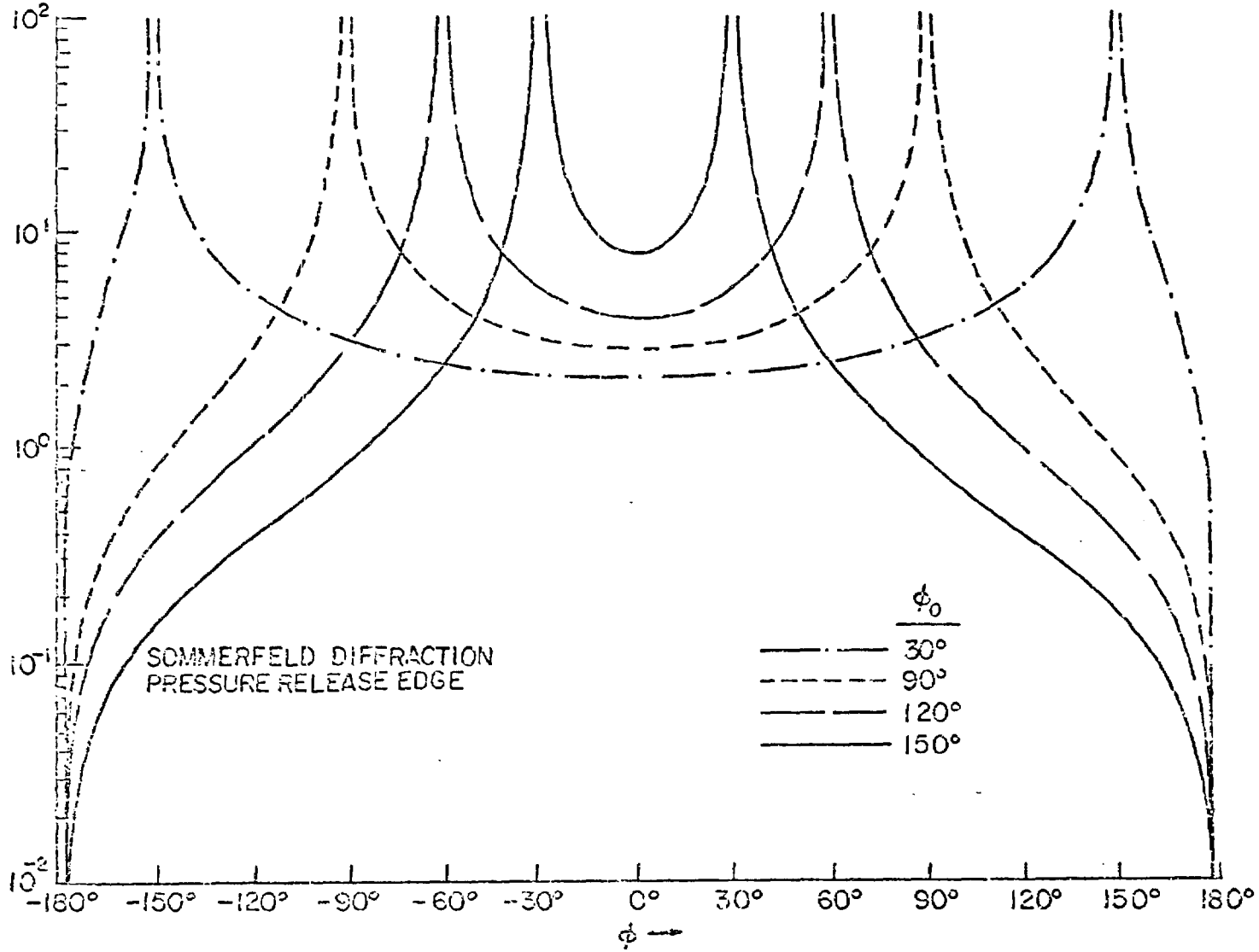

Figure 11.8b The Sommerfeld solution for diffraction from a pressure release edge is identical with the field when both surfaces are pressure release.

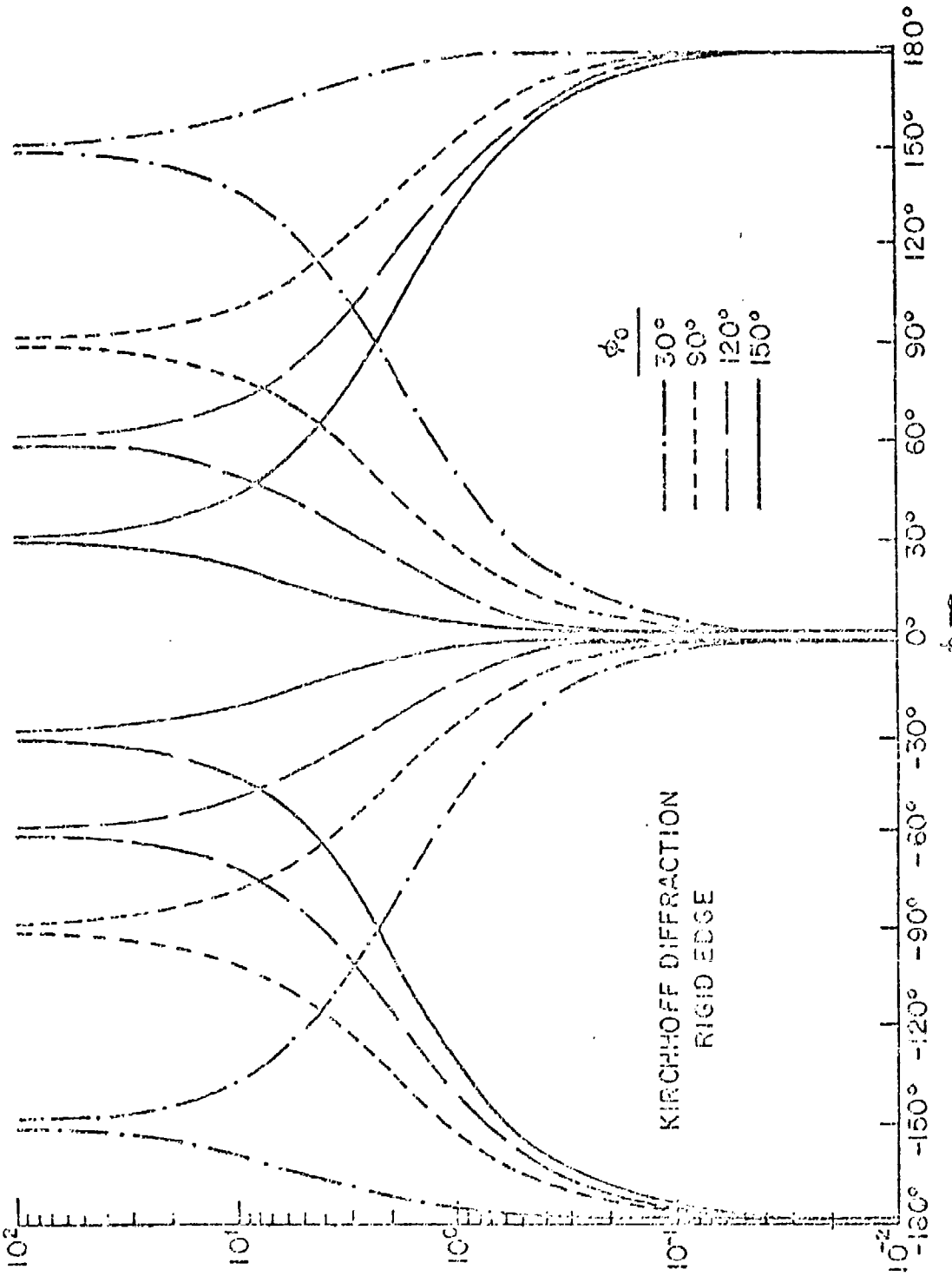

Figure 11.9a The Kirchhoff solution for diffraction from a rigid edge. The rear surface does not contribute.

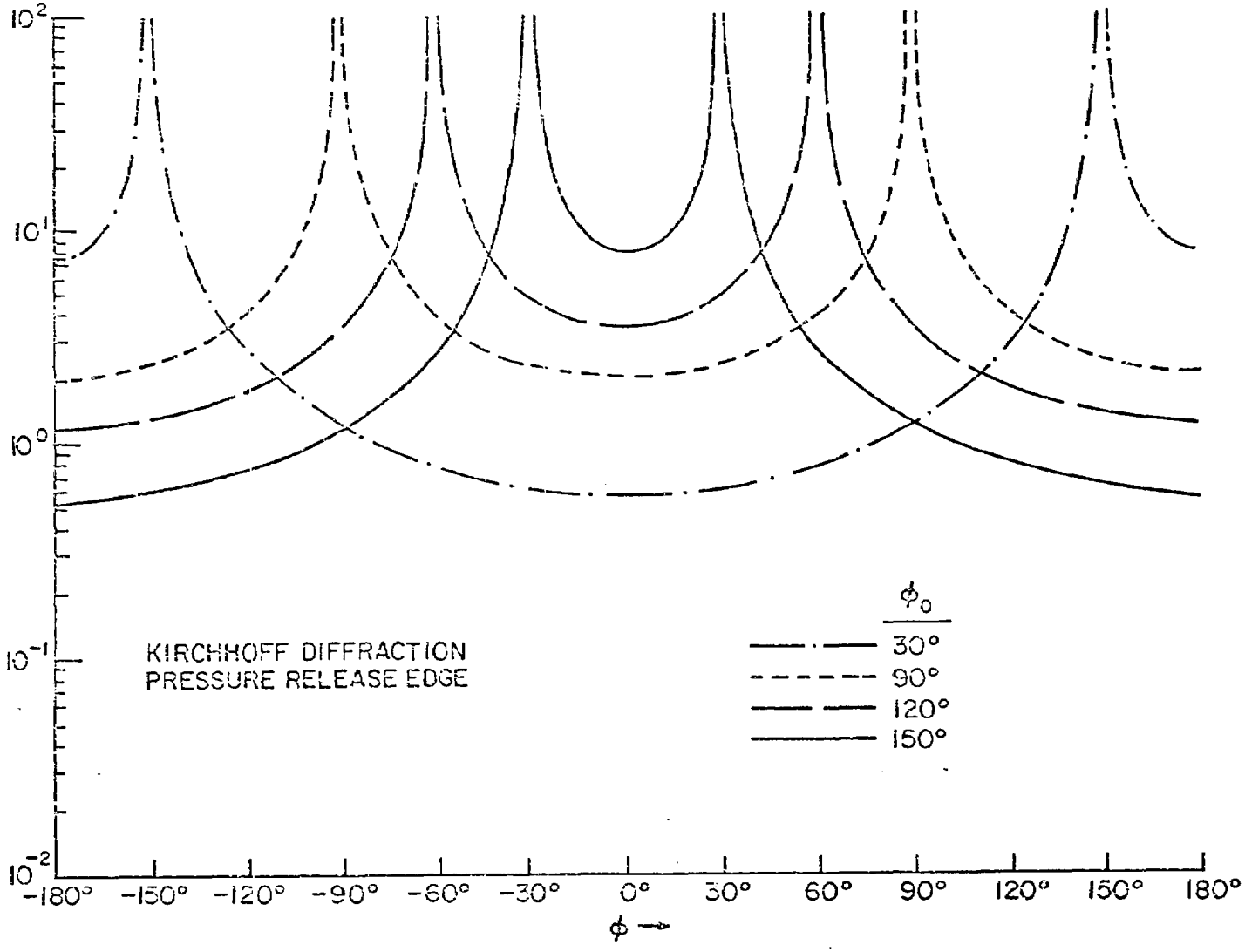

Figure 11.9b The Kirchhoff solution for diffraction from a pressure release edge. The rear surface does not contribute.

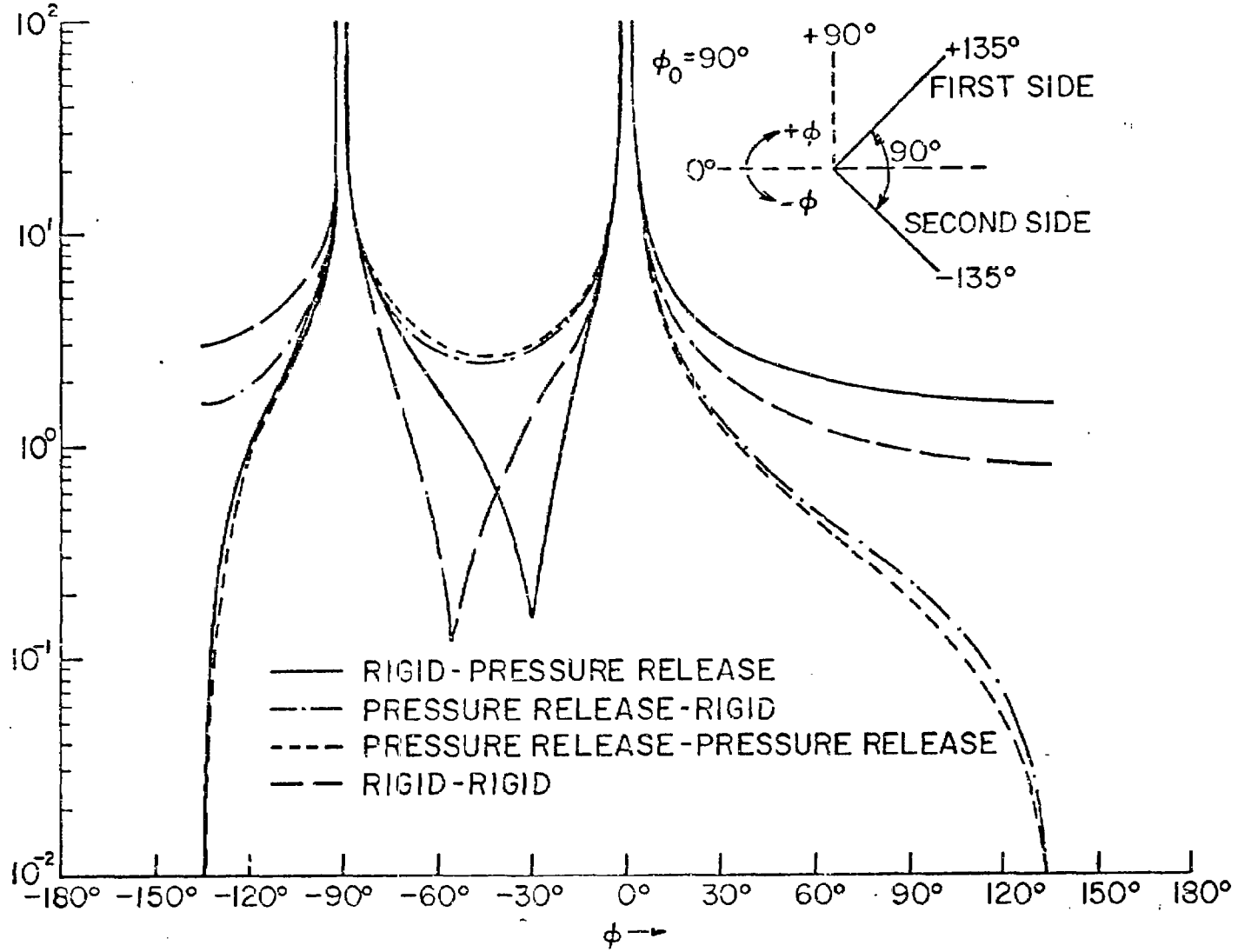

Figure 11.10a Diffraction from a 90° wedge for $\phi_0 = 90°$. The wedge surfaces satisfy the various combinations of rigid and pressure release boundary conditions indicated above.

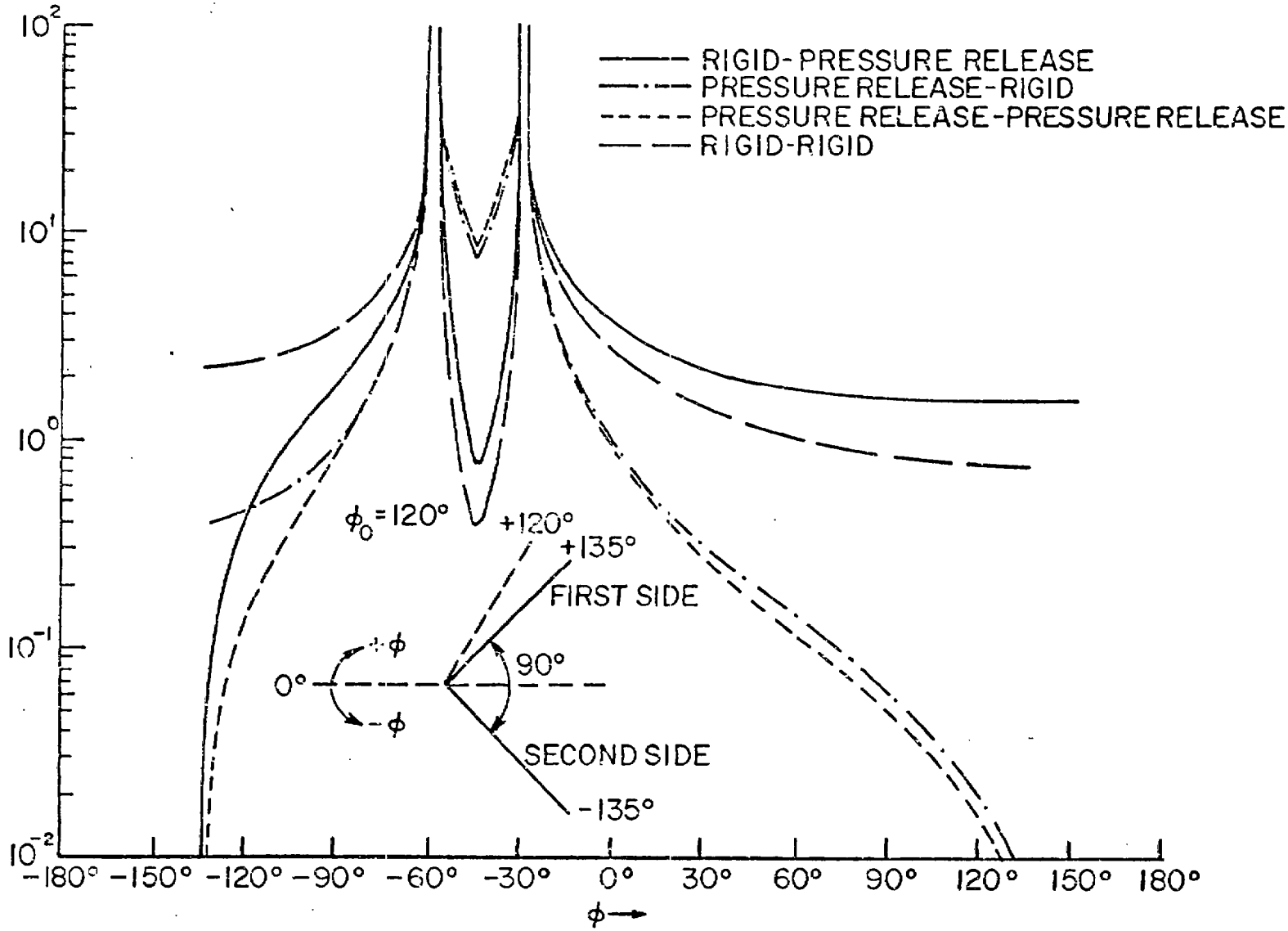

Figure 11.10b Diffraction from a 90° wedge for $\phi_0 = 120°$. The wedge surfaces satisfy the various combinations of rigid and pressure release boundary conditions indicated above.

REFERENCES

Papers by Malyuzhinets (The most important papers are numbered 1-4)

MALYUZHINETS, G.D.
USSR

The following papers were presented by AKIN personnel at the Third All-Union Symposium on Wave Diffraction, held September 24-30, 1964, in Tbilisi: Malyuzhinets, G.D., "One Theorem for Analytic Functions and its Generalizations for Wave Potentials." (2) Malyuzhinets, G.D., "On the Development of One Calculating Method of the Theory of Diffraction." (3) Malyuzhinets, G.D., "Investigation of Wave Diffraction." (4) Malyuzhinets, G.D., "Analytical Dependence on Parameter and Stationary Problems of Diffraction."

MALYUZHINETS, G.D.
USSR

The following paper was presented by AKIN personnel at the Second All-Union Symposium on Wave Diffraction, June 4-9, in Gorkiy, 1962: Fok, V.A., Vaynshteyn, L.A., Malyuzhinets, G.D., "Transverse Diffusion in the Diffraction of Short Waves on a Helical Cylinder."

MALYUZHINETS, G.D.
USSR

(4) Malyuzhinets, G.D., "The Excitation, Reflection, and Emission of Surface Waves on a Wedge with Given Impedances of the Faces," Doklady Akademii Nauk S.S.S.R., 1958, Vol 121, Nr 3, pp 436-439.

Malyuzhinets, G.D., "On Scattering of Sound Due to Irregularities of the Transition Layer in Seas," Akusticheskiy Zhurnal, 1959, Vol 5, Nr 1, pp 70-76.

Malyuzhinets, G.D., "Developments in Our Concepts on Diffraction Phenomena," Uspekhi Fizicheskikh Nauk, 1959, Vol 69, Nr 5, pp 321-334.

The following papers were presented by associates of AKIN at the Third International Congress on Acoustics in Stuttgart, Germany, on Sept 1-8, 1959: Malyuzhinets, G.D. (1) "The Development of

REFERENCES CONTINUED

Diffraction Appearance Concept," and (2) "The Sommerfeld Integrals and the Problem of Diffraction in Cone-Shaped Areas."

Malyuzhinets, G. D., "In Honor of His Fiftieth Birthday," Akusticheskiy Zhurnal, 1960, Vol 6, Nr 4, pp 419-528.

Malyuzhinets, G. D., Filippova, R. D., "Calculation of the Damping of Low-Frequency Sound Waves in Straight Lined Ducts," Promyshlennaya Aerodinamika, 1960, Vol 18, pp 3-11.

MALYUZHINETS, G.D.
USSR

Malyuzhinets, G. D., "Wave Diffraction," Encyclopedic Dictionary of Physics, Gosudartvennoye Naucknoye Izdatelstvo Sovetskaya Entsiklopediya, Moscow, 1960. Akusticheskiy Ahurnal, 1965, Vol 11, Nr 1, p 92.

Vaynshteyn, L. A., Malyuzhinets, G. D., "Transverse Diffusion during Diffraction at a Large Radius Waveguide Post. Part I. Asymptotic Diffraction Laws in Polar Coordinates," Radiotekhnika i Elektronika, 1961, Vol 6, Nr 9, pp 1489-1495.

Malyuzhinets, G. D., Vaynshteyn, L. A., "Transverse Diffusion for the Case of Diffraction in an Impedance Cylinder of Large Radius. Part I. Parabolic Equation in Ray Coordinates," Radiotekhnika i Elektronika, 1961, Vol 6, Nr 8, pp 1247-1258.

Malyuzhinets, G. D., "Research in the Field of Wave Diffraction," Vestnik Akademii Nauk S. S. S. R., 1961, Vol 31, Nr 1, pp 114-115.

Malyuzhinets, G. D., Tuzhilin, A. A., "The Electromagnetic Field Excited by an Electric Dipole in a Wedge-Shaped Region," Doklady Akademii Nauk S. S. S. R., 1962, Vol 146, Nr 5, pp 1039-1042.

Malyuzhinets of AFTN presented the following paper at the Conf on Physical Acoustics and Ultrasonics, March 3-7, 1955 in Moscow: "The Edge Effect of Large Radiators."

(1) Malyuzhinets, G. D., "Sound Radiation by Vibrating Sides of an Arbitrary Wedge," Akusticheskiy Zhurnal, 1955, Vol 1, Nr 2, pp 144-163.

(2) Malyuzhinets, G. D., "Audio Radiation by the Oscillating Boundaries of an Arbitrary Wedge - Part II," Akusticheskiy Zhurnal, 1955, Vol 1, Nr 3, pp 226-234.

REFERENCED CONTINUED

MALYUZHINETS, G.D.
USSR

The following paper was presented at the All-Union Conference on Acoustics, June 24-29, 1957, in Moscow: Malyuzhinets, G.D., "Emission and Diffraction of Sound."

The following paper was presented at the Fourth All-Union Acoustics Conf, May 26 to June 4, 1958, in Moscow: Malyuzhinets, G.D., "Transversal Amplitude Diffusion in Connection with the Refraction, Propagation and Reflection of Waves."

(3) Malyuzhinets, G.D., "Conversion Formula for Sommerfeld Integral," Doklady Akademii Nauk S.S.S.R., 1958, Vol 118, Nr 6, pp 1099-1102.

Malyuzhinets, G.D., "The Connection Between the Revision Formulas of the Sommerfeld Integral and the Formulas of Kontorovich-Zommerfelda," Doklady Akademii Nauk S.S.S.R., 1958, Vol 119, Nr 1, pp 49-51.

G.D. MALYUZHINETS

Moscow, Akusticheskiy Zhurnal, No 4, 1969, pp 629-630

Excerpts: Prof Georgiy Danilovich Malyuzhinetz, Doctor of Physicomathematical Sciences, died suddenly on 14 August 1969 at the age of 59. Malyuzhinets was a prominent Soviet specialist in acoustics and theory of wave diffraction, member of the Communist Party of the Soviet Union, and head of the laboratory of the Acoustics Institute of the USSR Academy of Sciences....

Malyuzhinets was very active in directing graduate students and in giving lectures both in schools (Moscow State University, Moscow Physicotechnical Institute and in research institutes. His comprehensive approach to scientific problems plus his great intuition in physics attracted the youth to him. Many young scientists did their dissertations under his direction or with his constant advice.

Malyuzhinets attached exceptional importance to the training of specialists in diffraction theory. He prepared and gave an original course on diffraction theory for students in the Moscow Physicotechnical Institute. He strove to set up diffraction theory as a speciality in the Mechanics and Mathematics Faculties of universities, for he was completely aware of the increasingly important role played by present-day mathematical methods in solving the problems of wave diffraction. As an active proponent of more mathematical training for scientists concerned with wave diffraction theory, Malyuzhinets spared no efforts to master for himself new mathematical methods and concepts....

REFERENCES CONTINUED

Similar Work with Students of Malyuzhinets and Others

M. S. Bobrovnikov and R. P. Starovoitova, Diffraction of Cylindrical Waves by an Impedance Wedge, Izv. vuzov, Fizika, 6, 163-176, (1963).

B. G. Nikolaev and M. V. Vasil'eva, "Quantitative Investigations of Wave Diffraction from Angular Domains," Uch. Sap. LGU, 32, 71-165 (1958).

A. V. Popov, Numerical Solution of the Wedge Diffraction Problem by the Transverse Diffusion Method, Soviet Physics - Acoustics, Vol. 15, (1969), p. 226.

M. P. Sakharova, Influence of the Edge of a Wedge with Vibrating Faces on the Radiated Acoustic Power, Soviet Physics - Acoustics, Vol. 12, (1966).

R. P. Starovoitova and M. S. Bobrovnikov, Excitation of an Impedance Wedge by a Filamentary Magnetic Source Located at the Vertex, Izv. vuzov, Fizika, 4, 130 (1962).

A. A. Tuzhilin, New Representations of Diffraction Fields in Wedge-Shaped Regions with Ideal Boundaries, Soviet Physics - Acoustics, Vol. 9, No. 2, (1963).

A. A. Tuzhilin, "Some Representations of the Wave Field Excited by an Electric or Magnetic Dipole in an Angular Region" [in Russian]. Annotation of Reports of the Second All-Union Symposium on Wave Diffraction, Moscow, Izd-vo AN SSSR (1962), p. 90.

V. Yu Zavadskii and M. P. Sakharova, Application of the Special Function $\Psi_\Phi(z)$ in Problems of Wave Diffraction in Wedge-Shaped Regions, Soviet Physics - Acoustics, Vol. 13, (1967), p. 487.

REFERENCES CONTINUED

V. Yu. Zavadskii and M. P. Sakharova, Tables of the Special Function $\varphi_{\phi}(z)$, Report of the Institute of Acoustics, Academy of Sciences of the USSR, Moscow (1960).

Plate Edge Reports by Malyuzhinets - Published after his death

G. D. Malyuzhinets and A. A. Tuzhilin, "Diffraction of Plane Sound Wave on a Thin Semi-Infinite Elastic Plate," Zh. Vychisl. Mat. Mat. Fiz., Vol. 10, No. 5, pp. 1210-1227, 1970.

G. D. Malyuzhinets and L. A. Wainstein, "Transversal Diffusion in Diffraction by an Impedance Cylinder of a Large Radius," Radiotekh. Elektron., Vol. 6; Pt. 1, No. 8, pp. 1247-1258; Pt. 2, No. 9, pp. 1489-1495, (1963).

G. D. Malyuzhinets, "Diffraction of Cylindrical and Plane Waves Propagating Along a Semi-Infinite Elastic Plate," Proc. Acoust. Inst. USSR Acad. Sci., Vol. 15, pp. 80-103, 1971.

Recent Western Publication About Malyuzhinets Theory

P. L. Christiansen, Comparison Between Edge Diffraction Processes, Proceedings of the IEEE, Vol. 62, No. 11, November 1974.

A. G. R. VanLennep, The Kernal of Sommerfeld's Transform as Solution to Difference Equations for a Class of Diffraction Problems, Journal of Applied Physics, Vol. 45, No. 10, October 1974.

DISTRIBUTION LIST FOR TECHNICAL MEMORANDUM - TM 75-01

Commander
Naval Sea Systems Command
Department of the Navy
Washington, DC 20362
Attention: Edward J. McKinney, Code 034B
Copy No. 1

Commander
Naval Sea Systems Command
Department of the Navy
Washington, DC 20362
Attention: Edward Liszka, Code 03A1
Copy No. 2

Commander
Naval Sea Systems Command
Department of the Navy
Washington, DC 20362
Attention: Chris Taylor, Code 0372
Copy No. 3

Commander
Naval Sea Systems Command
Department of the Navy
Washington, DC 20362
Attention: Library 09G32
Copy nos. 4 and 5

Commander
Naval Ship Research and Development Center
Department of the Navy
Washington, DC 20007
Attention: Maurcie Sevik, Code 900
Copy No. 6

Commander
Naval Ship Research and Development Center
Department of the Navy
Washington, DC 20007
Attention: Wayne Reader, Code 1945
Copy No. 7

Commander
Naval Ship Research and Development Center
Department of the Navy
Washington, DC 20007
Attention: Richard Biancardi, Code 1933
Copy No. 8

DISTRIBUTION LIST FOR TECHNICAL MEMORANDUM - TM 75-01 CONTINUED

Commander
Naval Ship Research and Development Center
Department of the Navy
Washington, DC 20007
Attention: Albert Tucker, Code 942
Copy No. 9

Commander
Naval Sea Systems Command
Department of the Navy
Washington, DC 20362
Attention: William August, Code 054A
Copy No. 10

Commander Naval Undersea Center
Pasadena Laboratory
3202 E. Foothill Blvd.
Pasadena, CA 91107
Attention: Douglas Chabries
Copy No. 11

Commander Naval Undersea Center
Pasadena Laboratory
3202 E. Foothill Blvd.
Pasadena, CA 91107
Attention: Carl Johanson
Copy No. 12

Commander
Naval Undersea Center
Pasadena Laboratory
3202 E. Foothill Blvd.
Pasadena, CA 91107
Attention: Joel Young
Copy No. 13

Commander
Naval Undersea Center
Pasadena Laboratory
3202 E. Foothill Blvd.
Pasadena, CA 91107
Attention: Jon Reeves
Copy No. 14

Commander
Naval Surface Weapons Center
White Oak
Silver Spring, MD 20910
Attention: Guillermo C. Gaunaurd
Copy No. 15

DISTRIBUTION LIST FOR TECHNICAL MEMORANDUM - TM 75-01 CONTINUED

Commander
Naval Surface Weapons Center
White Oak
Silver Spring, MD 20910
Attention: Walter Madigosky
Copy No. 16

Commander
Naval Underwater Systems Center
Newport Laboratory
Newport, RI 02840
Attention: Fred Canciliere
Copy No. 17

Commander
Naval Underwater Systems Center
Newport Laboratory
Newport, RI 02840
Attention: Dwain Hartge
Copy No. 18

Commander Naval Underwater Systems Center
Newport Laboratory
Newport, RI 02840
Attention: Edward Barile
Copy No. 19

Commander
Naval Underwater Systems Center
New London Laboratory
New London, CT 06321
Attention: Jan Holland
Copy No. 20

Commander Naval Coastal Systems Laboratory
Panama City, FL 32401
Attention: Bruce Nollle, Code 762
Copy No. 21

Commander
Naval Surface Weapons Center
White Oak
Silver Spring, MD 20910
Attention: Marshall J. Tino, Code 531
Copy No. 22

Commander
Naval Sea Systems Command
Department of the Navy
Washington, DC 20362
Attention: William Greenlaw, Code PMS 402B
Copy No. 23

DISTRIBUTION LIST FOR TECHNICAL MEMORANDUM - TM 75-01 CONTINUED

Commander
Naval Ship Research and Development Center
Department of the Navy
Washington, DC 20007
Attention: William Cramer, Code 1949
Copy No. 24

M. T. Pigott
Applied Research Laboratory
The Pennsylvania State University
P. O. Box 30
State College, PA 16801
Copy nos. 25, 26, 27, and 28